THE MULTIPLE ROLES OF A-TYPE LAMINS IN CELLULAR AGING, CELL CYCLE PROGRESSION AND THE DNA DAMAGE RESPONSE

Ian Gibbs-Seymour

Supervisor: Professor Chris Hutchison

A thesis submitted in partial fulfilment
of the requirements for the degree of

Doctor of Philosophy

School of Biological and Biomedical Sciences, University of Durham
2011

ABSTRACT

A-type lamins are a group of type V intermediate filaments whose main members are lamin A and C. Lamins A/C are components of the nuclear lamina and are encoded by the *LMNA* gene. Lamins A/C have a variety of cellular functions, including maintaining the structural integrity of the nucleus and the regulation of signal transduction pathways, transcription factors and DNA replication. Mutations in *LMNA* give rise to a diverse spectrum of diseases, termed laminopathies, which include premature aging syndromes.

In Chapter 3, I sought to understand the role of wild type lamin A in normal cellular aging. Lamin A C-terminal cysteine residues were irreversibly oxidized during the *in vitro* aging of human dermal fibroblasts (HDFs), which impaired the ability of lamin A to form disulfide bonds, causing loss of function. Furthermore, loss of these cysteine residues induced premature senescence, suggesting that these cysteine residues are important for lamin A function during cellular aging.

In Chapter 4, I extended previous findings implicating A-type lamins in the control of cell cycle progression. Loss of A-type lamins or its nucleoplasmic binding partner, LAP2α, caused delayed G_1/S-phase progression, reduced cellular proliferation and cell cycle exit. Proliferative defects could not be rescued via treatment with anti-oxidants.

In Chapters 5 and 6, I addressed the role of wild type mature lamin A/C in the DNA damage response (DDR). A-type lamins interact with the DDR mediator protein 53BP1 via its Tudor domain. Loss of *LMNA* caused endogenous DNA damage and loss of 53BP1 protein levels. Furthermore, loss of *LMNA* resulted in defective DNA repair that ultimately led to increased sensitivity to DNA damage.

Together, the data presented here extends previous findings implicating A-type lamins in cell cycle progression and provides novel insights into the cellular roles of A-type lamins in cellular aging and the DNA damage response.

CONTENTS

LIST OF FIGURES x

LIST OF SUPPLEMENTARY FIGURES xiii

LIST OF TABLES xiii

LIST OF ABBREVIATIONS xiv

DECLARATION xviii

ACKNOWLEDGEMENTS xix

DEDICATION xx

CHAPTER 1: INTRODUCTION 1

1.1 The nucleus: overview 1

1.2 Structure, assembly and regulation of the nuclear lamins 2

1.2.1 Lamin genes 2

1.2.2 Structure 4

1.2.3 Lamin assembly 5

1.2.4 Developmental regulation of lamins 6

1.2.5 Transcriptional regulation of lamins 7

1.2.6 Processing of prelamin A 8

1.3 Lamina function 12

1.3.1 Tensegrity element 12

1.3.2 Component of the nucleo-cytoskeletal structural framework 12

1.3.3 Chromatin scaffold 13

1.3.4 Transcription and proliferation 16

1.3.5 DNA replication 18

1.3.6 Epigenetics 18

1.3.7 DNA damage response 19

1.3.8 Mitosis 21

1.4 Lamina-Associated Proteins (LAPs) 23
1.5 Envelopathies 26
1.5.1 Laminopathies 26
1.5.2 Hutchinson-Gilford Progeria Syndrome (HGPS) 29
1.6 The DNA damage response 31
1.6.1 Sensing DNA damage and activating the DDR 31
1.7 Repair mechanisms and pathways 36
1.7.1 Mismatch repair (MMR) 37
1.7.2 Base excision repair (BER) 38
1.7.3 Nucleotide Excision Repair (NER) 40
1.7.4 Inter-strand crosslink (ICL) repair 42
1.7.5 Single-strand break (SSB) repair 43
1.7.6 Double strand break (DSB) repair 45
1.8 p53-binding protein (53BP1) 53
1.8.1 Structure of 53BP1 53
1.8.2 53BP1 in checkpoint control 54
1.8.3 53BP1 in DNA repair 54
1.8.4 Recruitment of 53BP1 to sites of DNA damage 55
1.9 DNA damage checkpoints 57
1.9.1 G_1/S-phase checkpoint 58
1.9.2 Intra-S-phase checkpoint 59
1.9.3 G_2/M-phase checkpoint 60
1.10 The importance of the DDR in human physiology 60
1.10.1 The DDR and cancer 60
1.10.2 The role of the DDR in premature aging 62
1.10.3 The role of DNA damage in cellular senescence 62
1.11 Aging 64
1.11.1 Overview 64
1.11.2 Cellular aging and senescence 65
1.11.3 p53 and p16-pRb pathways 74

1.12 The Cell Cycle 77
1.12.1 Overview 77
1.13 Cell cycle control 78
1.13.1 Cdks and cyclins 78
1.13.2 Phosphorylation events govern cdk activity 80
1.13.3 Ubiquitin-mediated proteolysis confers unidirectionality upon the cell cycle 82
1.13.4 Nuclear localisation regulates cdk activity 86
1.14 Cell cycle phases 87
1.14.1 G_0 and G_1-phase 87
1.14.2 S-phase 93
1.14.3 G_2/M-phase 96
1.15 When the cell cycle goes wrong: cancer 97

CHAPTER 2. MATERIALS AND METHODS 99
2.1 Cell Culture 99
2.1.1 Maintenance of human dermal fibroblasts 99
2.1.2 Maintenance of transformed cell lines 100
2.1.3 G_0 synchronisation by serum-starvation 100
2.1.4 Generation of stable U2OS cell lines 100
2.1.5 Drug/IR treatment 101
2.2 Plasmids 102
2.2.1 Flag-prelamin A 102
2.2.2 GFP-prelamin A and GFP-lamin C 102
2.2.3 HA-tagged 53BP1 102
2.3 Generation of amplified plasmid DNA 103
2.3.1 Transformation of DH5α *E.coli* 103
2.3.2. Plasmid purification 103
2.4 RNAi 103
2.4.1 siRNA sequences 103
2.4.2 Transfection of HDFs with siRNA 104

2.5 Plasmid transfection 106
2.5.1 Lipofectamine 2000 106
2.5.2 Amaxa nucleofection 106
2.5.3 Genejuice 106
2.6 Flow Cytometry 107
2.6.1 Estimation of S-Phase Fraction 107
2.6.2 Estimation of ROS Levels 108
2.7 Protein extraction 109
2.7.1 Preparation of whole cell extracts 109
2.7.2 Preparation of nuclear extracts 109
2.7.3 Biochemical fractionation 110
2.8 Western Blotting 113
2.8.1 Gel electrophoresis and immunoblotting 113
2.8.2 Membrane blocking and antibody incubations 113
2.8.3 Protein detection 114
2.8.4 Quantification of bands 114
2.8.5 Stripping of blots 114
2.9 Immunoprecipitation 115
2.9.1 Immunoprecipitation of endogenous lamin A/C complexes 115
2.9.2 Immunoprecipitation of GFP-lamin A complexes 115
2.10 Immunocytochemistry and confocal microscopy 116
2.10.1 Fixation and permeabilisation 116
2.10.2 Primary and secondary antibodies 116
2.10.3 Estimation of S-phase fraction and phase by EdU labelling 117
2.10.4 Confocal microscopy 117
2.10.5 ImageJ manipulation of micrographs 117
2.11 *In situ* nuclear matrix preparation 118
2.12 Senescence-associated β-galactosidase assay 118
2.13 Clonogenic assay 119
2.14 Laser micro-irradiation 119
2.15 Statistical analysis 120

CHAPTER 3: LAMIN A MODULATES THE CELLULAR RESPONSE TO OXIDATIVE STRESS 124
3.1 Introduction 124
3.1.1 Overview 124
3.2. Senescence-associated hyper-oxidation of cysteine residues in the lamin A tail 126
3.3 Temporary cell cycle arrest of HDF in response to mild oxidative stress is correlated with disulfide bond formation in lamin A. 132
3.4 HDF are hypersensitive to ROS stimulation in the absence of lamin A. ... 134
3.5 Loss of conserved C-terminal lamin A cysteine residues abrogates lamin A function and promotes cellular senescence. 137
3.6 Abrogation of lamin A function by C522/588/591A causes ROS intolerance in HDFs 142
3.7 Mild oxidative stress stimulates over-expression of AP-1 genes in the presence of Flag-C522/588/591A lamin A or absence of lamin A 149
3.8 Discussion 152
3.8.1 The oxidation status of lamin A cysteine residues influences cellular redox homeostasis and the onset of cellular senescence 152
3.8.2 Lamin A as a mediator of an adaptive response to oxidative stress .. 154
3.8.3 Possible synergy between oxidative thiol damage to lamin A and the accumulation of prelamin A and progerin during normal aging 156

CHAPTER 4: LAP2α-LAMIN A/C COMPLEXES GOVERN CELL CYCLE PROGRESSION IN HUMAN DERMAL FIBROBLASTS 157
4.1 Introduction 157
4.1.1 Overview 157
4.1.2 The role of LAP2α-lamin A/C complexes in G_1/S-phase transition 157
4.1.3 Current aims 159
4.2 Depletion of LAP2α or lamin A/C causes altered cell cycle progression in HDFs 160
4.3 Depletion of LAP2α or lamin A/C delays G_1/S-phase progression in HDFs 164

4.4 Depletion of LAP2α or lamin A/C causes transient cell cycle arrest in HDFs 169
4.5 Cell cycle arrest in LAP2α or lamin A/C depleted HDFs is correlated with high levels of ROS, but not increased double strand breaks 173
4.6 Discussion 180
4.6.1 LAP2α and lamin A/C are required for normal cell cycle progression in HDFs 180
4.6.2 LAP2α and lamin A/C prevent cell cycle arrest in HDFs 182
4.6.3 Reducing ROS levels associated with loss of LAP2α or lamin A/C cannot ameliorate proliferative defects 185

CHAPTER 5: THE ROLE OF A-TYPE LAMINS IN THE DNA DAMAGE RESPONSE 187
5.1 Introduction 187
5.1.1 Overview 187
5.1.2 Lamins and the DDR 189
5.1.3 Current aims 189
5.2 53BP1 co-fractionates with A-type lamins in HDFs 190
5.3 A-type lamins promote genome stability and mediate 53BP1 protein levels 193
5.4 53BP1 interacts with A-type lamins via its C-terminal domain, which is lost upon DNA damage 197
5.5 Lamin A/C-deficient cells display DNA repair defects and reduced cellular fitness in response to DNA damage 203
5.6 Discussion 207
5.6.1 Lamin A/C as a chromatin binding protein 207
5.6.2 A-type lamins do not relocalise to IRIF 208
5.6.3 A-type lamins mediate 53BP1 protein stability 209
5.6.4 A-type lamins promote genomic stability and efficient DNA repair 211

CHAPTER 6. MODELLING THE LAMIN A/C-53BP1 INTERACTION AND EXPLORATION OF DNA DAMAGE-DEPENDENT A-TYPE LAMIN PHOSPHORYLATION 215
6.1 Introduction 215
6.1.1 Lamin networks as indicators of molecular function 215
6.1.2 Current aims 216
6.2 Modelling the 53BP1-lamin A/C interaction 217
6.3 Potential for A-type lamins to be DNA damage-dependent targets of phosphorylation 224
6.4 Discussion 231
6.4.1 Modelling the 53BP1-lamin A/C interaction 231
6.4.2 A-type lamins as targets of DNA damage-dependent post-translational modifications 232

CHAPTER 7. GENERAL DISCUSSION 235
7.1 A-type lamins and thesis aims 235
7.2 Lamin A function is impaired during normal aging and is a key component of the cellular response to oxidative stress 236
7.3 Lamin A/C and LAP2α are important for cell cycle progression 238
7.4 Lamin A/C is a novel regulator of the DNA damage response 239
7.5 Linking aging, lamins and the DNA damage response 241
7.6 Conclusion 244

CHAPTER 8. SUPPLEMENTARY FIGURES 245

REFERENCES 252

LIST OF FIGURES

Figure 1.1. Overview of the structure of the nucleus. 2
Figure 1.2. General structure of lamin polypeptides 4
Figure 1.3. Processing pathway of wild type prelamin A and in disease 11
Figure 1.4. Chromosome territories in mammalian cells..... 15
Figure 1.5. Domain structure of LAP2 isoforms..... 25
Figure 1.6. Disease-causing lamin A/C mutations..... 28
Figure 1.7. Structure of the MRN complex and mode of action model.. 32
Figure 1.8. Eukaryotic mismatch repair pathway..... 38
Figure 1.9 Overview of BER pathway in mammalian cells..... 39
Figure 1.10 Overview of the NER pathway in mammalian cells. 41
Figure 1.11. Model of ICL repair highlighting the involvement of the FANC proteins 44
Figure 1.12. γ-H2AX-dependent signalling cascade following DNA damage 47
Figure 1.13. DSB repair pathways in mammalian cells 52
Figure 1.14 Domain structure of 53BP1 and two other mediators of the DDR, MDC1 and BRCA1 53
Figure 1.15 Checkpoint signaling initiates both a transient and sustained cell cycle arrest 58
Figure 1.16 Structure of human telomeres 70
Figure 1.17 The p53 and p16-pRb pathways govern cellular senescence..... 75
Figure 1.18 The eukaryotic cell cycle 78
Figure 1.19. Activity of cdks through the cell cycle 80
Figure 1.20 The ubiquitin-proteasome system (UPS) in the cell cycle 85
Figure 1.21 Domain structure pRb and post-translational modifications 89
Figure 1.22. Role of pRb in the cell cycle 90
Figure 1.23 Model of eukaryotic DNA replication 94
Figure 2.1. Schematic of biochemical fractionation procedure. 112
Figure 3.1. Conserved cysteine residues in the lamin A C-terminal 129

Figure 3.2. Hyper-oxidation of lamin A tail thiol residues in senescent fibroblasts 130
Figure 3.3. Age-dependent modifications to lamin A cysteine residues inhibit disulfide bond formation 131
Figure 3.4. The effects of mild and SIPS-inducing oxidative stress on lamin A disulfide bridge formation, nuclear morphology and growth 135
Figure 3.5. Cysteine-to-alanine mutations differentially affect lamin A disulfide formation. 138
Figure 3.6. A triple lamin A mutant C522/588/591A impairs cellular fitness which induces premature senescence 140
Figure 3.7. Absence of lamin A or presence of lamin A C522/588/591A cysteine mutant impairs ROS homeostasis in cells.. 144
Figure 3.8. HDFs expressing C522/588/591A lamin A mutant show intolerance to mild oxidative stress.. 147
Figure 3.9. C522/588/591A lamin A mutant induces expression of many stress-responsive genes 150
Figure 4.1. Loss of LAP2α or lamin A/C leads to delayed cell cycle progression. 162
Figure 4.2. Loss of LAP2α or lamin A/C causes delayed G_1/S-phase progression 167
Figure 4.3. Loss of nucleoplasmic LAP2α—lamin A/C complexes leads to transient cell cycle arrest in HDFs 171
Figure 4.4. Acute loss of nucleoplasmic LAP2α—lamin A/C complexes is not associated with activation of a DNA damage response 176
Figure 4.5. HDFs depleted of LAP2α or lamin A/C exhibit high levels of intracellular ROS that can be rescued with NAC treatment 178
Figure 4.6. Long-term NAC treatment fails to rescue growth defects associated with loss of LAP2α or lamin A/C in HDFs 179
Figure 5.1. The DNA damage response in mammalian cells. 188
Figure 5.2. 53BP1 cofractionates with lamin A/C in HDFs 192
Figure 5.3 A-type lamins promote 53BP1 stability and nuclear localisation 195

Figure 5.4. Depletion of A-type lamins promotes 53BP1 protein instability 196
Figure 5.5. A-type lamins interact with the 53BP1 C-terminus, which is lost upon DNA damage in a phosphorylation-dependent manner 199
Figure 5.6. Reintroduction of lamin A and C in Y259X cells restores 53BP1 nuclear localization 201
Figure 5.7. Generation of a U2OS/GFP-lamin A stable cell line 202
Figure 5.8. A-type lamin depletion inhibits DNA repair and reduces cellular fitness to DNA damage 205
Figure 6.1 DNA damage response proteins that interact either directly or indirectly (via BAF) with lamin A/C. 216
Figure 6.2. The type s Ig-like fold in the lamin A/C C-terminal 217
Figure 6.3. The lamin A/C Ig-like fold is predicted to interact with the Tudor domain of 53BP1 219
Figure 6.4. Lysine and arginine residues in the lamin A/C Ig-like fold 222
Figure 6.5. The lamin A/C Ig-like fold is predicted to interact with the Tudor domain of 53BP1. 223
Figure 6.6. Top result using GRAMM-X modeling server 224
Figure 6.7. Predicted phosphorylation sites in lamin A/C 225
Figure 6.8. SQ/TQ residues are conserved in the mammalian phylogeny 226
Figure 6.9. Assessing A-type lamin phosphorylation in response to DNA damage. 229
Figure 6.10. Comparison of potential ATM/ATR phosphorylation sites in lamin A/C with other known ATM/ATR targets 230

LIST OF SUPPLEMENTARY FIGURES

Figure 1. Age-dependent changes in nuclear architecture in HDFs 245
Figure 2. Cysteine sulfenic acid cycles 246
Figure 3. Effect of NAC on lamin A disulfide bond formation. 246
Figure 4. HDFs expressing Flag-C522A lamin A are phenotypically similar to HDFs expressing Flag-wt lamin A 247
Figure 5. Endogenous ROS levels in LBR and emerin-null HDFs 247
Figure 6. Cysteine residues in the LAP2α-specific C-terminal domain 248
Figure 7. LAP2α protein levels are down-regulated in quiescent HDFs 249
Figure 8. Knockdown efficiencies for clonogenic assay 249
Figure 9. Potential acetylation sites in lamin A/C 251

LIST OF TABLES

Table 1. Cdk and cyclin complexes during the cell cycle 79
Table 2. Antibodies used in this study. 121
Table 3. Literature based search for A-type lamin phosphorylation sites. 250

LIST OF ABBREVIATIONS

3D-FISH – three-dimensional fluorescence in situ hybridisation
ABC – ATPase binding cassette
AD – autosomal dominant
ADLD – autosomal dominant leukodystrophy
AP-1 – activator protein 1
APC – adenomatous polyposis coli
APC/C – anaphase promoting complex/cyclosome
APL – acquired partial lipodystrophy
ARE – anti-oxidant response elements
AT – ataxia telangiectasia
ATLD – ataxia-telangiectasia like disorder
ATM – ataxia telangiectasia mutated
ATMi – ATM inhibitor
ATR – ATM and Rad3-related
ATRIP – ATR-interacting protein
aWS – atypical Werner's syndrome
BAF - barrier-to-autointegration factor
BER – base excision repair
BRB – blot rinse buffer
BRCA1 – breast cancer 1, early onset
BrdU – bromodeoxyuridine
BSA – bovine serum albumin
Btf – Bcl-2-associated transcription factor
CAAX – where C is cysteine; A is any aliphatic amino acid; X is any of the following amino acids: S, M, C, A, Q or L
CAT – catalase
CBP – CREB-binding protein
Cdk – cyclin-dependent kinase
ChIP – chromatin immunoprecipitation
Chk1/2 – checkpoint kinase 1/2
CHO – Chinese hamster ovary
CIN – chromosomal instability
CKI – cdk inhibitor
CMT2B1 – Charcot-Marie-Tooth syndrome type 2b
CS – Cockayne Syndrome
CSR – class switch recombination
CTCF – CCCTC-binding factor
CtIP – C-Terminal Binding Protein Interacting Protein
DAPI – 4,6-diamindino-2-phenylindole
DCM-CD1 – dilated cardiomyopathy with conduction system defect
DDR – DNA damage response
DNA – deoxyribonucleic acid
DNA-PKcs – DNA protein kinase catalytic subunit
DP – dimerisation protein

ds – double-stranded
DSB – double strand break
DSP – dithiobis (succinimidyl propionate)
DTT – dithiothreitol
DUB – de-ubiquitylating enzyme
EDMD – Emery Dreifuss muscular dystrophy
EdU – 5-ethynyl-2'-deoxyuridine
EMT – epithelial-to-mesenchymal transition
ER – endoplasmic reticulum
ERCC1 – excision-repair cross-complementing group 1
ERK1/2 – extracellular signal-regulated kinase
ESCs – embryonic stem cells
ETC – electron transport chain
FA – Fanconi Anemia
FACS – fluorescence-activated cell sorting
feSEM – field emission scanning electron microscopy
FHA – forkhead-associated
FITC – fluorescein isothiocyanate
FLPD – Dunnigan-type familial partial lipodystrophy
FRAP – fluorescence recovery after photobleaching
FRET – fluorescence resonance energy transfer
GCL – germ-cell less
GFP – green fluorescence protein
GGR – global genomic repair
GPX – glutathione peroxidase
GSH – glutathione
GSK – glycogen synthase kinase
GST – glutathione S-transferase
H_2O_2 – hydrogen peroxide
γ-H2AX – phosphorylated histone H2AX
HA – hemagglutinin
HAT – histone acetyltransferase
HDAC – histone deacetylases
HDF – human dermal fibroblast
HEAT – Huntingtin, elongation factor 3 (EF3), protein phosphatase 2A (PP2A), and the yeast PI3-kinase TOR1
HEM – Hydropsectopic calcification-"moth-eaten"
HGPS – Hutchinson-Gilford Progeria Syndrome
HNPCC – hereditary nonpolyposis colorectal cancers
HR – homologous recombination
HRP – horseradish peroxidase
HU – hydroxyurea
ICL – intrer-strand crosslink
ICMT – isoprenylcysteine carboxy methyltransferase
IF – intermediate filament
Ig – immunoglobulin
IGF – insulin/insulin-like growth

ING – inhibitor of growth
INM – inner nuclear membrane
IR – ionizing radiation
IRIF – ionizing radiation induced foci
KASH – klarsicht, anc-1, syne homology
LADs – lamina-associated domains
LAP – lamina-associated polypeptide
LBR – lamin B receptor
LEM – LAP2, emerin, MAN1
LGMD 1B – limb girdle muscular dystrophy 1B
LINC – linker of nucleoskeleton and cytoskeleton
MADA - mandibuloacral dysplasia type A
MALDI-TOF/TOF – matrix-assisted laser desorption/ionization time-of –flight
MCM – mini-chromosome maintenance
MDC1 – mediator of DNA damage checkpoint protein 1
MDM2 – mouse double minute 2
MEFs – mouse embryonic fibroblasts
MI – microsatelittle instability
MMC – mitomycin C
MMEJ – microhomology mediated end joining
MMR – mismatch repair
MnSOD – manganese superoxide dismutase
MRN – Mre11, Rad50, NBS1
mRNA – messenger RNA
mTOR – mammalian target of rapamcyin
NAC – N-acetyl-L-cysteine
NADPH – nicotinamide adenine dinucleotide phosphate
NBS1 – Nijmegen breakage syndrome 1 (nibrin)
NCS – newborn calf serum
NEM – N-ethylmaleimide
NER – nucleotide excision repair
NES – nuclear export signal
NHEJ – non-homologous end joining
NLS – nuclear localization signal
NPC – nuclear pore complex
NuMA - nuclear mitotic apparatus protein
NuRD – nucleosome remodeling and deacetylases
O_2^- - superoxide radical
OH^- - hydroxyl radical
OIS – oncogene-induced senescence
ONM – outer nuclear membrane
ORC – origin recognition complex
OTUB1 – OTU domain-containing ubiquitin aldehyde-binding protein 1
PARP – poly (ADP-ribose) polymerase
PBS – phosphate buffered saline
PCNA – proliferating cell nuclear antigen
PHA – Pelger-Huet anomaly

PIAS – protein inhibitor of activated STAT
PIKK – phosphoinositide 3-kinase (PI3K)-related protein kinase
PKC – protein kinase C
POT1 – protection of telomeres 1
PP1 – type 1 protein phosphatase family
pRb – retinoblastoma protein
Rce1 – Ras-converting enzyme 1
RD – restrictive dermopathy
RER – rough endoplasmic reticulum
RFC – replication factor C
RING – really interesting new gene
RNA – ribonucleic acid
RNAi – RNA interference
RNS – reactive nitrogen species
ROS – reactive oxygen species
RPA – replication protein A
RXRβ - retinoic acid receptor β
SA β-gal – senescence-associated β-galactosidase
SAC – spindle assembly checkpoint
SAHF – senescence-associated heterochromatin foci
SDFs – senescence-associated DNA damage foci
SDSA – synthesis-dependent strand annealing
SDS-PAGE – sodium dodecyl sulfate polyacrylamide gel electrophoresis
SIPS – stress induced premature senescence
siRNA – small interfering RNA
SMC1 – structural maintenance of chromosomes protein 1A
SOD – superoxide dismutase
SREBP1 – sterol regulatory element-binding protein 1
ss – single-stranded
SCF – Skp1–Cul1–F-box
SSA – single-strand annealing
SSB – single-strand break
SUN1 – Sad1p, UNc-84
SWI/SNF – switch/sucrose nonfermentable
TCR – transcription coupled repair
TERT – catalytic subunit of telomerase
TFIIH – transcription factor IIH
TM – transmembrane
TRF – telomeric repeat binding factor
TRITC – tetramethylrhodamine B isothiocyanate
Trx – thioredoxin
TTD – trichothiodystrophy
UIM – ubiquitin-interacting motif
UPS – ubiquitin proteolysis system
XP – xeroderma pigmentosum
XPA, B, D, F, G – xeroderma pigmentosum group A, B, D, F, G
Zmpste24 – zinc metalloprotease related to the STE24 homolog in yeast

DECLARATION

The data presented within this thesis is the result of my own work. Any data cited from the unpublished or published work of another person(s) has been duly acknowledged. This data has not been presented in any previous thesis presented for a higher degree.

Name: Date:

ACKNOWLEDGEMENTS

"*If people did not sometimes do silly things, nothing intelligent would ever get done.*"

Ludwig Wittgenstein, Vermischte Bemerkungen

Firstly, I would like to thank my supervisor Professor Chris Hutchison for giving me the opportunity to study a gene that functions in many aspects of cell biology. I am also grateful for the encouragement and the freedom he has afforded me, which I believe has allowed me to fully engage with my project to explore many hypotheses. From this, I have the foundations that I hope will allow me to develop into an independent researcher in the future.

In the Hutchison laboratory, I am grateful to Mrs. Pamela Ritchie for all her help with many aspects of laboratory life. Furthermore, I am truly indebted to former lab members Dr. Vanja Pekovic and Dr. Ewa Markiewicz, each of whom made huge contributions to the techniques I have acquired over the past years. In addition, they also provided me with ideas and suggestions that have helped further my research. I also wish to thank Dr. Fahad Alzoghaibi and Dr. Georgia Salpingidou for FACS and technical advice, respectively. I would also like to thank the members of my Thesis Committee, Arto Määttä, Tony O'Sullivan and Roy Quinlan who provided invaluable input and perspectives in a relaxed, encouraging atmosphere. I am extremely grateful to the following, who, for various reasons, have helped me during my research: Dr. Christine Richardson, Dr. Tim Hawkins, Dr. Jen Topping (all University of Durham) for help with microscopy; Kuniyoshi Iwabuchi (Kanazawa Medical University, Japan) for supplying the 53BP1 expression constructs; members of the Quinlan laboratory: Terry Gibbons and Frederique Tholozan for invaluable help with molecular biology and microscopy, respectively; Dr. Nick Hole for use of the irradiator; Roland Foisner (University of Vienna, Austria) for support and advice; Manfred Wehnert (Ernst-Moritz-Arndt University, Germany) for supplying R453W cells.

DEDICATION

To my Mum and Dad, Anne and Richard

And

Ali, for her love, advice, support, encouragement and, more importantly, putting up with weekend visits to the lab.

CHAPTER 1: INTRODUCTION

1.1 The nucleus: overview

The nucleus is the keystone of all eukaryotic cells and functioned as one of the first evolutionary steps towards multicellularity (Pennisi, 2004; Lopez-Garcia and Moreira, 2006). The nucleus is responsible for a multitude of processes, including DNA replication, RNA production and the bi-directional transport of macromolecules (Lamond and Earnshaw, 1998). The compartmentalisation of these processes provides a means by which to regulate these and other metabolic processes in the nucleus, a step which is a necessary requisite for the evolution of complex organisms (Pennisi, 2004). Structurally, the nucleus is constructed of a three-dimensional interphase chromatin structure that lies within an internal nucleoplasm, all of which is enveloped by a double membrane, which comprises the inner nuclear membrane (INM) and the outer nuclear membrane (ONM) (Figure 1.1) (Maidment and Ellis, 2002; Worman and Courvalin 2005). The INM provides a physical attachment point to segregate chromatin into highly specific and defined chromosomal territories (Kind and van Steensel, 2010). Moreover, whilst the INM contains a unique set of proteins, the ONM is contiguous with the rough endoplasmic reticulum (RER) and thus shares similar protein content (Burke and Stewart, 2006). This double membrane creates a perinuclear space that is an extension of the ER lumen (Burke and Stewart, 2006). The double membrane is punctuated by a multi-protein complex called the nuclear pore complex (NPC) that tightly controls transport between the nucleoplasm and cytoplasm (Gorlich and Kutay, 1999; Lim and Fahrenkrog, 2006). Underlying the inner nuclear membrane is a filamentous meshwork called the nuclear lamina, containing A- and B-type lamins and lamin-binding proteins (Hutchison and Worman, 2004; Broers et al., 2006).

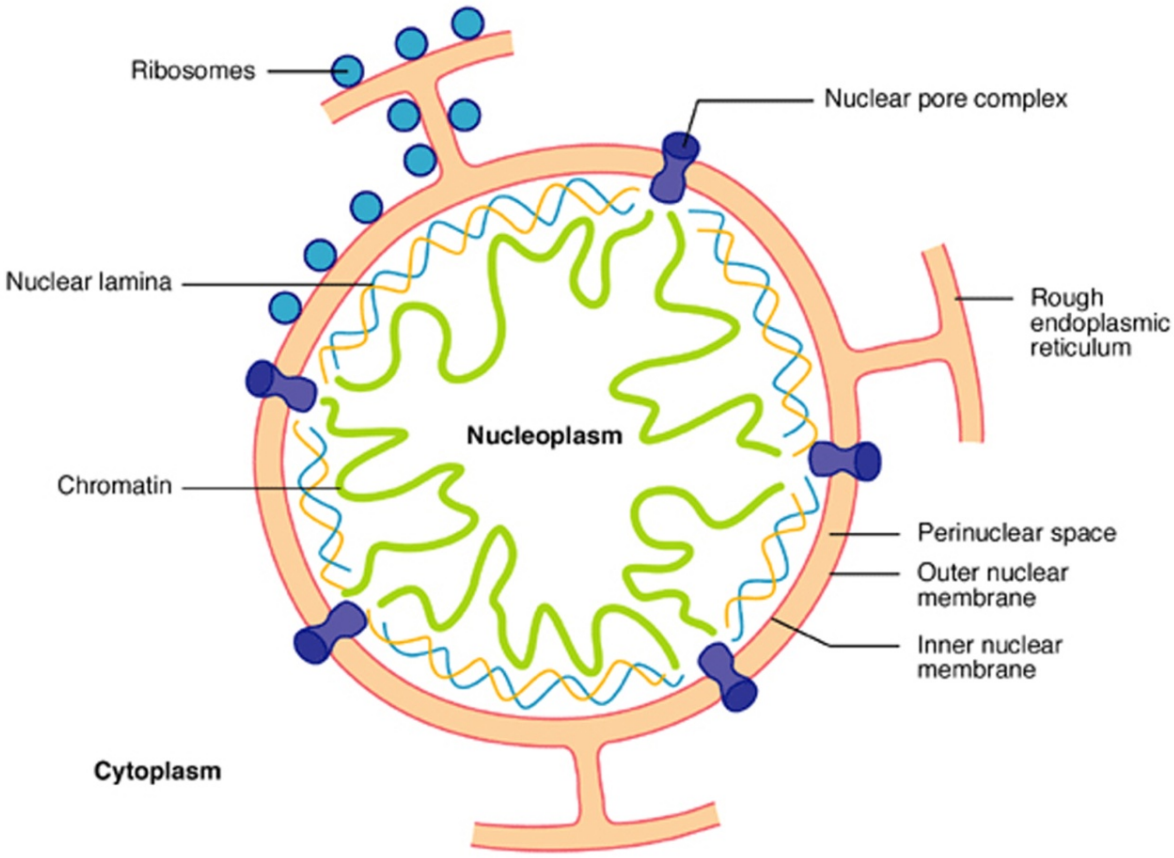

Figure 1.1. Overview of the structure of the nucleus. See text for details (Maidment and Ellis, 2002).

1.2 Structure, assembly and regulation of the nuclear lamins

1.2.1 Lamin genes

At least one lamin gene is found in all metazoans, with the exception of unicellular organisms (Cohen et al., 2001). Although no lamin genes have been identified in plants, electron microscopy of tobacco BY-2 cells has observed a highly organised filamentous protein structure underlining the INM that interconnects NPCs, suggesting that lamin-like proteins exist in plants (Fiserova et al., 2009; Fiserova and Goldberg, 2010; Graumann and Evans, 2011). Typically, invertebrates express only one lamin gene, which is a B-type lamin (Hutchison et al., 2001). One exception is *Drosophila melanogaster*, which expresses one B-

type lamin (Dm0) and one A-type lamin gene (lamin C) (Schulze et al., 2009). In contrast, vertebrates typically contain two B-type lamins genes and one A-type lamin genes (Hutchison et al., 2001). Again, one exception to this generality is *Xenopus*, which contains three B-type lamin genes (Melcer et al., 2007).

Seven different lamin polypeptides are encoded by three genes in humans (Hutchison and Worman, 2004). Firstly, the human *LMNA* gene on chromosome 1q21.2 is a 12 exon gene that encodes four A-type lamins, produced by alternative splicing: lamin A, lamin C, lamin AΔ10 and lamin C2 (Hutchison et al., 2001). The two major gene products are lamin A and C, whose protein sequences are identical for the first 566 amino acids but vary in their C-terminal, with lamin C containing five unique C-terminal amino acids and lamin A an additional 98 amino acids (Burke and Stewart, 2006). The lamin AΔ10 isoform lacks the amino acids encoded by exon 10, whilst lamin C2 is a male germline-specific isoform that is identical to lamin C except that its N-terminal contains a short non-helical segment arising from alternative splicing of mRNA initiated from a different start site (Furukawa et al., 1994; Alsheimer and Benavente, 1996; Machiels et al., 1996).

Two genes encode three separate B-type lamins. The *LMNB1* gene on chromosome 5q23.3–q31.1 encodes for lamin B1, whilst *LMNB2*, located on chromosome 19p13.3, encodes two alternatively spliced isoforms, lamin B2 and lamin B3 (Höger et al., 1990; Biamonti et al., 1992; Furukawa and Hotta, 1993; Lin and Worman, 1995; Wydner et al., 1996). Parenthetically, B-type lamins are the likely ancestral lamin, with A-type lamins arising as a result of a gene duplication of a B-type lamin gene during evolution and acquirement of an extra exon, which enables the last endoproteolytic cleavage step in the processing of prelamin A (see 1.2.5) (Goldberg et al., 2010).

1.2.2 Structure

The nuclear lamina was first identified by electron microscopy as a fibrous layer underlying the inner nuclear membrane (INM) and largely determines the overall structure of the nucleus during interphase (Fawcett, 1966; Burke and Stewart, 2002).The nuclear lamina consists of the nuclear lamins, which are classified as either A- or B-type depending on their sequence homology, structural features, biochemical properties, or their tissue expression specificity (Broers et al., 2006; Mattout et al., 2006). Lamins are type V intermediate filaments (IFs), having a typical tripartite domain structure, which includes an unstructured 'head' domain, an α-helical 'rod' domain and a globular 'tail' domain (Figure 1.2) (Hutchison and Worman, 2004). The α-helical rod domain is divided into four coiled-coil domains (1A, 1B, 2A, and 2B), separated by three flexible linker regions (L1, L12, L2), and characterised by the presence of heptad repeats within coil 1b (Hutchison and Worman, 2004). The nuclear targeting of lamins is facilitated by the presence of a NLS in the tail domain that interacts with importins and permits nuclear import (Broers et al., 2006). With the exception of lamin C, lamins are characterized by the presence of a CAAX motif at the very C-terminus, which is involved in the processing of the prepeptide to the propeptide (see 1.2.6) (Rusinol and Sinensky, 2006). Lamins also contain an S-type Ig-like fold between the rod domain and C-terminal, which is involved in various lamin-protein interactions as well as lamin-DNA interactions (Dhe-Paganon et al., 2002; Krimm et al., 2002).

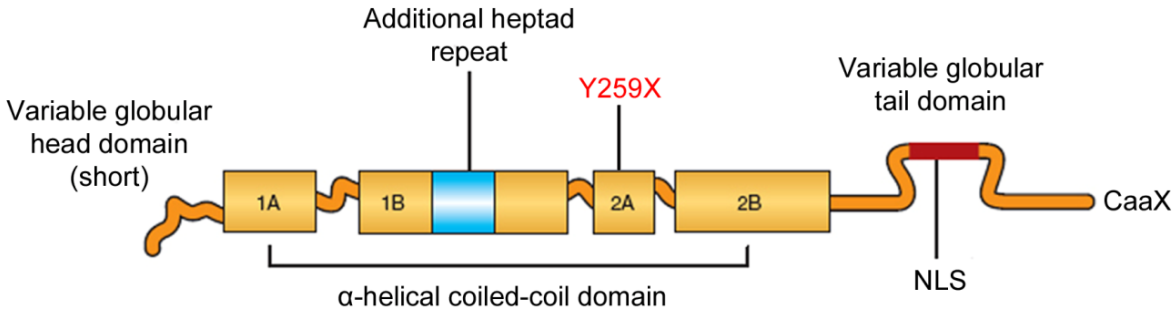

Figure 1.2. General structure of lamin polypeptides. See text for details, Y259X point mutation is shown (adapted from Hutchison and Worman, 2004).

1.2.3 Lamin assembly

The initial step in the assembly of nuclear lamins is the formation of lamin dimers (Stuurman et al., 1998). Lamins form obligate in-parallel in-register homodimers of ~50nm in length, which are formed from the interaction between two α-helical rod domains of each monomer. The homodimers then assemble longitudinally into polar head-to-tail tetrameric protofilaments, and these protofilaments then associate laterally in an anti-parallel half-staggered manner to form ~25nm beading filaments (Stuurman et al., 1998). These beading filaments are unstable *in vitro* and eventually form well-ordered paracrystalline arrays *in vitro*, which are not usually found *in vivo* (Herrmann and Aebi, 2004). Paracrystal formation suggests that *in vitro* lamin polymerization cannot fully recapitulate *in vivo* lamin polymerization, which therefore hints at other lamin-binding proteins being responsible for *in vivo* lamin assembly (Stuurman et al., 1998; Hutchison et al., 2001). Despite this, it was generally believed that lateral assembly of protofilaments produced 10nm lamin filament formation *in vivo*, and two sets of parallel 10nm filaments could then form at right angles to each other to produce an orthogonal network, with a repeat distance of ~50nm (Stuurman et al., 1998). However, this theory has recently been called into question (Goldberg et al., 2008). Using field emission scanning electron microscopy (feSEM), the authors showed that the lamina consists of only one 8–10 nm filament running parallel to another filament, rather than two sets at right angles. Moreover, the repeat distance was only ~15nm, not 50nm, as previously stated (Goldberg et al., 2008).

Although A- and B-type lamins interact *in vitro*, further evidence is needed to determine whether the complex nuclear lamina of mammalian somatic cells contains lamin heteropolymers or only homopolymers *in vivo* (Schirmer and Gerace, 2004). During mitosis, A- and B-type lamins exhibit different solubility properties. A-type lamins becoming solubilised, whilst B-type lamins remain membrane-bound, suggesting that lamin heterodimers may not form *in vivo*. In support of this, quantitative FRET (fluorescence resonance energy transfer) analysis concluded that lamins may exist as homopolymers with subsequent

interactions between both A- and B-type lamin homopolymers (Delbarre et al., 2006). Further to this, using high resolution microscopy it has been shown that A- and B-type lamins form separate filamentous networks within mammalian cells (Shimi et al., 2008). Despite the A- and B-type lamin networks being quite separate they do overlap and interact in places, which support the previous biochemical and FRET data outlined above (Shimi et al., 2008).

1.2.4 Developmental regulation of lamins

A- and B-type lamins are differentially regulated during development (Broers et al., 2006). At least one B-type lamin is expressed in all cell types throughout all developmental stages (Hutchison, 2002). Underlining the importance of B-type lamins in development, a mouse model with an insertional mutation in *Lmnb1* developed lung and bone defects causing death at birth, even though the mice continue to express lamin B2 (Vergnes et al., 2004). Furthermore, RNAi depletion of lamin B1 or lamin B2 in Hela cells demonstrated B-type lamins are essential for cell survival (Harborth et al., 2001). In contrast, A-type lamins are typically expressed in differentiated cells types and, in mice, lamins A and C are expressed between days 10-12 during embryogenesis, chiefly in the primordial muscle cells, suggesting that A-type lamins are not essential for development (Stewart and Burke, 1987, Rober et al., 1989). Moreover, embryonic stem cells (ESCs) do not express A-type lamins, further suggesting that A-type lamins have specific roles in differentiated tissues (Stewart and Burke 1987; Houliston et al., 1988; Röber et al., 1989; Constantinescu et al., 2006). As A-type lamin expression is preceded by differentiation, it has been suggested that A-type lamins are responsible for maintaining a differentiated state, rather than an active role in cell fate determination *per se* (Goldman et al., 2002). In keeping with this role, *Lmna*$^{-/-}$ mice exhibit no developmental defects but display severely retarded postnatal growth characterised by muscular dystrophy and cardiomyopathy (Sullivan et al., 1999). In humans, the presence of a homozygous Y259X mutation results in no functional lamin A/C protein, which caused death via respiratory failure after premature birth (Figure 1.2) (van Engelen et al., 2005).

1.2.5 Transcriptional regulation of lamins

A-type lamins are primarily regulated at the level of transcription, however, there is some evidence to suggest that they may be regulated at a post-transcriptional level (Lanoix et al., 1992; Alsheimer and Benavente 1996; Pugh et al., 1997). Various studies have defined several regulatory elements in the *LMNA* proximal promoter that are important in determining activity of the *LMNA* promoter. Firstly, there is a GC box that may bind Sp1/Sp3 transcription factors and an AP-1 motif that is able to bind the c-Jun and c-Fos transcription factors (Nakajima and Abe 1995; Tiwari et al., 1998; Muralikrishna et al., 2001). Furthermore, a GT-rich motif within the promoter region has the capacity to bind to both the Sp1/Sp3 transcription factors and the transcriptional coactivator CREB-binding protein (CBP) (Janaki Ramaiah and Parnaik, 2006). The *LMNA* promoter also contains a retinoic acid responsive element that promotes transcription upon retinoic acid treatment and also binds the transcription factors c-Jun and Sp1/Sp3 (Lebel et al., 1987; Okumura et al., 2000; Okumura et al., 2004). In addition to the promoter region, there are two regulatory regions within intron 1 of *LMNA*, footprinted region A (FPRA) and B (FPRB), which may bind hepatocyte nuclear factor-3β and the retinoic acid receptor β (RXRβ) transcription factors that have been suggested to control cell-type-specific transcription of *LMNA* (Arora et al., 2004). Interestingly, intron 1 of *LMNA* has a p53-binding site and is a transcriptional target of activated p53 in response to mitomycin C in HCT116 cells, a colon carcinoma cell line (Rahman-Roblick et al., 2007).

Recently, a novel study has shown that lamin B1 transcripts are targeted by the microRNA mir-23 (Lin and Fu, 2009). No study to date has addressed the role of microRNA control over *LMNA* transcripts. Indeed, possible miRNAs that target *LMNA* transcripts can be seen here:
http://refgene.com/search?q=4000&act=Search+GeneID%2C+Symbol+or+Acc%23

From this, one miRNA that targets *LMNA* transcripts is hsa-mir-30c-1, which is expressed in HL-60 leukaemia cells (Kasashima et al., 2004). In accordance, HL-60 cells are devoid of lamin A and C protein levels and have very low mRNA levels (due to spontaneously differentiating cells), therefore seemingly validating the targeting miRNA, hsa-mir-30c-1 (Paulin-Levasseur et al., 1988). Future studies into post-transcriptional regulation of lamin A/C transcripts will therefore be of interest, especially in cancers.

1.2.6 Processing of prelamin A

Lamins A, B1 and B2 are synthesised as precursor proteins that enter the nucleus via their NLS before extensive post-translational processing (Lehner et al., 1986; Lutz et al., 1992; Davies et al., 2009). The processing pathway occurs within the nucleus, rather than the cytoplasm, via a group of enzymes anchored within the INM (Barrowman et al., 2008). The processing pathway is initially dictated by a C-terminal CAAX motif (C = cysteine, A = any aliphatic amino acid, X = S, M, C, A, Q, L), which is present in all A- and B-type lamins except lamin C (Rusinol and Sinensky, 2006). Prelamin processing begins with the addition of a 15-carbon farnesyl lipid via a thioester linkage to the thiol group of the cysteine within the CAAX motif by a protein farnesyltransferase (Figure 1.3) (Davies et al., 2009). It is believed that farnesylation of the CAAX motif in lamins assists in their targeting to the nuclear envelope as evidence has shown that farnesylation increases the hydrophobicity of prelamin A and farnesyl-prelamin A binds avidly to membranes (Hennekes and Nigg, 1994; Silvius and l'Heureux, 1994). Indeed, inhibition of farnesylation with lovastatin caused nonfarnesylated prelamin A to accumulate in nucleoplasmic aggregates away from the nuclear envelope (Lutz et al., 1992). Once at the nuclear envelope, prelamins can be further processed and incorporated into the nuclear lamina (Holtz et al., 1989; Kitten and Nigg, 1991).

The second step, after farnesylation, is the removal of the –AAX from the CAAX motif by the zinc metalloproteinases Rce1 (Ras-converting enzyme 1) or Zmpste24 (Zinc metalloprotease related to the STE24 homolog in yeast) (Figure

1.3) (Bergo et al., 2002, Pendas et al., 2002; Corrigan et al., 2005). The newly exposed isoprenylcysteine is methylated by isoprenylcysteine carboxy methyltransferase (ICMT) (Figure 1.3) (Davies et al., 2009). Both these steps are dependent upon the preceding steps. Prelamin A is unique to the group of prelamins as it undergoes an additional endoproteolytic step that cleaves the last 15 amino acids, including the farnesylcysteine methyl ester, from the C-terminal to produce mature lamin A (Figure 1.3) (Davies et al., 2009). This step is carried out only by Zmpste24, which recognises the conserved RSYLLG sequence, producing mature lamin A which then integrates into the nuclear lamina (Corrigan et al., 2005).

The CAAX motif is conserved through vertebrate evolution, which suggests that the post-translational modifications to prelamin A have important functions. However, data from a variety of mouse models has called into question the relevance of the prelamin A processing pathway. Mice genetically engineered to express prelamin A only (no lamin C), mature lamin A only (no lamin C) and lamin C only (no lamin A) all appear phenotypically normal (Fong et al., 2006; Coffinier et al., 2010; Davies et al., 2010). At the cellular level, MEFs expressing only mature lamin A displayed a trivial increase in dysmorphic nuclei even though more lamin A was localised in the nucleoplasm (Coffinier et al., 2010). Importantly, the results suggest that by-passing the prelamin A processing pathway is compatible with survival (Coffinier et al., 2010). Moreover, it suggests that prelamin A processing is dispensable for lamin A incorporation into the nuclear lamina, a finding that underlines a prior study that has shown that microinjected mature lamin A incorporates into the nuclear lamina (Pugh et al., 1997). MEFs from mice that express lamin C only were also normal at the cellular level, with lamin C localised to the nuclear envelope independently of lamin A, a finding that is in contrast to previous findings (Pugh et al., 1997; Vaughan et al., 2001; Fong et al., 2006). Thus, it appears that lamins A or C are largely dispensable, together with the post-translational pathway that produces lamin A, at least in mice. One possibility is that both proteins may have redundant functions that may subsidise for loss of the other. Paradoxically, although by-

passing the prelamin A processing pathway appears to be compatbilte with survival, mutations in enzymes responsible for prelamin A processing give rise to a range of diseases in mice, including cardiomyopathy (in mice that express nonfarnesylated prelamin A) and premature aging syndromes (in mice null for *Zmpste24* or in mice expressing progerin or nonfarnesylated progerin) (see 1.8). In cells with *ZMPSTE24* deficiency, prelamin A undergoes the first three processing steps, but cannot undergo the last proteolytic cleavage step, causing prelamin A to be permanently carboxymethylated and farnesylated (Figure 1.3). In HGPS, prelamin A is translated with an internal 50 amino acid deletion that includes the last endoproteolytic cleavage site. Therefore, despite having a functional Zmpste24 protein, prelamin A is both carboxymethylated and farnesylated and, due to the deletion, slightly smaller in size than prelamin A found in cells with *ZMPSTE24* deficiency (Figure 1.3). The alterations to the prelamin A processing pathway shown here cause devastating premature aging syndromes, underlining that although by-passing the pathway altogether is compatible with survival, when the pathway is engaged any mutations within components of the pathway can have deleterious consequences for the organism (see 1.8). Future work may reveal distinct functions of the prelamin A processing pathway to help explain its evolutionary conservation.

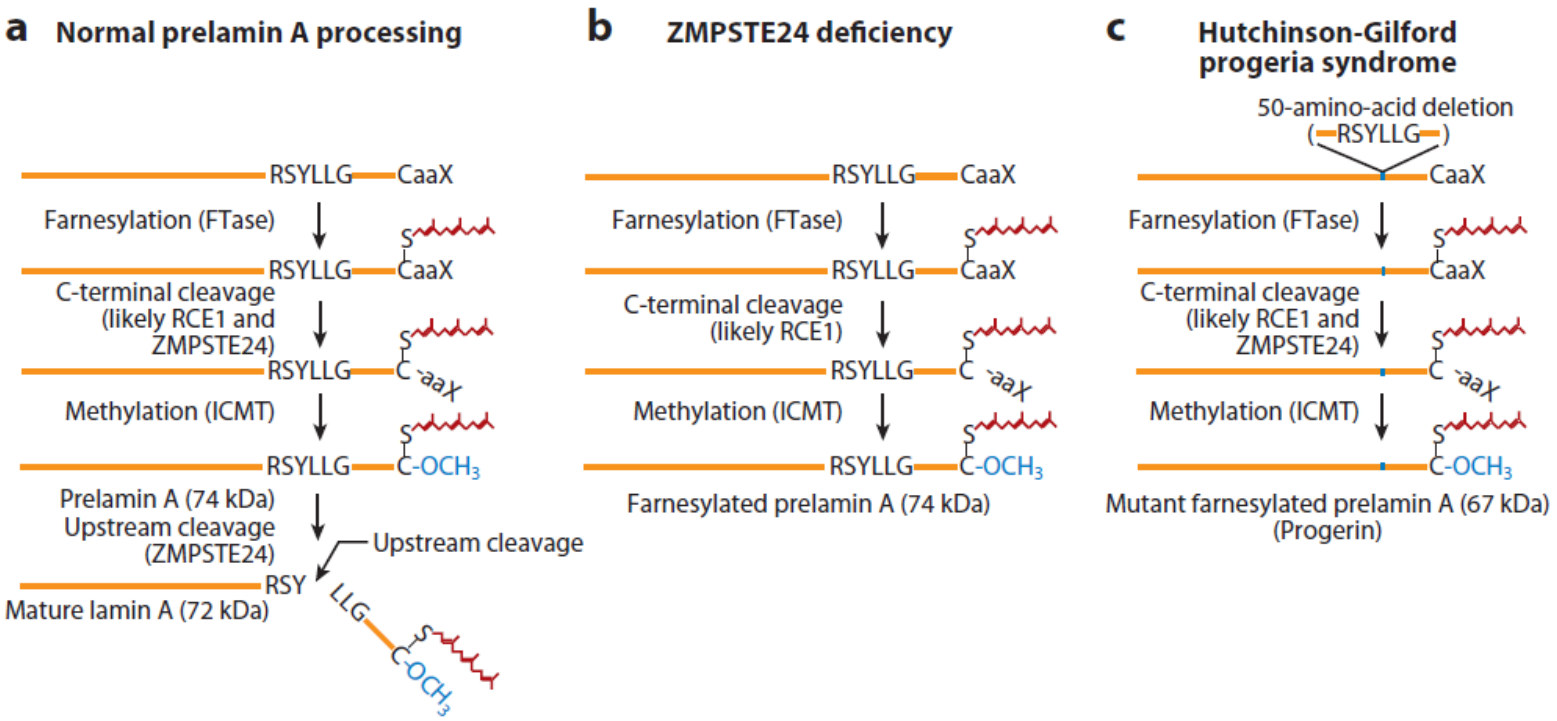

Figure 1.3. Processing pathway of wild type prelamin A and in disease. (**a**) Wild type prelamin A undergoes a series of post-translational processing steps before mature lamin A is formed. (**b**) Prelamin A found in Zmpste24-null cells is permanently farnesylated and carboxymethylated. (**c**) HGPS cells contain an internal deletion of 50 amino acids that removes the second endoproteolytic cleavage site, resulting in prelamin A that is both farnesylated and carboxymethylated, with the mutant product termed progerin. (Davies et al., 2009)

1.3 Lamina function

Far from merely being a structural component of the nucleus, lamins have a diverse range of cellular roles that influence a vast array of nuclear functions. Whilst it is beyond this thesis to describe all their functions in great depth, I will briefly cover the most relevant, providing the most salient points.

1.3.1 Tensegrity element

Whilst B-type lamins are ubiquitously expressed, A-type lamins are expressed only when ESCs differentiate, which is correlated with reduced nuclear deformability, suggesting that, analogous to intermediate filaments, A-type lamins have a structural role within the cell (Pajerowski et al., 2007). A-type lamins therefore confer structural stability to the nucleus and protect chromatin, which has led them to be described as a 'tensegrity element', which may be defined as "...a lightweight load-bearing structure that can re-adopt its initial shape after deformation..." (Hutchison, 2002; Hutchison and Worman, 2004). Underlining this, *Lmna*$^{-/-}$ MEFs exhibit impaired mechanical properties leading to reduced viability under mechanical stress, as well as de-regulated expression of genes associated with mechanical stress (Lammerding et al., 2004; Houben et al., 2007). Additionally, ectopic expression of lamin A in *Xenopus* oocytes, which normally only contain B-type lamins, increases the stiffness of the nuclei, reaffirming the mechanical properties A-type lamins exert on nuclei (Schape et al., 2009). Lastly, it has long been evidenced that a multitude of mutations in *LMNA* give rise to dysmorphic nuclei, again suggesting that A-type lamins are involved in the structural integrity of nuclei (Broers et al., 2006).

1.3.2 Component of the nucleo-cytoskeletal structural framework

A-type lamins are a component of a physical link between the nucleus and the cytoskeleton (Burke and Roux, 2009). This nucleo-cytoskeletal link is called the LINC complex and comprises SUN proteins, which reside at the INM, and nesprins, which primarily reside in the ONM (Burke and Roux, 2009). SUN1 and

SUN2 proteins and nesprins-1,-2 and -3α interact via their KASH domains in the perinuclear space (Hodzic et al., 2004; Worman and Gundersen, 2006; Burke and Roux, 2009). Nesprins interact with both the intermediate filament and the microfilament cytoskeletons via direct actin binding and plectin (Starr and Han, 2003; Tzur et al. 2006). Nesprin-1α is smaller in size than other nesprins so is localised to the INM where it interacts with lamins A/C and emerin (Broers et al., 2006; Wilhelmsen et al., 2006). Similarly, SUN1 and SUN2 may also interact with A-type lamins at the INM, but their retention at the INM is not dependent on A-type lamins (Crisp et al., 2006). Mutations that cause defects to components of the LINC complex can lead to impaired cell migration, nuclear positioning and decreased mechanical stress resistance (Houben et al., 2007; Ji et al., 2007; Lee et al., 2007; Houben et al., 2009)

1.3.3 Chromatin scaffold

It its simplest form, A-type lamins may function as a chromatin scaffold within the nucleus due to their ability to interact directly with polynucleosomes particles, chromatin, core histones and DNA via the lamin A/C Ig-like domain (Yuan et al., 1991; Luderus et al., 1992; Glass et al., 1993; Luderus et al., 1994; Taniura et al., 1995). Functionally, this scaffold role would also allow multiprotein complexes to interact with and regulate chromatin (Stierle et al., 2003). A-type lamins may also interact with chromatin indirectly via binding to barrier-to-autointegration factor (BAF), which itself associates with chromatin-interacting LEM-domain containing proteins (Andres and Gonzalez, 2009).

The spatiotemporal modulation of gene expression is essential for the life cycle of a cell. Therefore, to accomplish specific gene expression patterns, chromatin within eukaryotes is spatially arranged as either heterochromatin or euchromatin (Hubner and Spector, 2010). Whilst euchromatin is correlated with actively transcribed genes, densely packaged heterochromatin has been correlated with gene silencing, with cytological analyses of heterochromatin localisation revealing that it resides close to the INM (Akhtar and Gasser, 2007). Thus, above a simple

role for A-type lamins as a mere chromatin scaffold, it has been proposed that the A-type lamins and the nuclear lamina may segregate chromatin into active and inactive domains via interactions that anchor chromatin at the nuclear lamina (Sullivan et al., 1999; Goldman et al., 2004; Kind and van Steensel, 2010). Indeed, *in situ* expression studies and microarray analyses have shown that disruption to A- and B-type lamins causes deregulated gene expression, as well as expression of the lamin A mutant progerin (Vergnes et al., 2004; Frock et al., 2006; Malhas et al., 2007; Scaffidi and Misteli, 2008; Tang et al., 2008; Malhas et al., 2009). Furthermore, the use of the DamID technology with genome-wide sequencing has defined regions of the genome that are in contact with the nuclear lamina (Pickersgil et al., 2006; Guelen et al., 2008). From these studies, there are >1300 of these lamina-associated domains (LADs) in human fibroblasts, which range from between 0.5 to 10 Mb in size and contain genes that are expressed at relatively low levels, although there a small number of genes that are the exception and are still active in these domains (Guelen et al., 2008). LADs have been shown to have exquisitely sharp borders that are marked by sequences that promote binding of insulator proteins such as CTCF (Guelen et al., 2008). Interestingly, depletion of the Drosophila B-type lamin, Dm0, leads to the translocation of repressed gene clusters from the nuclear exterior to the nuclear interior where they become transcriptionally active (Shevelyov et al., 2009). In parallel to these studies, lamin A promotes transcriptional repression in both yeast and mammalian cells when it is tethered to specific promoters (Lee et al., 2009). Furthermore, the use of artificially tethered reporters has shown that if genes are directed towards the nuclear periphery then they are generally repressed, although the extent to which genes are silenced is thought to be dependent on both the local chromatin context and the regulatory sequences (Finlan et al., 2008; Kumaran and Spector, 2008; Reddy et al., 2008).

Lastly, lamins may also influence the positioning of chromosome territories (Figure 1.4) (Bridger et al., 2007). Chromosomes occupy distinct territories in interphase nuclei, although the positioning of territories is not static but rather a highly dynamic process whereby whole individual chromosomes or single genes

undergo rearrangements depending on the gene expression demands of the cell (Hubner and Spector, 2010). The gene-poor chromosome 18, which is normally found at the nuclear periphery, is localised within the nuclear interior in MEFs from *Lmnb1*$^{-/-}$ mice (Malhas et al., 2007). Similarly, in cells from patients with mutations in A-type lamins, chromosomes 13 and 18 were also relocalised towards the nuclear interior, suggesting that both A- and B-types can influence positioning of whole chromosomes (Meaburn et al., 2007; Mewborn et al., 2010). Furthermore, the nuclear periphery position of chromosome 4 is lost in human cells null for lamin A/C, further supporting a role for lamins in chromosome positioning (Masny et al., 2004).

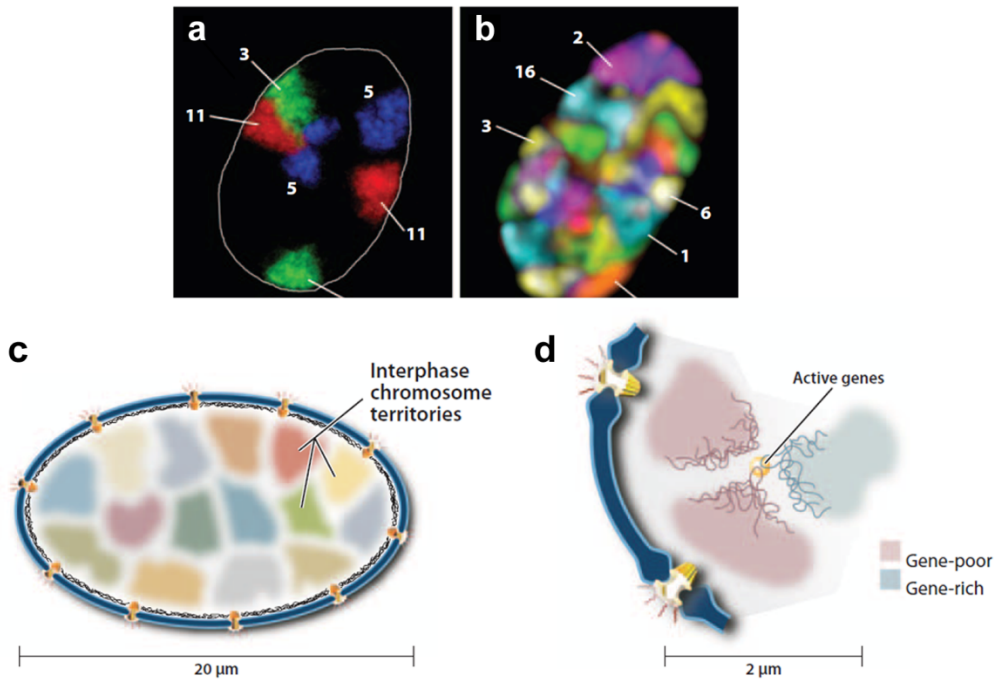

Figure 1.4. Chromosome territories in mammalian cells. (**a-b**) Images of three (a) and twenty-three (b) chromosomes were obtained after by 3D-FISH and chromosome painting. (**c**) Cartoon representation of the chromosome territories in an interphase nucleus. (**d**) Gene-poor regions are localized towards the nuclear periphery, whilst gene-rich regions are localized towards the interior. (Adapted from Hubner and Spector, 2010)

1.3.4 Transcription and proliferation

A variety of evidence suggests that A-type lamins have an active role in gene transcription, both directly and indirectly (Heessen and Fornerod, 2007). Firstly, expression of a dominant negative lamin A mutant in CHO or *Xenopus* nuclei inhibits the activity of RNA pol II (Spann et al., 2002). Furthermore, RNAi depletion of lamin B1 or lamin A/C overexpression in Hela cells caused inhibition of RNA pol II transcription (Kumaran and Spector, 2008; Shimi et al., 2008; Tang et al., 2008).

Data from a number of groups has shown that lamins interact with several transcription factors, which therefore implicates lamins in a number of cell signaling pathways that influence gene transcription (Heessen and Fornerod, 2007). Oct-1 is a transcription factor that interacts with lamin B1 and is sequestered at the nuclear envelope away from Oct-1 target genes (Imai et al., 1997). However, its dissociation from the nuclear lamina is associated with the up-regulation of pro-aging genes (Imai et al., 1997). The interaction between A-type lamins and transcription factors have been far more extensively studied (Andres and Gonzalez, 2009). The most notable is the interaction between lamin A/C and its nucleoplasmic binding partner, LAP2α, and the tumour suppressor pRb (Dechat et al., 2000; Markiewicz et al., 2002). This complex anchors hypophosphorylated pRb within the nucleus and therefore implicates A-type lamins in the pRb-E2F pathway and control of the G_1/S-phase transition. Indeed, loss of either lamin A/C or LAP2α in MEFs causes increased cellular proliferation due to deregulated pRb levels and/or phosphorylation status of pRb, which in turn promotes E2F-dependent gene transcription necessary for S-phase entry (Johnson et al., 2004; Naetar et al., 2007; Naetar and Foisner, 2009).

Lamin A/C also interact directly with TonEBP, SREBP1, Mel18, MOK2 and c-Fos, the latter being a member of the AP-1 family of transcription factors (Dreuillet et al., 2002; Lloyd et al., 2002; Zhong et al., 2005; Ivorra et al., 2006; Favale et al., 2007; Dreuillet et al., 2008; Harper et al., 2009). c-Fos has a DNA-binding domain

and a heterodimerisation domain, that allows it interact with other AP-1 family members (e.g. c-Jun) (Eferl and Wagner, 2003). Lamin A/C sequesters c-Fos at the nuclear envelope in serum-starved cells, thereby preventing AP-1 mediated gene transcription (Ivorra et al., 2006; Gonzalez et al., 2008). However, upon mitogenic stimulation, ERK1/2 interacts with lamins A/C and phosphorylates c-Fos, which releases it from the nuclear envelope, allowing it to promote transcription of target genes (Ivorra et al., 2006; Gonzalez et al., 2008). More recently, it was shown that upon mitogen stimulation, ERK1/2 displaces pRb from lamin A, facilitating its phosphorylation and inactivation, promoting G_1/S-phase transition (Rodriguez et al., 2009).

A-type lamins have been implicated in the regulation of transcription indirectly, via interactions with numerous lamin-binding proteins that themselves influence transcription. For example, firstly, the INM protein emerin is an A-type lamin binding protein that interacts with β-catenin via its APC-like domain (Markiewicz et al., 2006). β-catenin is a transcriptional cofactor of TCF/LEF and downstream effector of the canonical Wnt signaling pathway, which has roles in development and maintenance of stem cell niches (Clevers, 2006). Emerin acts so as to restrict the nuclear accumulation of β-catenin, thereby preventing its transcriptional activity (Markiewicz et al., 2006). In human cells null for emerin, from a patient with X-linked Emery Dreifuss muscular dystrophy, β-catenin accumulates in the nucleus, promoting cellular proliferation (Markiewicz et al., 2006).

Secondly, A-type lamins interact with INM proteins that contain a LEM (LAP2, Emerin, MAN1) domain, a 42 amino acid motif located in the nucleoplasm-facing N-terminus of these INM proteins (Broers et al., 2006). These LEM-domain proteins interact with a variety of transcriptional regulators, which therefore indirectly implicates A-type lamins in transcriptional control: the chromatin-interacting protein barrier-to-autointegration factor (BAF); germ-cell less (GCL), a transcription factor that binds to the DP3 subunit of E2F-DP heterodimeric transcription factors thus blocking E2F-DP-dependent gene expression in a pRb-independent manner; the death promoting transcriptional repressor Btf; the

transcriptional regulator Lmo7; the splicing factor YT521-B (Bengtsson and Wilson, 2004; Mansharamani and Wilson, 2005; Andres and Gonzalez, 2009).

1.3.5 DNA replication

The role of nuclear lamins in DNA replication has long been suggested, although the exact nature of this role is somewhat disputed (Broers et al., 2006). Early evidence came from studies using cell-free extracts from *Xenopus* eggs, in which deletion mutants of *Xenopus* lamin B3 or human lamin A or immunodepletion of *Xenopus* lamin B3 prevented lamina assembly and subsequently inhibited DNA replication (Ellis et al., 1997; Spann et al., 1997). The conclusion of both studies was that disrupting the nuclear lamina inhibited DNA replication. However, the temporal role of lamins in DNA replication is still unclear as findings from further studies showed that preventing lamina assembly inhibits the initiation of DNA replication, whilst the disruption of the lamina in nuclei that have already begun DNA replication does not affect further DNA synthesis (Ellis et al., 1997; Izumi et al., 2000). Furthermore, the nucleoplasmic lamin aggregates did not interfere with preassembled replication complexes (Izumi et al., 2000). There is therefore some inconsistency into the exact role of lamins in DNA replication. To complicate matters further, it has been reported that lamin B1 colocalises with sites of DNA replication foci during mid to late S-phase in mouse 3T3 cells (Moir et al., 1994). In contrast to this, lamin A/C has been shown to colocalise with sites of early replication in human fibroblasts, suggesting that lamin A/C has an organising role in early DNA replication sites, which also notably contained the pocket proteins pRb and p130 (Kennedy et al., 2000). More recently, it has been shown that PCNA interacts with the Ig-like fold in the C-terminus of A- and B-type lamins (Shumaker et al., 2008).

1.3.6 Epigenetics

In order to gain insights into the mechanistic basis of HGPS (see 1.5.2), research has found that cells from these patients exhibit considerable epigenetic changes (Scaffidi and Misteli, 2006; Shumaker et al., 2006; Liu et al., 2011). Firstly, HGPS

cells have gross loss of peripheral heterochromatin, underlining previous suggestions that A-type lamins act as a chromatin scaffold (Shumaker et al., 2006). Furthermore, *Lmna*$^{-/-}$ MEFs also display loss of some peripheral heterochromatin (Sillivan et al., 1999; Nikolova et al., 2004). Secondly, a variety of epigenetic histone marks are altered in HGPS cells, including reduced levels of trimethylated H3K9, reduced levels of trimethylated H3K27 and increased levels of trimethylated H4K20 (Scaffidi and Misteli, 2006; Shumaker et al., 2006). Mechanistically, these epigenetic alterations in HGPS may be mediated by chromatin remodelling proteins, such as the NuRD complex, components of which are reduced both in HGPS cells and in cells from old individuals (Pegoraro et al., 2009). Additionally, ING proteins interact with histones as well as histone deacetylases (HDACs) and histone acetyltransferases (HATs) to alter chromatin structure. It was recently shown that ING1 is a lamin A binding protein and exhibits reduced levels in HGPS cells (Han et al., 2008). Together, these studies suggest that A-type lamins influence epigenetic changes to chromatin indirectly via interactions with various chromatin remodelling proteins.

The functional relevance of these epigenetic alterations to the pathology of HGPS has yet to be fully understood. However, recent data from another prelamin A processing mutant may help understand how epigenetic changes are associated with premature aging. It was shown that *Zmpste24*$^{-/-}$ MEFs display a grossly altered epigenetic landscape, with hypermethylated rRNA and hypoacteylated histones HB and H4, which was correlated with altered gene expression profiles that affect cellular proliferation and metabolic processes that are known to be impaired in *Zmpste24*$^{-/-}$ MEFs (Varela et al., 2005; Osorio et al., 2010). Moreover, these changes occur naturally during normal aging, suggesting some mechanistic links between premature aging and the normal aging process.

1.3.7 DNA damage response

DNA repair was first explored in Hutchinson-Gilford Progeria Syndrome (HGPS) some 38 years ago, before it was known that the disease was caused by a

mutation in *LMNA* (Epstein et al., 1973). This study found that HGPS cells exhibited a failure to rejoin DNA ends in response to DNA damage induced by IR. Surprisingly, this finding was not followed up for some time. Recently, the link between A-type lamins and the DDR was explored using *Zmpste24*$^{-/-}$ MEFs and HGPS patient cells (Liu et al., 2005; Varela et al., 2005). In both these cells prelamin A exists permanently in a carboxymethylated and farnesylated form, which is correlated with gross changes in nuclear architecture (Davies et al., 2009). In response to a range of genotoxic stresses (IR, UV, camptothecin mitomycin C and etoposide), *Zmpste24*$^{-/-}$ MEFs showed reduced survival when assessed by colony-forming assay, suggesting that prelamin A effects numerous repair pathways (Liu et al., 2005). Both *Zmpste24*$^{-/-}$ MEFs and HGPS cells exhibit increased levels of endogenous DNA damage as assessed by increased levels of γ-H2AX (Liu et al., 2005, Varela et al., 2005; Scaffidi and Misteli, 2006). Furthermore, the recruitment of DNA repair factor 53BP1, a component of the NHEJ pathway, was delayed by ~ 2 hours in both *Zmpste24*$^{-/-}$ MEFs and HGPS cells in response to IR, suggesting that the presence of unprocessed prelamin A inhibits the upstream signaling events necessary for the recruitment of 53BP1 (Liu et al., 2005). Additionally, 53BP1 complexes take longer to dissociate in *Zmpste24*-null MEFs and HGPS cells, suggesting impaired DNA repair in these cells. Transient overexpression of wild type Zmpste24 in *Zmpste24*$^{-/-}$ MEFs reversed these effects, drawing a direct link to prelamin A as being the primary cause (Liu et al., 2005). The impaired recruitment of 53BP1 in GFP-LAΔ50 transfected Hela cells in response to cisplatin treatment was also confirmed in a separate study (Manju et al., 2006). In parallel to this, it was also observed that the number of Rad51 foci, a marker of homologous recombination, was reduced in response to DNA damage in both *Zmpste24*$^{-/-}$ MEFs and HGPS cells (Liu et al., 2005). The DDR apical kinases, ATM and ATR, were both activated in HGPS and restrictive dermopathy (RD) cells (human fibroblasts harbouring a homozygous mutation in Zmpste24) as well as their downstream effector kinases, Chk1 and Chk2 (Liu et al., 2006).

The DNA repair defects observed in RD and HGPS cells may be partly attributable to the incorrect localisation of the NER pathway protein XPA at progerin-induced DSBs (Liu et al., 2007). Furthermore, the MRN complex component Rad50 could not be correctly localised to endogenous DSBs in HGPS and RD cells, underlining that progerin-induced XPA localisation to DSBs inhibits correct DSB recognition (Liu et al., 2007). In response to camptothecin XPA did not localise to DNA lesions, thus suggesting that the incorrect localisation of XPA is specific to DSBs generated by progerin. Together, these studies indicate that the production of mutant lamin A activates DNA damage response pathways caused by the production of endogenous DNA damage.

Recently, a study has shown that *Lmna*$^{-/-}$ MEFs exhibit reduced ability to process dysfunctional telomeres, which has been correlated with the loss of 53BP1 protein levels by proteasomal degradation in these cells (Gonzalez-Suarez et al., 2009). 53BP1 is a mediator protein of the DDR, involved directly in DNA repair and signalling (Fitzgerald et al., 2009). Therefore, as a modulator of 53BP1 levels, A-type lamins have been implicated in the DDR (Gonzalez-Suarez et al., 2009).

1.3.8 Mitosis

Mammalian cells employ an ‘open’ method of mitosis, that is, the nuclear envelope must be disassembled and then reassembled during mitosis. As mentioned briefly above, A- and B-type lamins exhibit different properties during this disassembly/reassembly process (Cohen et al., 2001). The nuclear envelope is first disassembled during late prophase via phosphorylation, and hence depolymerisation, of lamins by cdk1 and protein kinase C (PKC) in combination with the physical action of microtubules pulling the nuclear envelope apart (Broers et al., 2006). Whereas A-type lamins are depolymerised and dissociate from the nuclear lamina during early prophase, B-type lamins dissociate in late prophase, which is when full nuclear envelope breakdown occurs (Broers et al., 2006; Dechat et al., 2010). After nuclear envelope breakdown, A-type lamins become

solubilised within the cytoplasm whereas the majority of B-type lamins are insoluble and remain nuclear membrane-bound, which disperses into the ER.

Lamins are dephosphorylated by protein phosphatase 1a during the telophase-G1 transition, which allows their reassembly into the nuclear lamina (Thompson et al., 1997; Hutchison et al., 2001). Nuclear envelope reassembly has been shown to exhibit a spatiotemporal hierarchy of protein assembly around the chromosome surfaces (Broers and Ramaekers, 2004). Firstly, LAP2α and BAF assemble at the ends of chromosomes, followed by LBR, emerin and LAP2β (Broers et al., 2006). Next, B-type lamins polymerise and associate with chromosomes during mid-to-late telophase via a membrane-bound anchor, most likely LBR and LAP2β, which interacts with the B-type lamin rod domain (Hutchison, 2002). However, the exact timing of when B-type lamins reassemble into a nuclear membrane structure has been disputed using various cell models (Broers et al., 1999; Moir et al., 2000; Lopez-Soler et al., 2001; Broers et al., 2006). In contrast to B-type lamins, the majority of A-type lamin assembly occurs during late telophase once the nuclear envelope and NPCs are assembled (Dyer et al., 1999; Broers et al., 2006). A small fraction of A-type lamins has been shown to associate with chromosomes earlier in Hela cells than in mouse cells, colocalising with emerin in the central core region of chromosomes (Dechat et al., 2004; Dechat et al., 2007).

1.4 Lamina-Associated Proteins (LAPs)

The lamina-associated proteins (LAPs) are a diverse group of LEM-domain containing INM proteins that were originally characterised by their resistance to biochemical extraction (Senior and Gerace, 1988; Foisner and Gerace, 1993; Gerace and Foisner, 1994). The LAP1 family is encoded for by the *LAP1* gene and produces three splice isoforms, A, B and C (Foisner and Gerace, 1993). LAP1 isoforms are type II INM proteins that are developmentally regulated and interact with both A- and B-type lamins (Martin et al., 1995; Maison et al., 1997). The LAP2 family of proteins is the best characterised of the LAPs (Broers et al., 2006). There are six isoforms of the alternatively spliced *LAP2* gene, α, β, γ, δ, ε, and ζ (Dechat et al., 2000b). Four of these, LAP2β, γ, δ and ε, are type II INM proteins that contain N-terminal LEM domains and a single transmembrane (TM) domain (Figure 1.5). Two LAP2 proteins, LAP2α and ζ, do not contain TM domains and are thus nucleoplasmic (Figure 1.5). Whilst LAP2ζ shares the first 219 N-terminal amino acids of LAP2β, γ, δ and ε, LAP2α contains a unique large C-terminal domain (Figure 1.5) (Dechat et al., 2000b).

The LAP2 proteins that are targeted to the INM, LAP2β, γ, δ and ε, are expressed throughout development, are essential for cellular survival (for LAP2β) and primarily bind B-type lamins (Furukawa et al., 1995; Furukawa et al., 1998; Lang et al., 1999; Dechat et al., 2000b; Harborth et al., 2001). However, it has also been shown that *Xenopus* XLAP2β is able to interact *in vitro* with both A- and B-type lamins, although this has yet to be shown for human LAP2β (Lang and Krohne, 2003). Functionally, LAP2β has roles in nuclear reassembly and interacts directly with DNA via its LEM-like domain in its N-terminal and indirectly with DNA via its LEM domain interaction with BAF (Ulbert et al., 2006; Margalit et al., 2007). Moreover, LAP2β interacts with chromatin protein HA95 via its C-terminal region (Martins et al., 2003; Ulbert et al., 2006). These studies have led to the suggestion that LAP2β may regulate higher order chromatin structure. Indeed, it has been suggested that LAP2β may repress transcription via interactions with the germ cell less (GCL), a transcriptional repressor, and histone deacetylase (HDAC),

which is known to silence gene transcription (Sadoni et al., 1999; Nill et al., 2001; Zink et al., 2004; Somech et al., 2005). Another LAP2 isoform, LAP2ζ, acts so as to inhibit LAP2β-mediated transcriptional repression by competition for BAF (Shaklai et al., 2008). It will be of interest to determine the inter-relationships between the various LAP2 isoforms and how they regulate one another functions.

The molecular function of the LAP2 isoform, LAP2α, also suggests that the LAP2 proteins are involved in higher order chromatin structure during cell cycle-dependent nuclear structure dynamics and transcriptional regulation (Vlcek and Foisner, 2007). Firstly, several lines of evidence suggest that LAP2α regulates chromatin structure. LAP2α is localised to the nucleoplasm during interphase, where it preferentially binds A-type lamins both *in vitro* and *in vivo* (Dechat et al., 2000a; Markiewicz et al., 2002). During mitosis, LAP2α localises to telomeric chromosome regions in a phosphorylation dependent manner along with LAP2β, BAF and emerin (Vlcek and Foisner, 2007). LAP2α associates with chromosomes early during nuclear envelope reassembly, before LAP2β-bound membranes and the bulk of lamins have assembled around chromosomes (Vlcek et al., 1999; Vlcek et al., 2001; Gajewski et al., 2004). LAP2α contains both LEM and LEM-like domains that allows interaction with DNA both indirectly (via BAF) and directly, respectively (Dechat et al., 2000b). LAP2α and BAF are highly mobile within the nucleoplasm during interphase, as assessed by FRAP, suggesting that LAP2α-lamin A/C-BAF interactions may be involved in the dynamic organisation of chromatin (Vlcek and Foisner, 2007).

The most compelling evidence for a role of LAP2α in transcriptional regulation is based on its interaction with the tumour suppressor, pRb (see 1.6.4) (Markiewicz et al., 2002). LAP2α-lamin A/C complexes tether hypophosphorylated pRb within the nucleoplasm (Markiewicz et al., 2002; Pekovic et al., 2007). Therefore, it is likely that LAP2α-lamin A/C complexes govern the G_1/S-phase transition by controlling pRb localisation and possibly phosphorylation status. Active pRb blocks E2F-dependent gene transcription via a variety of methods including the recruitment of the SWI/SNF chromatin remodelling complex, polycomb group

proteins, histone deacetylases as well as histone and DNA methyltransferases (Stevaux and Dyson, 2002; Frolov and Dyson, 2004; Korenjak and Brehm, 2005; Galderisi et al., 2006). pRb is inactivated by the sequential phosphorylation by cyclin-cdk complexes during G1-phase (Korenjak and Brehm, 2005). The LAP2α C-terminal domain interacts with the pocket C domain of pRb, whilst ChIP analyses have shown LAP2α to be present at E2F-dependent gene promoters, suggesting that LAP2α-lamin A/C complexes may physically repress E2F-dependent transcription by interaction with pRb (Dorner et al., 2006).

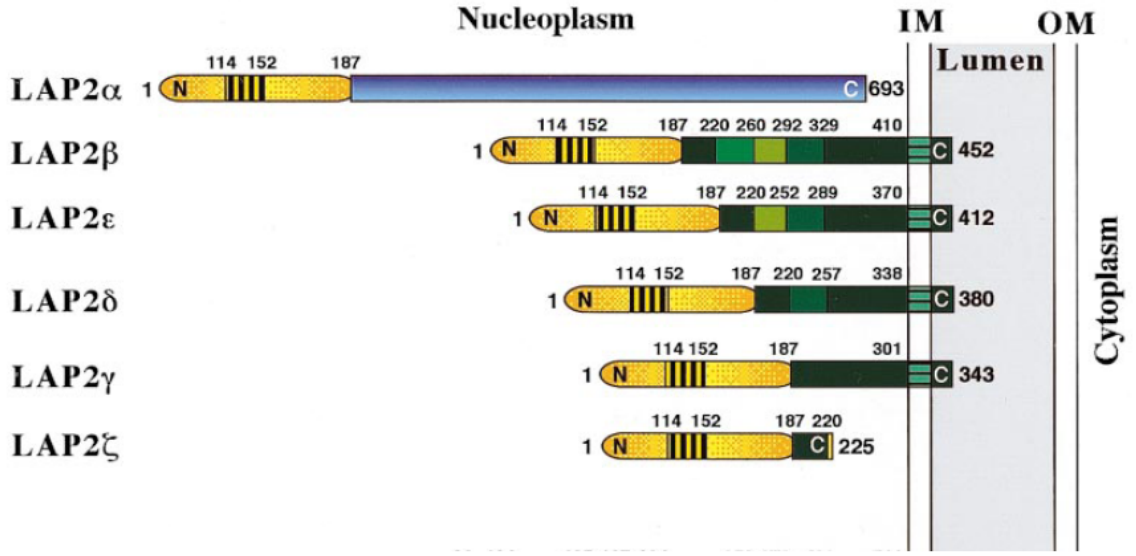

Figure 1.5. Domain structure of LAP2 isoforms. Of the six alternatively spliced isoforms of LAP2 in mammalian cells, LAP2β,γ,δ and ε isoforms display sequence similarity and differ via small insertions in the nucleoplasmic domain (shaded green boxes) and contain TM domains which span the INM. LAP2α has a common N-terminal (yellow), which contains the conserved LEM domain (hatched box), and a unique C-terminal (blue) without a TM domain. (Dechat et al., 2000)

1.5 Envelopathies

The importance of the nuclear envelope is perhaps best exemplified by its implication in the pathogenesis of a variety of diseases. Mutations within genes that encode nuclear envelope proteins are termed envelopathies (Burke and Stewart, 2006). Whilst I will not go into great detail here, a thorough review of these diseases is provided by Broers et al., 2006 and Worman and Bonne, 2007. Envelopathies include an autosomal recessive form of cerebellar ataxia (where nesprin 1 is mutated), PHA and HEM/Greenberg skeletal dysplasia (lamin B receptor, LBR), X-linked Emery Dreifuss muscular dystrophy (EDMD, emerin), dilated cardiomyopathy (LAP2α), and three skeletal diseases: osteopoikilosis, Buschke-Ollendorff syndrome and melorheostosis (all MAN1), (Broers et al., 2006; Worman and Bonne, 2007).

1.5.1 Laminopathies

Mutations in both A- and B-type lamins give rise to a wide spectrum of diseases collectively called laminopathies, which are themselves a subsection of envelopathies (Gruenbaum et al., 2005; Broers et al., 2006; Burke and Stewart, 2006; Mattout et al., 2006; Worman and Bonne, 2007). Primary laminopathies arise from mutations within *LMNA*, *LMNB1*, or *LMNB2*, whilst secondary laminopathies arise from disease-causing mutations within *ZMPSTE24*. Disease-causing mutations within *LMNA* were first identified in 1999, however mutations within the two lamin B genes have only recently been discovered. Duplication of *LMNB1* causes adult-onset autosomal dominant leukodystrophy (ADLD) and Barraquer-Simmons syndrome is a sporadic acquired partial lipodystrophy resulting from mutation within *LMNB2* (APL) (Hegele et al., 2006; Padiath et al., 2006).

By comparison, there are now more than 255 mutations that have been documented within *LMNA* (http://www.dmd.nl/lmna_home.html). Mutations within *LMNA* give rise to a remarkable number of different clinical disease phenotypes that have been loosely grouped together in terms of phenotypic characteristics

(Figure 1.6). Those that affect striated muscle include autosomal dominant Emery-Dreifuss muscular dystrophy (AD-EDMD), dilated cardiomyopathy with conduction system defect (DCM-CD1) and limb girdle muscular dystrophy 1B (LGMD 1B) (Bione et al., 1994; Bonne et al., 1999; Fatkin et al., 1999; Bonne et al., 2000; Muchir et al., 2000). Charcot-Marie-Tooth syndrome type 2b (CMT2B1) is an autosomal recessive axonal disease caused by mutations within *LMNA* (De Sandre-Giovannoli et al., 2002; Chaouch et al., 2003; Tazir et al., 2004). A third group of laminopathies are those involving lipodystrophies. Lipodystrophies are a heterogeneous group of disorders characterised by complete or partial loss of adipose tissue and is often associated with insulin-resistant diabetes mellitus; one of these caused by *LMNA* mutations is Dunnigan-type familial partial lipodystrophy (FLPD) (Kobberling and Dunnigan, 1986; Garg et al., 1999; Hegele et al., 2000; Reitman et al., 2000; Lelliott et al., 2002; Agarwal and Garg, 2006). Finally, the fourth group may be classified as premature aging disorders; these include atypical Werner's syndrome, mandibuloacral dysplasia type A (MADA), restrictive dermopathy (RD) and Hutchinson-Gilford progeria syndrome (HGPS) (Novelli et al., 2002; Chen et al., 2003; Cao and Hegele, 2003; De Sandre-Giovannoli et al., 2003; Eriksson et al., 2003; Hegele, 2003; Navarro et al., 2004; Filesi et al., 2005; Levy et al., 2005; Moulson et al., 2005; Toth et al., 2005).

'Secondary' laminopathies are caused by mutations in proteins that are responsible for processing prelamin A (Broers et al., 2006). The only mutations documented thus far in the genes of this processing pathway are in *ZMPSTE24*, which causes both MAD and RD (Broers et al., 2006).

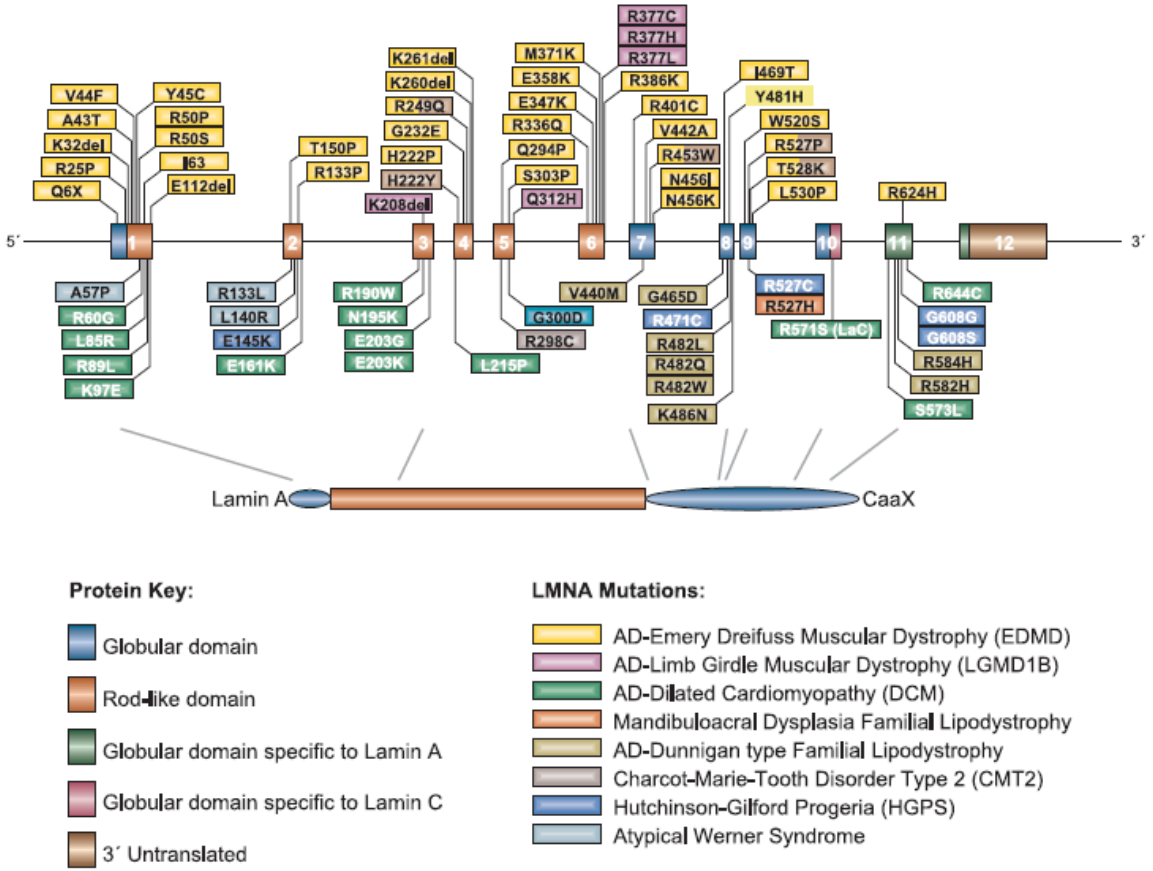

Figure 1.6. Disease-causing lamin A/C mutations. Comprehensive diagram showing the positions of mutations in *LMNA* and the laminopathy they cause (Burke and Stewart, 2006).

1.5.2 Hutchinson-Gilford Progeria Syndrome (HGPS)

Hutchinson-Gilford Progeria Syndrome (HGPS) is a rare devastating premature aging laminopathy, with a reported incidence of 1:4-8 million (Novelli and D'Apice, 2003; Pollex and Hegele, 2004; Martin, 2005). Patients usually die between 12-15 years with the majority (~90%) of patients dying from stroke or coronary failure (Hennekam, 2006). HGPS patients appear normal at birth, but within one year exhibit several features that are associated with normal aging, such as alopecia, atherosclerosis, osteolysis, lipodystrophy, scleroderma and speckled skin pigmentation (Pollex and Hegele, 2004). However, HGPS patients do not exhibit cognitive degeneration, cataract formation or any increase in tumour susceptibility, which therefore redefines HGPS a segmental progeroid syndrome, as all the age-related symptoms are not fully recapitulated (Mounkes and Stewart, 2004).

The genetic causes of HGPS had long been a mystery since its first diagnosis over a century ago. However, in 2003, three independent groups showed that mutations in *LMNA* were responsible for this disease. Classical autosomal dominant HGPS arises from a *de novo* germline mutation in *LMNA* that only affects lamin A but not lamin C (Eriksson et al., 2003; De Sandre-Giovannoli et al., 2003; Cao and Hegele, 2003). The most common HGPS-associated mutation is the d*e novo* point mutation 1824C>T, which results in a silent base substitution G608G (GGC>GGT) within exon 11 (Eriksson et al., 2003). In addition, two other *de novo* mutations were found to cause HGPS, G608S (GGC>AGC) and a heterozygous base substitution in exon 2, E145K (GAG>AAG) (Eriksson et al., 2003). The G608G mutation activates a cryptic splice within exon 11 of *LMNA*, resulting in a loss of 150 nucleotides from mature mRNA. This translates as an internal 50 amino acid deletion near the C-terminus, resulting in a mutant lamin A protein product termed progerin (Eriksson et al., 2003). This deletion removes the second endoproteolytic cleavage site, preventing the final processing step to

mature lamin A, thus progerin is both carboxymethylated and farnesylated (Figure 1.3) (Goldman et al., 2004).

Progerin acts in a dominant negative fashion with progerin transcript levels ~40% of total lamin A transcripts, indicating that use of the splice site is incomplete (Reddel and Weiss, 2004). As A-type lamins are involved in a vast array of cellular functions, research has focussed on which of these functions are altered in HGPS fibroblasts. Progerin is less mobile within the nucleus and primarily localises to the nuclear envelope due to the presence of a farnesyl group, which anchors it within the INM (Dahl et al., 2006). Progerin exerts its toxic effect at the nuclear envelope by disrupting A- and B-type lamin homopolymer formation (Delbarre et al., 2006). Furthermore, fibroblasts from HGPS patients display a characteristic set of nuclear envelope defects and abnormalities, such as blebbing, NPC clustering and loss of peripheral heterochromatin (Eriksson et al., 2003; Goldman et al., 2004). Downstream of these nuclear alterations, HGPS cells exhibit defects in mitosis, altered cell cycle profiles with reduced S-phase content, reduced cellular proliferation, increased endogenous DNA damage, deregulated gene expression profiles, an altered epigenetic landscape and defects in cellular signalling (Scaffidi and Misteli, 2006; Shumaker et al., 2006; Cao et al., 2007; Dechat et al., 2007; Han et al., 2008; Andres and Gonzalez, 2009; Pegoraro et al., 2009). Together, this research highlights deleterious effects that mutant lamin A production has on a wide range of cellular functions, indicating the important roles that A-type lamins play in normal cells.

1.6 The DNA damage response

1.6.1 Sensing DNA damage and activating the DDR

The first critical step in the DDR is the sensing of the damage itself. Early studies identified the PCNA-like protein complex Rad9-Hus1-Rad1 and Rad17 as potential sensors (Volkmer and Karnitz, 1999; Weiss et al., 2000). Rad17 shares homology with the five subunits of replication factor C (RFC) and during replication RFC binds DNA which in turn recruits PCNA to form a sliding clamp to stabilise DNA polymerases. Therefore, by analogy, during DNA damage, it has been postulated that Rad17 binds to DNA ends and recruits the Rad9-Hus1-Rad1 complex (Green et al., 2000).

Several lines of evidence now suggest that the Mre11-Rad50-NBS1 (MRN) complex is a *bona fide* sensor in the DDR and recent advances into its biological function has led it to be labelled "...a flexible scaffold that acts as a combined sensor, signaling and effector complex via dynamic states that control biological outcomes to DSBs..." (Williams et al., 2010). Structurally, the MRN complex is a heterohexamer, consisting of dimers of its three constituents (Figure 1.7a,b). The first component of the complex is the SMC family member, Rad50, which contains an ABC ATPase domain at both the N- and C-terminals. The collapse of the intervening sequence between ATPase domains results in the formation of an anti-parallel coiled-coil which extends from the 'head' domain and forms a Zn-hook domain at the apex of the Rad50 coiled-coil (Hopfner et al., 2002). The next component, Mre11, which binds to Rad50 to form the core 'head' complex (M_2R_2), has N-terminal phosphoesterase and C-terminal DNA-binding domains and participates in both ssDNA endonuclease and 3'-5' dsDNA exonuclease activities that are essential for the DNA repair process (Trujillo et al., 1998; Hopfner et al., 2001; Williams et al., 2007). The last component of the MRN complex is NBS1 (also known as nibrin or p95), which forms a flexible adaptor linkage to the Mre11-Rad50 core complex, acting as a signaling and protein-interaction module. NBS1

contains an N-terminal phospho-protein binding domain and a C-terminal Mre11-binding domain, tethering its signalling capabilities to Mre11 and Rad50.

It is possible to divide the roles of the MRN complex into three distinct biological functions: sensing DNA damage, catalysing DNA processing and signaling. The MRN complex is recruited to DNA ends independently of any other protein, suggesting that it is the initial primary DNA damage sensor. In response to DNA damage, the MRN complex functions as a macromolecular dimer (Williams et al., 2009). Each Mre11 monomer interacts with one Rad50 monomer at the intersection of its globular and coiled-coil domains, and together two subunits generate the M_2R_2 head domain (Figure 1.7b) (Williams et al., 2010). The Mre11-Rad50 head domain senses and binds broken DNA ends and bridges the gap between strands (Figure 1.7c-d). Furthermore, the Rad50 Zn-hooks can bridge homologous sister chromatids during homologous recombination repair (Figure 1.7c-d). Whilst this mechanism describes the sensing of broken DNA ends, the MRN complex is also responsible for the initial processing of DNA ends.

Figure 1.7. Structure of the MRN complex and mode of action model. (**a**) Domain structure of Mre11, Rad50 and NBS1. (**b**) The MRN complex consists of a heterohexamer, with two subunits each of Mre11, Rad50 and NBS1. The head domain consists of an Mre11 dimer and two Rad50 ABC ATPase domains, whilst the coil and hook domains are composed of the remaining residues of Rad50. NBS1 associate with Mre11 and forms a flexible adaptor region, which is essential for various signaling functions. (**c-d**) Proposed model for MRN function. See text for details (taken from Lamarche et al., 2010; Williams et al., 2009, 2010).

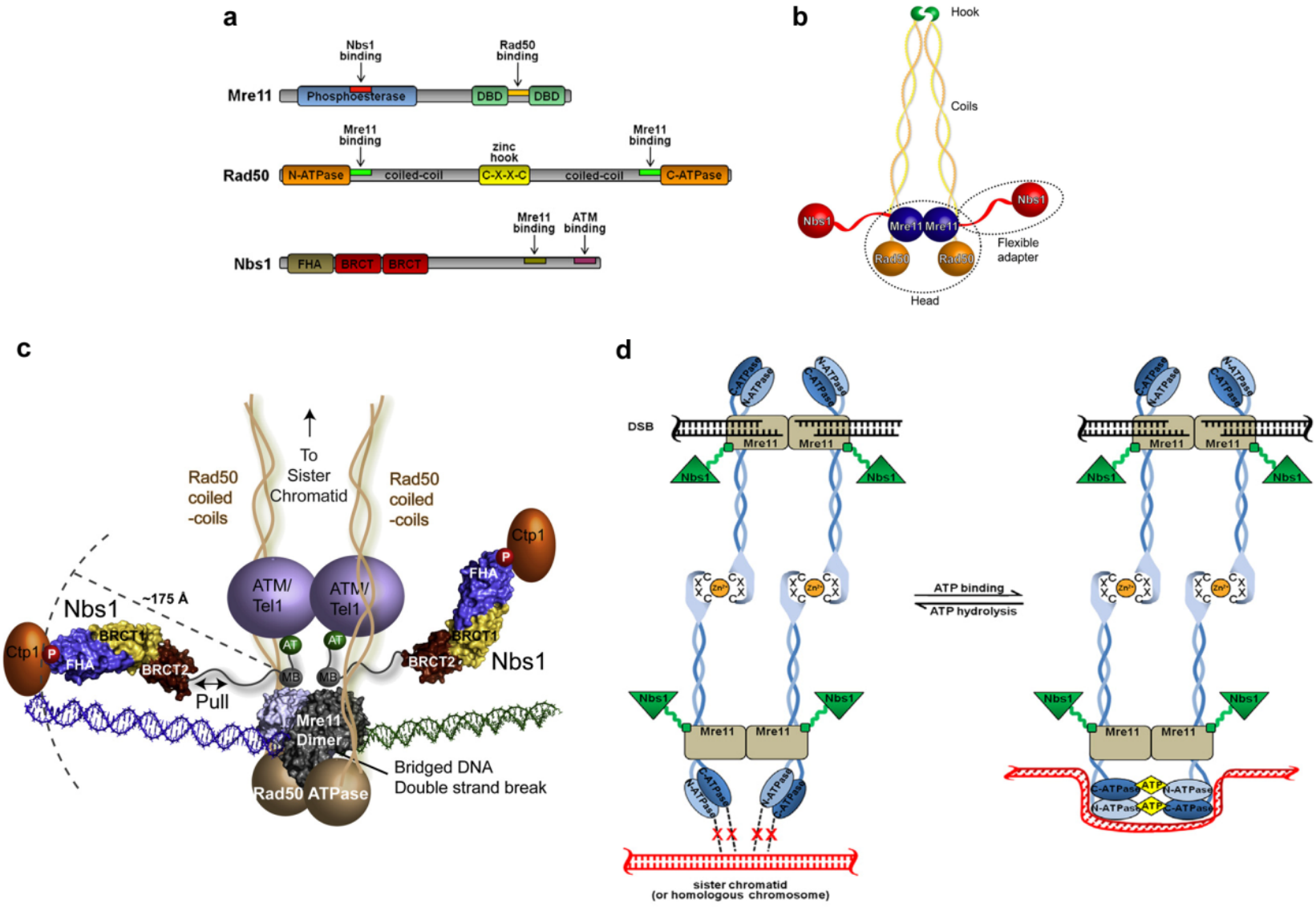
a
Nbs1 binding
Rad50 binding
Mre11
Phosphoesterase
DBD
DBD
Mre11 binding
zinc hook
Mre11 binding
Rad50
N-ATPase
coiled-coil
C-X-X-C
coiled-coil
C-ATPase
Mre11 binding
ATM binding
Nbs1
FHA
BRCT
BRCT
b
Hook
Coils
Nbs1
Nbs1
Mre11
Mre11
Rad50
Rad50
Flexible adapter
Head
c
To Sister Chromatid
Rad50 coiled -coils
Rad50 coiled -coils
ATM/ Tel1
ATM/ Tel1
Ctp1
P
FHA
BRCT1
BRCT2
Nbs1
~175 Å
Ctp1
P
FHA
BRCT1
BRCT2
Nbs1
Pull
Mre11 Dimer
Bridged DNA Double strand break
Rad50 ATPase
d
DSB
Mre11
Mre11
Nbs1
Nbs1
ATP binding
ATP hydrolysis
sister chromatid
(or homologous chromosome)

Predictably, as a DNA damage sensor, mutations in components of the MRN complex lead to various disease phenotypes. NBS1 is mutated in Nijmegen breakage syndrome (NBS), a rare autosomal-recessive disease characterized by microcephaly, growth retardation, immunodeficiency, hypersensitivity to ionizing radiation and predisposition to cancer (Carney et al., 1998; Matsuura et al., 1998; Varon et al., 1998). Mutations in Rad50 also lead to an NBS-like phenotype (Waltes et al., 2009). Furthermore, hypomorphic Mre11 mutations lead to radiosensitivity and genomic instability in ataxia-telangiectasia like disorder (ATLD) (Stewart et al., 1999).

These disease phenotypes overlap with those of ataxia telangiectasia (AT), a disease characterised by cerebellar ataxia, telangiectasia, immune defects and lymphoid cancer predisposition. AT is caused by mutations in the protein ATM (ataxia telangiectasia mutated), a serine/threonine protein kinase in the phosphoinositide 3-kinase (PI3K)-related protein kinase (PIKK) family (Lavin, 2008). The similar phenotypes observed for mutations in the MRN complex and ATM reflects their role as early components of the DDR and their role in sensing DNA damage. Indeed, for some time it was believed that ATM was the primary sensor of DNA damage. However, recent evidence implicates MRN as being upstream of ATM activation and thereby underlines the second function of the MRN complex, its ability to initiate the DDR signaling cascade.

The primary signaling mechanism of the MRN complex is carried out by NBS1, which interacts with the HEAT-repeats of ATM via its C-terminus and is required for the recruitment of ATM to DNA breaks (Falck et al., 2005; You et al., 2005). Moreover, once activated, ATM may phosphorylate NBS1 on Ser-278 and Ser-343 residues (Difilippantonio and Nussenzweig, 2007). How the recruitment of ATM to the MRN complex activates ATM is a question of on-going debate. Initial evidence suggested ATM was activated by conformational relaxation changes in DNA structure surrounding a DNA break (Bakkenist and Kastan, 2003). Later reports however have shown that a functional MRN complex is required for complete ATM activation (Uziel et al., 2003; Lee and Paull, 2004, 2005).

Furthermore, ATM activation is inhibited in both NBS and ATLD cells in response to DNA damage, underlining its dependency on the MRN complex (Uziel et al., 2003).

Regardless of the mode of its activation, upon DNA damage ATM dissociates from a constitutive dimer into activated monomers, whereby they can phosphorylate a range of cellular substrates (e.g. p53, Chk2, BRCA1) involved in a diverse range of cellular processes, including DNA repair, cell cycle control and transcriptional control (Bakkenist and Kastan, 2003; Matsuoka et al., 2007). ATM undergoes autophosphorylation on a least three residues, S367, S1899 and S1987, with phosphorylation of S1987 important for the transition from inactive dimer to active monomer (Bakkenist and Kastan, 2003; Kozlov et al., 2006). The autophosphorylation of ATM leads to its widespread and rapid phosphorylation throughout the nucleus and in this manner is able to propagate the damage signal. Whether ATM autophosphorylation is a cause or consequence of its activation remains to be determined, as there are several conflicting reports (Lavin, 2008).

In concert with phosphorylation, ATM also undergoes acetylation at Lys3016, which leads to its DNA damage-dependent activation (Sun et al., 2005, 2007). Building on this, further studies have revealed that ATM exists in its inactive state in a complex with the acetyltransferase Tip60. Upon DNA damage Tip60 binds histone H3K9me3 residues around the DNA break, which facilitates acetylation of ATM, thereby activating it (Sun et al., 2009). It therefore appears that the concerted efforts of autophosphorylation, acetylation and MRN binding have the cumulative effect of activating ATM during DNA damage.

Related to ATM is another DNA damage kinase of the PIKK family, ATR (ATM and Rad3 related). Whilst ATM is activated in response to double strand breaks *in vivo*, ATR is activated by UV and agents that cause replication stress (Abraham, 2001; Li and Zou, 2005). The importance of ATR to organismal survival is demonstrated by ATR knockout mice, which results in embryonic lethality (Brown

et al., 2000; de Klein et al., 2000). Furthermore, hypomorphic mutations in human ATR give rise to the autosomal recessive disorder Seckel syndrome, which shares characteristics with AT (O'Driscoll et al., 2003). Both ATM and ATR preferentially phosphorylate SQ/TQ residues, thus they share similar target substrates (Matsuoka et al., 2007; Stokes et al., 2007). In human cells, ATR exists in a stable heterodimer with ATRIP (ATR-interacting protein) (Cortez et al., 2001). In response to UV damage or replication stress, generation of single-stranded DNA (ssDNA) is bound by replication protein A (RPA) to prevent the formation of higher order structures. RPA coated ssDNA then recruits the ATR-ATRIP heterodimer and activated ATR phosphorylates downstream targets such as Chk1, which is responsible for phosphorylating Cdc25A, thus inhibiting the firing of replication origins (Zou and Elledge, 2003; Sancar et al., 2004).

Together with ATM and ATR, the other major PIKK in mammalian cells is DNA-PK, which consists of a trimer of DNA-PK catalytic subunit (DNA-PKcs) and a dimer of Ku70/Ku80 (Sancar et al., 2004). DNA-PK plays an important role in the response to double strand breaks and the non-homologous end joining pathway as well as phosphorylating target substrates (see 1.7.6.3).

1.7 Repair mechanisms and pathways

Due to its very nature, DNA can be damaged in a variety of ways, including base damage (reduced, oxidized, or fragmented bases), DNA backbone damage (abasic sites and single- or double-strand DNA breaks), and cross-links (DNA-protein cross-links and inter-strand or intra-strand cross-links) (Hoeijmakers, 2001; Jackson and Bartek, 2009; Ciccia and Elledge, 2010). As a result of these genomic insults, evolution has provided various repair pathways (some of which may only repair one single type of DNA lesion) that are responsible for maintaining genomic stability and the fidelity of DNA that can be broadly categorised into six different, but partly overlapping, DNA repair pathways: direct repair, base excision repair (BER), mismatch repair (MMR), nucleotide excision repair (NER), repair of inter-strand cross-links (ICLs), double-strand break (DSB)

repair (Sancar et al., 2004). Here, I will briefly summarise the first five of these pathways, but explore the last, DSB repair, in more detail.

1.7.1 Mismatch repair (MMR)

MMR is responsible for removing mispaired, inserted or deleted nucleotides (1-10 bases) during replication when the DNA polymerase exonuclease 3'-5' proof-reading fails, and in doing so MMR increases the fidelity of DNA replication ~1000 fold (Kunkel and Erie, 2005; Jun et al., 2006; Hsieh and Yamane, 2008). Defects in the MMR pathway are linked to microsatelittle instability (MI), which is implicated in most cancers including hereditary nonpolyposis colorectal cancers (HNPCC) (Hoeijmakers, 2001).

In eukaryotes, there are two complexes that initiate the MMR pathway (Figure 1.8). Firstly, the MutSα dimer (composed of MSH2 and MSH6) recognises 1-2 base insertion/deletions and single base-base mismatches. Secondly, the MutSβ dimer (composed of MSH2 and MSH3) may recognise base insertions/deletions with two or more bases (Larrea et al., 2010). Interaction of these dimers with mismatched DNA initiates the interaction of MutL heterodimers to the mismatched DNA. There are three MutL heterodimers in eukaryotes: MutLα (composed of MLH1 and PMS2), MutLβ (composed of MLH1 and MLH3) and MutLγ (composed of MLH1 and PMS1) (Kunkel and Erie, 2005; Jascur and Boland, 2006; Jun et al., 2006). Whilst the MutLα and MutLβ heterodimers have endonuclease activities, the resulting nick can be utilized various exonucleases including Exo1 (Kunkel and Erie, 2005; Jascur and Boland, 2006; Jun et al., 2006). Alternatively, Exo1-independent strand displacement synthesis may occur via DNA pol δ (Kadyrov et al., 2009). The DNA is then resynthesised by the concerted actions of replication factor C (RFC), proliferating cell nuclear antigen (PCNA) and DNA pol δ (Modrich, 2006).

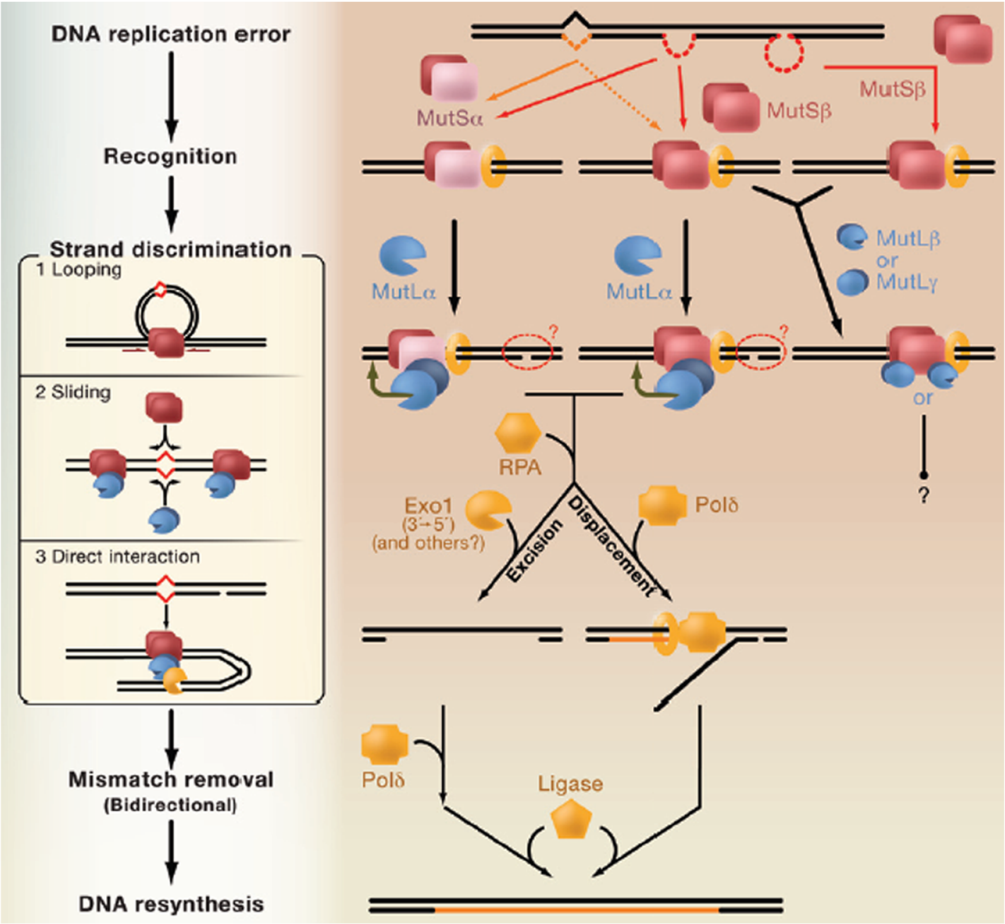

Figure 1.8. Eukaryotic mismatch repair pathway. Mismtached bases are recognised by MutSα or MutSβ, before recruitment of either MutLα, β or γ proteins depending on the type of mismatch. Further processing allows resynthesis of the DNA strand (Larrea et al., 2010).

1.7.2 Base excision repair (BER)

BER is responsible for the removal of damaged bases and is initiated by a plethora of DNA glycosylases, which each deal with a specific type of damaged base. Glycosylases flip the damaged base out of the DNA helix to form an abasic site (AP site) (Fromme at al., 2004). The damaged base is cleaved from the sugar-phosphate backbone by APE1 (Fortini and Dogliotti, 2007). Depending on the type of lesion, BER proceeds by either short- or long-patch pathways. In the short-patch pathway (where a single nucleotide is replaced), DNA pol β performs

a one-nucleotide gap-filling reaction and removes the 5'-terminal baseless sugar residue via its lyase activity, which is then followed by sealing of the remaining nick by the XRCC1–ligase3 complex (Hoeijmakers, 2001). In contrast, in the long-patch pathway (where 2-10 nucleotides are newly synthesised), a large complex involving DNA pol δ/ε and proliferating cell nuclear antigen (PCNA) together with the FEN1 endonuclease to remove the DNA flap and DNA ligase 1 for sealing (Figure 1.9) (Sancar et al., 2004).

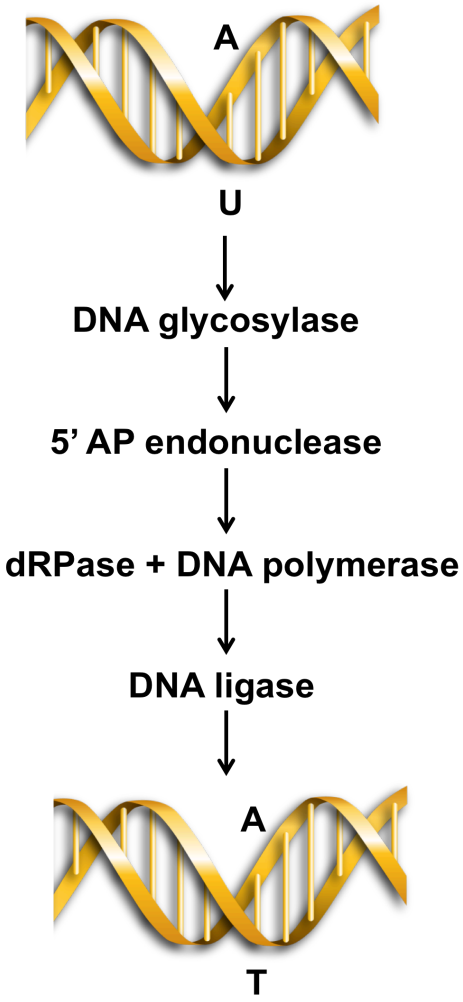

Figure 1.9. Overview of base excision repair (BER) pathway in mammalian cells. Damaged bases are recognised by DNA glycosolases, followed by the action of an endonuclease, gap filling and then ligation.

1.7.3 Nucleotide Excision Repair (NER)

NER is the major mechanism for removal of a variety of structurally and chemically unrelated bulky DNA lesions such as chemical adducts and the dimerized pyrimidine bases induced by UV radiation (Hanawalt, 2007; Hoeijmakers, 2009). Defects in NER cause diseases such as xeroderma pigmentosum (XP), Cockayne Syndrome (CS), and trichothiodystrophy (TTD) (Thoma and Vasquez, 2003). There are two major NER sub-pathways: global genomic repair (GGR), which eliminates lesions from the entire genome, and transcription coupled repair (TCR), which efficiently removes lesions from the transcribed strand of active genes. Both sub-pathways follow the same basic repair steps and require more than 25 proteins for DNA damage recognition, dual-incision, excision, repair synthesis, and ligation (Thoma and Vasquez, 2003). In GGR, DNA damage-induced helical distortion is recognized by the XPC and XPD (or UV-DDB) protein complexes. In TC-NER, damage is recognised by the CSB and CSA proteins, which respond to the stalling of RNA polymerase II (Hanawait and Spivak, 2008). In both cases, the next step involves the recruitment of transcription factor IIH (TFIIH). The two helicase subunits of TFIIH, XPB and XPD, both act to unwind DNA, allowing damage recognition by xeroderma pigmentosum group A (XPA), whilst RPA arrives at the same time to help in verifying the presence of DNA lesions (Nouspikel, 2009). Endonuclease xeroderma pigmentosum group G (XPG) and the xeroderma pigmentosum group F-excision-repair cross-complementing group 1 (XPF–ERCC1) complex are responsible for the 3' and 5' DNA incisions, respectively, creating a single-stranded oligonucleotide ~ 24-32 nucleotides in length (Coin et al., 2008; Hoeijmakers, 2009). Binding of XPG induces the release of XPC, whereas XPF–ERCC1 triggers excision of the damaged DNA and the release of XPA and TFIIH (Coin et al., 2008). Subsequently, the newly formed gap in the DNA is filled by DNA polymerase δ/ε, replication factor C (RFC), proliferating cell nuclear antigen (PCNA), RPA and DNA ligase I or a complex of XRCC1 and DNA ligase III (Figure 1.10) (Park and Choi, 2006).

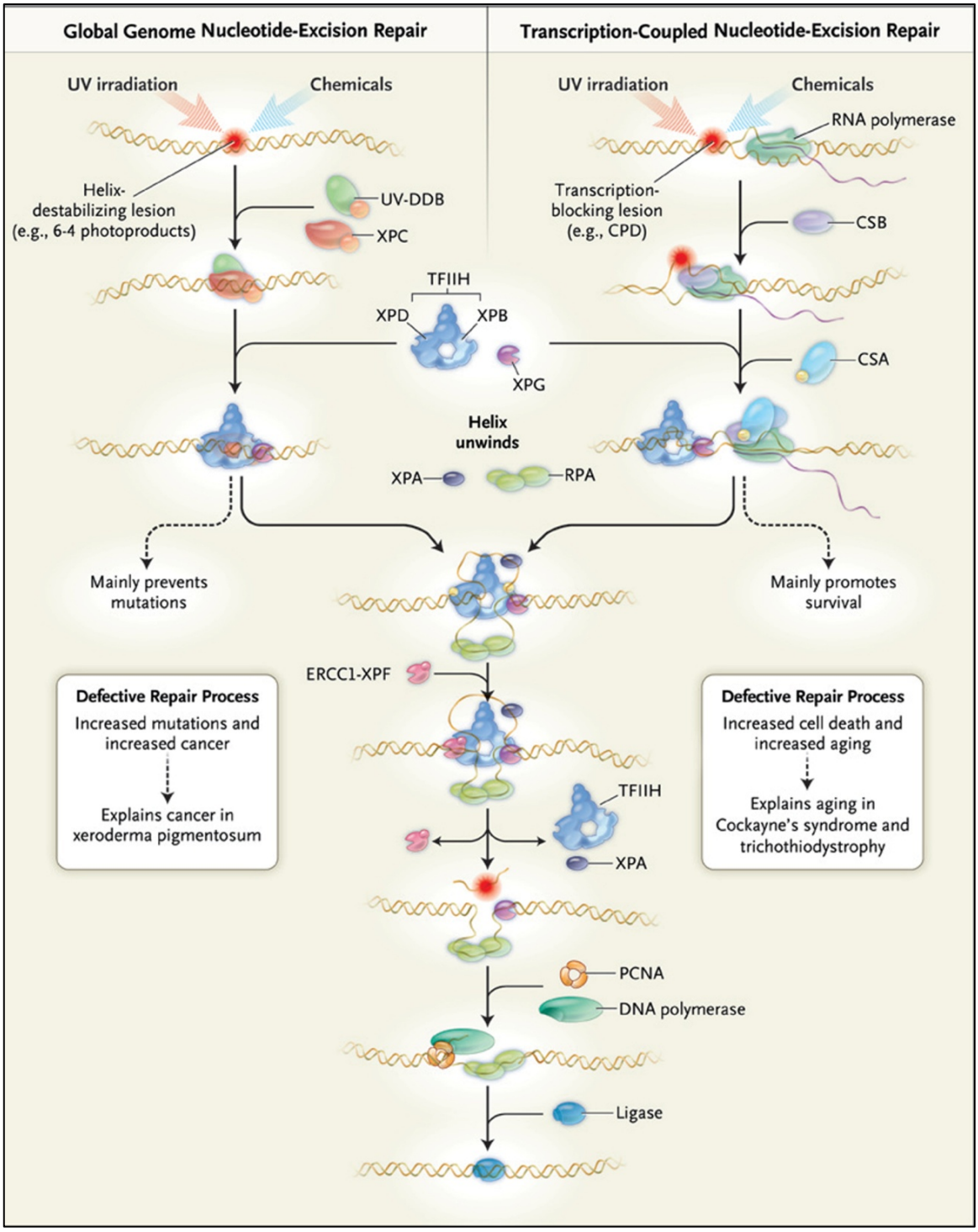

Figure 1.10. Overview of the nucleotide excision repair (NER) pathway in mammalian cells. UV-induced DNA damage is proceesed by one of two branches of NER, namely global genome repair (GGR) or transcription-coupled repair (TCR). The two pathways converge when TFIIH is recruited, which then

facilitates the recruitment of downstream factors necessary for damage sensing and repair. See text for details (Hoeijmakers, 2009).

1.7.4 Inter-strand crosslink (ICL) repair

Inter-strand crosslinks may be caused by a range of chemicals (e.g. nitrogen mustards, mitomycin C, cisplatin) and result from the formation of covalent linkages between DNA strands to create a bi-directional block to replication polymerases (Smogorzewska et al., 2010). To counteract this life-threatening lesion, the Fanconi Anemia (FA) pathway has evolved to target this specific form of DNA damage (Liu et al., 2010). FA is a rare inherited disease characterised by genomic instability, congential malformations, bone marrow failure and cancer predisposition (Alter et al., 2003; Wang et al., 2007). Cells from FA patients are hypersensitive to DNA inter-strand crosslinking (ICL) agents such as mitomycin C (MMC) and cisplatin. There are thirteen distinct Fanconi anemia genes that have been shown to interfere with the DNA-replication-dependent repair of lesions involving crosslinked DNA at stalled replication forks. Furthermore, it seems likely that all thirteen are needed for efficient ICL repair (Niedernhofer et al., 2005; Moldovan and D'Andrea., 2009). Central to the FA pathway is the FANCI-FANCD2 (ID) complex (Garcia-Higuera et al., 2001; Smogorzewska et al., 2007). The ID complex is chromatin bound, and when it encounters a DNA replication structure stalled due to a DNA crosslink, it becomes phosphorylated by the ATR/ATRIP kinase, which is localized through recognition of RPA at the lesion (Zou and Elledge, 2003). Phosphorylation of both FANCI and FANCD2 is required for ID function (Andreassen et al., 2004; Ho et al., 2006; Ishiai et al., 2008). Upon phosphorylation, eight FA proteins (A, B, C, E, F, G, L, and M) are assembled into the nuclear FA core complex that mono-ubiquitylates its two substrates, FANCI and FANCD2, a reaction that also requires the FA-associated proteins FAAP100 and FAAP24 (Garcia-Higuera et al., 2001; Taniguchi et al., 2002; Ciccia et al., 2007; Collis et al., 2008). The ubiquitylated ID complex then accumulates at the site of damage and directs repair (Smogorzewska et al., 2007; Raschle et al., 2008; Knipscheer et al., 2009). Exactly how it does it this unclear. However, using

a cell-free system, it has been suggested that monoubiquitylation of FANCD2 is required for the unhooking of the ICL (Knipscheer et al., 2009). Unhooking involves incisions on both sides of the ICL, followed by bypass synthesis over the lesion on the remaining intact strand using a translesion polymerase. Both the incision step and the bypass polymerase step are dependent upon ubiquitylation of the ID complex (Raschle et al., 2008; Knipscheer et al., 200;). Double strand breaks generated by unhooking are resected and one of them initiates homologous recombination to complete ICL repair (Figure 1.11) (Moldovan and D'Andrea, 2009; Kee and D'Andrea, 2010).

1.7.5 Single-strand break (SSB) repair

Single-strand breaks may form in response to ROS, IR and as a result of inherent BER processes (Caldecott, 2008). Initial sensing of SSBs is carried by the zinc finger domains of PARP1 and PARP2, whose binding to DNA causes their activation and they subsequently synthesise poly(ADP-ribose) (PAR) chains at the sites of damage, notably on histones H1, H2B and PARP1 itself. The assembly is transient and rapid, with the PAR chains disassembled by PARG (Schreiber et al., 2006). Recent evidence suggests that the addition of PAR chains (PARylation) leads to local chromatin relaxation, which is necessary for the recruitment of other chromatin modifying enzymes and DNA repair proteins (Ahel et al., 2008; Ahel et al., 2009; Chou et al., 2010; Larsen et al., 2010; Polo et al., 2010; Smeenk et al., 2010). XRCC1 is recruited to PAR chains and facilitates the recruitment of downstream effectors such as Xip1 such as DNA polymerase b, PNK, and the nucleases APE1, APTX, and APLF (Caldecott, 2008). The processed ends are then directed into the short- or long-patch BER pathways.

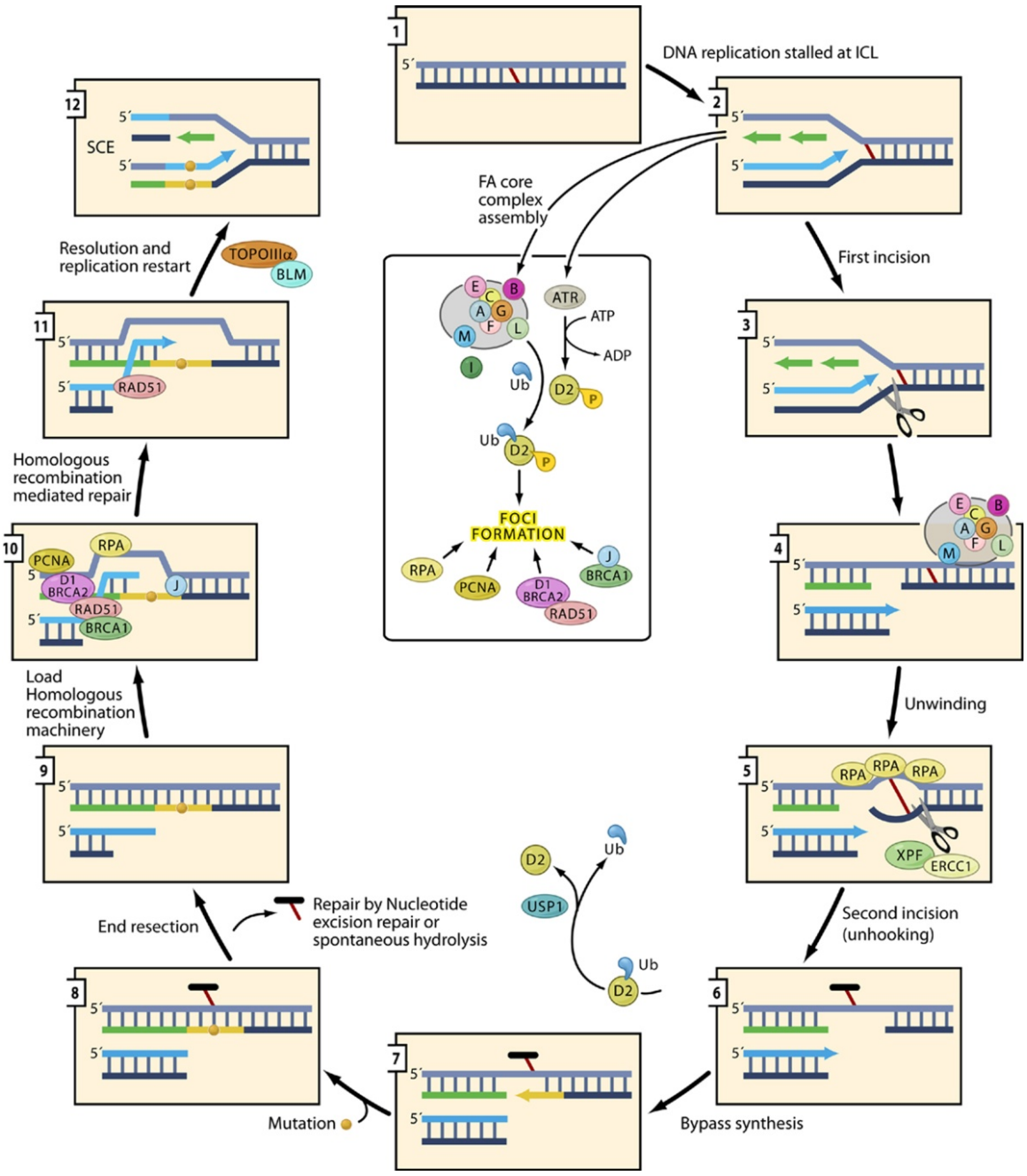

Figure 1.11. Model of ICL repair highlighting the involvement of the FANC proteins. Inter-strand crosslinks, produced either by crosslinking reagents or the convergance of two replisomes, are recognised by the FA complex, which triggers the ubiquitylation of FANCD2 and FANCI. Nucleases then excise the ICL, which is subsequently repaired by homologus recombination before replication restart (Nierdernhofer et al., 2005).

1.7.6 Double strand break (DSB) repair

Among the various forms of DNA damage that are inflicted by mutagens, DSBs are the most dangerous cytotoxic lesions. DSBs can be caused by ionizing radiation, radiomimetic chemicals, ROS, and mechanical stress on chromosomes (Mackinnon and Caldecott, 2007; Jackson and Bartek, 2009). DSBs can also be the result of normal V(D)J recombination or abnormal replication fork arrest and collapse (Polo and Jackson, 2011). Defects in DSB repair result in genomic instability and apoptosis at the cellular level, and lead to increased predisposition to cancer in animal models and in people (Halazonetis et al., 2008; Jackson and Bartek, 2009). DSBs are repaired using two main pathways, either by homologous recombination repair (HRR), which usually occurs in S and G_2-phases, or non-homologous end-joining (NHEJ) mechanisms, which normally occurs in G_1-phase (Hiom, 2010; Kass and Jasin, 2010). Cells have evolved interwoven mechanisms for the detection of DSBs and recent work has implicated a variety of cellular processes in the complex task of both signalling and repairing DSBs, such as post-translational modifications (phosphorylation, acetylation, ubiquitylation, SUMOylation), transcriptional silencing and altered chromatin dynamics (Ciccia and Elledge, 2010).

1.7.6.1 γ-H2AX-dependent signalling cascade in response to DSBs

In addition to the MRN complex, DSBs can be sensed by PARP, Ku70/80 and RPA (with processing) (Uziel et al., 2003; Falck et al., 2005; Ciccia and Elledge, 2010; Polo and Jackson, 2011). Furthermore, MRN and Ku70/80 contribute to full ATM and DNA-PKcs activation (Falck et al., 2005; Al-Hakim et al., 2010). Following DSB formation, the MRN complex component NBS1 binds ATM via its C-terminal domain. Once ATM has been activated it phosphorylates an extensive network of cellular substrates, such as proteins involved in DNA repair and cell cycle progression (Matsuoka et al., 2007; Derheimer and Kastan, 2010). One of the first substrates to be phosphorylated by ATM is histone variant H2AX on Ser139, which can also be phosphorylated by two other PIKKs, ATR and DNA-PK

(Rogakou et al., 1999; Burma et al., 2001; Stiff et al., 2004; Attikum and Gasser, 2009). The H2AX variant constitutes ~ 10-15% of total H2A in higher eukaryotes and upon DNA damage its phosphorylation may spread up to 1-2 megabases from the DSB in an asymmetrical manner, a process which is responsible for the retention of downstream DDR proteins rather than their initial recruitment (Rogakou et al., 1998; Celeste et al., 2003; Stucki and Jackson, 2006; Berkovich et al., 2007; Meier et al., 2007; Savic et al., 2009; Iacovoni et al., 2010). Coupled to γ-H2AX production is the dephosphorylation of Y142 of H2AX, which appears to be a prerequisite for Ser139 phosphorylation (Cook et al., 2009; Xiao et al., 2009). Another substrate of ATM, MDC1 (mediator of the DNA-damage checkpoint 1) then sequentially binds γ-H2AX via its C-terminal BRCT repeats (Goldberg et al., 2003). Further to this, MDC1 also interacts with the NBS1 N-terminal FHA domain. Upon DNA damage, MDC1 is phosphorylated by casein kinase 2 (CK2) at SDT (Ser-Asp-Thr) repeats in its N-terminal. These phosphorylated repeats serve as a ligand for the NBS1 FHA domain, which helps to maintain MRN-ATM at sites of DNA damage and allows further accumulation of γ-H2AX at regions flanking the DSB (Chapman and Jackson, 2008 Melander et al., 2008; Spycher et al., 2008). The MDC1 FHA domain can also bind ATM, thus it is clear that MDC1 serves as a platform for the assembly of proteins integral to the DDR (Lou et al., 2006). This positive feedback mechanism allows further retention of downstream proteins at sites of DNA damage and has therefore led MDC1 to be termed the “...master regulator...” of the DDR (Stucki and Jackson, 2004). The RING-finger E3 ubiquitin ligase protein RNF8 also binds MDC1 phospho-TQ sites via its N-terminal FHA domain and ubiquitylates H2A and H2AX at DSBs via K63-linkages (Huen et al., 2007; Kolas et al., 2007; Mailand et al., 2007). Another ubiquitin ligase, RNF168, recognises ubiquitin chains and catalyses the further K63 ubiquitylation of H2A and H2AX (Doil et al., 2009; Stewart et al., 2009). The recently identified E3 ubiquitin ligase, HERC2, facilitiates assembly of the RNF/Ubc13 complex by interacting withn the FHA domain of RNF8 in a phopsphorylation-dependent manner (Bekker-Jensen et al., 2010; Bekker-Jensen and Mailand, 2010). The K63 ubiquitin chains serve as a

recruitment signal for the BRCA1-A complex via the UIM motif in RAP80 (Figure 1.12) (Huen and Chen, 2010). The RNF8-RNF168 axis is also responsible for the recruitment of the mediator protein 53BP1 to sites of DNA damage. Therefore, histone ubiquitylation is essential for the assembly of DNA repair factors at DSBs (Bekker-Jensen and Mailand, 2010).

As another level of complexity to these assembly events, recent advances have shown a role for SUMOylation as a regulatory post-translational modification in the DDR to add the aforementioned acetylation, phosphorylation and ubiquitylation modifications (Galanty et al., 2009; Morris et al., 2009). It was shown that two SUMO ligases, PIAS1 and PIAS4, localise to DSBs, with PIAS1 responsible for SUMOylating BRCA1 and stimulating its E3 ubiquitin ligase activity, whilst PIAS4 is responsible for SUMOylating the RNF8/Ubc13 complex thereby stimulating its ubiquitin ligase activity (Galanty et al., 2009; Morris et al., 2009).

Typically, proteins involved in the antagonistic post-translational modification (e.g. de-ubiquitylation, de-SUMOylation, de-phosphorylation) localise to the DSB microenvironment simultaneously. Recently, the de-ubiquitylating enzyme (DUB) OTUB1 was shown to inhibit RNF168-dependent ubiquitylation by direct inhibition of Ubc13 (Nakada et al., 2010). Therefore, the apparently overt complexity of DDR protein assembly has been suggested to facilitate exquisite fine control of DNA repair mechanisms as the requirement for different repair choices play out (Figure 1.12) (Cicca and Elledge, 2010).

Figure 1.12. γ-H2AX-dependent signalling cascade following DNA damage. Following IR, PARP1/2 and MRN are recruited to the DSB. MRN and Tip60 activate ATM, which in turn phosphorylates p53, Chk2 and H2AX. MDC1 binds γ-H2AX, which is responsible for the recruitment of downstream substrates RNF8, RNF168, BRCA1 and 53BP1. See main text for details. (Ciccia and Elledge, 2010)

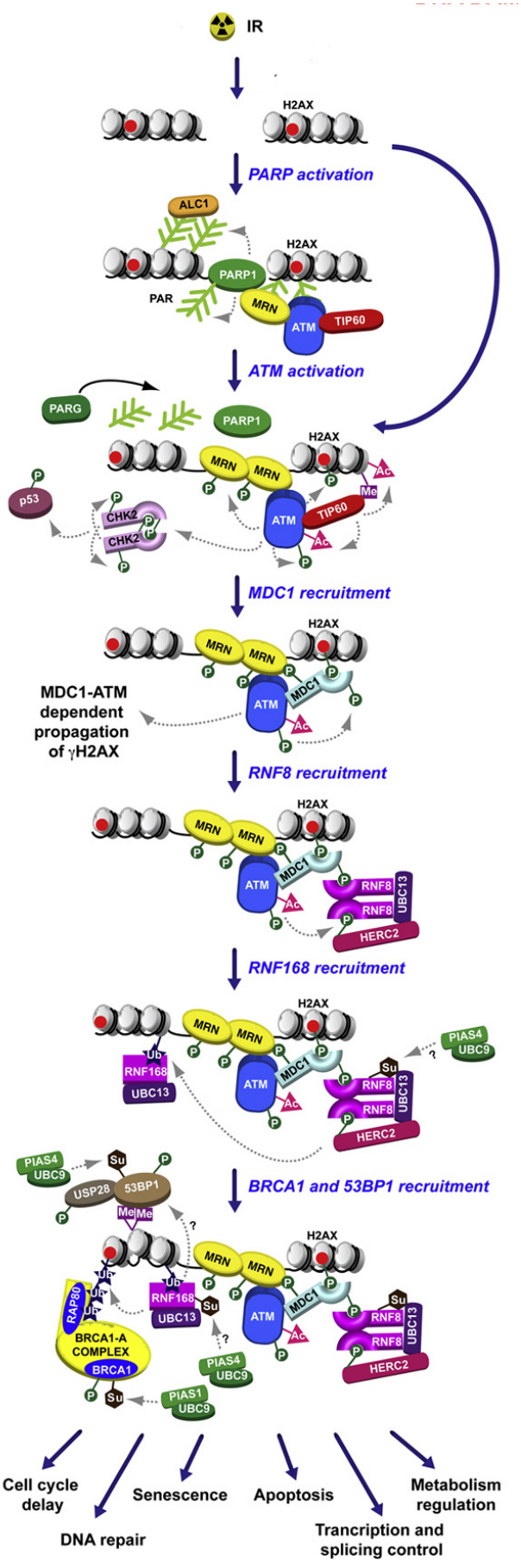
IR
H2AX
PARP activation
ALC1
PARP1
PAR
MRN
ATM
TIP60
ATM activation
PARG
p53
CHK2
Ac
Me
MDC1 recruitment
MDC1-ATM dependent propagation of γH2AX
RNF8 recruitment
RNF8
UBC13
HERC2
RNF168 recruitment
Ub
RNF168
UBC13
PIAS4
UBC9
Su
BRCA1 and 53BP1 recruitment
USP28
53BP1
RAP80
BRCA1-A COMPLEX
BRCA1
PIAS1
Cell cycle delay
Senescence
Apoptosis
Metabolism regulation
DNA repair
Trancription and splicing control

1.7.6.2 Homologous recombination (HR)

The HR repair pathway is an accurate repair process that depends on an intact sister chromatid as a template. Initial sensing is carried out by the MRN complex and is associated with a DSB signalling cascade involving histone modifications. Furthermore, the Mre11 component of the MRN complex acts together with CtIP, Exo1 and helicases to stimulate the resection of the 5' ends of the DSB to generate 3' ssDNA overhangs (Mimitou and Symington, 2008, Zhu et al., 2008; Nicolette et al., 2010). It should be noted that Mre11 possess intrinsic 3'-5' exonuclease activity and only through interaction with other factors, notably CtIP and Exo1, can it promote initial 5'-3' resection necessary for homologous recombination (Huertas, 2010, Lamarche et al., 2010; Nicolette et al., 2010). Once resection is complete, RPA binds immediately to ssDNA and BRCA2 facilitates the replacement of RPA by the Rad51, a DNA-dependent ATPase, to form nucleoprotein filaments (Kass and Jasin, 2010). Formation of this nucleoprotein filament facilitates strand exchange during which the ssDNA invades the homologous duplex DNA template to generate a D-loop structure. D-loop formation can then be resolved by multiple mechanisms. The first is called synthesis-dependent strand annealing (SDSA) and involves the extension of the 3' end of the D-loop by repair synthesis leading to its annealing with the resected strand of the second end (Figure 1.13) (Heyer et al., 2010). The second mechanism involves the production of a Holliday junction if the two sisters exchange, which can be resolved by nucleolytic processing by Gen1 and the Slx1-Slx4 nuclease complex (Hiom, 2010). Resolution of the Holliday junction results in either crossover or non-crossover products, with the former having deleterious effects, such as loss of heterozygosity (Figure 1.13) (Kass and Jasin, 2010). However, typically HR is an accurate repair pathway (i.e. forming non-crossover products) if a sister chromatid is present, faithfully restoring the DSB (Ciccia and Elledge, 2010).

1.7.6.3 Non-homologous end joining (NHEJ)

The first step of NHEJ is the binding of the Ku70/80 heterodimer to the double-stranded ends of the DSB (Mahaney et al., 2009; Roberts et al., 2010). Whilst Ku70/70 possesses some end processing ability, it also functions to recruit DNA-dependent protein kinase catalytic subunit (DNA-PKcs), a step that translocates Ku70/80 inwards (Roberts et al., 2010). Binding of DNA-PKcs to DNA stimulates its own autophosphorylation, an event that induces a large conformational change in DNA-PK, leading to its dissociation from DNA either before or after end processing events (Sibanda et al., 2010). After DNA-PKcs binding, further proteins are recruited to process the DNA ends, one of which is the endonuclease, Artemis, which is phosphorylated by DNA-PK. Another protein recruited is the polynucleotide kinase, phosphatase (PNKP), which is responsible for removing 3'-phosphate groups and adds 5'-phosphate groups to DNA ends (Koch et al., 2004). The MRN complex and DNA polymerases μ and λ, which fills in missing nucleotides, are also required for the end processing of DSBs. Lastly, DNA-PK recruits the x-ray repair cross-complementing protein 4 (XRCC4) and DNA ligase IV complex as well as XLF, which are involved in the ligation of the DSB (Figure 1.13) (Mahaney et al., 2009). Whilst DSBs with flushed 5'-phosphorylated ends or complementary overhangs are re-ligated effectively, where nucleotides have become altered, lost or need processing then genetic material may be lost after this re-ligation step, therefore defining the NHEJ pathways as typically error-prone (Hiom, 2010).

1.7.6.4 Alternative non-homologous end joining (alt-NHEJ) and single-strand annealing (SSA)

When the classical NHEJ pathway is blocked, then Ku70/80-dependent NHEJ cannot proceed and cells may use alternative NHEJ pathways (sometimes called microhomology mediated end joining, MMEJ) (McVey and Lee, 2008). Although the exact mechanism is unknown, it appears that limited end resection by MRN and CtIP occurs prior to DNA ligation. Furthermore, this may be aided by small

microhomologies that may help to align broken strands of DNA (Simsek and Jasin, 2010).

A distinct pathway separate from HR is single-strand annealing (SSA). If there are repetitive DNA sequences on either side of a DSB then, following resection, the strands can be annealed by Rad52, followed by the removal of DNA flaps by XPF/ERCC1 (Hartlerode and Scully, 2009). The action of EPF/ERCC1 results in the loss of genetic material from between the repetitive sequences and hence this repair pathway is inherently error-prone.

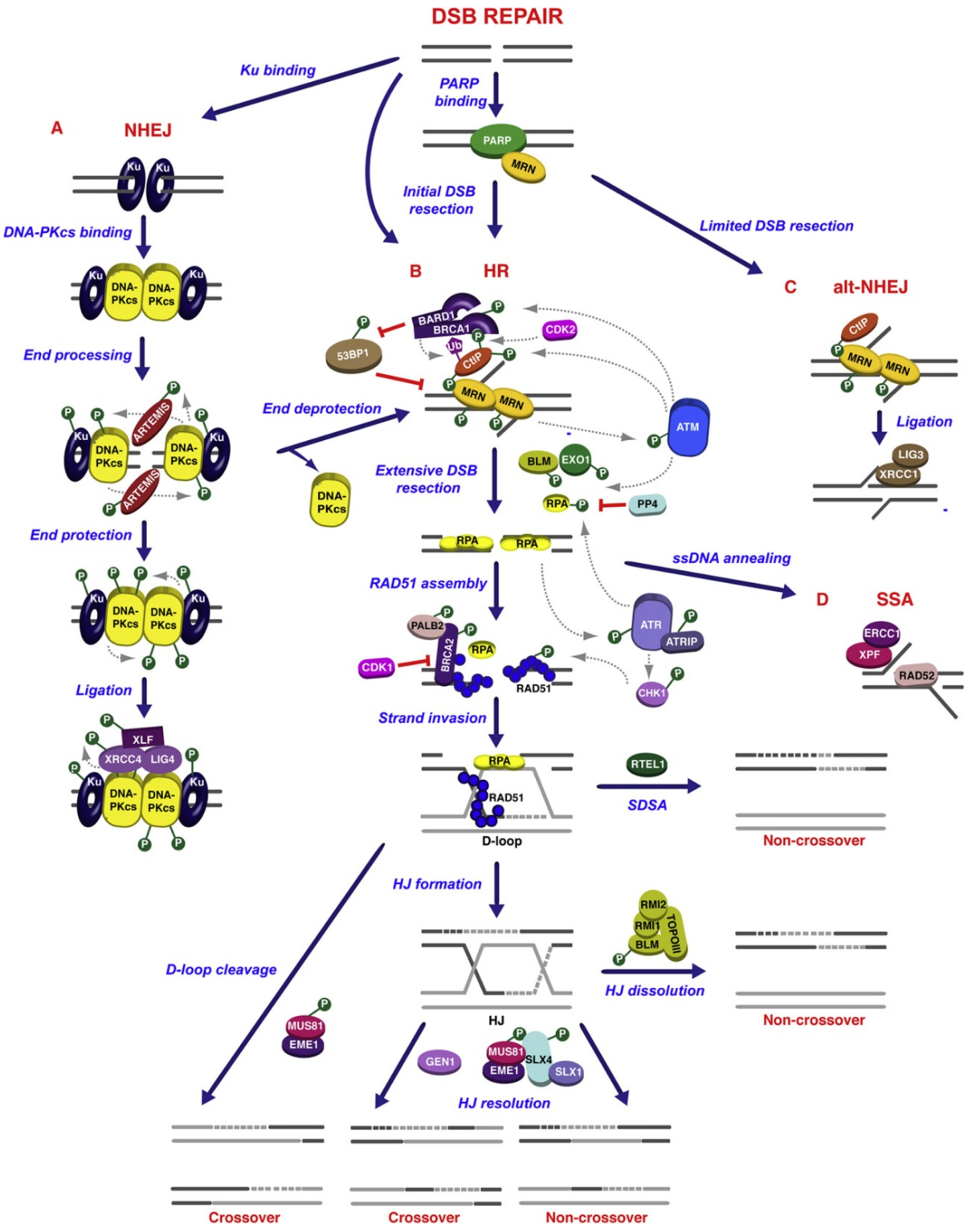

Figure 1.13. DSB repair pathways in mammalian cells. DSBs are principally repaired by either homologous recombination (HR) or non-homologous end-joining (NHEJ). See text for details (Ciccia and Elledge, 2010).

1.8 p53-binding protein (53BP1)

The p53 binding protein, 53BP1, together with proteins such as BRCA1, MDC1 and TopBP, has been classified as a mediator of the DNA damage response (Wang et al., 2002). 53BP1 was first identified as a p53-interacting protein using a yeast two hybrid assay with the p53 central domain as bait (Iwabuchi et al., 1994). Since then various studies have underlined its importance in the in the DDR via its impact on checkpoint activation and its role in DNA repair.

1.8.1 Structure of 53BP1

53BP1 is a large protein (1972 amino acids) with an N-terminal region rich in phosphorylation sites. The C-terminal domain consists of an oligomerisation domain (OD), a region required for γ-H2AX interaction, a Tudor domain and a tandem BRCT domain (Figure 1.14) (Fitzgerald et al., 2009).

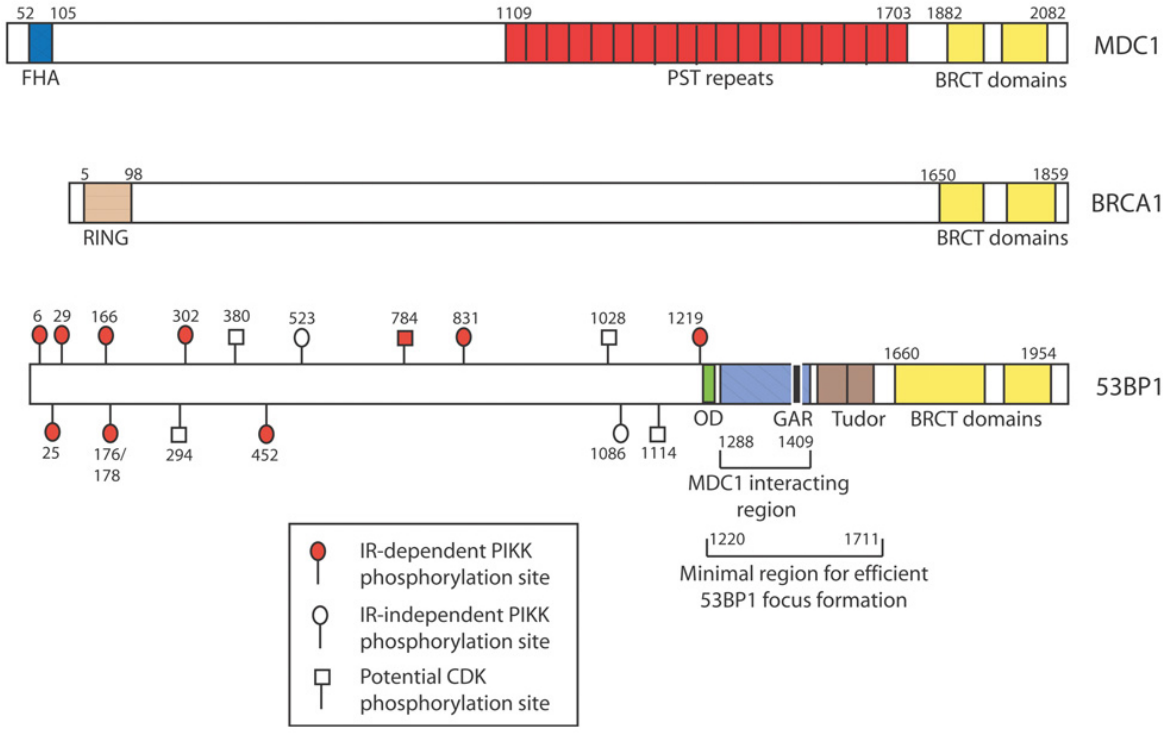

Figure 1.14. Domain structure of 53BP1 and two other mediators of the DDR, MDC1 and BRCA1 (Fitzgerald et al., 2009).

The N-terminal region of 53BP1 has been shown to be rich in both IR-dependent and IR-independent phosphorylation sites, with 32 potential SQ/TQ sites (Ward et al., 2003; Jowsey et al., 2007; Fitzgerald et al., 2009; Lee et al., 2009). The role of IR-dependent phosphorylation of 53BP1 is discussed below. 53BP1 also contains 41 SP/TP sites, which are targets for CDK phosphorylation, but the exact role for these CDK sites remains to be determined (Jowsey et al., 2007; Fitzgerald et al., 2009).

1.8.2 53BP1 in checkpoint control

A role for 53BP1 in both the intra-S-phase and G_2/M-phase checkpoints has been suggested (DiTullio et al., 2002; Fernandez-Capetillo et al., 2002; Wang et al., 2002). In the latter study, U2OS cells depleted of 53BP1 exhibited ineffective checkpoint arrest, with a defective G_2/M checkpoint only apparent in response to low doses of IR (Wang et al., 2002). In contrast, subsequent reports have failed to detect any defective intra-S-phase and G_2/M-phase checkpoints (Iwabuchi et al., 2006).

53BP1 is a phosphorylation target of ATM/ATR in response to DNA damage (Ward et al., 2003). Moreover, in 53BP1-depleted cells, the phosphorylation of downstream targets including Chk2, BRCA1 and SMC1 was shown to be inhibited (DiTullio et al., 2002; Wang et al., 2002). 53BP1 also potentiates the autophosphorylation ATM at Ser1982, although the exact mechanism of how it carries out this function remains unclear (Wilson and Stern, 2008).

1.8.3 53BP1 in DNA repair

53BP1 has been implicated as a facilitator in the NHEJ repair pathway and in the absence of 53BP1 cells exhibit increased genomic instability (Adams and Capenter, 2006; Nakamura et al., 2006). Specifically, mice null for 53BP1 exhibit defects in class switch recombination (CSR) and V(D)J recombination, two processes that produce DNA intermediates with DSBs (Manis et al., 2004; Ward et al., 2004; Difilippantonio et al., 2008). Long-range rearrangements from distal

gene segments were diminished in 53BP1-null thymocytes, suggesting that 53BP1 is involved in promoting NHEJ during V(D)J recombination by facilitating the mobility of broken DNA ends (Difilippantonio et al., 2008). Indeed, 53BP1 increases the mobility of uncapped telomere ends (achieved by using *TRF2*-deficient cells) therefore increasing their capacity to be fused (Dimitrova et al., 2008). The ability of 53BP1 to modulate chromatin mobility has also implicated it in the repair of heteromchromatin, which is repaired relatively late in the repair process due to remodelling events (Noon et al., 2010).

Recently, a role for 53BP1 in the choice between DSB repair pathways (HR vs NHEJ) has been established (Nakamura et al., 2006; Xie et al., 2007). Whilst 53BP1 promotes NHEJ, disruption to 53BP1 activity leads to increased HR pathway choice (Nakamura et al., 2006; Xie et al., 2007). Furthermore, importantly, loss of 53BP1 leads to the increased viability of *Brca1*-null cells and *Brca1*$^{\Delta 11/\Delta 11}$ mice, which express a truncated form of the protein (Cao et al., 2009; Bouwman et al., 2010). Moreover, *Brca1*$^{\Delta 11/\Delta 11}$*53bp1*$^{-/-}$ mice develop normally and do show premature aging or increased cancer rates. In this context, loss of 53BP1 in *Brca1*-deficient cells leads to increased HR, which is initiated by DNA end resection (Bouwman et al. 2010; Bunting et al., 2010). This therefore suggests that 53BP1 promotes the NHEJ pathway by inhibiting DNA end resection, thus inhibiting HR (Boulton, 2010). Limiting resection may be important for the long duration needed for long-range rejoining events during NHEJ (Goodarzi et al., 2010). The molecular mechanism for 53BP1 inhibition of the HR remains to be determined, though it has been postulated that BRCA1 ubiquitylation of CtIP may enhance its ability to promote resection (Boulton, 2010).

1.8.4 Recruitment of 53BP1 to sites of DNA damage

53BP1 is recruited to DSBs via both γ-H2AX-dependent and independent mechanisms (Yuan et al., 2010; Pei et al., 2011). The γ-H2AX dependent mechanism was described previously. However it remains to be clarified how histone ubiquitylation regulates the recruitment of 53BP1 to DSBs as 53BP1 does

not contain any ubiquitin binding domains (Bekker-Jensen and Mailand, 2010). One possibility is that there is an ubiquitin-binding protein that may facilitate 53BP1 recruitment to DSBs, or that 53BP1 does have some intrinsic ubiquitin binding ability. Interestingly, 53BP1 associates with the de-ubiquitylating enzyme USP28. Another theory posits that histone ubiquitylation promotes local chromatin relaxation, which in turn exposes histone residues. Accordingly, 53BP1 has been shown to bind both H3K79me2 and H4K20me2 via its Tudor domain (Huyen et al., 2004; Botuyan et al., 2006). Until recently, it was believed that H4K20me2 levels did not change upon DNA damage, indicating that *de novo* histone methylation is not promoting 53BP1 recruitment (Fitzgerald et al., 2009). This therefore suggested that alterations in the chromatin structure imposed during DNA damage promoted the exposure of H3K79me2 and H4K20me2 residues that bind 53BP1 (Fitzgerald et al., 2009). This proposal has been challenged very recently by the finding that a methyltransferase, MMSET, actually causes local accumulation of methylated H4K20, which is undetectable by western blot due to the high background levels of this modification in cells (Pei et al., 2011). Down-regulation of MMSET or mutation of critical residues in its methyltransferase domain inhibited 53BP1 recruitment to IRIF, but not the formation of γ-H2AX or recruitment of MDC1 and RNF8 (Pei et al., 2011). MMSET recruitment to IRIF does seem to require both γ-H2AX and MDC1 with MMSET interacting with MDC1 in a DNA damage-dependent manner, which was correlated with its phosphorylation at S102 by ATM (Pei et al., 2011). Importantly, MMSET recruitment to IRIF was not affected by RNF8, suggesting that 53BP1 may be recruited to DSBs by both RNF8-dependent and independent mechanisms (Pei et al., 2011).

53BP1 may also be recruited to DSBs in a γ-H2AX-independent manner, as exemplified using H2AX-null cells (Celeste et al., 2003). 53BP1 interacts with the MRN complex, via NBS1, and requires the MRN complex for transient tethering at DSB sites (Lee et al., 2010; Yuan and Chen, 2010).

1.9 DNA damage checkpoints

In response to genotoxic insults, cells must initiate checkpoints to attenuate cell cycle progression and arrest replication, therefore preventing DNA lesions from being converted to inheritable mutations (Zhou and Elledge, 2000; Lukas et al., 2004; Bartek and Lukas, 2007). Cell cycle arrest is essential to allow DNA repair or, if the damage is beyond repair, engage an apoptotic or senescence pathway. After DNA damage, the two apical PIKKs, ATM and ATR, are activated and are responsible for downstream signaling events that play the central roles in initiating the checkpoints (Li and Zou, 2005; Cimprich and Cortez, 2008). As mentioned previously, ATM is activated primarily in response to DNA double-strand breaks, whereas ATR is activated by a broad array of DNA damage and replication interference (Jackson and Bartek, 2009). ATM and ATR phosphorylate two major signal-transducing kinases, Chk1 and Chk2, which in turn regulate downstream targets, such as Cdc25 and p53, to control cell cycle progression and DNA synthesis (Shiloh, 2003; Bartek and Lukas, 2007). The Cdc25 family of phosphatases are key targets of Chk1 and Chk2 and three isoforms exist in mammalian cells, A, B and C (Aressy and Ducommun, 2008). Whilst Cdc25A controls cell cycle progression through S-phase and mitosis, Cdc25B and C control mitotic entry. The spatiotemporal regulation of damage signals is integrated into three distinct cell cycle checkpoints: G_1/S-phase, intra-S phase and G_2/M-phase. Before describing each of these, it is noteworthy to highlight that DNA damage checkpoints operate at two levels. The initial checkpoint response causes a rapid cell cycle arrest and generally proceeds by the phosphorylation of target substrates (e.g. Cdc25) to impede cell cycle progression. The second layer to this checkpoint activation is a delayed and sustained response from the cell cycle machinery, as a result of transcriptional activation in response to DNA damage (Lukas et al., 2004). This slower response is essential as it allows the integration of the DDR signals over time (Figure 1.15).

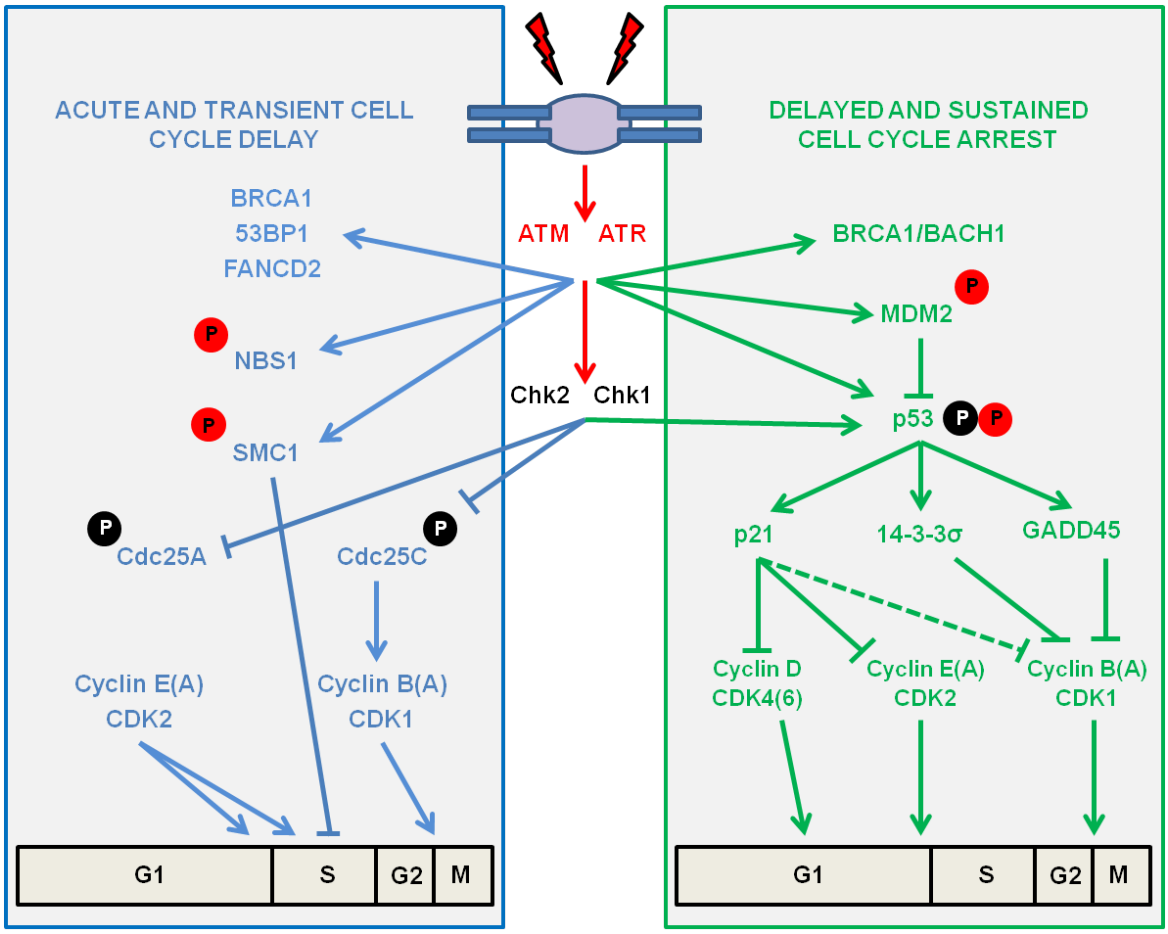

Figure 1.15 Checkpoint signaling initiates both a transient and sustained cell cycle arrest. DNA damage induces both a rapid transient cell cycle arrest via protein-protein signalling, and also a transcriptional program to enforce and sustain the cell cycle arrest. The apical PIKKs ATM and ATR, together with the Chk1 and Chk2 kinases initiate a cascade of signalling ensuring activation of cell cycle checkpoints (Lukas et al., 2004).

1.9.1 G_1/S-phase checkpoint

Damage induced during G_1-phase initiates a checkpoint that prevents the initiation of DNA replication in the presence DNA lesions. The cellular target of active unphosphorylated Cdc25A is the cdk2-cyclin E complex. Cdc25A dephosphorylates the cdk2-cyclin E complex, which maintains its active state, thus promoting cell cycle progression. In response to DNA damage, Chk1 and Chk2 phosphorylate Cdc25A, which in turn is ubiquitylated by the $SCF^{\beta TrcP}$

ubiquitin ligase, thus inducing its degradation via the ubiquitin-proteasome pathway (Mailand et al., 2000). The CDK2-cyclin E complex is therefore hyperphosphorylated, at Tyr15 of CDK2, rendering it inactive and hence promoting a G_1/S-phase arrest (Mailand et al., 2000; Bartek and Lukas, 2001; Falck et al., 2001). This rapid p53-independent pathway of phosphorylation and ubiquitylation is responsible for the initial early response to DNA damage. However, for a sustained cell cycle arrest, DNA-damage dependent transcriptional activation of p53 is necessary. Both ATM/ATR and Chk1/Chk2 can phosphorylate p53 in response to DNA damage at various residues (Milczarek et al., 1997). As well as phosphorylation, p53 undergoes a myriad of other post-translational modifications that, together, results in its stabilisation and the activation of its DNA-binding domain, enhancing its transcriptional ability (Vousden and Prives, 2009). One target of p53-dependent transcription is the cell cycle inhibitor, $p21^{WAF1}$, which suppresses CDK2-cyclin E, therefore reinforcing the G_1 checkpoint arrest initiated by Cdc25A destruction (Figure 1.15) (Poehlmann and Roessner, 2010). Interestingly, it has been shown recently that p53 undergoes oscillations driven by the continued activation of ATM due to the persistence of DNA damage in a feedback mechanism involving WIP1 phosphatase and MDM2 E3 ubiquitin ligase (Batchelor et al., 2008; Loewer et al., 2010). This suggests a regulatory feedback mechanism where DNA damage can signal to cell cycle regulators, thereby facilitating crosstalk between the two pathways.

1.9.2 Intra-S-phase checkpoint

DNA damage encountered during S-phase results in the destruction of Cdc25A, therefore inhibiting the loading of Cdc45 onto DNA pre-replication complexes (Bartek and Lukas, 2001; Falck et al., 2001). This pathway initiates and sustains the intra-S-phase checkpoint response that can last several hours and is independent of both p53 and p21 (Bartek and Lukas, 2001).

1.9.3 G_2/M-phase checkpoint

The G_2/M checkpoint prevents cells from entering mitosis with DNA lesions and therefore transmitting the damage to daughter cells (Lukas and Bartek, 2004). The G_2/M checkpoint functions in a similar fashion to the G_1/S checkpoint with an initial rapid transient response and a delayed sustained response. The initiating step for mitotic entry is the activation of the CDK1-cyclin B1 complex by dephosphorylation. Activated CDK1-cyclin B1 activates Cdc25C and inactivates Wee1, therefore forming two positive feedback loops. In response to DNA damage, Chk1 and Chk2 phosphorylate Cdc25C and therefore prevent the dephosphorylation of the CDK1-cyclin B1 complex necessary for mitotic entry (Figure 1.15).

1.10 The importance of the DDR in human physiology

1.10.1 The DDR and cancer

Defects in genes that encode members of the DDR are found in most cancer types. Furthermore, the broad range of diseases caused by mutations in DDR proteins exemplifies their importance to human physiology (Hoeijmakers, 2009; Jackson and Bartek, 2009: Kerzendorfer and O'Driscoll, 2009; Negrini et al., 2010; Ciccia and Elledge, 2010; Hanahan and Weinberg, 2011). For example, defects in the nucleotide excision repair pathways proteins XPA-XPG can cause xeroderma pigmentosum, a disease characterised by hypersensitivity to UV and which results in a 2000-fold higher risk of skin cancer in patients than the general population (Hoeijmakers, 2009). Defects in the mismatch repair pathway are associated with hereditary non-polyposis colon cancer, whilst mutations in the base excision have been associated with colorectal tumours (Negrini et al., 2010). Mutations in DDR genes that predispose patients to the development of various cancers are characterised by chromosomal instability (CIN) and include *BRCA1*, *BRCA2*, *BRIP1*, *Rad50*, *NBS1*, *WRN*, *BLM* and *REQL4* (Jackson and Bartek, 2009).

Hereditary cancers caused by mutations in DDR genes support the mutator hypothesis of cancer development, which posits that "...genomic instability is present in precancerous lesions and drives tumour development by increasing the spontaneous mutation rate..." (Loeb, 1991; Kinzler and Vogelstein, 1997; Halazonetis et al., 2008; Negrini et al., 2010). Therefore, patients with hereditary mutations in DDR proteins may exhibit increased genomic stability and cancer development if a single event leads to loss of any remaining wild type allele (Negrini et al., 2010). Interestingly, the evidence for mutations in DDR genes found in sporadic cancers is severely lacking. The past few years have seen the fruition of high-throughput cancer genome sequencing studies that have detailed the mutations and chromosomal rearrangements in various cancer types (Sjoblom et al., 2006; Wood et al., 2007; Ding et al., 2008; Jones et al., 2008; Parsons et al., 2008; Parsons et al., 2011; Varela et al., 2011). An analysis of five of these studies by Negrini et al., (2010) showed a paucity of mutations in DDR genes (Sjoblom et al., 2006; Wood et al., 2007; Ding et al., 2008; Jones et al., 2008; Parsons et al., 2008). The authors of this analysis go on to argue that the mutator hypothesis predicts that mutations in DDR genes would be frequent in sporadic cancer development, which is in stark contrast to the high-throughput sequencing data. Therefore, they suggest that the CIN seen in sporadic cancers may be explained by the oncogene-induced DNA replication stress model, which postulates that the oncogene-induced collapse or replication forks results in DSBs and genomic instability (Bartkova et al., 2005; Bartkova et al., 2006; Di Micco et al., 2006; Halazonetis et al., 2008; Negrini et al., 2010). However, this model is by no means complete, for example telomere erosion and epigenetic modifications are not taken into account by high-throughput sequencing. Furthermore, recessive mutations in DDR genes are necessary for loss-of-function in most cases, which would be rare events in sporadic cancers. Thus, further work is needed to identify genes responsible for CIN in sporadic cancers and define the role of the DDR in cancer progression

1.10.2 The role of the DDR in premature aging

Defects in several DNA repair proteins lead to various premature aging phenotypes, some of which also exhibit increased cancer incidences (Hoeijmakers, 2009). In general, defects in genes that encode DNA repair proteins involved in preventing mutagenesis are generally associated with a predisposition to cancer. Alternatively, defects in genes that encode proteins that protect cells from the cytotoxic effects of DNA damage exhibit low rates of cancer and a premature aging phenotype (Garinis et al., 2008). For example, mutations in the GG-NER pathway protein XPA give rise to xeroderma pigmentosum, which is characterised by cancer predisposition but not a premature aging phenotype (Ciccia and Elledge, 2010). In contrast, mutations in the TC-NER pathway give rise to Cockayne Syndrome, a segmental premature aging disorder. Both humans and mouse models do not show increased rates of cancer despite this pathway being involved in the DNA repair process. It has been suggested that the premature aging phenotype and low incidences of cancer is because the TC-NER pathway constitutes only a small part of all the DNA repair pathways. However, defects in this pathway do induce cell death and thus prevents these mice from developing cancer (Hoeijmakers, 2009). This example highlights the balance between anti-aging and anti-cancer pathways that cells must engage to protect the genome. In the case of Cockayne Syndrome, the anti-cancer pathway results in increased cell death and senescence, which promotes aging, but prevents tumour formation (Garinis et al., 2008).

1.10.3 The role of DNA damage in cellular senescence

Senescent cells exhibit a range of different cellular characteristics compared to replicative cells, including gene expression profiles, ROS levels, telomere length and morphology (Campisi, 1998). Cells will undergo replicative senescence due to the erosion of telomere ends, i.e. telomere-dependent senescence (Toussaint et al., 2000; Passos et al., 2007). This process is non-stress induced. However, if cells are exposed to oxidative stress, then a variety of DNA damage occurs, including oxidized bases, SSBs and DSBs. DSBs trigger a DNA damage

response that, if persistent, can activate senescence via the p53 and pRb tumour suppressors (Campisi, 2005). Thus, cells may undergo senescence as a response to persistent DSBs, which is telomere-independent and may be called stress induced premature senescence (SIPS) (Passos et al., 2007). As mentioned above, oncogene-induced DNA replication stress causes activation of the DDR , resulting in oncogene-induced senescence (OIS), a process that acts as a barrier to malignant progression (Bartkova et al., 2005; Braig et al., 2005; Bartkova et al., 2006; Di Micco et al., 2006; Bartek et al., 2007). Functionally, senescence represents an example of limited investment in long-term somatic maintenance and repair function (Kirkwood, 2005). On one hand, senescent cells cannot initiate tumours once they have exited the cell cycle, yet their presence within the cellular milieu has negative consequences on surrounding cells as they behave in an "...antisocial manner...", secreting growth factors and proteases that both encourage nearby tumors to metastasize and degrade tissue function (Campisi, 2005).

1.11 Aging

1.11.1 Overview

Organismal aging, as a process, has been succinctly described as the "...overall decline in the functional capacity of various organs to maintain baseline tissue homeostasis and to respond adequately to physiological needs under stress..." (Sahin and DePinho, 2010). The underlying causes of aging are therefore likely to be numerous and complex depending on the tissue type. For example, how does brain tissue, a largely non-proliferative tissue age compared to intestinal tissue, which is highly proliferative? To answer such questions, some 300 theories of aging have been postulated (Kirkwood, 2005). It is generally believed that stochastic damage to proteins and DNA, as a result of both endogenous (radical oxygen and nitrogen species) and exogenous (e.g. radiation, chemicals) reagents, accumulates during an organism's lifetime to contribute to tissue decline and aging (Campisi, 2003; Hasty et al., 2003). Therefore, mechanisms to repair this damage are at the centre of the aging phenotype as deterioration of their function over time causes deleterious effects on tissue homeostasis and tumour suppression (Kirkwood, 2006; Garinis et al., 2008). Underlining this, mutations in genes involved in preserving genomic stability can give rise to various premature aging syndromes, with some displaying increased risk of cancer (Jackson and Bartek, 2009; Sinclair and Oberdoerffer, 2009; Ciccia and Elledge, 2010). However, the stochastic damage model of aging has been challenged by the finding that mutations in the insulin/insulin-like growth (IGF) factor signalling pathway actually extend lifespan in *C.elegans, Saccharomyces cerevisiae* and *Drosophila melanogaster* (Schumacher et al., 2008). In mice, various genetic changes that lead to extended lifespan are all characterised by downregulation of the IGF signalling pathway, suggesting that this pathway is central to organismal aging (Monnat Jr, 2007; Schumacher et al., 2008). In addition genetic components of the target of rapamcyin (mTOR) pathway and the mitochondrial electron transport chain may also extend lifespan if they are downregulated (Vijg and Campisi, 2008). In addition, dietary restriction can extend lifespan by

dampening the three pathways mentioned above. Organisms thus seem to exhibit a degree of plasticity in terms of longevity that may be influenced by intrinsic and extrinsic factors (Kirkwood, 2006; Vijg and Campisi, 2008).

From an evolutionary perspective, various hypotheses exist as to why organisms age (Kirkwood, 2002). One prevailing hypothesis is the 'disposable soma theory', which posits that aging results from a trade-off between reproduction and somatic maintenance/repair (Kirkwood, 2002). This theory suggests that extrinsic mortality is a central driver of longevity. Thus, for short-lived organisms, with high extrinsic mortality, there is little selective pressure to invest energy in maintenance/repair pathways necessary to preserve somatic cells. In contrast, long-lived organisms require functional maintenance/repair pathways to preserve somatic tissues and ensure longevity (Kirkwood, 2002). Therefore, in the case of humans, eliminating extrinsic hazards means that aging can be seen as the persistence of genotypes that have escaped natural selection (Campisi, 2003). In essence, aging is a result of the decline in the force of natural selection (Campisi, 2003). In this context, it is important to consider another evolutionary theory of aging, the concept of 'antagonistic pleiotropy' (Campisi, 2003). This posits that a gene, genetic pathway or process may be beneficial to an organism in young age, but deleterious to an organism in old age (Campisi and D'Adda di Fagagna, 2007). In this scenario, because the force of natural selection diminishes with age, genes that benefit an organism in early life but have deleterious effects in later life are not selected against, allowing their generational persistence (Campisi, 2003). One such mechanism that exhibits antagonistic pleiotropy is cellular senescence, which may act as a tumour suppressor in young age, yet contribute to the decline in tissue homeostasis in old age (Campisi and D'Adda di Fagagna, 2007).

1.11.2 Cellular aging and senescence

Most somatic cells have a limited capacity to divide *in vitro*, first recognised nearly fifty years ago (Hayflick and Moorhead, 1961). After a finite number of divisions, somatic cells enter a permanent G_1-phase arrest termed cellular senescence

(Campisi, 2003). Despite their non-proliferative state, senescent cells are still viable and metabolically active within their tissue niche. Senescent cells have several notable features that distinguish them from non-senescent cells. This senescent phenotype includes apoptosis resistance, altered gene expression profiles with the notable upregulation of several CKIs, the formation of senescence-associated heterochromatin foci (SAHF), senescence-associated DNA damage foci (SDFs), the secretion of pro-inflammatory cytokines termed the senescence-associated secretory phenotype (SASP) and an increase in senescence-associated β-galactosidase activity (SA β-gal) as well as a loss of proliferative markers such as PCNA and BrdU incorporation (Campisi and D'Adda di Fagagna, 2007; Coppe et al., 2010; Freund et al., 2010).

Although senescence has been extensively characterised using a variety of cell types *in vitro*, its relevance to aging *in vivo* has recently emerged (Minamino and Komuro, 2008). Using senescence markers as described above, several studies have shown that tissues from human, primates and rodents contain senescent cells that increase with the age of the tissue, most notably in renewable tissues (Janzen et al., 2006; Krishnamurthy et al., 2006; Molofsky et al., 2006; Jeyapalan et al., 2007). Importantly, senescent cells have been shown at sites of age-related diseases such as osteoarthritis and atherosclerosis and their presence has also been shown inhibit liver fibrosis (Vasile et al., 2001; Krizhanovsky et al., 2008). Thus, understanding *in vitro* senescence pathways and mechanisms will help unravel how and why senescence contributes to aging *in vivo*.

Senescence can either derive from telomere-dependent or independent mechanisms (Touissant et al., 2000; Campisi and D'Adda di Fagagna, 2007). Telomere-dependent senescence results from telomere erosion with each cell division and this is termed replicative senescence, whilst telomere-independent mechanisms (e.g. sub-lethal exposure to oxidative stress and radiation or telomere uncapping) lead to stress-induced premature senescence (SIPS) (Toussaint et al., 2000).

1.11.2.1 Telomere-dependent or replicative senescence

To counter the problems of having linear chromosomes, i.e. how to prevent end degradation and recognition of the ends as double strand breaks, cells have evolved telomeres, structures that adorn the ends of chromosomes (Blasco, 2007). In germline cells and some cancers, telomeres are maintained by the enzyme telomerase (O'Sullivan and Karlseder, 2010). However, telomerase is not expressed in most normal cells and progressive telomere shortening occurs as somatic cells divide *in vitro*, which culminates in permanent cell cycle arrest termed replicative senescence (Toussaint et al., 2000; de Lange, 2005). Cells that fail to undergo replicative senescence in the presence of dysfunctional telomeres display gross genomic instability, which in turn promotes malignant tumorigenesis (Artandi and DePinho, 2000). Overexpression of TERT, the catalytic subunit of telomerase, in somatic human cells allows infinite cell divisions, underlining that telomerase expression circumvents replicative senescence (Bodnar et al., 1998). A correlation between increased telomere length and longevity has been reported in centenarians, suggesting that telomere length is an important determinant of human aging (Atzmon et al., 2010). Moreover, reduced telomere length has been correlated with increased risk of cardiovascular disease, dementia and aging of the immune system (Blasco, 2007; Sahin and DePinho, 2010). Various segmental and unimodal premature aging syndromes are associated with dysfunctional telomere maintenance, such as the Werner's syndrome, ataxia telangiectasia (AT), dyskeratosis congenita, Hutchinson–Gilford progeria syndrome (HGPS) and Bloom syndrome (Blasco, 2007; Sahin and DePinho, 2010).

Whilst telomere shortening in humans is associated with replicative senescence, mouse cells, which contain long (>20 kb) telomeres and express telomerase, undergo only a few population doublings in culture before undergoing senescence, therefore suggesting that telomere shortening is not the primary cause of senescence in mouse cells (Campisi, 2005; Campisi and D'Adda di Fagagna, 2007). The early senescence of mouse cells is associated with the high levels of oxygen (20%) used in culture conditions, which causes irreversible DNA

damage (Parrinello et al., 2003). Importantly, culturing mouse cells at lower physiological oxygen levels (3%) allows unlimited proliferation (Parrinello et al., 2003). Recently, ground-breaking studies utilising *Tert*$^{-/-}$ mice have yielded important insights into the role of telomeres in aging (Jaskelioff et al., 2011; Sahin et al., 2011). In the first study, the authors used a mouse model that allowed for the reactivation of telomerase in prematurely aged adult mice and showed that age-related decline phenotype of a number of tissues was reversed within 4 weeks of reactivation (Jaskelioff et al., 2011). This study highlights that aging may be prevented be targeting telomere structure and or regulation. The second study from the same group showed that telomere dysfunction causes activated p53 to suppress the master regulators of mitochondria, the *PGC-1* genes, which in turn leads to age-related mitochondrial dysfunction. Mitochondrial dysfunction then leads to oxidative stress by increased ROS levels, causing damage to both nuclear and mitochondrial DNA. This cycle contributes to the aging phenotype and provides a clear link between telomere loss and signalling events between the nucleus and mitochondria (Sahin et al., 2011).

Structurally, telomeres are long repetitive stretches of tandem DNA repeats (5'-TTAGGG-3') that are bound by proteins that make up the shelterin complex (Figure 3.1) (de Lange, 2005; Blasco, 2007). In humans, these tandem repeats vary between chromosomes, but are typically 9-15 kb, whereas mouse cells have exceptionally long telomeres and can be up to 100 kb (O'Sullivan and Karlseder, 2010). DNA polymerases cannot completely replicate the ends of DNA by lagging strand synthesis, a phenomenon termed the 'end replication problem', which results in the loss of 50-200 base pairs during each round of DNA replication. Thus, many cell divisions are required before telomere length is sufficiently shortened to elicit senescence promoting signals. However, as little as one shortened telomere is sufficient to trigger senescence (Martens et al., 2000; Hemann et al., 2001).

Telomeric DNA ends with a single-stranded 3' G-rich overhang of 50-300 nucleotides, which folds back onto duplex telomeric DNA forming a 'T-loop', a large circular structure (Figure 1.16) (de Lange, 2005; Blasco, 2007). The T-loop has been proposed to exist in two conformations: open and closed. The closed conformation forms a protective barrier to the end of the chromosome, preventing both telomerase access and the recognition of the end as a double strand break by ATM and ATR kinases.

As telomeric DNA is quite distinct in its properties, a plethora of proteins known as the shelterin complex have evolved to facilitate its stability and regulation by interacting directly or indirectly with the telomeric DNA, such as TRF1, TRF2 (both of which bind the double-stranded telomeric DNA), POT1 (which attaches to the single-stranded overhang), Rap1, TIN2 and TIP1 (De Lange, 2005; Blasco, 2007). Together, the shelterin complex covers both the double and single-stranded DNA of telomeres and also participates in cell-cycle dependent interactions with a number of different proteins (Blasco, 2007). Furthermore, the shelterin complex also prevents the activation of DNA damage signaling pathways, with TRF2 inhibiting ATM and POT1 inhibiting ATR (Figure 1.16).

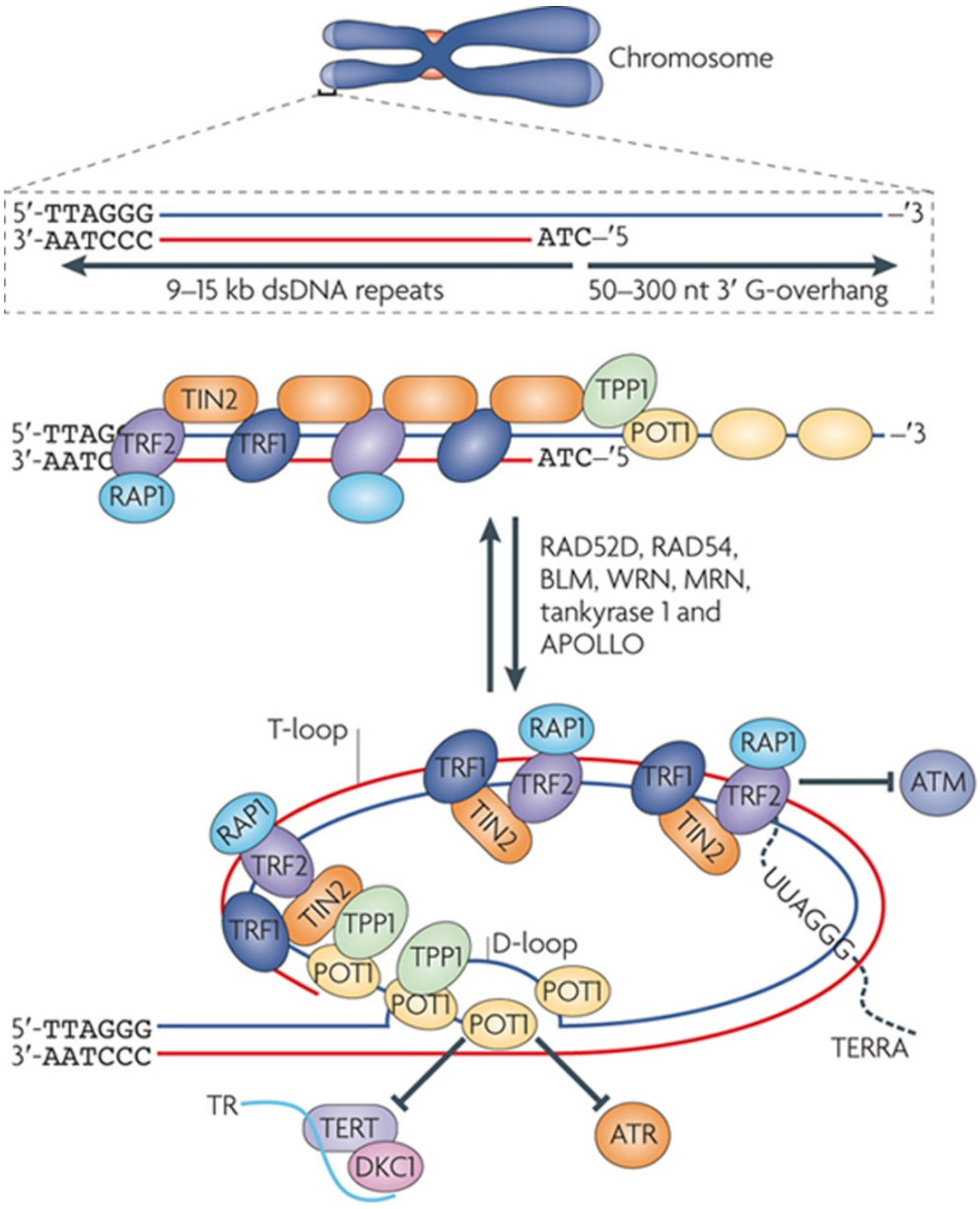

Figure 1.16 Structure of human telomeres. The chromosomes end in a structure called a telomere. Telomeres consist of TTAGGG repeats that may extend for numerous kilobases, resulting in a G-rich leading strand and a C-rich lagging strand (top). The G-rich strand extends for 50-300nt, forming a 3' G-overhang or G-tail (top). Numerous proteins, assemble at telomeres, forming the 'shelterin complex' (top and bottom). This complex protects the chromosome ends via the formation of a telomeric T-loop structure (bottom) (O'Sullivan and Karlseder, 2010).

1.11.2.2 Telomere-independent senescence or stress-induced premature senescence (SIPS)

Human fibroblasts may also undergo telomere-independent senescence due to chronic DNA damage or telomere uncapping, oxidative damage due to ROS and activation of oncogenes (Campisi and D'Adda di Fagagna, 2007). Telomere-independent senescence has also be termed 'stress induced premature senescence (SIPS) (Toussaint et al., 2000).

1.11.2.2.1 DNA damage

Chronic activation of the DNA damage response may induce senescence without the loss of telomeres (Toussaint et al., 2000; Suzuki et al., 2001). The major cause of senescence due to DNA damage is the persistent presence of double strand breaks, which may arise from both exogenous and endogenous reagents, e.g. radiation or replication fork collapse. Activation of the DNA damage response (DDR) by DSBs induces cell cycle arrest via both p53-p21 and p16-pRb pathways (see 3.1.3) (Herbig et al., 2004; Jacobs and de Lange, 2004). Telomere uncapping or disruption to proteins involved in the shelterin complex may also activate DDR-dependent senescence independent of telomere length (Chen et al., 2008). For instance, expression of dominant negative TRF2 mutants leads to dysfunctional telomeres, without telomere length shortening, and activates the DDR, leading to premature senescence (Takai et al., 2003). The importance of the DDR in aging is perhaps best exemplified by the range of different premature aging diseases associated with mutations in genes important to this pathway (Jackson and Bartek, 2009). Furthermore, a range of mouse models that have DDR proteins knocked-out exhibit premature aging phenotypes at both the organismal and cellular level, for instance *Brca1*, *Ku80*, *Ku70*, *Xrcc4*, *DNA-PKcs*, *Ercc1*, *Xpf1* and *Wrn* (Lombard et al., 2005).

1.11.2.2.2 Oxidative damage

The ‘free radical theory of aging’ posits that the balance between the production and elimination of intracellular reactive oxygen and/or nitrogen species (ROS/RNS) is the major determinant of cellular lifespan (Harman 1956). Whilst normal levels of intracellular ROS are required for signalling pathways, higher levels of ROS cause direct damage to a range of macromolecules, including lipids, protein, RNA and DNA (Blumberg, 2004). ROS are generated primarily in the mitochondria through aerobic respiration, the products of which include superoxide radical (O_2^-) and hydroxyl radical (OH^-), and non-radical molecules like hydrogen peroxide (H_2O_2) (Kregel and Zhang, 2007). As an extension of the free radical theory of aging, a mitochondrial theory of aging has been proposed, which speculates that electrons leaking from the electron transport chain produce ROS, which in turn damages the mitochondrial DNA, leading to further increases in intracellular ROS levels and a decline in mitochondrial function (Wallace, 2005). As direct evidence for this, studies suggest that mitochondrial DNA damage is increased with aging (Hamilton et al., 2001; Hagen et al., 2004). Furthermore, an ‘inflammatory theory of aging’ has been suggested which postulates that pro-inflammatory gene expression is activated by the age-dependent increase in oxidative stress, which in turn leads to inflammation in a multitude of tissues and organs (Chung et al., 2006). Regardless of the theory, it is clear that intracellular ROS are also involved in pathogenesis of many age-related conditions, including cancer, atherosclerosis and neurodegenerative diseases (Haddad et al., 2004).

Mammalian cells are armed with a number of sophisticated antioxidant defence mechanisms that function to balance excessive ROS and prevent accumulation of ROS-induced oxidative damage (Kregel and Zhang, 2007). Primary antioxidant enzymes, including catalase (CAT), superoxide dismutase (SOD) and glutathione peroxidase (GPX) function in a series of integrated reactions to convert ROS to more stable molecules, such as H_2O and O_2. Furthermore, a multitude of secondary enzymes act synergistically with small molecular weight antioxidants (e.g., GSH, NADPH, thioredoxin (Trx), vitamins E and C, and trace metals, such

as selenium) to form redox cycles that provide cofactors for primary antioxidant enzyme functions (Kregel and Zhang, 2007). Small molecular weight antioxidants can also function as direct scavengers of ROS. In addition, ROS activates many transcription factors involved in stress signalling pathways such as Sp-1, AP-1 and NF-κB, which bind to anti-oxidant response elements (ARE) in gene promoters and regulate expression of stress response genes, some of which include those encoding the major anti-oxidant enzymes (Haddad, 2002). Another important aspect of redox homeostasis in cells involves the balance between reduced and oxidised forms of thiols. Protein thiols can serve as essential redox sensors in cells, which undergo reversible redox modifications in response to oxidative stress (Eaton 2006). Accumulating evidence suggests that thiol-based disulfide bridge formation represents a common strategy by which proteins respond to oxidative stress and mediate transient activation of protective stress responses (Linke and Jakob 2003). One important aspect of these protective stress responses is the ability of cells to undergo temporary growth arrest that allows time for repair of damaged DNA, regeneration of oxidized proteins and recovery of redox balance (Davies et al., 1999). At the cellular level, inability to recover the redox balance can lead to SIPS in human fibroblasts, which can be achieved experimentally by treatment with sub-lethal levels of oxidative stress such as H_2O_2 (Chen et al., 2004; Chen et al., 2005). Moreover, disruption to the anti-oxidant defence systems would thus also be predicted to induce SIPS. Indeed, inhibition of SOD1, which detoxified the superoxide anion, causes cells to undergo premature senescence (Blander et al., 2003). Conversely, increasing SOD1 levels actually increases cellular longevity in primary fibroblasts and reduces the rate of telomere shortening (Serra et al., 2003).

1.11.2.2.3 Oncogenic induced senescence (OIS)

Another form of telomere-independent senescence can be triggered by the expression of oncogenes, such as *H-RASG*^{12V} (Serrano et al., 1997; Wei et al., 1999; Gorgoulis and Halazonetis, 2010). Oncogene activation deregulates DNA replication, causing DSBs that trigger a sustained DDR, which causes cells to

enter senescence, preventing further proliferation (Bartkova et al., 2006; Di Micco et al., 2006). Evidence suggests that OIS operates *in vivo* as well as *in vitro*, underpinning this mechanism as an anti-tumorigenesis pathway (Gorgoulis and Halazonetis, 2010). OIS also induced large-scale chromatin changes, which may be visualised by the formation of several DNA-dense nuclear foci termed senescence-associated heterochromatin foci (SAHF) (Narita et al., 2003; Zhang et al., 2005; Di Micco et al., 2007). SAHF formation is under the control of the p16-pRb pathway and its proposed role is to repress local E2F-dependent gene transcription by promoting a repressive chromatin environment and also promoting global silencing via heterochromatin formation (Campisi, 2005). Recent evidence suggests that gene silencing and SAHF are two distinct pathways in OIS (Di Micco et al., 2011). Local gene silencing is dependent on the ATM-p53 pathway, which inhibits proliferation, whilst SAHF is governed by the ATR kinase and acts to dampen the DDR (Di Micco et al., 2011). The authors suggest that SAHF may therefore act to protect cell viability against apoptosis by reducing DDR signaling, although the physiological benefits of this remain to be determined.

1.11.3 p53 and p16-pRb pathways

The p53 and p16-pRb pathways are the two major tumour suppressor pathways that are engaged in response to senescence-inducing signals (Campisi, 2005). Various signals activate either one or both pathways, for example, oncogenic Ras activates both pathways. In the p53 pathway, DNA damage activates the *CDKN2A* locus, whose gene product ARF or p14 sequesters the E3 ubiquitin-protein ligase HDM2, which itself promotes p53 degradation (Campisi and D'Adda di Fagagna, 2007). Thus, p53 levels are increased, which in turn promotes transcription of target genes, one of which includes p21, a potent CKI that enforces cell cycle arrest by suppressing the inactivating phosphorylation of pRb (Figure 1.17). Oncogenic signals may also lead to the engagement of the p16-pRb pathway, usually by the induction of $p16^{INK4A}$, the other product of the *CDKN2A* locus. $p16^{INK4A}$ is a potent CKI that inhibits pRb phosphorylation, thereby

enforcing G_1-phase arrest and inhibiting E2F-dependent gene transcription, which is necessary for G_1/S-phase progression. Crosstalk between the two pathways also serves to control cellular proliferation and enforce senescence. From the p16-pRb pathway, E2F induces ARF expression whilst pRb also regulates p53 through a trimeric p53-HDM2-pRb complex (Campisi and D'Adda di Fagagna, 2007).

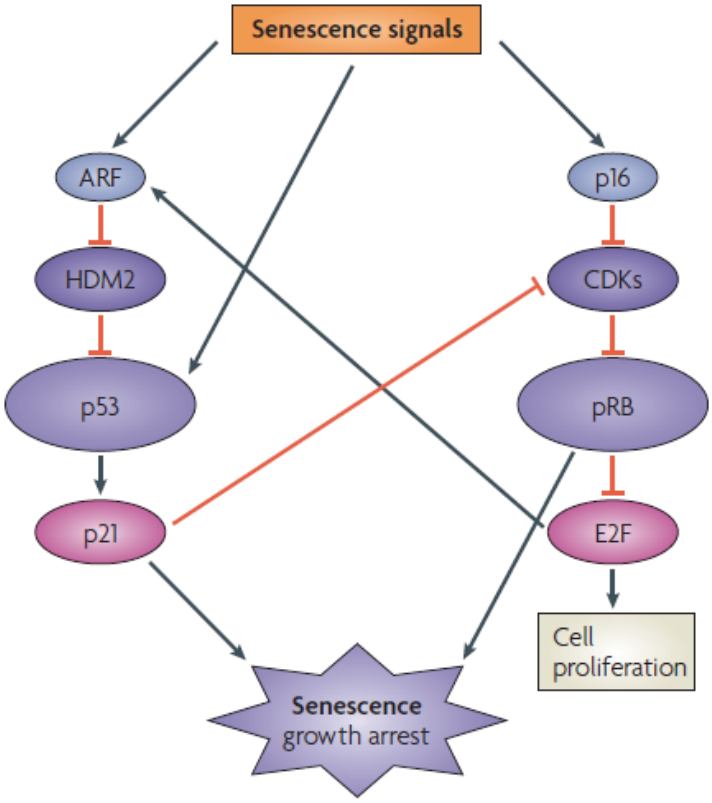

Figure 1.17 The p53 and p16-pRb pathways govern cellular senescence. Various signals such as dysfunctional telomeres, DNA damage, and excessive mitogenic signals (e.g. oncogenes) may trigger entry into senescence. Entry into senescence is channelled via the pRb or p53 pathways, however some signals (such as oncogenic Ras) engage both pathways. Moreover, there may be crosstalk between the pathways: p53 induces expression of p21, which inhibits pRB phosphorylation and E2F can induce ARF expression, which engages the p53 pathway (Campisi and D'Adda di Fagagna, 2007).

1.11.4 Aging: a trade-off between senescence and cancer

Within the context of aging, senescence can be seen as a tumour suppressor pathway in young organisms, acting to halt the potential transformation of cells that might promote cancer and ultimately organismal death. However, as explained above, senescent cells also secrete a range of factors that have been shown to actually promote cancer progression by stimulating proliferation, promoting angiogenesis and inducing epithelial-to-mesenchymal transition (EMT), a process which has been shown to aid cancer metastasis and invasiveness (Krtolica et al., 2001; Coppe et al., 2006; Coppe et al., 2008; Thiery et al., 2009). The antagonistic pleiotropy of senescent cells highlights that one pitfall of tumour suppression is their contribution to age-related tissue decline and thus they have a central role in the aging process (Campisi, 2005).

1.12 The Cell Cycle

1.12.1 Overview

The cell cycle is a highly complex and meticulously coordinated set of unidirectional spatiotemporal events that govern the production of two daughter cells from one mother cell. The controlled regulation of the cell cycle is vital for organismal development and tissue regeneration and renewal. Extensive work over the past century has shed light on the exquisite control of the numerous steps of cell cycle, the molecular basis of which is highly conserved throughout evolution (Nurse, 2000). The cell cycle is divided into four phases: G_1, S, G_2 and M. G_1-phase is the first gap phase whereby cells decide whether to divide or not, DNA replication then occurs during S-phase and the second gap phase, G_2, prepares the cell for mitosis or M-phase (Figure 1.18). During G_1-phase the integration of pro- and anti-growth signals dictates whether the cell passes a specialised commitment point, called the restriction point (Figure 1.18 'R'). If the cell passes the restriction point it is fully committed to DNA replication and completing a cell cycle (Vermuelen et al., 2003). If the cell decides not to pass the restriction point it may exit the cell cycle, either transiently or permanently, in a phase termed as G_0. If a cell encounters problems during the cell cycle then checkpoints are activated that halt progression until the problem is either rectified. Importantly, deregulation of the cell cycle machinery may lead to chronic proliferation of cells, a fundamental trait of all cancers (Hanahan and Weinberg, 2011). Whilst it would be impossible to describe all the proteins and mechanisms involved in the cell cycle in this thesis, I will cover some of the major proteins that are essential to drive this process.

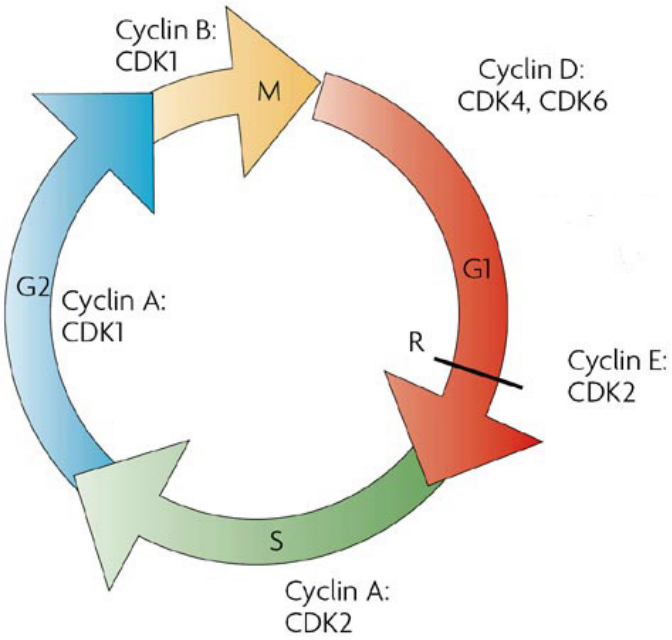

Figure 1.18 The eukaryotic cell cycle. The cell cycle is divided into four stages: two gap phases (G1 and G2), S-phase and mitosis (M-phase) (Dehay and Kennedy, 2007).

1.13 Cell cycle control

1.13.1 Cdks and cyclins

Central to the core of cell cycle regulation is the oscillatory action of the "...cell cycle engines..." cyclin dependent kinases (cdks) (Nurse, 2000). Cdks are serine/threonine protein kinases that are activated at specific stages of the cell cycle to phosphorylate targets substrates (Morgan, 1995). To date, nine cdks have been identified in mammals, five of which are active during the cell cycle (Vermeulen et al., 2003). Cdks may interact with more than one cyclin, which has been suggested to potentiate substrate selectivity for the cdk (Table 1) (Schafer, 1998). Interestingly, the activity of cdk1 alone is sufficient to drive the cell cycle during the early development of cell lineages (Santamaria et al., 2007).

Cdk	Cyclin	Cell cycle phase activity
Cdk4	Cyclin D1, D2, D3	G_1 phase
Cdk6	Cyclin D1, D2, D3	G_1 phase
Cdk2	Cyclin E	G_1/S phase
Cdk2	Cyclin A	S phase
Cdk1 (Cdc2)	Cyclin A	G_2/M phase
Cdk1 (Cdc2)	Cyclin B	M phase
Cdk7	Cyclin H	CAK, all cell cycle phases

Table 1. Cdk and cyclin complexes during the cell cycle. (Vermeulen et al., 2003)

Whilst cdk protein levels remain stable throughout the cell cycle, cyclin protein levels exhibit oscillatory fluctuations through the cell cycle. In this way cyclins are able to periodically activate cdks at the appropriate stage of the cell cycle and this mechanism provides the primary means of regulating the cell cycle (Figure 1.19) (Murray, 2004). The one exception is cyclin D, which is expressed in direct response to mitogenic signals and remains relatively high throughout the cell cycle (Assoian and Zhu, 1997). To date, sixteen cyclins have been identified in mammals, although not all are involved in cell cycle regulation (Johnson and Walker, 1999). Cyclins D1, D2 and D3 associate with cdk4 and cdk6 and regulate entry into G_1 past the restriction point (Bartek et al., 1997). Another G_1 cyclin, cyclin E associates with cdk2 and is essential for G_1/S-phase progression. Cyclin A interacts with cdk2 and is required for S-phase progression, whilst the association between cyclin A associates and cdk1 during late G_2 and early M-phase promotes entry into mitosis (Bardin and Amon, 2001). During mitosis, cyclin

B associates with cdk1 and governs progression through M-phase (Arellano and Moreno, 1997).

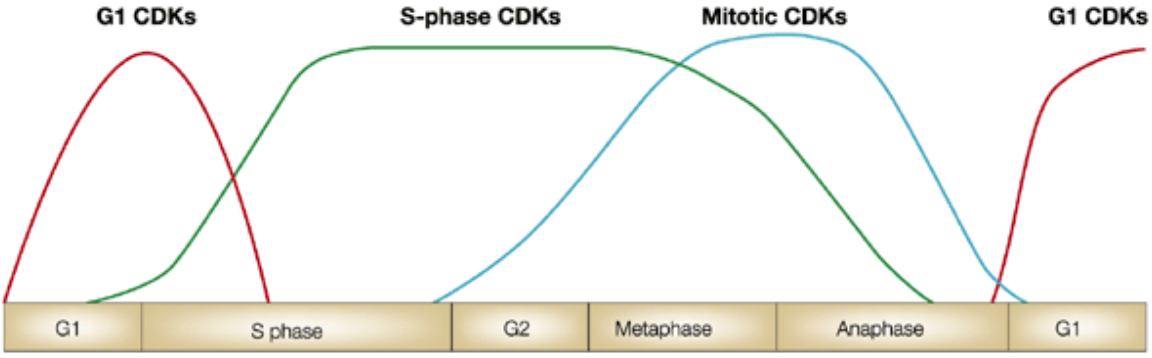

Figure 1.19. Activity of cdks through the cell cycle. Cdk activation requires interaction with a cyclin subunit (see Table 1) and phosphorylation of the cdk subunit by the CAK (Bardin and Amon, 2001).

Recent data from knockout mice has questioned the absolute requirement for D-type and E-type cyclins, cyclin D-dependent cdk4 and cdk6 and cyclin E-dependent cdk2 in cell cycle progression (Sherr and Roberts, 2004). Genetic ablation of all these cell cycle genes suggests that a degree of compensation may exist in the absence of a specific cdk-cyclin complex. It has also been suggested that other cdks, removed from the core control of the cell cycle during evolution, may step-in if required, "...the defeated remains of (other) ancestrally dominant kinases can be glimpsed in both DNA replication (the Cdc7/Dbf4 kinase/activator couple) and in mitosis (Polo and others)..." (Murray, 2004).

1.13.2 Phosphorylation events govern cdk activity

As well as associating with cyclins, complete cdk activation is also dependent upon phosphorylation of the cdk subunit on conserved threonine and tyrosine residues (Arellano and Moreno, 1997). Cdk1 is the prototypic cdk, being originally identified as cdc2 in yeast (Draetta et al., 1988). Depending on the residue, phosphorylation of cdk1 may be either stimulatory or inhibitory. For full activation, cdk1 must be phosphorylated on threonine 161 (Thr160 for cdk2 and Thr172 for

cdk4) by the cdk7-cyclin H complex, known as the cdk-activating kinase (CAK). Threonine 161 of cdk1 is within a T-loop motif, which, in its inactive unphosphorylated state, folds so as to sterically block cyclin binding. Subsequent phosphorylation of Thr161 induces a conformational change in the T-loop to enhance binding of cyclins (Jeffrey et al., 1995). In contrast, inhibitory phosphorylation of cdk1 is carried out on threonine 15 and/or threonine 14 by the Wee1 and Myt1 kinases (Nurse, 2004). The Thr14/15 residues are within the cdk1 kinase domain, and phosphorylation therefore inhibits its kinase ability. Wee1 kinase action is necessary on cdk1-cyclin complexes as they enter the nucleus to prevent premature mitotic progression (Heald et al., 1993). Dephosphorylation of Thr14/15 by Cdc25 phosphatase is required for cdk1 activation and cell cycle progression (Lew and Kornbluth, 1996; Schafer, 1998). Three isoforms of Cdc25 exist in mammalian cells: A, B and C (Aressy and Ducommum, 2008). Whilst Cdc25A controls cell cycle progression through S-phase and mitosis, Cdc25B and C control mitotic entry. Activated cdk1-cyclin complexes may phosphorylate both Wee1 and Cdc25C, which inactivates and activates them, respectively, therefore forming both a positive and negative feedback loop (Vermeulen et al., 2003).

Cdk activity may also be regulated physically, either by interaction with the cdk or cdk-cyclin complex, by cdk inhibitors (CKIs). There are two distinct protein families in metazoans that encode CKIs, INK4 and Cip/Kip (Sherr and Roberts, 1999). The Cip/Kip protein family includes $p21^{Waf1/Cip1/Sid1}$ (p21, encoded by *CDKN1A*), $p27^{Cip2}$ (p27, encoded by *CDKN1B*) and $p57^{Kip2}$ (p57, encoded by *CDKN1C*) (Susaki and Nakayama, 2009). The Cip/Kip family function to modulate cdk4,6-cyclin and cdk 2-cyclin complex activity by directly binding to both cdk and cyclin subunits (Sherr and Roberts, 1995; Hengst and Reed, 1998; Besson et al., 2008). Functionally, p21, p27 and p57 differ slightly in their specific biological roles depending on the cellular signals. For example, p21 has a well-established role in DNA synthesis and the DNA damage response. In the former it binds and inhibits PCNA (Waga et al., 1997). In the latter, p21 is a transcriptional target of activated p53 in response to DNA damage, therefore enforcing cell cycle checkpoints in G_1 and G_2 (Elledge, 1996; Gartel and Tyner, 1999). Furthermore, $p21^{-/-}$ MEFs exhibit a

failure to undergo DNA damage dependent cell cycle arrest (Deng et al., 1995). In contrast to p21, p27 functions in quiescent cells and mitogen-starved cells to enforce cell cycle exit and becomes rapidly degraded upon cell cycle entry (Besson et al., 2006). Crystal structures of p27 bound to the cyclin A-cdk2 complex revealed that p27 inserts itself into the catalytic cleft on cdk2 therefore preventing catalytic activity (Russo et al., 1996). The cellular proliferation restraining function of p27 is particularly striking in *p27*$^{-/-}$ mice, which exhibit organ hyperplasia and increased body size (Fero et al., 1996). Results from this knockout mouse highlights the importance of CKIs in development and underline that effective cell cycle exit (i.e. for terminal differentiation) is essential for tissue homeostasis and ultimately organismal survival.

The second protein family of CKIs consists of p15^{INK4b} (encoded by *CDKN2B)*, p16^{INK4a} (encoded by *CDKN2A*), p18^{INK4c} (encoded by *CDKN2C*) and p19^{INK4d} (encoded by *CDKN2D*) (Gil and Peters, 2006; Kim and Sharpless, 2006). The INK4 family of CKIs inhibit G_1 cdk4,6 in a mechanism distinct from the Cip/Kip CKIs, which have broader targets (Lukas et al., 1999). The INK4 family bind stably with cdk4,6 before they are able to interact with cyclins, therefore preventing their association and thus inhibits the phosphorylation of pRb and maintains cells in G_1 (see 1.14.1) (Brotherton et al., 1998; Russo et al., 1998; Murray, 2004). The expression of INK4 family proteins has been associated with permanent exit from the cell cycle into senescence (Campisi, 2005; Janzen et al., 2006). The induction of senescence plays an important role as an anti-tumorigenesis barrier and homozygous mutations in the INK4 CKIs are frequently found in various cancer subtypes (see 1.15) (Sharpless, 2005).

1.13.3 Ubiquitin-mediated proteolysis confers unidirectionality upon the cell cycle

Coupled to the activation of cdks is the ubiquitin proteolysis system (UPS), which is responsible for the timely destruction of cyclins through the cell cycle. The temporal irreversible destruction of cyclins during the cell cycle ensures that the

cell cycle may only proceed in one direction (Vodermaier, 2004). Two main ubiquitin ligases control the destruction of the cell cycle machinery: the SCF (Skp1–Cul1–F-box protein) complexes and the anaphase promoting complex/cyclosome (APC/C) (Vodermaier, 2004). Functionally, the F-box subunit within the SCF complex regulates substrate specificity (Jin et al., 2004). To date, there are sixty-nine F-box proteins, each of these F-box 'adaptors' may interact with multiple substrates, therefore providing a vast range of potential targets for the SCF complex (Skaar and Pagano, 2009). In contrast, the APC/C complex has two 'adaptor' proteins, Cdh1 and Cdc20, which are activated at different points in the cell cycle, G_0/G_1 and M-phases respectively, and recognise substrates on the basis of a degradation motif (degron) in their target proteins (Cardozo and Pagano, 2007).

APC/C^{Cdc20} levels are low in G_1-phase, but increase during S and G2-phases (Skaar and Pagano, 2009). In M-phase, APC/C^{Cdc20} forms but only becomes active until chromosomes are attached to the spindle and the Spindle Assembly Checkpoint (SAC) is satisfied. Upon activation, it promotes metaphase to anaphase transition by targeting Securin and Shugoshin for degradation, and also targets p21 for degradation during prometaphase (Frescas and Pagano, 2008). APC/C^{Cdh1} cooperates with APC/C^{Cdc20} to reset the cell cycle (i.e. to low cdk activity) and inhibits cdk2 and cdk1 activity by targeting cyclin A and B for destruction as well as Cdc20 and Cdc25A, thereby inhibiting APC/C^{Cdc20} activity. During G_1, APC/C^{Cdh1} also targets Skp2/Cks1, therefore preventing the premature degradation of SCF^{SKP2} targets such as p27 and thus acts to prevent G_1 progression (Figure 1.20) (Peters, 2006). From late G_1 to the end of mitosis, cdk-dependent phosphorylation of Cdh1 prevents its assembly into the APC/C core, which inhibits the activity of the APC/C^{Cdh1} complex (Peters, 2006). Furthermore, the APC/C^{Cdh1} complex is also inhibited by physical interaction with Emi1, allowing accumulation of mitotic cyclins (Figure 1.20). After the destruction of mitotic cyclins by APC/C^{Cdc20} Cdh1 is activated to form the APC/C^{Cdh1} complex and the APC/C subunit cycle may start again.

Two of the most widely studied SCF complexes are SCF^{SKP2} and $SCF^{\beta\text{-}TrCP1}$ (Figure 1.20). SCF^{SKP2} is responsible for ubiquitylating the CKI p27 in the presence of the accessory protein Cks1, but only when specific residues of p27 are phosphorylated (Nakayama et al., 2004; Guardavaccaro and Pagano, 2006). SCF^{SKP2} also promotes the degradation of p21, therefore acting as a positive regulator of the cell cycle by activating cdk1 and cdk2 (which are active from late G1 to anaphase, which is denoted as C-phase in Figure 1.20) (Frescas and Pagano, 2009). In contrast, $SCF^{\beta\text{-}TrCP1}$ acts as both a positive and negative regulator of the cell cycle by targeting Emi1, Wee1, claspin and Cdc25A. The $SCF^{\beta\text{-}TrCP1}$-mediated targeting of Emi1 in early prometaphase is dependent upon the prior phosphorylation of Emi1, the APC/C^{Cdh1} complex inhibitor, by both cdk1 and Plk1 (Yamasaki and Pagano, 2004).

Together, the concerted efforts of both the SCF and APC/C ubiquitin ligases, i.e. by regulating each other's activity, in combination with the oscillatory cdk activity network, help drive the cell cycle and provide unidirectional regulatory layers to the process that, unchecked, could result in uncontrolled proliferation and cancer (see 1.15).

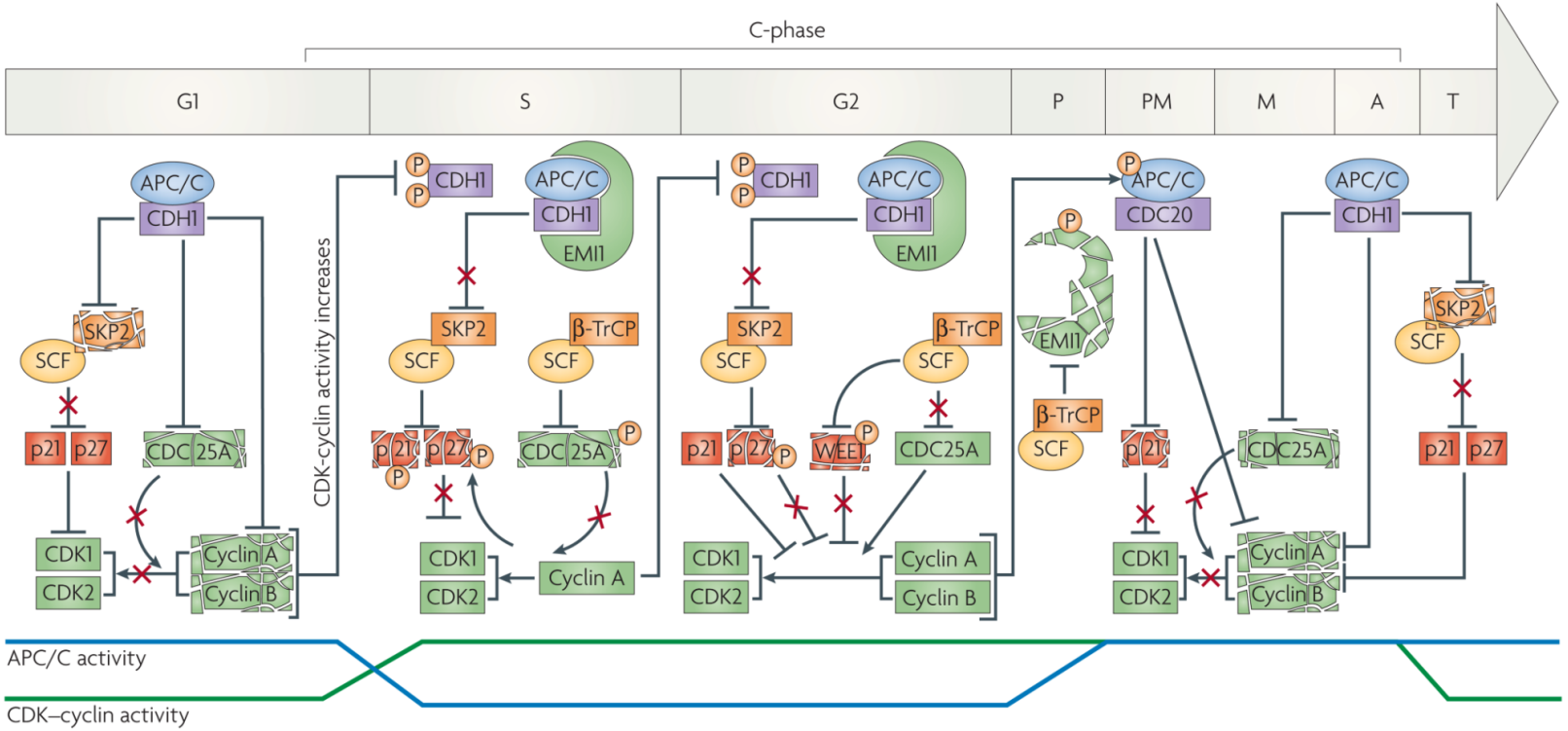

Figure 1.20. The ubiquitin-proteasome system (UPS) in the cell cycle. The combined actions of the APC/C and SCF ubiquitin ligases, in concert with the oscillatory nature of cdk activity, govern the cell cycle. Cdk-cyclin activity increases from late-G1 to anaphase (denoted as C-phase). APC/C^{Cdh1} helps reset the cell cycle (i.e. low cdk activity) by targeting cyclins A and B, as well as Cdc20 and Cdc25A. APC/C^{Cdc20} promotes metaphase to anaphase transition by targeting securing and Shugoshin for degradation. SCF^{SKP2} promotes degradation of the CKIs p21 and p27, whilst $SCF^{\beta\text{-}TrCP1}$ targets Cdc25A, Wee1 and Emi1 for degradation (Frescas and Pagano, 2009).

1.13.4 Nuclear localisation regulates cdk activity

The subcellular localisation of the cell cycle machinery plays an important role in the spatiotemporal regulation of the cell cycle (Takizawa and Morgan, 2000). Cyclins E and A both exhibit constitutive nuclear localisation, probably reflecting their vital roles in S-phase, i.e. DNA replication and prevention of re-replication. In contrast, cdk-cyclin D1 complexes are exported from the nucleus to the cytoplasm for proteolysis after phosphorylation by GSK3β (Diehl et al., 1998). The intracellular trafficking of cdk1-cyclin B complexes is by far the most studied among the cell cycle complexes. During interphase, cdk1-cyclin B complexes are sequestered in the cytoplasm, but during G_2-phase, are imported into the nucleus (Li et al. 1997). B-type cyclins contain a nuclear export signal (NES), which mediates an association with CRM1, the nuclear export protein, therefoe promoting its nuclear export and cytoplasmic localisation (Yang et al., 1998). Phosphorylation of cyclin B1 at prophase attenuates its nuclear export, whilst cyclin B2 remains in the cytoplasm until nuclear envelope breakdown.

The mechanism of nuclear import for the various cyclins varies dramatically, suggesting that they have evolved import mechanisms based on their temporal function within the cell cycle. Strikingly, neither cyclins nor their interacting cdks contain any putative classical nuclear localisation signals (NLS) (Yang and Kornbluth, 1999). However, studies revealed that, for cyclin B1 and cyclin E, the import signal is contained within these cyclins, yet they use distinct mechanisms for import (Moore et al., 1999). Cyclin E interacts with the importin α adaptor subunit of the importin α-β heterodimer and in this way acts as a classical basic NLS-containing protein. Cyclin B1, by contrast, is imported via interaction with importin β in the notable absence of the importin α adaptor subunit (Moore et al., 1999). It has been suggested that the non-classical import mechanism of cyclin B1 ensures a low import rate during interphase, therefore preventing inappropriate M-phase entry (Yang and Kornbluth, 1999).

1.14 Cell cycle phases

1.14.1 G_0 and G_1-phase

After cells have completed a cell division they are faced with the vital decision of whether to divide again or exit the cell cycle. The decision to engage another round of cell division is a highly regulated, multi-faceted process requiring the correct temporal functions of proteins to ensure the inheritance of preserved genomic material. Firstly, if the appropriate mitogenic signals are absent, cells enter G_0. This state may be applied to cells that exited the cell cycle permanently, such as nerve or muscle cells, or transiently, regardless, in both cases the cells are said to be quiescent. The G_0 state may also be applied to senescent cells, which are those cells that have exited the cells permanently but have engaged a different biochemical cellular program rendering them nonviable, therefore making them quite distinct from quiescent cells. As mentioned previously, the CKIs, including the Cip/Kip and INK4 families, have a prominent role in maintaining cells in a G_0. For example, $p15^{INK4b}$ and $p16^{INK4A}$ inhibit cdk-cyclin D complexes, whilst p21 and p27 inhibit cdk-cyclin D and cdk-cyclin E complexes. The ultimate downstream effector of all the pathways is the tumour suppressor, the retinoblastoma protein (pRb). The concerted synergy of the CKIs is to prevent phosphorylation of pRb, which is keenly inactivated by cdk-cyclin dependent phosphorylation, thereby allowing cell cycle progression, as discussed below. Furthermore, other members of the pRb protein family have prominent roles in actively maintaining cells in G_0, which will also be discussed below.

1.14.1.1 The Rb-E2F pathway

The tumour suppressor, pRb, is so named because it was identified as the primary cause of the rare childhood cancer retinoblastoma. Cloning of *RB* and the subsequent identification of homozygous inactivating mutations of *RB* supported earlier hypotheses that retinoblastoma was caused by two mutations, or two ‘hits’, which was then predicted to functionally inactivate a tumour suppressor gene (Knudson, 1971; Cavenee et al., 1983; Dunn et al., 1988). Studies to delineate its

function have shown that the *RB* gene product pRb is critically involved in cell cycle regulation along with two other family members, p107 and p130, in nearly all cell types (Dyson, 1998). pRb, p107 and p130 are collectively termed pocket proteins because their similar primary sequences form a bipartite pocket domain structure, which is important for interactions with both cellular proteins and viral oncoproteins, thus enabling pRb to exert its cellular function (Figure 1.21). Specially, pRb is a 928 amino acid protein that contains three important domains: A, B and C (Burkhart and Sage, 2008). The A and B domains form the AB pocket, which is critical for interaction with various proteins, including the transcription factor E2F (Figure 1.21). The AB pocket is separated by a spacer region, which in p107 and p130 contains a cdk-cyclin binding site, though it is absent from pRb (Zhu et al., 1995; Munger et al., 2003). The C domain of pRb enhances binding of the AB pocket to E2F (~ 10-fold) (Qin et al., 1992). The pocket proteins are also able to interact with proteins that contain an L-X-C-X-E domain, such as D-type cyclins and HDAC (Figure 1.21) (Giacinti and Giordano, 2006). In contrast, E2F proteins do not have any L-X-C-X-E domains, and in this way pRb may interact with both E2F proteins and L-X-C-X-E domain-containing proteins as the binding sites are distinct from each other (Figure 1.21). Furthermore, the growth suppressing activities of pRb require both the E2F interaction and L-X-C-X-E domains (Giacinti and Giordano, 2006).

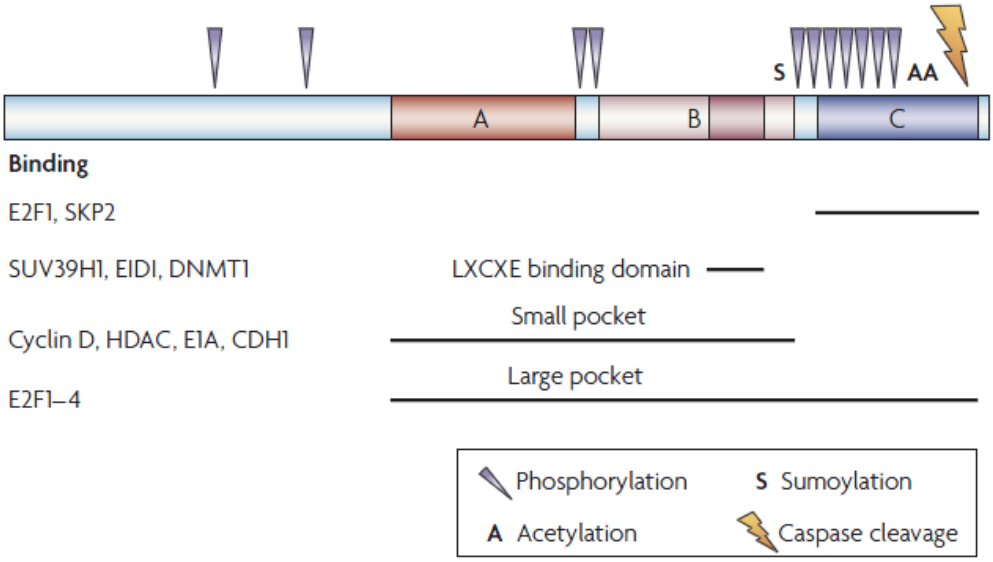

Figure 1.21 Domain structure pRb and post-translational modifications. pRb has three pocket domains: A, B and C. The pocket domains may interact with a variety of proteins important for cell cycle regulation, such as E2F and proteins with an L-X-C-X-E domain (Burkhart and Sage, 2008).

Functionally, pRb has been widely studied as a tumour suppressor for its role as a central regulator of the cell cycle as it acts an inhibitor of the G_1-S-phase transition (Knudsen and Knudsen, 2008). The inactivation of pRb by cdk-cyclin complex-dependent phosphorylation is the molecular switch to drive cell cycle progression past the irreversible restriction or R-point, analogous to START in yeast (Lundberg et al., 1999). Past this point in G_1, cells are inextricably committed to replicate their DNA via the engagement of a major transcriptional program in a mitogen-independent manner. In its hypophosphorylated state, pRb suppresses G_1-S transition by binding to the E2F transcription factor, which regulates the expression of S-phase genes (Figure 1.22) (Mittnacht, 1998). pRb is thought to inhibit E2F-dependent transcription in two ways. Firstly, pRb binds to the transactivation domain of E2F therefore inhibiting its transcriptional activity. Secondly, pRb promotes the active repression of gene expression by recruiting histone deacetylases (HDACs), SWI/SNF chromatin remodelling complexes, Polycomb group proteins and methyltransferases (Knudsen and Knudsen, 2008).

In response to mitogenic signals, D-type cyclins are rapidly transcribed via the action of the Ras-Raf-MAPK signaling pathway (Lundberg and Weinberg, 1999). Activated cdk4,6-cyclin D complexes act to phosphorylate pRb on various serine and threonine residues, therefore inactivating it and allowing expression of a multitude of E2F-responive genes necessary for cell cycle progression, including cyclin E and A (Figure 1.22) (Bartek and Lukas, 2001). Microarray analyses highlights that E2F targets approximately 150–200 genes (Knudsen and Knudsen, 2008). E2F1-3 functions by recruiting proteins that promote an open chromatin structure, allowing the transcription machinery access to promoters, for example the basal transcription factor TFIID and other co-activators, such as histone acetyltransferases, p300 and CBP, GCN5 and TIP60 are all recruited to gene promoters (Figure 1.22) (Chen et al., 2009). Activated cdk2-cyclin E complexes in late G_1 further phosphorylate pRb in cooperation with cdk4,6-cyclin D complexes, and in this way the pRb-E2F pathway acts in a feed forward mechanism to enhance pRb phosphorylation (Figure 1.22) (Mittnacht, 1998). pRb is maintained in a phosphorylated state until late mitosis until it is dephosphorylated by members of the type 1 protein phosphatase family (PP1).

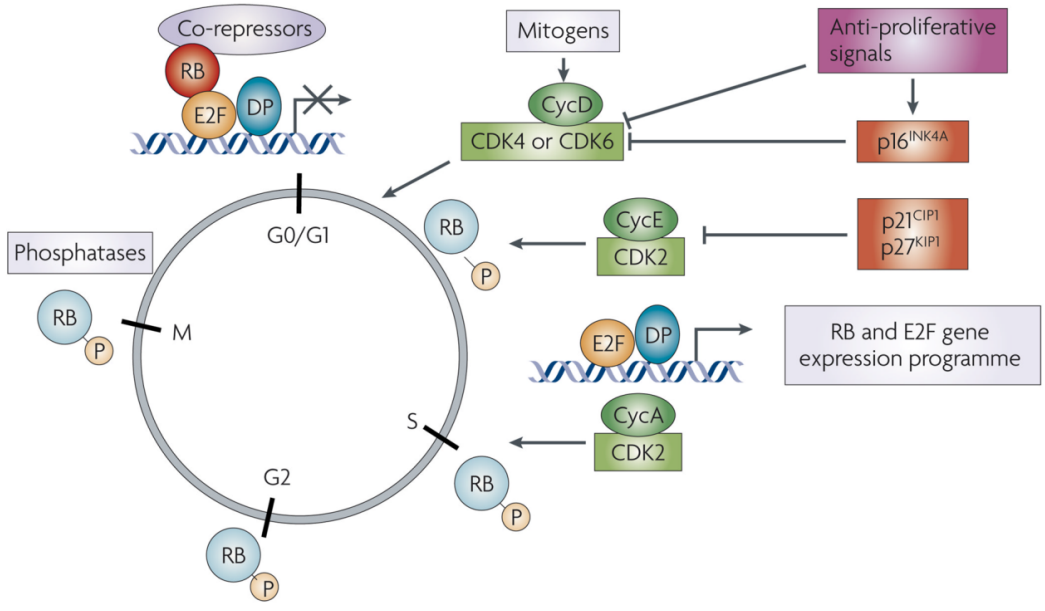

Figure 1.22. Role of pRb in the cell cycle. pRb is phosphorylated, and in turn inactivated by cdk-cyclin complexes leading to E2F-dependent gene expression required for S-phase progression (Knudsen and Knudsen, 2008).

The number of E2F family members is quite extensive, broadening the ways in which cell cycle progression is regulated. Furthermore, not all E2Fs are transcriptional activators, some act so as to repress transcription (Chen et al., 2009). To date, there are ten E2F family members: E2F1, E2F2, E2F3a, E2F3b (all activators); E2F4, E2F5, E2F6, E2F7a, E2F7b, E2F8 (all repressors). The E2F activators contain sequence-specific DNA-binding domains and a dimerisation domain, which enables binding with one of three dimerisation partners (DP1-3) (Chen et al., 2009). Interaction with the DP proteins allows E2F to bind DNA and stabilises the interaction with pocket protein, although they do not determine the specificity of the interacting pocket protein (Giacinti and Giordano, 2006; Polager and Ginsberg, 2008). Notably, E2F7 and 8 do not dimerise with DP proteins, but rather may homodimerise or form E2F7/E2F8 heterodimers. Activator E2Fs also contain a cdk-binding domain and NLS near the N-terminus. The C-terminus contains a transcriptional transactivation domain, which enables activation of gene expression, and pRb-binding domain within this transactivation domain, allowing pRb to actively repress E2F-mediated gene expression (Giacinti and Giordano, 2006; Polager and Ginsberg, 2008). The E2F repressor group proteins also contain a DNA-binding domain and pRb-binding domain whilst they contain a NES instead of a NLS (for E2F4 and E2F5). E2F6-8 do not contain pRb-binding domains, indicating that their repressor function in the cell cycle is independent of the pocket proteins.

The various combinations that may exist between the E2F family and the pocket proteins (pRb, p107 and p130) show a degree of specificity in the interactions, which suggests that the biological functions of the pocket proteins are not wholly redundant. For example, pRb interacts with E2F1-4, although E2F4 mainly interacts with p107 and p130 and E2F5 associates predominantly with p130 (Attwooll et al., 2004; Cobrinink, 2005; Chen et al., 2009). Functionally, the plethora of E2Fs, in conjunction with their interacting pocket protein, appear to have specific functions within the cell cycle either due to their expression levels or their activation, or both. Temporally, in G_0, E2F4 and E2F5, whose protein levels are unchanged throughout the cell cycle, associate with p107 and p130 and other

co-repressors (e.g. histone deacetylases (HDACs), the DNA methyltransferase DNMT1 and C-terminal binding protein (CtBP)) to repress E2F-responsive genes. Upon mitogenic signalling, cdk4,6-cyclin D phosphorylation of pRb inactivates pRb repressor function, therefore promoting the transcription of E2F-responsive genes, including *E2F1-3*, in late G_1. The repressor E2Fs, E2F6,7 and 8, which function independently of the pocket proteins, mediate the repression of the transcription program, including *E2F1*, therefore acting to antagonise E2F1-3 activator function (Chen et al., 2009).

Pocket proteins may also control the G_1/S-phase transition in an E2F-independent manner. Firstly, p107 and p130, but not pRb, may bind cdk4,6-cyclin D and cdk2-cyclin E complexes (Zhu et al., 1995). In contrast, pRb interacts with the F-box protein Skp2, which is part of the SCF ubiquitin ligase complex (see 1.13.3) (Ji et al., 2004). This interaction inhibits the ubiquitylation and thus degradation of p27, which leads to increased p27 levels and inhibits G_1/S-phase progression (Wang et al., 2010). pRb also induces PML body formation and suppress Ras signalling, two functions which ultimately also lead to inhibition of proliferation in an E2F-independent manner (Cobrinink, 2005).

1.14.1.2 The Myc pathway

Acting synergistically with the Rb-E2F pathway to the control the G_1/S-phase transition is the Myc pathway (Bartek and Lukas, 2001). The *c-myc* gene product is proto-oncogene and transcription factor of the bHLH/LZ protein family, whose expression is rapidly induced by mitogenic signalling. Myc may act as both a transcriptional activator and repressor depending on its interacting partners, with one estimate suggesting that it may regulate up to 15% of all genes (Dominguez-Sola et al., 2007; Cotterman et al., 2008). Myc promotes the production of proteins that promote G_1/S-phase including D-type cyclins, cyclin E and Cdc25. Moreover, Myc also functions indirectly by sequestering p27 into cdk4-cyclin D complexes, enabling its phosphorylation and subsequent UPS-mediated degradation (Bartek and Lukas, 2001). Silencing of either the Rb-E2F or Myc

pathway is not enough to inhibit cell cycle progression, probably as a result of over-lapping gene targets, but inhibition of both pathways prevents S-phase entry.

1.14.1.3 Cdk2-cyclin E is a G_1/S-phase convergence point

The synergistic actions of the Rb-E2F and Myc pathways cooperate to inactivate pRb and promote the entry into S-phase. The regulation of the abundance and activity of cdk2-cyclin E complexes by these two convergent pathways has been suggested to be the rate-limiting step that is essential for S-phase entry (Sherr and Roberts, 1999; Nilsson and Hoffmann, 2000). As well as phosphorylating pRb and p27, the cdk2-cyclin E complex promotes phosphorylation of p220NPAT, a protein involved in the activation of histone gene promoters during DNA replication. Furthermore, the Cdc45 protein, which loads DNA polymerase α onto replication origins, is activated by cdk2-cyclin E complexes, providing evidence for an essential role for cdk2-cyclin E in G_1/S-phase control (Zou and Stillman, 1998).

1.14.2 S-phase

Whilst a thorough discussion of S-phase is beyond the scope of this thesis, I will cover the salient conceptual points important in the context of the cell cycle. The basic machinery of DNA replication is highly conserved throughout evolution, with higher organisms adapting more elaborate strategies in order to replicate larger segments of DNA (Kelly and Brown, 2000). Two problems must therefore be overcome in eukaryotes for replicating such a large amount of genetic material. First, DNA replication must be initiated at the multiple sites at the correct time in the cell cycle and, secondly, these initiation sites must be prevented from firing in the newly synthesised daughter chromosomes (Kelly and Brown, 2000). These events are regulated extensively within the framework of the cell cycle and checkpoint pathways, which arrest cell cycle progression in response to replication stress, thereby inhibiting the transmission of damaged DNA to daughter cells.

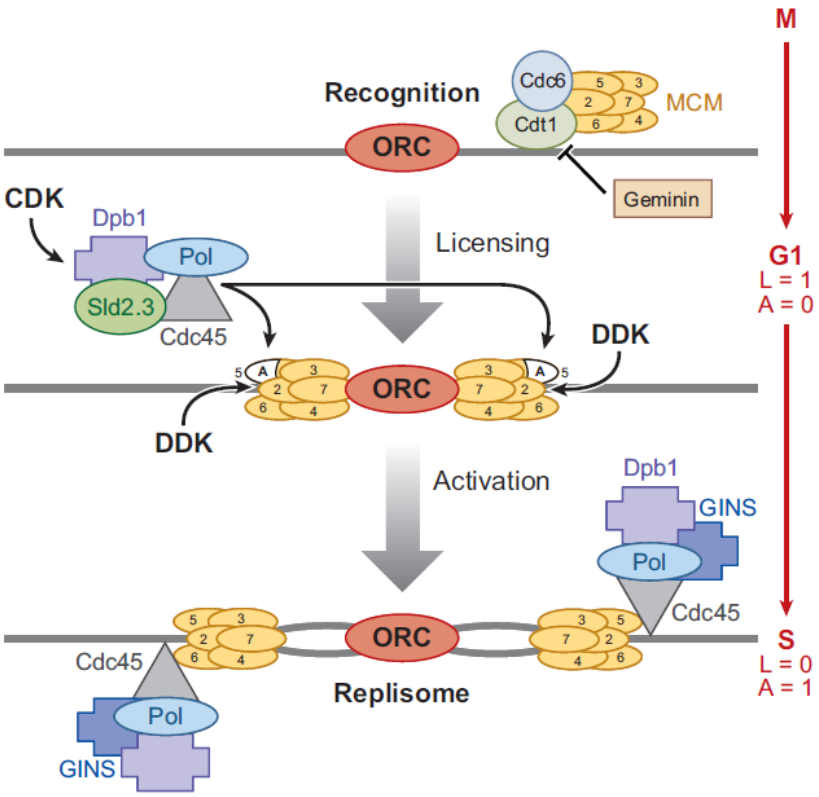

Figure 1.23 Model of eukaryotic DNA replication. ORC binds origins of replication, which then allows Cdt1 and Cdc6 to load MCM2-7 onto chromatin. CDK and DDK govern the loading of the replisome and activation of MCM2-7 complex (adapted from Sclafani and Holzen, 2007).

DNA replication is initiated at specific DNA sites called origins of replication. These sequences are bound by the origin replication complex (ORC) during G_1-phase (Masai et al., 2010). Studies using a range of organisms has highlighted that ORCs vary in their ability to recognise specific DNA sequences and in higher eukaryotes ORC displays no DNA binding sequence specificity, suggesting that other factors such as chromatin structure may influence ORC association (Sclafani and Holzen, 2007). The minichromosome maintenance (MCM) complex is a heterohexameric assembly of MCM 2,3,4,5,6 and 7 subunits. The MCM complex is loaded onto the chromatin-bound ORC by Cdc6 and Cdt1 during late mitosis-early G_1-phase to form a prereplicative complex (pre-RC) (Figure 1.23) (Blow and Gillespie, 2008). Once MCM has loaded onto ORC, origins are said to be 'licensed'. Re-replication from licensed sites is inhibited by blocking MCM

loading during S, G_2 and M-phases via the action of cdks (Nguyen et al., 2001; Blow and Dutta, 2005). In this way, origins are either licensed (L = 1, A = 0) or activated (L = 0, A = 1), like binary code (See Figure 1.23). This is accomplished in a number of ways. Firstly, cdk-mediated phosphorylation of ORC results in its degradation by SCF^{Skp2} during S-phase (Mendez et al., 2002). Cdc6 is stabilised during G_1-phase by cdk-dependent phosphorylation, which prevents its association with APC/C, however, as APC/C is inactivated during G1, Cdc6 stabilisation is decreased, thereby inhibiting replication licensing (Duursma and Agami, 2005; Mailand and Diffley, 2005). Cdt1 levels are regulated in two ways. Firstly, it may be signalled for SCF^{Skp2}-dependent and independent degradation after initial phosphorylation by either cdk2 or cdk4 (Blow and Dutta, 2005). Secondly, Cdt1 is stabilised by binding to the cell cycle regulated protein geminin, which is expressed during S, G_2 and early mitosis, therefore inhibiting the loading of the MCM complex onto origins (Blow and Dutta, 2005). Interestingly, cells contain far more licensed pre-RCs that are eventually fired, i.e. they prepare an excess of potential DNA replication start sites and in this way DNA replication displays great plasticity (Gilbert, 2004). It has been shown that cells use ‘dormant’ origins if the replication machinery is stalled in response to DNA damage (Masai et al., 2010). The selection of origins fired during S-phase may be regulated either at the pre-RC assembly step or the actual activation step (Masai et al., 2010). Furthermore, origins are temporally regulated during S-phase and although the long standing dogma of euchromatin being replicated during early S-phase and heterochromatin being replicated during late S-phase holds true in some instances, recent evidence suggests that the temporal differences in replication timing is likely due to three-dimensional chromatin structure and nuclear architecture (Hiratani et al., 2009).

Once licensed, i.e. by the loading of MCM2-7 helicase onto ORC by Cdc6 and Cdt1, the process of firing them needs to be activated at the appropriate stage. The two major protein kinases responsible for this are cdk and Cdc7-Dbf4, which activate the MCM helicase. Cdc7-Dbf4 is absent in G1-phase due to degradation via APC/C^{Cdh1}, which is itself inactivated as cells enter S-phase, therefore allowing

Cdc7-Dbf4 levels to rise. MCM complexes are loaded in excess at origins and once activated by cdk and Cdc7-Dbf4, are able to interact with Cdc45, a protein that loads the replisome (multi-protein replication fork complex) and moves with the replication fork and is necessary for fork initiation and elongation (Masai et al., 2010). Various other proteins, such as the GINS complex, Sld2 and 3, MCM10 and Dpb11 are involved in facilitating the activation of the MCM2-7 helicase and loading the replisome (Figure 1.23) (Diffley and Labib, 2002).

1.14.3 G_2/M-phase

Once a cell has replicated its genetic material, before it can divide its progression is halted until cdk1-cyclin B complexes are activated and several G_2/M checkpoints must be satisfied. During G_2, phosphorylation on Thr168 of cdk1 allows binding to cyclin B. However, the cdk1-cyclin B complex is inactivated by phosphorylation of cdk1 on Thr14/15 by Wee1 and Myt1. At the end of G_2 and beginning of mitosis, these two residues are dephosphorylated by Cdc25. Activated cdk1-cyclin B then phosphorylates Cdc25, activating it and initiating a positive feedback loop, whilst also phosphorylating Wee1, thereby inactivating it, providing a negative feedback loop (Vermeulen et al., 2003). Phosphorylation by cdk1 and Plk1 of Wee1 promotes its degradation after ubiquitylation by $SCF^{\beta\text{-}TrCP}$. Activated cdk1-cyclin B1 complexes promote chromatin condensation and mitotic spindle assembly, whilst phosphorylating a range of other targets, including nuclear lamins (inducing nuclear envelope breakdown) and histone H1 (Nigg, 2001; Yu and Yao, 2008). Activated cdk1-cyclin B and Plk1 also phosphorylate Emi1, the APC/C inhibitor, stimulating degradation by via $SCF^{\beta\text{-}TrCP}$ in prophase (Hansen et al., 2004). Cdk1 also phosphorylates APC/C, which promotes interaction with Cdc20, and this activated APC/C^{Cdc20} complex targets cyclin A destruction during prometaphase (Vodermaier, 2004). After prometaphase, the spindle assembly checkpoint (SAC) prevents chromosome segregation until all chromosome are aligned correctly (Nasmyth, 2005). A single unattached kinetochore is sufficient to inhibit activation of APC/C (Musacchio and Hardwick, 2002). Once the SAC has been satisfied, anaphase commences via the activity of

APC/C^{Cdc20}, which targets the Separase inhibitor, Securin, for degradation, allowing sister chromatids to be pulled apart (Nasmyth, 2005). APC/C^{Cdc20} also targets cdk1-cyclin B complexes for degradation at this stage. Later in mitosis, during telophase, Cdh1 is activated in the absence of cdk activity and dephosphorylating action of Cdc14p, and forms the APC/C^{Cdh1} complex, which targets APC/C^{Cdc20} for degradation and remains active through to G_1 in the two daughter cells (Nigg, 2001).

1.15 When the cell cycle goes wrong: cancer

The cell cycle machinery is a prime target for the progression of cancer as it provides the potential to allow unlimited cell divisions and bypasses checkpoint controls even in the presence of genomic instability (Hanahan and Weinberg, 2011). The number of cell cycle-related genes mutated in cancer, the types of mutations found, and how they impact on the cell cycle is far too numerous to cover here. However, in light of what I have discussed previously, I will simplify the discussion to proteins that drive G_1/S-phase and G_2/M-phase transitions.

Both the pRb-E2F and Myc pathways that govern the G_1/S-phase transition are targets in cancer (Hanahan and Weinberg, 2000). As the restriction-point in G_1 governs the decision to commit to cell division, there is great selective pressure in cancers to bypass this decision point by promoting the pRb-E2F pathway (Bartek et al., 1997). The G_1/S-phase regulators may be seen as either proto-oncogenes (E2F, Myc, cyclins D1, D2 and E, cdk4 and 6, Cdc25) or tumour suppressors (p53, pRb, p15, p16, p21, p27) (Bartek et al., 1997; Sherr, 2004). Tumour suppressor genes encode proteins that inhibit cell cycle progression and loss-of-function mutations in these genes may cause the the resulting oncoprotein to become non-functional and therefore oncogenic. In contrast, proto-oncogenes generally undergo gain-of-function mutations resulting in an oncoprotein that may be refractory to normal regulatory mechanisms that governs its activity (Sherr, 2004). These two groups either drive proliferation by encouraging cell cycle proliferation (proto-oncogenes) or through their inability to inhibit the cell cycle

(tumour suppressors) (Sherr, 2004). The promotion of oncogenesis by either proto-oncogenes or tumour suppressors, or both, proceeds by several distinct mechanisms (Bartek et al., 1997). These include gene amplification, chromosomal translocations or inversions, activating or inactivating mutations, promoter silencing, increased/decreased protein turnover and altered protein-protein interactions (Bartek et al., 1997). Whilst pRb function is completely lost in retinoblastoma, it is also found to be mutated in a great number of cancer types, for example, in 80% of small cell lung cancer cases (Sherr and McCormick, 2002). Furthermore, inactivating mutations in p16 are frequently found in cancers, for example, in up to 80% of pancreatic cancer cases (Kamb, 1998; Sherr and McCormick, 2002). It has been estimated that ~ 90% of all cancers have a deregulated pRb-E2F pathway (Hall and Peters, 1996). The pRb-E2F pathway is thus particularly susceptible to mutations causing this a shift towards uncontrolled proliferation. Moreover, upstream mitogenic signalling mutations in genes such as *Ras* also contribute to increased use of the pRb-E2F pathway by promoting pRb phosphorylation (Peeper et al., 1997).

Mutations in G_2/M-phase genes are less profound numerically than those that control the G_1/S-phase transition, presumably because mutations in these genes would undermine the bypass of G_1/S-phase control, i.e. it is essential that a cancer cell retains the ability to divide having gone through G_1 and S-phase (Bartek et al., 1997). However, *Cdc25* is deregulated in cancer and can be overexpressed in certain cancer types, leading to unscheduled cdk-cyclin activation (Nilsson and Hoffmann, 2000).

CHAPTER 2. MATERIALS AND METHODS

2.1 Cell Culture

2.1.1 Maintenance of human dermal fibroblasts

Wild type human dermal fibroblasts (HDFs) have previously been isolated from neonate and juvenile foreskin and cryopreserved (Bridger et al., 1993). The 2DD strain of HDFs used in this study were cultured in Dulbecco's modified Eagle's medium (DMEM, Invitrogen) supplemented with 10% (v/v) FBS (Sigma) (from now on referred to as 10% DMEM) with the addition of 10 units/ml penicillin (Invitrogen) and 50 µg/ml streptomycin (Invitrogen) at 37ºC in a humidified incubator with 5% CO_2. During this study only early passage HDFs (p8-p12) were used.

HDFs were grown in 75 cm^2 culture flasks (Nunc) with a media change every 2-3 days. Once the cells had reached approximately 70-80% confluency they were subcultured and reseeded at 3 x 10^5 cells per 75 cm^2 culture flask. For subculturing, cells were washed once with Versene buffer (137 mM NaCl, 2.7 mM KCl, 8 mM Na_2HPO_4, 1.5 mM KH_2PO_4, 1.5 mM EDTA pH 7.4) and then detached from the culture flask by the addition of Versene buffer plus 10% (v/v) trypsin (Sigma) and placed for a maximum of 5 minutes at 37ºC in a humidified incubator with 5% CO_2 to aid detachment. Subsequently, trypsin was inactivated via the addition of 10% DMEM and antibiotics. The cells were transferred to a sterile 30 ml universal tube and centrifuged at 200 x *g* for 5 minutes. The media was aspirated off and the cells were then thoroughly resuspended and counted using a haemocytometer to determine the cell density and thereafter seeded into 75 cm^2 flasks.

HGPS fibroblasts (AG06297) carrying classical G608G mutation in the *LMNA* gene and fibroblasts from young (GM0323; eight year old) and old (GM09588; eighty-five year old) healthy individuals were obtained from the Coriell Cell

Repository. HDFs from a patient with lethal foetal akinesis harbouring a homozygous Y259X mutation in the *LMNA* gene were obtained as an autopsy sample after an informed consent and were a kind gift from Dr. Jos Broers. AD-EDMD (Emery-Dreyfuss muscular dystrophy) fibroblasts carrying the R453W mutation in the *LMNA* gene, X-EDMD HDFs carrying a mutation in the *STA* gene, and HDFs from patients with Greenberg dysplasia carrying a mutation in the *LBR* gene were a kind gift from Dr. Manfred Wehnert.

2.1.2 Maintenance of transformed cell lines

HEK293T and U2OS cells (a kind gift from Eric Schirmer, University of Edinburgh) were maintained in 10% DMEM. They were typically split at a ratio of 1:10 and routinely passaged every 2-3 days.

2.1.3 G_0 synchronisation by serum-starvation

Synchronisation of HDFs in the reversible G_0 phase (quiescence) of the cell cycle has been described previously (Bridger et al., 1993). In order to induce quiescence, HDFs were seeded at a density of 3 x 10^5 cells per 75 cm^2 culture flask and cultured in 10% DMEM and antibiotics at 37ºC in a humidified incubator with 5% CO_2. Cells were allowed to proliferate up to approximately 70-80% confluency, at which point the media was aspirated from the culture flasks and cells were washed once with, and then maintained in, DMEM supplemented with 0.5% (v/v) FBS and antibiotics for 3-5 days at 37ºC in a humidified incubator with 5% CO_2. G_1 arrested cells were confirmed by immunofluorescence staining with Ki67 antibody.

2.1.4 Generation of stable U2OS cell lines

U2OS cells were transfected with either GFP-pMax (Lonza) or GFP-prelamin A using Lipofectamine 2000 (see 2.5.1). After 24 hours, cells were plated in 10 cm dishes with the addition of 800 µg/ml G418. Selection in G418-supplemented media continued for 7-14 days. Single isogenic clones were then created by

cloning in 96-well plates before propagation and use. Levels of GFP-expression were assessed by microscopy and western blotting.

2.1.5 Drug/IR treatment

Etoposide and hydroxyurea were purchased from Sigma. Etoposide powder was dissolved in DMSO to a final stock concentration of 10 mM and kept in the dark at 4ºC. Unless stated otherwise, cells were treated with 20 μM etoposide for 30 minutes. Hydroxyurea (HU) was dissolved in MilliQ water to a final stock concentration of 0.5 M and discarded after immediate use. HU was used at a final concentration 20 mM and was applied to cells overnight (16-20 hours). Bleomycin sulphate was purchased from Calbiochem, dissolved in MilliQ water to produce a stock concentration of 5 mg/ml and stored in the dark at -20ºC. Bleomycin sulphate was applied for 1 hour and used at a final concentration of 20 μg/ml. After all treatments, cells were either assayed immediately or at later time points, in which case cells were then washed twice with sterile PBS and re-fed with 10% DMEM and antibiotics. N-acetyl-L-cysteine (NAC) was purchased from Sigma, dissolved in MilliQ water to a stock solution of 0.5 M and applied to cells to final concentration of 10 mM. Hydrogen peroxide (H_2O_2) was purchased from Sigma and comes as a stock solution of 8.8 M. In order to treat cells with μM quantities of H_2O_2, the stock solution was diluted in MilliQ water to produce a working stock solution of 4 mM before subsequent addition to cells at the concentrations indicated in the text. Ionizing radiation treatment was performed with a NDT 320 irradiator using a Comet MXR-321 X-ray tube (130 kV, 5 mA) at a dose rate of 1.9 Gy/min. Cells were irradiated before being returned to 37ºC 5% CO_2 incubators for the time indicated in the text. Caffeine (Sigma) was made fresh by dissolving in water at a stock concentration of 0.5 M and added to cells at a final concentration of 20 mM for 1 hour prior to irradiation. MG-132 (Calbiochem) was used at a concentration of 30 μM and added to culture medium for 6 hours.

2.2 Plasmids

2.2.1 Flag-prelamin A

Prelamin A cDNA was previously cloned into the mammalian expression vector pSVK3 (Amersham Pharmacia Biotech Inc), which has an N-terminal Flag-tag and a multiple cloning site downstream from an SV40 early promoter and an ampicillin resistance cassette (Östlund et al., 2001). The construct was kindly provided by H.J. Worman (Departments of Medicine and of Anatomy and Cell Biology, Columbia University College of Physicians and Surgeons, New York, USA). Flag-prelamin A cysteine mutants (see text for specific details) were kindly provided by V.Pekovic (University of Durham).

2.2.2 GFP-prelamin A and GFP-lamin C

Prelamin A cDNA was previously cloned by a member of our laboratory into pEGFP-C2 (Clontech Inc), which contains a multiple cloning site downstream from the cytomegalovirus early promoter and expresses the gene with an N-terminus EGFP fusion (Vaughan et al., 2001). Lamin C was previously cloned into the pS65T expression vector and was previously obtained from Dr Jos Broers (Department of Molecular Cell Biology and Genetics, University of Maastricht, The Netherlands).

2.2.3 HA-tagged 53BP1

HA-tagged 53BP1 expression constructs were kindly provided by Kuniyoshi Iwabuchi (Department of Biochemistry, Kanazawa Medical University, Japan). Various cDNA fragments were previously cloned into the mammalian expression construct pCMH6K, which contains an N-terminal tag with an influenza virus hemagglutinin (HA) epitope (Iwabuchi et al., 2003).

2.3 Generation of amplified plasmid DNA

2.3.1 Transformation of DH5α *E.coli*

Expression constructs were used to transform competent DH5α *E.coli* cells. Briefly, 100µl of *E.coli* cells were thawed on ice for 10 minutes. After which time, 1-1000 µg of plasmid DNA was added to the cells and mixed carefully using a pipette, then left for up to 30 minutes on ice. The cells were then placed at 42ºC for 90 seconds, then returned to ice for exactly 2 minutes. Next, 1ml of room temperature LB was added to the cells and then incubated at 37ºC for 90 minutes with shaking at 225-250 rpm. Cells were then plated onto LB agar containing 100 µg/ml ampicillin or 30 µg/ml kanamycin (depending of the expression construct) and allowed to grow for 16-20 hours at 37ºC. From these plates, clearly isolated colonies were chosen and grown in LB with 100 µg/ml ampicillin or 30 µg/ml kanamycin for 16 hours with shaking at 225-250 rpm before conducting small scale DNA purification of the culture.

2.3.2. Plasmid purification

Small and large-scale DNA purification was carried out according to the manufacturer's guidelines (Promega).

2.4 RNAi

2.4.1 siRNA sequences

Knockdown of target proteins was achieved by following standard laboratory protocols that had previously been adapted from published protocols (Elbashir et al., 2001; Harborth et al., 2001; Pekovic et al., 2007). The negative control and LAP2α siRNA sequences were obtained from Ambion, whilst the lamin A/C siRNA sequence was obtained from Qiagen. Alternatively, to determine transfected cells, these oligos were purchased from the same companies with a 5'-Cy3 tag. Upon arrival, siRNA duplexes were resuspended in nuclease-free water to give a final working concentration of 20 µM (for Oligofectamine transfection) or 40 µM (for

Amaxa transfection), aliquoted and stored at -20˚C until use. The sequences of LAP2α and lamin A/C siRNAs have been selected from the open reading frames of both LAP2α and lamin A/C mRNAs to obtain 21-nt sense and 21-nt antisense strand with symmetric 2-nt 3′-overhangs of identical sequence. The negative control siRNA is targeted against a sequence that does not have any significant sequence similarity to mouse, rat or human transcript sequences (note: sequence details not available from supplier). The LAP2α siRNA sequence is targeted against the LAP2α-specific exon 4 of *TMPO* such that no other isoforms should be targeted. The LAP2α and lamin A/C siRNA sequences were as follows:
LAP2α sense: 5′-GCU AAG AAA GUA CAU ACU U tt-3′
LAP2α anti-sense: 5′-AAG UAU GUA CUU UCU UAG C tg-3′
Lamin A/C sense: 5′-CUG GAC UUC CAG AAG AAC A tt-3′
Lamin A/C anti-sense: 5′-UGU UCU UCU GGA AGU CCA G tt-3′.

2.4.2 Transfection of HDFs with siRNA

2.4.2.1 Oligofectamine siRNA transfection

In order to knockdown endogenous LAP2α or lamin A/C, HDFs were either synchronised as previously described or used during log-phase growth and then transfected with the appropriate siRNA. On the day of transfection, siRNA was allowed to thaw to room temperature before use. Following this, 15 µl of Oligofectamine (Invitrogen) was mixed gently with 60 µl warmed DMEM (note: DMEM was not supplemented with 10% FBS or antibiotics) and incubated for 5-10 minutes at room temperature. During this time period 15 µl of negative control, LAP2α or lamin A/C siRNA was mixed gently with 250 µl of warmed DMEM. After 5-10 minutes, the two mixtures were combined by gentle tapping and allowed to incubate for 20 minutes at room temperature. Whilst allowing this transfection complex to form, synchronised HDFs were washed with Versene buffer and then detached with Versene buffer and trypsin as described previously, then neutralised with 10% DMEM and no antibiotics. Cells were counted using a haemocytometer to determine the cell density and then seeded at a density of 1 x

10^5 into 60mm plates (Nunc) in the presence of 2660 µl 10% DMEM and no antibiotics. After the 20 minute incubation period, the siRNA/Oligofectamine mixture was added dropwise across the 60mm culture dish resulting in a final concentration of 100 nM of the siRNA. The culture dish was placed at 37ºC in a humidified incubator with 5% CO_2 and after 24 hours the media was aspirated off and replaced with fresh DMEM supplemented with 10% FBS and no antibiotics. Cells were then assayed at various times post-transfection.

2.4.2.2 Amaxa siRNA transfection

As an alternative transfection methodology, HDFs were transfected with siRNA by electroporation using the Amaxa Normal Human Dermal Fibroblast Nucleofector kit (Lonza). Cells were used at 80-90% confluency and on the day of transfection HDFs were washed with Versene buffer before trypsinisation and subsequent resuspension in 10% DMEM plus antibiotics. HDFs were then counted and aliquoted at 5 x 10^5 per 15 ml falcon tube before being pelleted at 200 x *g* for 5 minutes at room temperature. The media was then completely removed from the falcon tube and the pellet was resuspended in 100 µl room temperature Nucleofector solution and 5 µg of the appropriate siRNA. The suspension was transferred to a cuvette and electroporated using program U-23 as suggested by the supplier. The suspension was then supplemented with 1 ml 10% DMEM before gentle transfer to a 10 cm plate. The culture dish was placed at 37ºC in a humidified incubator with 5% CO_2 and after 24 hours the media was aspirated off and replaced with fresh 10% DMEM. For immunofluorescence studies, cells were trypsinised 24 hours post-transfection and plated onto glass coverslips before fixation at the times indicated in the text.

2.5 Plasmid transfection

2.5.1 Lipofectamine 2000

Plasmid transfection was carried out according to the manufacturer's instructions (Invitrogen). Briefly, cells were plated in 2ml 10% DMEM without antibiotics 24 hours prior to transfection in 6-well plates so as to be 90-95% confluent the next day. On the day of transfection, 250µl of DMEM was mixed with 5 µl of Lipofectamine 2000 for 5 minutes at room temperature. During this time 4.0 µg of plasmid DNA was diluted in 250 µl of DMEM and the two solutions were then mixed gently and incubated for 20 minutes at room temperature. This solution was then added to adherent cells for 24 hours, after which time it was replaced with fresh 10% DMEM. Plasmid expression was assayed by immunofluorescence or western blotting after 48 hours.

2.5.2 Amaxa nucleofection

HDFs were transfected with 3 µg plasmid DNA by electroporation using the Amaxa Normal Human Dermal Fibroblast Nucleofector kit (Lonza). The methodology was the same for siRNA transfection (see 2.4.2.2).

2.5.3 Genejuice

U2OS/GFP-lamin A cells were plated to 70-80% confluency in 10 cm dishes 24 hours before transfection. The following day cells were transfected with HA-53BP1 constructs using Genejuice (Genejuice:DNA ratio, 3:1) with a total of 6 µg DNA per plate. Protein extracts were prepared 24 hours post-transfection for GFP-Trap immunoprecipitation.

2.6 Flow Cytometry

2.6.1 Estimation of S-Phase Fraction

In order to estimate S-phase fraction the Click-iT EdU flow cytometry assay kit was obtained from Invitrogen. HDFs were synchronised as described above and transfected with negative control, LAP2α or lamin A/C siRNA. The media was changed after 24 hours with fresh DMEM supplemented with 10% FBS and no antibiotics. After 42 hours EdU (5-ethynyl-2'-deoxyuridine), an analogue of bromo-deoxyuridine (BrdU), was added to the culture dishes to a final concentration of 50 μM for 1 hour. The cells were washed, detached and neutralized with fresh 10% DMEM and subsequently centrifuged in 15 ml falcon tubes at 200 x *g* for 5 minutes. Cells were then washed once with 3 ml ice-cold 1% bovine serum albumin (BSA) in phosphate-buffered saline (PBS) and pelleted by centrifugation at 500 x *g* for 5 minutes (these centrifugation parameters are used for the rest of this flow cytometry protocol). The supernatant was removed and the pellet resuspended in 100 μl 1% BSA in PBS. An equal volume of 4% paraformaldehyde in PBS was added to fix the cells and the mixture was incubated for 15 minutes at room temperature, protected from light. Cells were then washed once with 3 ml 1% BSA in PBS, pelleted, the supernatant removed and the cells resuspended in 100 μl of 1% BSA in PBS. At this point samples were kept for up to one week at 4˚C or processed immediately. The cells were then permeabilised with 100 μl of Triton X-100-based permeabilisation reagent and mixed thoroughly. The cells were washed with 3 ml 1% BSA in PBS, pelleted and the supernatant removed. The Click-iT reaction cocktail was prepared and 0.5 ml added to the cells, which were then incubated for 30minutes at room temperature, protected from light. The cells were washed with 3 ml 1% BSA in PBS, pelleted, the supernatant removed and the cells were resuspended in 0.5 ml 1% BSA in PBS. The cells were then mixed thoroughly with 5 μl of 20 mg/ml Ribonuclease A. Finally, 2 μl of CellCycle 488-red (7-amino-actinomycin D) was added to the cells, mixed well and incubated at room temperature for 30 minutes protected from light. Samples were kept on ice before cell cycle analysis on a

Becton Dickinson FACSCalibur flow cytometry. For the detection of EdU, with Alexa Fluor 488 azide, a 488nm excitation with green emission filter was used. The fluorescent signal generated by the Alexa Fluor 488 azide was detected with logarithmic amplification. For the detection of the Click-iT EdU CellCycle 488-red, a red emission filter was used and the fluorescent signal generated by the CellCycle stain was detected with linear amplification. A minimum of 5,000 cells were analysed per sample and the percentage of cells in each phase of the cell cycle was determined using FlowJo software.

2.6.2 Estimation of ROS Levels

Intracellular ROS levels were estimated using the cell permeant indicator 5-(and-6)-chloromethyl-2',7'-dichlorodihydrofluorescein diacetate, acetyl ester (CM-H_2DCFDA) (Molecular Probes). The dye is non-fluorescent until the removal of acetate groups by intracellular esterases and oxidation occurs within the cell. CM-H_2DCFDA was resuspended in 86 µl of DMSO to produce a 1 mM stock solution. Cells were washed twice with PBS before CM-H_2DCFDA was added to serum-free phenol-free low glucose DMEM (Invitrogen) at a final concentration of 5 µM and subsequently added to the cells for 1 hour at 37ºC. Cells were washed once with PBS before being scraped into 0.5 ml PBS. Intracellular ROS levels were then analysed using FACSCalibur flow cytometer with appropriate settings (excitation 485-95nm; emission 520-25nm). Data were collected as histograms from 10,000 single-cell events and median fluorescence intensity of FL1 peaks was analysed using FlowJo software. To measure the rate of intracellular ROS production, cells were treated with 100µM H_2O_2 during the last 20-30min of incubation with carboxy-H_2DCFDA in serum-free phenol-free DMEM. To measure the rate of intracellular ROS elimination, H_2O_2-treated cells were allowed to recover for 1h in phenol-free serum-free medium containing carboxy-H_2DCFDA. For anti-oxidant treatments, cells were incubated with 10 mM NAC for 1h in serum-free phenol-free low glucose DMEM containing 5 µM CM-H_2DCFDA. As a background control, cells were incubated in phenol-free serum-free DMEM without CM-H_2DCFDA.

2.7 Protein extraction

2.7.1 Preparation of whole cell extracts

Cells grown on plates were washed twice with ice-cold PBS before being scraped into the same buffer and centrifuged at 1000 x *g* for 5 minutes at 4ºC. Cell pellets were then lysed in ice-cold hypotonic buffer (10 mM Tris pH 7.4, 10 mM KCl, 3 mM $MgCl_2$, 0.1% Triton X-100), containing freshly added complete protease and phosphatase inhibitor (Thermo) and 500 units/ml RNase-free DNase I (Sigma/Roche) for 10-15 minutes on ice. An appropriate volume of 2X/5X sample buffer was added to the extract and then boiled for 5 minutes at 95ºC before loading onto SDS-PAGE gels or freezing. Alternatively, washed and pelleted cells were lysed directly into 2X sample buffer and boiled for 5 minutes at 95ºC. Extracts were then drawn through a 23G needle to reduce viscosity or sonicated (3 x 5 seconds followed by 30 seconds intervals; 10 µm amplitude) before loading onto SDS-PAGE gels or freezing.

2.7.2 Preparation of nuclear extracts

Cells were pelleted as above before lysis in ice-cold hypotonic buffer containing freshly added complete protease and phosphatase inhibitor for 10 minutes on ice. Extracts were then subjected to homogenization with 10 rotating strokes of a tight fitting pestle in a Dounce homogenizer. Nuclei were then collected by centrifugation at 4000 rpm for 5 minutes at 4ºC. Nuclei were then resuspended in hypotonic buffer containing freshly added complete protease and phosphatase inhibitor and 500 units/ml RNase-free DNase I for 10 minutes on ice. An appropriate volume of 2X/5X sample buffer was added to the extracts before boiling for 5 minutes at 95ºC. Samples were then frozen or loaded onto SDS-PAGE gels.

2.7.3 Biochemical fractionation

Biochemical fractionation of cells was carried out according to standard laboratory protocols (Pekovic et al., 2007). All steps were carried out on ice and all buffers were ice-cold and supplemented with freshly added complete protease and phosphatase inhibitor. Furthermore, 40 mM NEM was added to all buffers to prevent protein oxidation during the fractionation. Typically, 10 x 10cm plates of 70-80% confluent cells were washed once in ice-cold PBS before being scraped and aliquoted into 5 x 15ml falcon tubes and collected by centrifugation at 1000 x *g* for 5 minutes at 4ºC. Cell pellets were then resuspended in 200µl CSK buffer (10 mM PIPES pH 6.8, 10 mM KCl, 300 mM sucrose, 3 mM $MgCl_2$, 1 mM EGTA pH 8.0), transferred to 5 x 1.5ml micro-centrifuge tubes and collected by centrifugation. This and all subsequent centrifugation steps were carried out at 4000 rpm for 5 minutes at 4ºC unless stated otherwise. Supernatants were discarded and one pellet, named P1, which represents the whole cell extract, was snap frozen in liquid nitrogen before use later in the procedure. The remaining four cell pellets were subsequently resuspended in 200µl CSK/T buffer (CSK buffer supplemented with 0.5% Triton X-100) for 5 minutes before centrifugation. The four supernatants were collected into a tube labelled S2 and snap frozen whilst one pellet was labelled P2 and also snap frozen. The remaining three cell pellets were resuspended in RSB buffer (42.5 mM Tris-HCl pH 8.3, 8.5 mM NaCl, 2.6 mM $MgCl_2$), centrifuged and supernatants discarded. The three cell pellets were then resuspended in 200µl RSB-Magik buffer (RSB buffer containing 1% (v/v) Tween 20 and 0.5% (v/v) sodium deoxycholate) for 5 minutes and centrifuged. The three supernatants were collected and in tube labelled S3 and snap frozen with one cell pellet labelled P3. The remaining two cell pellets were resuspended in 200µl extraction buffer (10 mM PIPES pH 8.3, 250 mM ammonium sulphate, 300 mM sucrose, 3 mM $MgCl_2$, 1 mM EGTA pH 8.0), centrifuged and the supernatants discarded. The two pellets were then resuspended in room temperature digestion buffer containing 500 U/ml RNase-free DNase I (Sigma/Roche) for 20 minutes at room temperature before subsequent centrifugation. The two supernatants were pooled in a tube labeled

S4 and snap frozen with one pellet labeled P4. The remaining pellet was resuspended in extraction buffer for 5 minutes before centrifugation for 10 minutes. The last supernatant, labeled S5, and last pellet, P5 were then snap frozen (Figure 2.1). All pellets were then thawed and resuspended in 200µl hypotonic buffer (see 2.7.1) for 15 minutes on ice before addition of 50µl 5X sample buffer, boiled for 5 minutes, then frozen. For P1, the extract was passed through a 23G needle to reduce viscosity. All supernatants were thawed and an appropriate volume of 5X sample buffer (e.g. 200µl to S2 and 50µl to S5) was added to the extracts before boiling for 5 minutes and freezing. For western blot analysis, an equal volume of sample was loaded from each fraction.

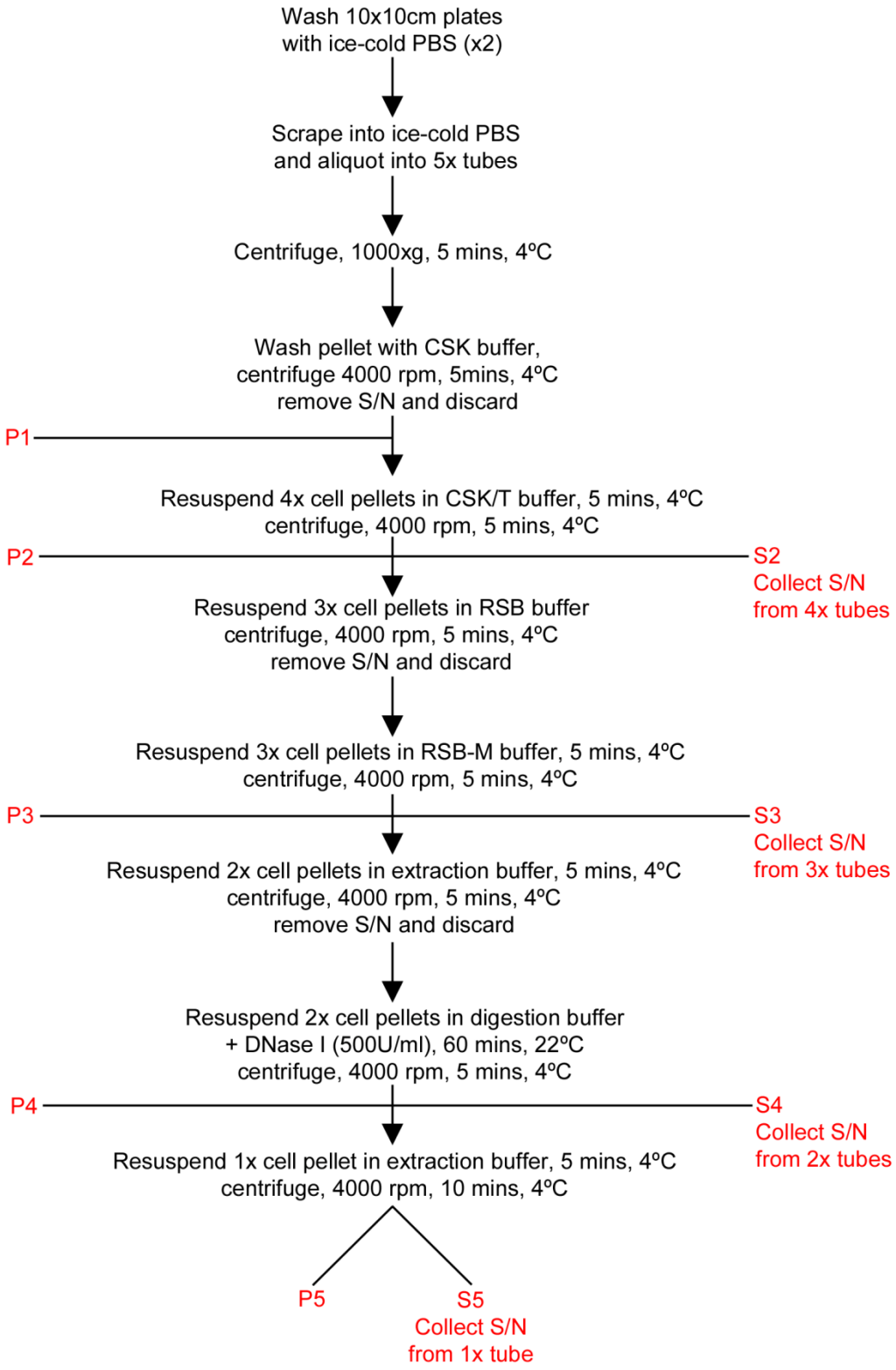

Figure 2.1. Schematic of biochemical fractionation procedure.

2.8 Western Blotting

2.8.1 Gel electrophoresis and immunoblotting

Samples were separated by one-dimensional SDS-PAGE, which was carried out according to standard protocols (Markiewicz et al., 2002). Sample protein was loaded as well as 10 µl of prestained protein ladder (Fermentas) to ensure correct separation of proteins, correct electrotransfer and for determining the molecular weight of detected proteins. Proteins were separated on various percentage gels run at 100V in tank buffer (25 mM Tris [pH 8.3], 192 mM Glycine, 0.1% SDS) until the bromophenol blue in the sample buffer had run out of the gel. Proteins were then electrophoretically transferred to a nitrocellulose membrane (0.2mm, Whatman) in transfer buffer (25 mM Tris-Cl [pH 9.2], 200 mM glycine, 0.1% SDS, 20% methanol) using the Mini Transblot system (Bio-Rad), which was run at 100V, 250 mA for 1.5 hours or 30V, 90 mA overnight at 4ºC.

2.8.2 Membrane blocking and antibody incubations

Post-transfer, membranes were rinsed once in blot rinse buffer (BRB, 10 mM Tris-HCl [pH 7.4], 150 mM NaCl, 1 mM EDTA) for 5 minutes with constant agitation. Membranes were then blocked in 5% (wt./vol.) nonfat dry milk or BSA in BRB-T (10 mM Tris-HCl [pH 7.4], 150 mM NaCl, 1 mM EDTA, 0.1% Tween-20) for either 1 hour at room temperature or overnight at 4˚C, both with constant agitation. Primary antibodies were diluted in their appropriate incubation buffer and applied to the membrane overnight at 4˚C. After primary antibody incubation, membranes were washed three times for 10 minutes each with BRB-T at room temperature with constant agitation. Membranes were then incubated with the appropriate secondary antibody diluted with 5% (wt./vol.) nonfat dry milk or 5% BSA in BRB-T at a concentration of [1:2000] for 1 hour at room temperature with constant agitation. The secondary antibodies used were donkey anti-mouse IgG conjugated to horseradish peroxidase (HRP) or donkey anti-rabbit IgG conjugated to HRP (both Stratech). Membranes were then washed three times for 10 minutes each with BRB-T at room temperature with constant agitation.

2.8.3 Protein detection

Immunological detection of proteins on the membranes was performed with the Enhanced Chemiluminescence kit (ECL; GE Healthcare). ECL reagents were mixed and added to the membranes, which were then exposed to Hyperfilm ECL films (GE Healthcare). The bands were visualised using a Compact X4 Automatic X-ray Film Processor (Xograph Imaging Systems Ltd).

2.8.4 Quantification of bands

The signals obtained for the protein bands were quantified by densitometry using one of two methods. Firstly, the autoradiogram was scanned into Adobe Photoshop using a ScanJet 6300C (Hewlett Packard) and the resulting image was saved and then processed using the ImageJ software. Alternatively, the densitometry was performed using Image Gauge analysis software (FujiFilm). Background signal was always subtracted from the signal obtained for each band.

2.8.5 Stripping of blots

The Re-Blot Plus kit was purchased from Millipore. The antibody stripping solution was prepared according to the manufacturer's instructions and applied to the membrane with gentle mixing for 15 minutes at room temperature. The membrane was then washed twice for 5 minutes with 5% (wt./vol.) nonfat dry milk or 5% BSA in BRB-T before re-probing with the desired antibody.

2.9 Immunoprecipitation

2.9.1 Immunoprecipitation of endogenous lamin A/C complexes

Proliferating wild type HDFs grown in 10 cm plates were first cross-linked *in vivo* using DSP (Dithiobis[succinimidyl propionate]) (Pierce), essentially as described (Fujita et al., 2002). Briefly, HDFs were washed twice with room temperature PBS pH 8.0 before adding 10 ml PBS per 10 cm plate with DSP added to a final concentration of 1 mM. Plates were swirled for 15 minutes at room temperature before the addition of 1 M Tris-HCl pH 7.5 to a final concentration of 25 mM for 15 minutes at room temperature to quench the reaction. Plates were then washed in ice-cold PBS, pelleted and lysed in NP-40 buffer (50 mM Tris-HCl pH 7.5, 150 mM NaCl, 1% NP-40, 100 mM EDTA) containing freshly added complete protease and phosphatase inhibitor (Thermo) for 20 minutes on ice. Extracts were then sonicated for 3 x 10 seconds (amplitude 10 μm) with 30 second intervals. Lysates were then cleared by centrifugation at 12,0000 rpm for 10 minutes and added to pre-equilibrated Dynabeads Protein G (Invitrogen) with pre-bound lamin A/C (sc-7292, Santa Cruz) or unspecific IgG overnight at 4ºC. Beads were then washed four times with NP-40 buffer before addition of 2X sample buffer and boiled for 10 minutes at 95ºC before loading onto SDS-PAGE gels.

2.9.2 Immunoprecipitation of GFP-lamin A complexes

For 293T and U2OS immunoprecipitations, cells washed and scraped into ice-cold PBS before centrifugation at 1000 x *g* for 5 minutes. Cell pellets were then lysed in NP-40 buffer (see above) for 20 minutes on ice before centrifugation at 12,000 rpm for 10 minutes. Clarified extracts were then added to pre-equilibrated GFP-Trap M beads (Chromotek) overnight at 4ºC. Beads were washed and bound proteins eluted as for HDFs.

2.10 Immunocytochemistry and confocal microscopy

2.10.1 Fixation and permeabilisation

Cells grown on glass coverslips were washed once with PBS and fixed for 15 minutes at room temperature with 4% formaldehyde (AnalaR) in PBS. Coverslips were then washed three times for 5 minutes each with PBS. Cells were then permeabilised with 0.5% Triton X-100 (Sigma) in PBS for 5 minutes at 4°C. Again, coverslips were washed three times for 5 minutes each with PBS. In order to ensure specificity of antibody binding, cells were incubated with blocking buffer (1% NCS (v/v) in PBS) for 45-60 minutes at room temperature.

2.10.2 Primary and secondary antibodies

Blocking buffer was aspirated off and coverslips were incubated with primary antibodies in a moist chamber for 1 hour at room temperature or overnight at 4ºC. Primary antibodies were diluted in 1% NCS in PBS; those used and their dilutions can be seen in Table 2. Following primary antibody incubation, cells were washed five times in five changes of PBS. Secondary antibodies were applied for 1 hour at room temperature in a moist chamber protected from light. The secondary antibodies used were a combination of donkey anti-mouse IgG or donkey anti-rabbit IgG (both Stratech) each conjugated to either tetramethylrhodamine B isothiocyanate (TRITC) or fluorescein isothiocyanate (FITC) and diluted 1:100 in 1% NCS in PBS. Coverslips were washed five times in five changes of PBS before a final wash in distilled water. Coverslips were mounted on to glass slides in 30% (v/v) glycerol containing 12% (v/v) Mowiol (Sigma), 2mg/ml 4,6-diamindino-2-phenylindole (DAPI) and 2.5% (v/v) 1,4-diazobicyclo-[2.2.2]-octane (DABCO; Sigma).

2.10.3 Estimation of S-phase fraction and phase by EdU labelling

HDFs were synchronised in G_0 as described above and transfected with negative control, LAP2α or lamin A/C siRNA on coverslips. In order to visualise replication factories, 23 hours post-transfection, and every three hours thereafter, HDFs were labelled for 1 hour with EdU (5-ethynyl-2'-deoxyuridine) to a final concentration of 10 μM for 1 hour. After the 1 hour labelling period, HDFs were washed with PBS, fixed and permeabilised as described above. To detect EdU incorporation, coverslips were incubated with 50 μl Click-iT reaction cocktail for 30 minutes at room temperature according to the manufacturer's instructions (Invitrogen). Coverslips were then mounted onto glass slides with DNA visualised using DAPI as described above.

2.10.4 Confocal microscopy

Micrographs of immunostained cells were taken with a confocal imaging system (LSM510 Meta; Carl Zeiss MicroImaging Inc) with LSM510 image browser software equipped with a 40x / 1.3 oil-immersion lens and photomultiplier tube. A dynamic range adjustment was used to optimize the signal for the fluorophores, and images were collected in multichannel mode. Images were imported into ImageJ, where they were merged and scale bars added before subsequent collation using Adobe Photoshop 7.0.

2.10.5 ImageJ manipulation of micrographs

For fluorescence signal profiles, fluorescence output along defined paths was determined using the 'Plot Profile' macro in the ImageJ software package. Alternatively, fluorescence signal intensity of defined regions was measured using the polygon selection tool in ImageJ. Non-specific background fluorescence was subtracted from results. Data was then exported into Excel for statistical analysis. Nuclear outlines were produced using the 'Threshold' and 'Find Edges' functions in ImageJ.

2.11 *In situ* nuclear matrix preparation

The sequential treatment of HDFs on coverslips with detergents, nucleases and salt was essentially as described (Pekovic et al., 2007). All buffers contained freshly added protease inhibitor cocktail (Sigma). HDFs were grown for 48-72 hours on coverslips before treatment with IR (3 Gy) and allowed to recover for 1 hour. Cells were then washed twice with ice-cold PBS before the addition of CSK/T (see 2.7.3) for 10 minutes at 4ºC. Cells were then incubated in extraction buffer (see 2.7.3) for 5 minutes at 4ºC. To digest DNA, coverslips were then incubated in digestion buffer with the addition of 500 U/ml DNase I (Sigma) for 30 minutes at room temperature. Cells were then incubated in extraction buffer to terminate the digestion for 5 minutes at 4ºC. HDFs were fixed at various times during the extraction procedure (i.e. unextracted, CSK/T and after the last extraction buffer step) and processed for immunofluorescence as described above.

2.12 Senescence-associated β-galactosidase assay

The Senescence β-Galactosidase Staining Kit was purchased from Cell Signaling to histochemically detect β-galactosidase activity in cells at pH 6 (Dimri et al., 1997). Cells were washed once with PBS and fixed with a mixture of 2% formaldehyde and 0.2% glutaraldehyde in PBS for 15 minutes at room temperature. Cells were washed twice with PBS and then stained overnight at 37ºC with 40 mM citric acid/sodium phosphate [pH 6.0], 150 mM NaCl, 2 mM $MgCl_2$, 5 mM potassium ferrocyanide, 5 mM potassium ferricyanide and 1 mg 5-bromo-4chloro-3-indolyl-βD-galactopyranoside (X-gal). Cells were then checked under the microscope for the development of blue colour and, for long-term storage, the staining solution was removed and cells were overlaid with 70% glycerol and stored at 4ºC.

2.13 Clonogenic assay

The colony formation assay was performed exactly as described (Franken et al., 2006). U2OS cells were transfected twice in 24 hours with siRNA and then harvested by trypsinisation after 48 hours from the initial transfection. Cells were counted and then plated by serial dilution into 60mm culture dishes. The initial seeding density (100-1000) was dependent upon the severity of the treatment as judged by preliminary experiments. Cells were allowed to adhere for approximately 24 hours and then treated with the indicated dose of IR. Cells were returned to the incubator for 12 days. After this time dishes were washed once with PBS before staining with a solution of 6% glutaraldehyde (vol/vol) and 0.5% crystal violet (wt.vol) in dH_2O for 30 minutes at room temperature. Dishes were then rinsed and the number of colonies formed counted. The surviving fraction at each IR dose was calculated based on the plating efficiency of the untreated plates.

2.14 Laser micro-irradiation

To induce localised tracts of double-strand breaks, a protocol was adapted from established methods (Lukas et al., 2003). Cells were grown in a 2-well Lab-tek II chamber slide system and pre-sensitised by incubation with 10μM BrdU (Sigma) in phenol-free 10% DMEM (Invitrogen) for 24 hours prior to laser irradiation. Cells were then mounted on the stage of a Zeiss Axiovert 200 microscope integrated with the PALM microbeam workstation (P.A.L.M. Laser Technologies, Bernried, Germany). Cells were visualized under visible light and nuclei were targeted using the supplied software. The irradiation was carried out with a pulsed nitrogen laser, set at 50% power output, which was coupled to the bright field path of the microscope and focussed through a LD 40x NA 0.55 Zeiss objective to produce a beam width of approximately 1 μm. Some 50-150 cells were irradiated within 5 minutes with each cell exposed to the laser for less than 500-ms, before being immediately returned to a 37ºC 5% CO_2 incubator. Cells were then fixed at the times indicated in the text and processed for immunofluorescence as outlined

above. Three independent experiments were performed to confirm the validity of the observations with non-irradiated cells acting as an internal control for the effect of the induced DNA damage and the antibodies used in the experiment.

2.15 Statistical analysis

Graphs were produced in Excel (Microsoft) and the standard deviation calculated using the same software. To determine any statistical significance between the results a two-tailed Student *t* test was carried out using Excel.

Table 1. Antibodies used in this study.

(IF = immunofluorescence; IB = immunoblotting; m = monoclonal; p = polyclonal)

Antibody Name	Target	Antibody Type	Dilution		Source
			IF	IB	
Jol2	Lamin A/C	Mouse (m)	1:200	1:200 5% Milk	Dyer et al., (1997)
Jol4	Lamin A	Mouse (m)	Undiluted	1:10	Dyer et al., (1997)
636	Lamin A/C	Mouse (m)	1:5000		Santa Cruz
RαLA	Lamin A	Rabbit (p)	1:5000	1:2000 5% milk	Sigma
133A2	Lamin A	Mouse (m)	1:500		Immuquest
RαLC	Lamin C	Rabbit (p)	1:2000		Immuquest
LAP15	LAP2α	Mouse (m)	1:10	1:100 5% milk	Dechat et al., (1998)

IQ175	LAP2α	Rabbit (p)	1:2000	1:2000 5% milk	Immuquest
AC-40	β-actin	Mouse (m)		1:2000 5% milk	Sigma
JBW301	Phospho-histone H2AX (Ser139)	Mouse (m)	1:500	1:1000 5% milk	Upstate
2577	Phospho-histone H2AX (Ser139)	Rabbit (p)	1:100		Cell Signalling
Phospho-Chk2 (Thr68)	Phosphothreonine 68	Rabbit (p)	1:100	1:1000 5% milk	Cell Signalling
NB100-304	Total 53BP1	Rabbit (p)	1:500	1:2000 5% milk	Novus Biologicals
Ki67	Ki67	Rabbit (p)	1:200		Dako
WA3	β-tubulin	Mouse (m)		1:1000 5% milk	Kind gift from Dr. Karakesisoglou (University of Durham)

H-92	Rad51	Rabbit (p)	1:50	1:200 5% milk	Santa Cruz
F-7	HA-tag	Mouse (m)		1:200 5% milk	Santa Cruz
Anti-GFP	GFP-tag	Mouse (m)		1:5000 5% milk	Roche
ATM/ATR substrate motif	Phospho-SQ/TQ	Rabbit (p)		1:500 5% BSA	Cell Signalling
H2A	Histone H2A	Rabbit (p)		1:1000 5% BSA	Cell Signalling
2D9A12	$p16^{INK4a}$	Mouse (m)		1:1000 5% milk	Abcam
PC-10	PCNA	Mouse (m)		1:5000 5% milk	Abcam

CHAPTER 3:
LAMIN A MODULATES THE CELLULAR RESPONSE TO OXIDATIVE STRESS

3.1 Introduction

3.1.1 Overview

Aging affects nearly all metazoans, thus how and why organisms age has been, and will continue to be, widely and extensively researched throughout the world (Kenyon, 2005; Kirkwood, 2005). In the UK, 16% of the population were aged 65 and over in 2009, with this estimated to rise to 23% by 2034 (www.statistics.gov.uk). Furthermore, the number of people aged over 85 was ~ 660,000 in 1984 and whilst the number reached 1.4 million in 2009, it is estimated that by 2034 this number will have reached 3.5 million people, accounting for 5% of the population. Importantly, age is a major risk factor associated with a number of medical conditions, most notably, cancer, cardiovascular disease, type II diabetes, pulmonary disease, stroke, dementia and arthropathies. Therefore, understanding the fundamental biological pathways that govern aging is essential for improved medical care necessary to provide healthcare for our aging population.

3.1.5 The role of A-type lamins in senescence and aging

Progeroid syndromes are diseases characterised by premature aging of one (unimodal) or many, but not all (segmental), tissue types. Our understandings of the pathways that cause premature aging provide evidence that these pathways may underlie the normal aging process. A-type lamins were first linked to the aging process by the finding that Hutchinson-Gilford progeria syndrome (HGPS), was caused by a point mutation in *LMNA*, leading to the production of a truncated lamin A protein called progerin (De Sandre-Giovannoli et al., 2003; Eriksson et al., 2003). Three further premature aging diseases that may arise from mutations in

LMNA, atypical Werner's syndrome (aWS), mandibuloacral dysplasia (MAD) and restrictive dermopathy (RD) are phenotypically similar to HGPS patients, yet display slightly milder symptoms (Broers et al., 2006). These diseases are part of a wider set of diseases, termed laminopathies, which arise from mutations of *LMNA*. Laminopathies collectively affect mesenchymal tissues and exhibit phenotypes that may be found in normally aged tissues, which has led A-type lamins to be labelled 'guardians of the soma' (Hutchison and Worman, 2004). Moreover, a range of laminopathy mouse models have reduced longevity, whilst RNAi of Ce-lamin in *C.elegans* leads to a decrease in lifespan (Haithcock et al., 2005; Stewart et al., 2007).

At the cellular level, the link between lamin A/C and senescence has been provided by insights from HGPS patient cells (Kudlow et al., 2007). HGPS cells exhibit reduced proliferative capacity *in vitro*, and therefore undergo senescence earlier than from healthy donors (Goldman et al., 2004; Liu et al., 2011). Importantly, normal human cells, from both young and old individuals, expressed a basal level of progerin by sporadically activating the same cryptic splice site found in HGPS cells (Scaffidi and Misteli, 2006). Coupled to this, human fibroblasts from old patients exhibited increased nuclear abnormalities, which is correlated with reduced nucleoplasmic lamin A/C levels and reduced levels of HP1γ and H3K9 methylation (Scaffidi and Misteli, 2006). Furthermore, progerin expression was found in skin tissues from healthy aged individuals (McClintock et al., 2007). In contrast to this, one study has found decreased expression of lamin A in different cell types of old mice (Duque et al., 2006).

3.1.6 Current aims

Various studies suggest that a number of mechanisms could be at work by which prelamin A may influence cellular senescence. However, no study so far has addressed the role, if any, that mature lamin A plays in cellular senescence. Therefore, in this chapter I explore the role of mature lamin A in cellular senescence with further exploration of its role in the oxidative stress response.

3.2. Senescence-associated hyper-oxidation of cysteine residues in the lamin A tail

Human dermal fibroblasts (HDFs) that have been aged *in vitro* to reach replicative senescence exhibit a range of dysmorphic nuclear shapes that are reminiscent of those observed in fibroblasts from patients with Hutchinson-Gilford Progeria Syndrome (HGPS) (Supplementary Figure 1a-c) (Goldman et al., 2004). To assess if altered protein levels of lamin A/C and lamin B2 contributed to this cellular phenotype, cellular extracts were prepared from wild type HDFs at different population doublings. Immunoblotting revealed that total protein levels of lamin A/C and lamin B2 were unchanged during cellular aging, ruling out the possibility that the increased dysmorphic nuclear shapes observed in senescent cells were due to altered protein levels (Supplementary Figure 1d). Previous studies have shown that oxidative damage during cellular aging can lead to protein unfolding (Friguet, 2006) and that protein thiols are prime targets of oxidative modifications (Eaton, 2006). I therefore investigated whether lamin A/C could be a target of oxidative thiol damage in during the aging of HDFs *in vitro*, which might account for the accumulation of dysmorphic nuclei. To assess the potential contribution of thiols, multiple sequence alignments of lamins A, C, B1 and B2 revealed that lamin A contains three unique cysteine residues (C570, C588 and C591) in its specific C-terminal tail domain and shares a single cysteine residue with lamin C in the common IgG domain (C522), whilst none of these cysteine residues are present in lamins B1 or B2 (Figure 3.1a). Importantly, three cysteines (C522, C588 and C591) are conserved throughout the mammalian phylogeny (Figure 3.1b).

Cysteine residues in proteins can form disulfide bonds under oxidizing conditions, which can be detected on non-reducing SDS-PAGE as slower-migrating protein species, for inter-molecular complexes, or faster-migrating protein species for intra-molecular disulfide bonds (Benham et al*.,* 2000). To investigate the availability of cysteine residues to form disulfide bonds in lamins A/C, cell extracts from HDFs at increasing population doublings (p12, p24 and p40) were resolved

on non-reducing or reducing SDS-PAGE and probed with anti-lamin A (Jol4) and anti-lamin C (RαLC) antibodies. Under non-reducing conditions lamin A was weakly detected as a monomer in young (p12) HDFs but exhibited two band shifts to the positions of the slower-migrating lamin A homodimer and faster-migrating protein species (Figure 3.2a). Under reducing conditions, lamin A was detected only as a monomer across all three population doublings confirming that both the slower- and faster-migrating bands of lamin A in young (p12) HDFs were disulfide-dependent (Figure 3.2a). A progressive decline in the amounts of both inter- and intra-molecular disulfide species with increasing population doublings was coupled to the accumulation of lamin A monomers at p40 (Figure 3.2a). In contrast to lamin A, lamin C migrated as a monomer across all three population doublings under both non-reducing and reducing conditions (Figure 3.2b). These findings suggest that the cysteine residues in the lamin A tail promote both inter and intra-disulfide bond formation (Figure 3.2c). Note the inter-molecular bonds could form with other lamin A polypeptides or with other lamin A binding proteins (e.g. LAP2α). Lastly, as HDFs age *in vitro*, cysteine residues in lamin A become progressively less available for forming disulfide bonds.

Protein thiols can undergo different degrees of oxidation, which can be either reversible (sulfenic acid) or irreversible (sulfinic and sulfonic acids) (Poole et al., 2004) (Supplementary Figure 2). To investigate if cysteine residues in lamin A become irreversibly oxidized in senescent HDFs, and therefore explain why they become progressively less available for forming disulfide bonds as HDFs age, MALDI-TOF/TOF peptide mass fingerprinting in conjunction with reductive thiol-trapping alkylation was used. Three cysteine-containing peptides of lamin A were identified in the Mascot database: αα516-27, which contains C522, and αα585-97 and αα583-97 (the latter having one missed cleavage site at R585), both containing C588 and C591 (Figure 3.2d). In young (p12) HDFs, the observed and predicted masses of each peptide corresponded to the mass difference of either one (αα516-27) or two (αα583-97 & αα585-97) alkylation adducts, indicating an absence of reduction-resistant oxidative modifications (Figure 3.2d). In contrast, in senescence (p40) HDFs, the observed and predicted peptide masses differed by

32Da (αα516-27) or 48Da + a mass of one alkylation adduct (αα583-97 & αα585-97) (Figure 3.2d). The observed peptide modifications were resistant to DTT reduction and corresponded to those expected for irreversible oxidation to sulfinic (SO_2H) and sulfonic (SO_3H) acids respectively. Together, this data shows that lamin A cysteines are targets of irreversible oxidative modifications in senescent (p40) HDFs, which most likely explains the observed decrease in disulfide bond formation under oxidizing conditions shown previously.

HDFs from old individuals also display increased dysmorphic nuclei similar to senescent HDFs from young individuals (Scaffidi and Misteli, 2006). Therefore, to interrogate the ability of lamin A cysteine residues to form disulfide bonds in HDFs from old individuals, cell extracts were resolved on non-reducing or reducing SDS-PAGE and probed with anti-lamin A (Jol4) antibody as described previously. Under non-reducing conditions, HDFs from an old individual (aged 84) displayed a reduction in both the slower-migrating lamin A homodimer and faster-migrating protein species (Figure 3.3a). Quantification of band intensities revealed reductions of ~70% and ~50%, respectively, for inter- and intra-disulfide bond formation (Figure 3.3b). Under reducing conditions, lamin A migrated as a monomer, confirming that both the slower- and faster-migrating bands of lamin A in HDFs were disulfide-dependent (Figure 3.3a) In sum, this extends the previous findings and suggests that reduced lamin A disulfide bond formation may occur *in vivo* during the normal aging of healthy individuals.

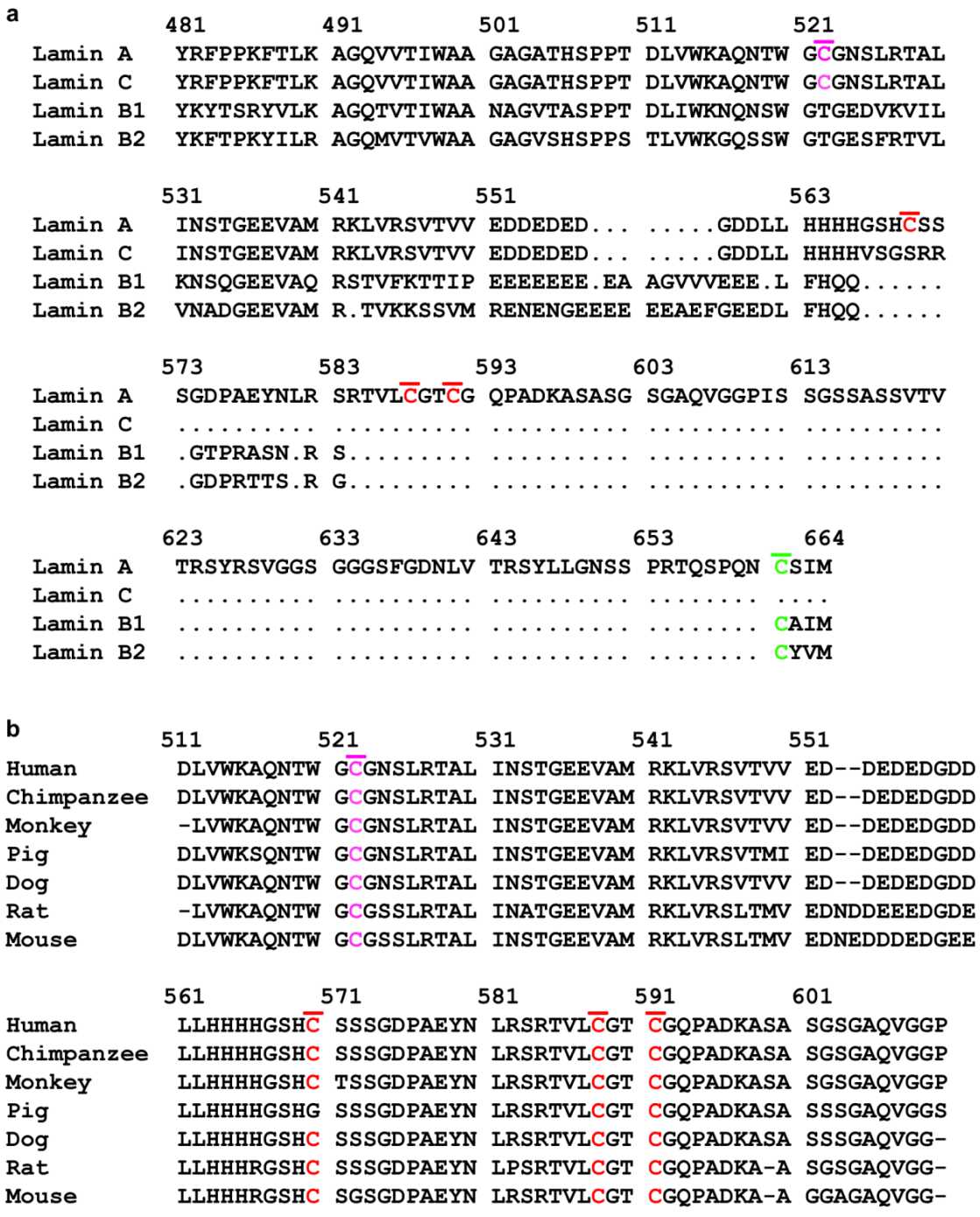

Figure 3.1. Conserved cysteine residues in the lamin A C-terminal. (a) Multiple sequence alignment of the C-terminal regions from human A- and B-type lamins. Cysteine residues are labelled as follows: a single cysteine common to the IgG domain of lamins A and C (purple), three lamin A specific cysteines (red) and a CAAX-box associated cysteine (green). (b) A-type lamin C-terminal sequence alignment of various mammalian species with labelling as in (a).

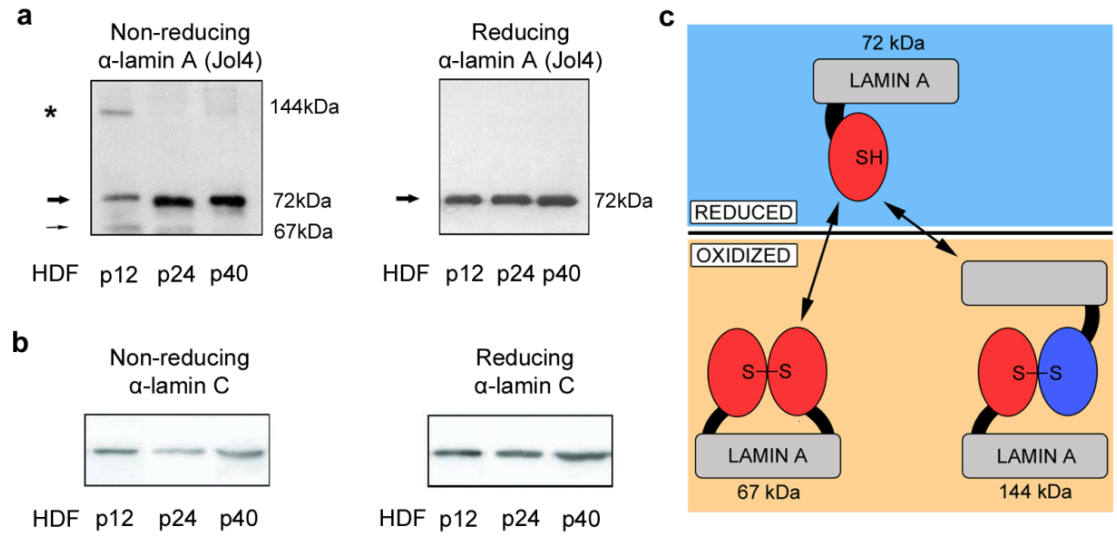

d

PDL	Residue number	Observed mass	Predicted mass	Δ mass	Sequence	Modification
p12	516-527	1431.6	1306.6	125	K AQNTWGCGNSL R	NEM
p40	516-527	1338.6	1306.6	32	K AQNTWGCGNSL R	SO_2H
p12	583-597	1785.7	1535.7	250	R SRTVLCGTCGQPAD K	2 x NEM
p40	583-597	1708.7	1535.7	173	R SRTVLCGTCGQPAD K	NEM + SO_3H
p12	585-597	1542.6	1292.6	250	R TVLCGTCGQPAD K	2 x NEM
p40	585-597	1465.6	1292.6	173	R TVLCGTCGQPAD K	NEM + SO_3H

Figure 3.2. Hyper-oxidation of lamin A tail thiol residues in senescent fibroblasts. (**a,b**) Protein extracts from p12-40 HDFs were subjected to non-reducing or reducing SDS-PAGE and immunoblotted against Jol4 (a) to detect lamin A or RαLC (b) to detect lamin C. Thick arrow, lamin A (72kDa); thin arrow, lamin A intra-molecular disulfide (~67kDa). *, lamin A inter-molecular disulfide (~144kDa). (**c**) Cartoon showing redox-dependent formation of lamin A intra- and inter-molecular disulfides (S-S). Note the inter-molecular bonds could form with other lamin A polypeptides or with other lamin A binding proteins (e.g. LAP2α). SH, cysteine sulfhydryl group. (**d**) MALDI-TOF/TOF peptide mass fingerprinting of lamin A peptides isolated from p12 and p40 HDF in the presence of NEM. Three lamin A cysteine-containing peptides αα516-27 (C522), αα583-97 and αα585-97 (C588 and C591) were identified in Mascot database (C570-containing peptide was not detected and could not be analysed). The mass differences (in daltons)

between observed and predicted peptide mass peaks, the amino acid sequence of modified peptides and their corresponding modifications are listed. SO_2H = sulfinic acid, SO_3H = sulfonic acid.

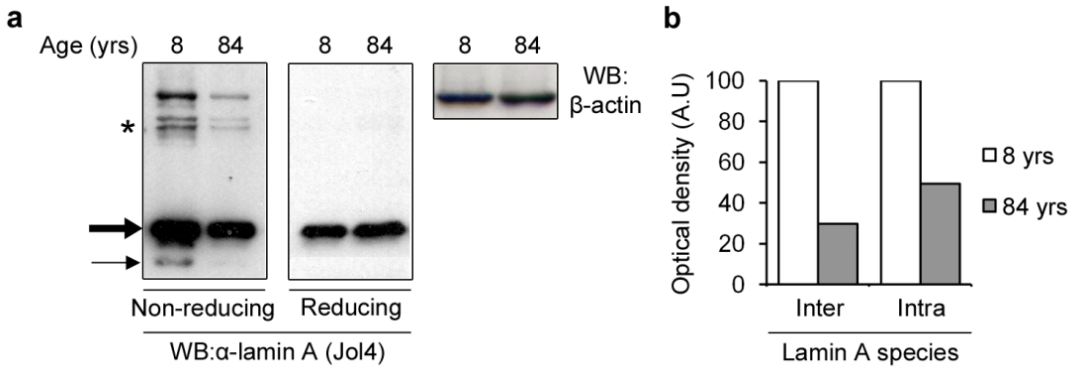

Figure 3.3. Age-dependent modifications to lamin A cysteine residues inhibit disulfide bond formation. (**a**) HDF protein extracts from young and old individuals were subjected to either non-reducing or reducing SDS-PAGE and immunoblotted with anti-lamin A (Jol4) antibody. Representative blots were selected from two repeat experiments using two young and three old donors. Thick arrow, lamin A; *, lamin A inter-molecular dimers; thin arrow, lamin A intra-molecular disulfides. (**b**) Optical densitometry of non-reducing blots was performed to determine the relative proportion of inter-molecular dimers and intra-molecular disulfides in protein extracts from young and old donors and the values obtained for protein bands were normalised to those of the corresponding monomeric lamin A.

3.3 Temporary cell cycle arrest of HDF in response to mild oxidative stress is correlated with disulfide bond formation in lamin A.

HDFs enter a state of stress induced premature senescence (SIPS) following exposure to high levels of oxidative stress, whilst exposure to mild oxidative stresses elicits a protective stress response leading to temporary growth arrest (Davies, 1999). Furthermore, it has been proposed that the formation of disulfide bonds may act as part of a protective response to mild oxidative stress (Eaton, 2006). Hydrogen peroxide (H_2O_2) is the most widely used pro-oxidant as it is produced physiologically and serves as an essential second messenger in redox signalling (Toussaint et al., 2000). Since I have shown that lamin A forms disulfide bonds in young HDFs but not in senescent HDFs, I investigated whether lamin A forms disulfide bonds *in vivo* in response to oxidative stress. Based on the prior data and the above hypotheses of Davis et al. and Eaton, I anticipated that mild oxidative stress would cause a temporary cell cycle arrest and the formation of lamin A disulfide bonds, whereas excessive oxidative stress would cause entry into a senescent state and inhibit the formation of lamin A disulfide bonds.

Firstly, I assessed the proliferation of HDFs in the presence of either low or high levels of oxidative stress. Young (p12) HDFs were treated *in vivo* with either 150μM or 350μM H_2O_2 alone, or following anti-oxidant pre-treatment with N-acetyl cysteine (NAC) (Figure 3.4a). The viability of HDFs was not affected by any of the treatments (not shown). After the treatments, HDFs were either cultured for 72h or were reseeded and cultured for an additional 24h, before being assessed for cellular morphology, expression of proliferation markers, expression of senescence-associated β-galactosidase (SA β-gal) activity and nuclear morphology. In response to 150μM H_2O_2 alone, HDFs entered a state of growth arrest, demonstrated by reduced expression of the proliferation marker Ki67 (<30%) (Figure 3.4b). The growth arrest was readily reversible following reseeding in the absence of H_2O_2, as assessed by the spindle-shaped cell morphology (Figure 3.4a) and a high Ki67+ index (>70%, Figure 3.4b). Treatment

of HDFs with 150μM H_20_2 did not affect nuclear morphology (Figure 3.4e) or induce expression of SA β-gal (Figure 3.4d). In contrast, in response to 350μM H_2O_2, HDFs entered a state of stress induced premature senescence as shown by a flattened cell morphology (Figure 3.4a), greatly reduced Ki67 labelling (<20%, Figure 3.6c) and high SA β-gal activity (>50%, Figure 3.4d). Notably, none of these phenotypes was reversed by re-seeding in the absence of H_2O_2. Premature entry into a senescent state was correlated with greatly increased numbers of abnormally shaped nuclei (Figure 3.4e). Pre-treatment of HDFs with the free radical scavenger N-acetyl cysteine (NAC) prevented both the transient effects of 150μM H_2O_2 and the senescence inducing effects of 350μM H_2O_2 (Figure 3.4a-e).

To analyse the ability of lamin A to form disulfide bonds in response to oxidative stress, young (p12) HDFs were treated with either 150μM or 350μM H_2O_2 *in vivo*. Cell extracts were prepared in the presence of the alkylating agent N-ethylmaleimide (NEM) and resolved on non-reducing or reducing SDS-PAGE. In untreated cells, both faster and slower migrating forms of lamin A were weak but detectable with an anti-lamin A (Jol4) antibody (Figure 3.4f). The detection of the faster and slower migrating bands increased significantly after treatment with 150μM H_2O_2, suggesting enhanced intra- and inter-disulfide bond formation in response to mild oxidative stress (Figure 3.4f). Neither species was detected in the presence of 350μM H_20_2, suggesting that thiol residues were unavailable for disulfide bond formation (Figure 3.4f). Under reducing conditions, lamin A was detected as a monomer after each H_2O_2 treatment confirming that the slower and faster migrating species were disulfide-dependent (Figure 3.4f). Importantly, following NAC pre-treatment there was no increase in the level of disulfide bonds formation in the presence of 150μM H_2O_2, neither was there any elimination of disulfides following 350μM H_2O_2 (Supplementary Figure 3). Taken together, these findings show that in response to mild oxidative stresses HDFs enter a state of temporary cell cycle arrest, which is correlated with disulfide bond formation in lamin A. Moreover, in the absence of effective ROS scavenging, high levels of oxidative stress promote stress induced premature senescence and this is

correlated with the appearance of dysmorphic nuclei and absence of disulfide bond formation in lamin A.

3.4 HDF are hypersensitive to ROS stimulation in the absence of lamin A.

Whilst the data presented thus far has determined a correlation between senescence and oxidation of lamin A cysteine residues preventing intra- and inter-disulfide bond formation, senescence is also correlated with the appearance of dysmorphic nuclei. One interpretation of this may be the presence of non-functional lamin A in the nuclear lamina. Thus, to determine the role of lamin A in cellular senescence, I investigated the cellular response to mild oxidative stress in HDFs harbouring a homozygous mutation Y259X in the *LMNA* gene, which are null for expression of lamins A/C (Muchir et al., 2003). I hypothesized that in the absence of lamin A, these HDFs would be more sensitive to mild oxidative stresses and therefore have an increased likelihood of undergoing stress induced premature senescence instead of temporary growth arrest. Wild-type and Y259X HDFs were either left untreated or treated *in vivo* with 150μM H_2O_2 and analysed for their proliferative capacity, SA β-gal activity and nuclear morphology. As observed previously, Y259X HDFs showed a reduced Ki67 proliferative index and an increased percentage of dysmorphic nuclei and SA β-gal activity when compared to wild type HDFs (Figure 3.4g-i) (Pekovic et al., 2007). In response to 150μM H_2O_2, wild-type HDFs entered a growth arrest as shown by a ~2.5 fold reduction in expression of Ki67, but re-entered the cell cycle following reseeding as shown by re-expression of Ki67 (Figure 3.4g). Treatment of wild type HDFs with 150μM H_2O_2 did not induce either SA β-gal activity or the appearance of dysmorphic nuclei (Figure 3.4h,i). In contrast, treatment of Y259X HDFs with 150μM H_2O_2 led to a ~2 fold reduction in Ki67 expression that was not reversible following re-seeding (Figure 3.4g), and caused them to enter stress induced premature senescence as shown by a >2 fold increase in both SA β-gal activity and the percentage of dysmorphic nuclei (Figure 3.4h,i). Taken together, these results suggest that lamin A is essential for cellular resilience to oxidative stress.

Figure 3.4. The effects of mild and SIPS-inducing oxidative stress on lamin A disulfide bridge formation, nuclear morphology and growth. (**a-e**) HDFs were treated with 150 or 2x 350μM H_2O_2 alone or after pre-incubation with 10mM NAC. (a) Phase contrast images were taken within one week of H_2O_2 treatments (left and middle panels), or following additional reseeding for 24h (right panels). Bar, 20μm. (b) The fraction of Ki67 +ve nuclei determined before reseeding. (c) The fractions of Ki67 +ve nuclei, (d) SA β-gal +ve HDFs and (e) dysmorphic nuclei determined after reseeding. (**f**) Protein extracts from 150, 250 or 2x 350μM H_2O_2-treated HDFs were prepared with 40mM NEM, resolved on non-reducing/reducing SDS-PAGE and probed with JoL2. Thick arrow, lamin A (72kDa); arrowhead, lamin C (65kDa); thin arrow, lamin A intra-molecular disulfide (~67kDa); *, lamin A inter-molecular dimer (~144kDa). (**g-i**) Wild-type and lamin A/C -/- HDFs (Y259X) were left untreated or treated with 150μM H_2O_2 and the fractions of Ki67 +ve nuclei (g), SA β-gal +ve cells (h) and dysmorphic nuclei (i) determined before or after reseeding. Fractions were calculated by scoring 300 cells from random fields on triplicate coverslips in three independent experiments. Means ± S.D. are shown. *, $p<0.05$ relative to 150μM H_2O_2-treated HDFs without NAC (c-e) or untreated lamin A/C -/- HDFs (g-i).

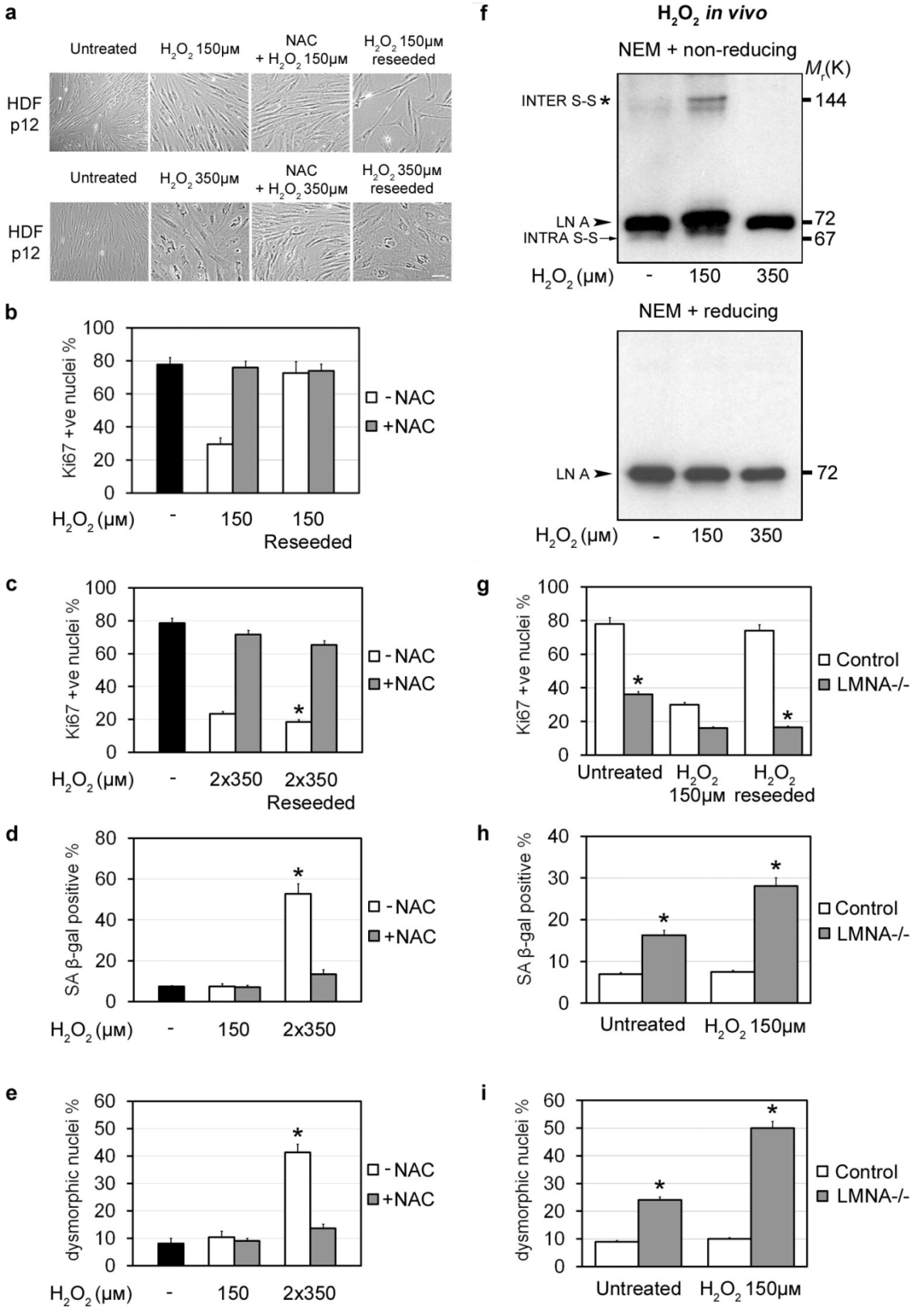
a
Untreated
H2O2 150μM
NAC + H2O2 150μM
H2O2 150μM reseeded
HDF p12
Untreated
H2O2 350μM
NAC + H2O2 350μM
H2O2 350μM reseeded
HDF p12
b
Ki67 +ve nuclei %
100
80
60
40
20
0
- NAC
+NAC
H2O2 (μM) - 150 150 Reseeded
c
Ki67 +ve nuclei %
- NAC
+NAC
H2O2 (μM) - 2x350 2x350 Reseeded
d
SA β-gal positive %
80
60
40
20
0
- NAC
+NAC
H2O2 (μM) - 150 2x350
e
dysmorphic nuclei %
60
50
40
30
20
10
0
- NAC
+NAC
H2O2 (μM) - 150 2x350
f
H2O2 in vivo
NEM + non-reducing
Mr(K)
INTER S-S *
144
LN A
INTRA S-S
72
67
H2O2 (μM) - 150 350
NEM + reducing
LN A
72
H2O2 (μM) - 150 350
g
Ki67 +ve nuclei %
100
80
60
40
20
0
Control
LMNA-/-
Untreated
H2O2 150μM
H2O2 reseeded
h
SA β-gal positive %
40
30
20
10
0
Control
LMNA-/-
Untreated
H2O2 150μM
i
dysmorphic nuclei %
60
50
40
30
20
10
0
Control
LMNA-/-
Untreated
H2O2 150μM

3.5 Loss of conserved C-terminal lamin A cysteine residues abrogates lamin A function and promotes cellular senescence.

As the data has implicated lamin A in the cellular response to oxidative stress, which is correlated with intra- and inter-disulfide bond formation in lamin A, I sought to assess whether the redox-dependent disulfide bond formation in lamin A is associated with an adaptive response to oxidative stress. To this end, I used a panel of cysteine-to-alanine Flag-tagged lamin A constructs including the single mutants C522A, C588A, C591A, a double mutant C588/591A and a triple mutant C522/588/591A. Wild-type and mutant constructs were then expressed in young (p12) HDFs. Cell extracts were prepared in the presence of NEM and were resolved on either non-reducing or reducing SDS-PAGE and immunoblotted with anti-Flag or anti-lamin A (Jol4) antibodies. Under non-reducing conditions, Flag-wt lamin A was detected as a monomer as well as the slower and faster-migrating protein bands, indicating the formation of both intra- and inter-molecular disulfide bonds (Figure 3.5a). Mutants C588A and C591A also formed intra and inter-molecular disulfide bonds (Figure 3.5a). In contrast, whilst mutant C522A readily formed inter-molecular disulfides, intra-molecular disulfides were undetectable (Figure 3.5a). Furthermore, disulfide bond formation was nearly undetectable in the double mutant (C588/591A) and completely undetectable in the triple mutant (C522/588/591A) (Figure 3.5a). As expected, Flag-lamin A proteins migrated as monomers under reducing conditions (Figure 3.5b). The level of over-expression of lamin A was then investigated by immunoblotting with an anti-lamin A (Jol4) antibody. The results indicated that on average there was a ~2 fold increase in the level of lamin A following transfection, suggesting an approximate 1:1 ratio of endogenous compared to Flag-lamin A (Figure 3.5c). This panel of lamin A constructs were therefore used to determine which cysteine residues in lamin A were important for cellular resilience to ROS and in determining whether disulfide bond formation is a component of an adaptive cellular response to oxidative stress.

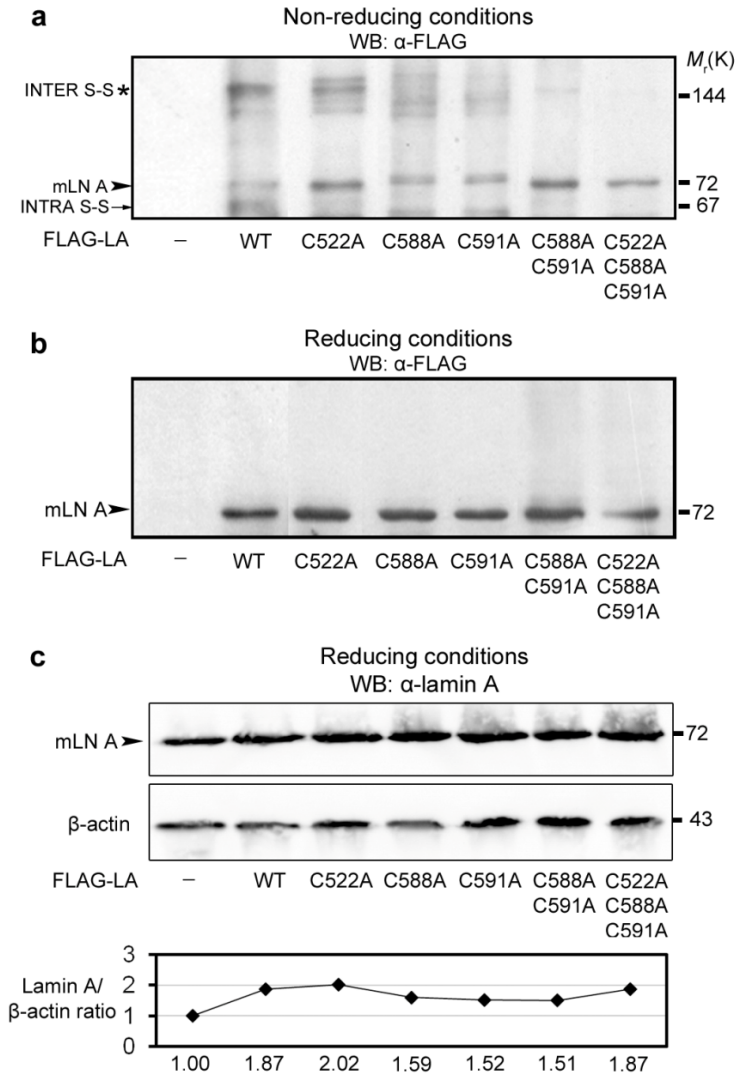

Figure 3.5. Cysteine-to-alanine mutations differentially affect lamin A disulfide formation. (**a-b**) HDF were transfected with Flag-wt or one of five different Flag-cys-ala lamin A constructs. Protein extracts prepared in the presence of NEM were resolved on non-reducing (a) or reducing (b) SDS-PAGE and probed with anti-Flag M2 antibodies. Lanes contain untransfected control (-), wild type lamin A (WT), C522A, C588A, C591A single lamin A mutants, C588/591A double lamin A mutant or C522/588/591A triple lamin A mutants. Arrowhead, lamin A monomer; arrow intra-molecular disulfide species; *, inter-molecular disulfides species. (**c**) HDF were transfected with the same constructs and probed with anti-lamin A (133A2) or anti-β-actin antibodies. The graph shows

the fold expression of cys-ala lamin A protein relative to endogenous lamin A in untransfected control and normalized to β-actin following optical densitometry.

In order to investigate the effects of the lamin A mutants on nuclear morphology and cellular proliferation, young HDFs (p12) were transfected with either Flag-wild type (Flag-wt) lamin A or one of the cysteine-to-alanine lamin A mutants. As expected, Flag-wt lamin A localised both to the nuclear envelope and to the nucleoplasm and >85% of transfected HDFs showed normal nuclear morphology (Figure 3.6a,b). Each of Flag-C522A, C588A and C591A lamin A also localised strongly to the nuclear envelope and transfected HDFs displayed normal nuclear morphology (Figure 3.6a,b). Flag-C588/591A lamin A also localised to the nucleus but displayed elevated (~20% of transfected cells) levels of nuclei containing aggregates of Flag-tagged proteins (Figure 3.6a,b). In contrast, expression of Flag-C522/588/591A lamin A resulted in gross disorganisation within nuclei and ~45% of transfected HDFs displayed dysmorphic nuclear shapes (Figure 3.6a,b). A range of assays were then utilised to assess the affect of each mutant on proliferation and senescence. Firstly, the Ki67 index, a marker of actively dividing cells, and proliferation rates of HDFs did not differ significantly following transfection with Flag-wt, C522A, C588A or C591A lamin A (Figure 3.6c,d). Transfection with Flag-C588/591A lamin A did not significantly affect the proliferation index but did significantly impair the growth rate of HDFs (Figure 3.6c,d). Finally, transfection with Flag-C522/588/591A lamin A significantly reduced the proliferation index (to <40%) and halved the growth rate of HDF when compared Flag-wt lamin A and the single mutants (Figure 3.6c,d). I then investigated the possible emergence of a senescent phenotype to account for the reduced Ki67 and growth rates, either by expression of SA β-gal or by cell morphology. Consistent with the above findings, only HDFs expressing Flag-C522/588/591A lamin A were able to induce cellular senescence in a significant fraction (>25%) (Figure 3.6e). Furthermore, only HDFs expressing Flag-C522/588/591A lamin A exhibited a flattened enlarged cellular morphology, indicative of entry into senescence (Figure 3.6f) (Dimri et al., 1995). Taken

together, this data suggests two important results. Firstly, the ability of lamin A to form intra- and inter-molecular disulfide bonds is not directly linked to entry into a senescent state, since neither the expression of Flag-C522A lamin A (which is unable for form intra-molecular disulfide bonds) nor Flag-C588/591A lamin A (which is unable for form any disulfide bonds) were able to induce a senescent phenotype, although the Flag-C588/591A lamin A mutant does impair growth rates. Secondly, the loss of all three C-terminal cysteine residues generates a phenotype that is remarkably similar to a lamin A null phenotype suggesting a complete abrogation of lamin A function (compare Figures 3.4 and 3.6).

Figure 3.6. A triple lamin A mutant C522/588/591A impairs cellular fitness which induces premature senescence. (**a**) HDFs (p12) were transfected with Flag-wt (WT) or one of C522A, C588A, C591A, C588/591A or C522/588/591A lamin A constructs and immunostained with anti-Flag M5 antibody and DAPI. Micrographs are displayed as two-colour merged images (Flag, red; DAPI, blue). Scale bar = 10μm. The fraction of Flag +ve cells showing dysmorphic nuclei (**b**) or Ki67 ve+ cells (**c**) for each construct used is shown. Fractions were calculated by counting 300 cells from triplicate coverslips in three independent experiments. (**d**) Growth curves of cells transfected with WT, or each of the cys-ala lamin A mutants. (**e**) The fractions of SA β-gal +ve transfected HDFs were calculated by counting 300 cells in triplicate wells in three independent experiments. (**f**) Phase contrast images of Flag-wt, Flag-C522A C588A, C591A, C588/591A or C522/588/591A mutant lamin A transfected HDFs. Scale bars = 20μm. Means ± S.D. are shown. *, $p<0.05$ relative to Flag-wt HDFs.

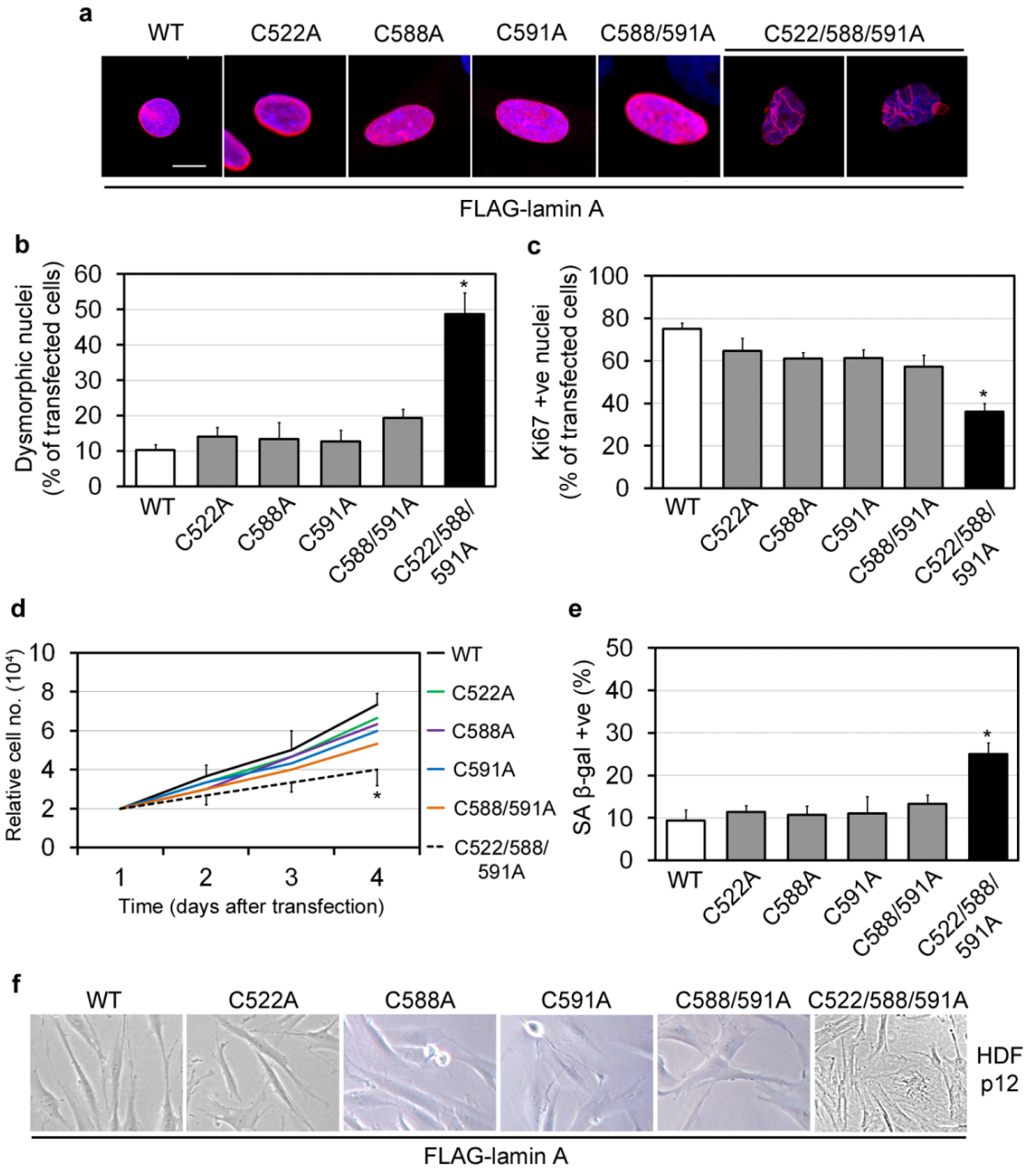
a
WT
C522A
C588A
C591A
C588/591A
C522/588/591A
FLAG-lamin A
b
Dysmorphic nuclei (% of transfected cells)
0
10
20
30
40
50
60
*
WT
C522A
C588A
C591A
C588/591A
C522/588/ 591A
c
Ki67 +ve nuclei (% of transfected cells)
0
20
40
60
80
100
*
WT
C522A
C588A
C591A
C588/591A
C522/588/ 591A
d
Relative cell no. (10⁴)
0
2
4
6
8
10
1
2
3
4
Time (days after transfection)
*
WT
C522A
C588A
C591A
C588/591A
C522/588/ 591A
e
SA β-gal +ve (%)
0
10
20
30
40
50
*
WT
C522A
C588A
C591A
C588/591A
C522/588/ 591A
f
WT
C522A
C588A
C591A
C588/591A
C522/588/591A
HDF p12
FLAG-lamin A

3.6 Abrogation of lamin A function by C522/588/591A causes ROS intolerance in HDFs

To further investigate the finding that the lamin A mutant C522/588/591A abrogates lamin A function, I compared ROS generation in a broad spectrum of cell types with various *LMNA* backgrounds. These included HDFs expressing either Flag-wt lamin A or Flag-C522/588/591A lamin A, HDFs functionally null for lamin A/C (Y259X), HDFs from a HGPS patient harbouring the classical G608G mutation and HDFs expressing a mutant lamin A/C (R453W) that causes Autosomal dominant Emery Dreifuss Muscular Dystrophy (AD-EDMD). HDFs were treated with mild levels of oxidative stress (150μM H_2O_2) and the levels of ROS before or after treatment were determined using a ROS-sensitive fluorescent dye (Figure 3.7e). Representative cytograms from wild type, Y259X, G608G and R453W HDFs are shown (Figure 3.7a-d). In HDFs expressing Flag-C522/588/591A lamin A, basal levels of ROS were ~3 fold higher when compared to HDFs expressing Flag-wt lamin A (Figure 3.7e). The presence of single lamin A mutants did not affect basal levels of ROS (e.g. C522A, Supplementary Figure 4). Upon stimulation with 150μM H_2O_2, ROS levels increased by ~2 fold in HDFs expressing Flag-wt lamin A, whereas in HDFs expressing Flag-C522/588/591A lamin A, ROS levels became saturated (Figure 3.7e). These data suggest that in the presence of Flag-C522/588/591A lamin A, ROS homeostasis is disturbed and HDFs become hypersensitive to oxidative stress. Similarly, the basal levels of ROS were ~2.5 fold higher in Y259X HDFs, compared to those expressing Flag-wt lamin A, and increased still further upon stimulation with H_2O_2 (Figure 3.7e). In contrast, whilst HDFs expressing progerin or R453W displayed basal levels of ROS that were ~1.5 fold higher than controls, upon stimulation with H_2O_2 ROS levels were only slightly elevated and did not exceed the levels observed following H_2O_2 stimulation in the controls (Figure 3.7e). Importantly, pre-treatment of HDFs with the ROS scavenger NAC abrogated the effects of H_2O_2 stimulation in all cases (Figure 3.7e). I also investigated ROS levels in HDFs from patients with X-linked EDMD, which are null for the inner nuclear membrane protein emerin and

from patients with Greenberg Dysplasia, which are null for the inter nuclear membrane protein Lamin B receptor (LBR). I found that both basal levels and stimulated levels of ROS were identical to controls (Supplementary Figure 5 and data not shown). Taken together, these data suggest that hypersensitivity to oxidative stress is a phenotype that occurs specifically due to the loss of conserved cysteine residues in the lamin A tail or absence of lamin A, rather than the general NE defects or with disease associated mutations in the *LMNA* tail domain. To confirm this finding, I also investigated the cellular responses to mild oxidative stress in HDFs from HGPS and AD-EDMD, harbouring G608G and R453W mutations, respectively. As for wild type HDFs, both the G608G and R453W HDFs entered a reversible cell cycle arrest following stimulation with 150μM H_20_2 (Figure 3.7f) and this treatment did not significantly increase the fraction of cells expressing SA β-gal (Figure 3.7g) or the percentage of dysmorphic nuclei (Figure 3.7h). Therefore, these data confirm that the presence of functional lamin A is required for resilience to cellular ROS and that elimination of the conserved cysteine residues in the lamin A tail abrogates lamin A function.

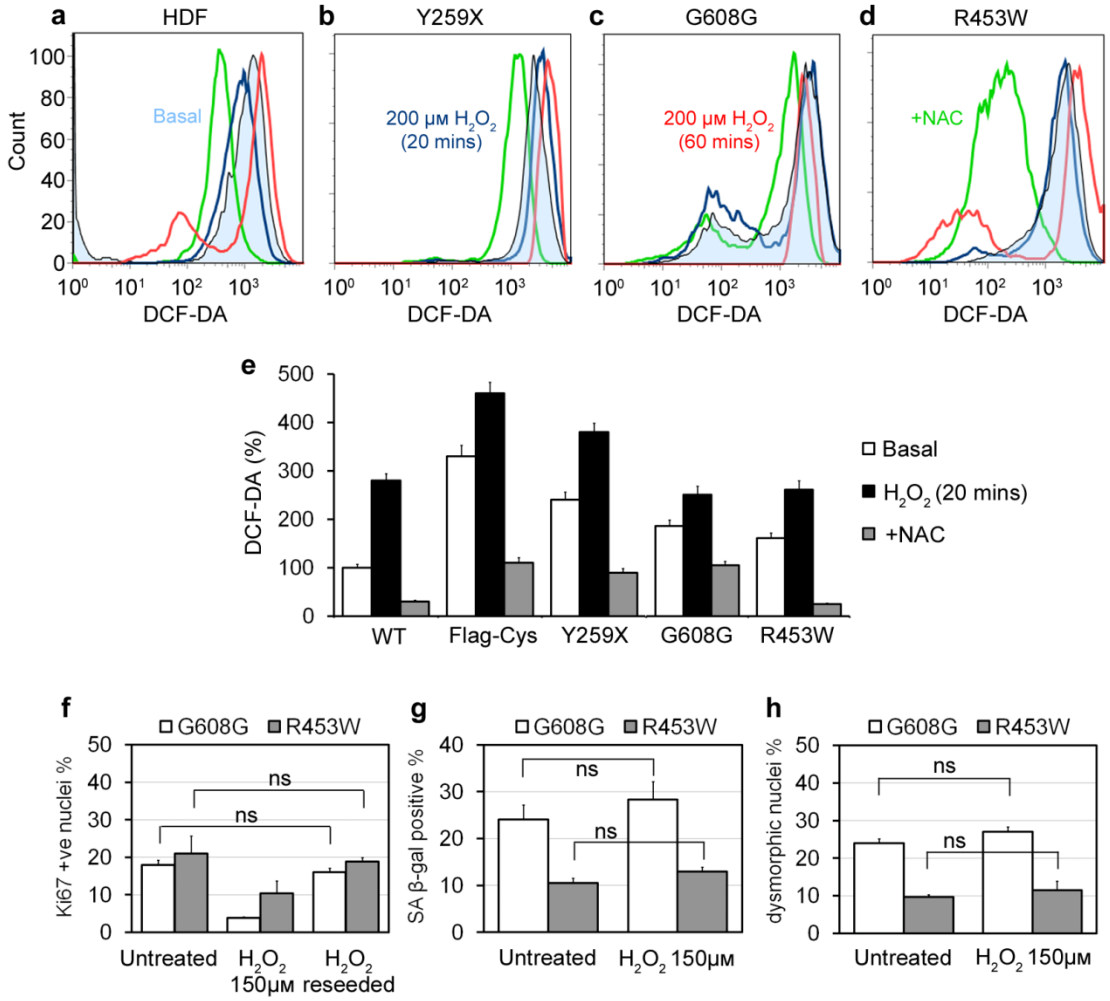

Figure 3.7. Absence of lamin A or presence of lamin A C522/588/591A cysteine mutant impairs ROS homeostasis in cells. (**a-d**) Basal intracellular ROS levels were determined by measuring relative DCF fluorescence in HDFs, Y259X, HGPS (G608G) and AD-EDMD (R453W) cells under basal conditions, following 200μM H_2O_2 stimulation for 30min, or after antioxidant treatment with 10mM NAC. Representative cytograms are shown. (**e**) Data from (a-d) with the addition of HDFs transfected with Flag-wt or C522/588/591A lamin A (Flag-Cys). DCF fluorescence is expressed as % relative to Flag-wt HDFs or control HDFs (not shown) which is set at 100%. The increase or decrease in DCF fluorescence following H_2O_2 or NAC treatments, respectively is expressed as % relative to the basal level for each culture. Means ± S.D. are shown. *, $p<0.05$ compared to Flag-wt HDFs or control HDFs. (**f-h**) Patient HDFs expressing progerin or AD-

EDMD mutation R453W were left untreated or treated with 150μM H_2O_2 and the fractions of Ki67 +ve cells (f), SA β-gal +ve cells (g) and dysmorphic nuclei (h) determined before and after reseeding. Fractions were calculated by scoring 300 cells from random fields on triplicate coverslips in three independent experiments. Means ± S.D. are shown. NS = not significant when comparing untreated cells with 150μM H_2O_2-treated cells after reseeding for each culture.

Since HDFs expressing Flag-C522/588/591A lamin A appear to be hypersensitive to oxidative stress, I predicted that the deleterious effects of this mutant on cell proliferation arose as a direct result of the increased cellular accumulation of ROS. To test this hypothesis, I investigated both nuclear morphology and cell proliferation in conditions that either increase or decrease cellular ROS. I assessed nuclear morphology and SA β-gal activity following stimulation with 150μM H_2O_2. As expected, there was no significant increase in dysmorphic nuclei or SA β-gal expression (<5%) in H_2O_2-treated HDFs expressing Flag-wt lamin A (Figure 3.8a,b). In contrast, H_2O_2-treated HDFs expressing Flag-C522/588/591A lamin A showed increases of 23% and 14% in dysmorphic nuclei and SA β-gal expression, which were effectively prevented by NAC pre-treatment (Figure 3.8a,b). Importantly, direct treatment of these fibroblasts with NAC (in the absence of H_2O_2) reduced basal levels of dysmorphic nuclei and SA β-gal activity to levels similar to those observed in HDFs expressing Flag-wt lamin A (Figure 3.8a,b). These results suggest that the induction of dysmorphic nuclei and stress induced premature senescence in HDFs expressing Flag-C522/588/591A lamin A results from higher levels of ROS accumulating in these cells, since they could be prevented by exogenous treatments with anti-oxidants.

Oxygen tension is another factor that can modulate cellular ROS levels (Parrinello et al., 2003), and under standard culture conditions oxygen tension is relatively high (20.6%). Cells were therefore cultured under low (5%) oxygen tension to investigate whether this would ameliorate the deleterious effects of expressing Flag-C522/588/591A lamin A. A comparison between basal ROS levels in HDFs

expressing Flag-wt lamin A and Flag-C522/588/591A lamin A revealed that, as previously observed, under standard culture conditions, basal ROS levels were significantly higher in HDFs expressing Flag-C522/588/591A lamin A mutant compared to Flag-wt lamin A (Figure 3.8c). In contrast, basal ROS levels in HDFs expressing the mutant were reduced by ~2.5 fold in 5% oxygen as compared to 20.6% oxygen (Figure 3.8c). Similar reductions in cellular ROS were also observed following pre-treatment with NAC (Figure 3.7). Since ROS are major inducers of DNA damage, which is known to result in senescent arrest (Gorbunova et al., 2002), I examined whether increased ROS levels in HDFs expressing Flag-C522/588/591A lamin A were accompanied with the formation of DNA damage foci. When grown under standard oxygen tension, the fraction of cells displaying DNA damage foci was ~3 fold greater in HDFs expressing Flag-C522/588/591A lamin A compared to HDFs expressing Flag-wt lamin A (Figure 3.8d). As expected, the fraction of HDFs displaying DNA damage foci declined significantly when they were grown under low oxygen tension (Figure 3.8d). Similarly, the levels of both dysmorphic nuclei and SA β-gal activity were also significantly decreased in HDFs expressing Flag-C522/588/591A lamin A in 5% oxygen as compared to 20.6% oxygen conditions (Figure 3.8e,f). In sum, these data suggests that HDFs expressing C522/588/591A lamin A have reduced tolerance to oxidative stress, leading to a number of deleterious cellular effects including accumulation of ROS, ROS-induced DNA damage and premature entry into senescence. Moreover, deleterious cellular effects can be ameliorated either by application of exogenous ROS scavengers or by growth under low oxygen tension. This data strongly suggests that loss of the conserved cysteine residues in the lamin A tail reduces cellular fitness by rendering fibroblasts hypersensitive to ROS.

Figure 3.8. HDFs expressing C522/588/591A lamin A mutant show intolerance to mild oxidative stress. (**a-b**) HDFs expressing Flag-wt or C522/588/591A lamin A were left untreated or treated with 150μM H_2O_2 in the presence or absence of 10mM NAC. Alternatively, transfected cultures were treated with 10mM NAC in the absence of H_2O_2 stimulation. (a) The fraction of Flag +ve dysmorphic nuclei or (b) SA β-gal +ve cells were determined 72h after H_2O_2 stress. Fractions were calculated by scoring 300 cells on triplicate coverslips in three independent experiments. (**c-f**) Transfected HDFs were assessed under standard (20.6%) or low (5%) oxygen tension for basal ROS levels (c) and for fractions of Flag +ve nuclei showing either γ-H2AX DNA damage foci (d), dysmorphic nuclei (e), or SA β-gal +ve cells (f). Fractions were scored by counting 300 nuclei on triplicate coverslips from three independent experiments. Means ± S.D. are shown. *, $p<0.05$ relative to untreated Flag-C522/588/591A lamin A HDFs (a-b), or Flag-wt lamin A HDFs at 21% O2 (c-f). **, $p<0.05$ relative to untreated Flag-C522/588/591A lamin A HDFs (a-b), or Flag- C522/588/591A HDFs at 21% O2 (c-f).

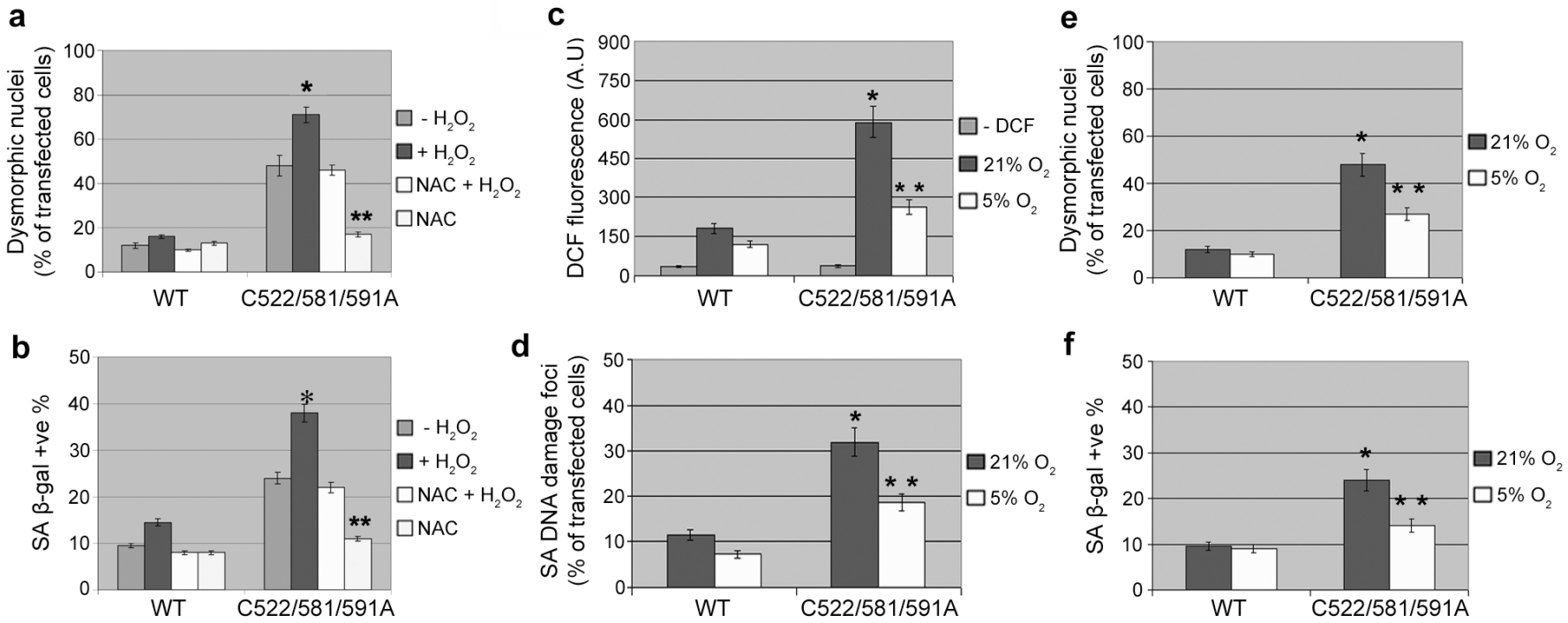
a
Dysmorphic nuclei (% of transfected cells)
100
80
60
40
20
0
*
**
- H_2O_2
+ H_2O_2
NAC + H_2O_2
NAC
WT
C522/581/591A
b
SA β-gal +ve %
50
40
30
20
10
0
*
**
- H_2O_2
+ H_2O_2
NAC + H_2O_2
NAC
WT
C522/581/591A
c
DCF fluorescence (A.U)
900
750
600
450
300
150
0
*
**
- DCF
21% O_2
5% O_2
WT
C522/581/591A
d
SA DNA damage foci (% of transfected cells)
50
40
30
20
10
0
*
**
21% O_2
5% O_2
WT
C522/581/591A
e
Dysmorphic nuclei (% of transfected cells)
100
80
60
40
20
0
*
**
21% O_2
5% O_2
WT
C522/581/591A
f
SA β-gal +ve %
50
40
30
20
10
0
*
**
21% O_2
5% O_2
WT
C522/581/591A

3.7 Mild oxidative stress stimulates over-expression of AP-1 genes in the presence of Flag-C522/588/591A lamin A or absence of lamin A

The previous data shows that the absence of lamin A or the presence of a lamin mutant lacking conserved C-terminal cysteine residues causes ROS intolerance. To begin to understand the mechanism behind ROS intolerance, I investigated whether expression of transcription factors that can activate anti-oxidant enzymes or expression of the genes encoding the anti-oxidant enzymes themselves is impaired in HDFs null or expressing various forms of *LMNA*. To assess this, qPCR was used to quantify the expression of these genes in the presence or absence of mild oxidative stress (150μM H_2O_2) in HDFs expressing Flag-wt lamin A or Flag-C522/588/591A lamin A, and also in HGPS HDFs harbouring the classical G608G mutation and in lamin A null (Y259X) HDFs. The expression levels of all the genes assessed were similar in HDFs expressing Flag-wt lamin A and HGPS HDFs (Figure 3.9). In contrast, in HDFs expressing Flag-C522/588/591A lamin A or HDFs null for lamin A (Y259X), genes in the AP-1 and NF-κB family, c-fos and p65, were both significantly up-regulated following mild oxidative stress, although levels of expression of Sp1 were similar to controls (Figure 3.9). The likely down-stream targets of AP-1 and NF-κB, including manganese superoxide dismutase (MnSOD), catalase (CAT) and glutathione S-transferase (GST) were also all significantly up-regulated following mild oxidative stress in both HDFs expressing Flag-C522/588/591A lamin A and HDFs null for lamin A (Y259X), suggesting that the anti-oxidant defence pathways were activated (Figure 3.9). Interestingly, the level of activation of c-fos, which exhibited a ~6 fold activation following oxidative stress, has previously been reported only in response to chronic (500μM H_2O_2) oxidative stress (Chaum et al., 2009). Taken together, whilst these data do not reveal the mechanism behind ROS intolerance they do confirm our hypothesis that loss of lamin A function does lead to hypersensitivity to and intolerance of ROS.

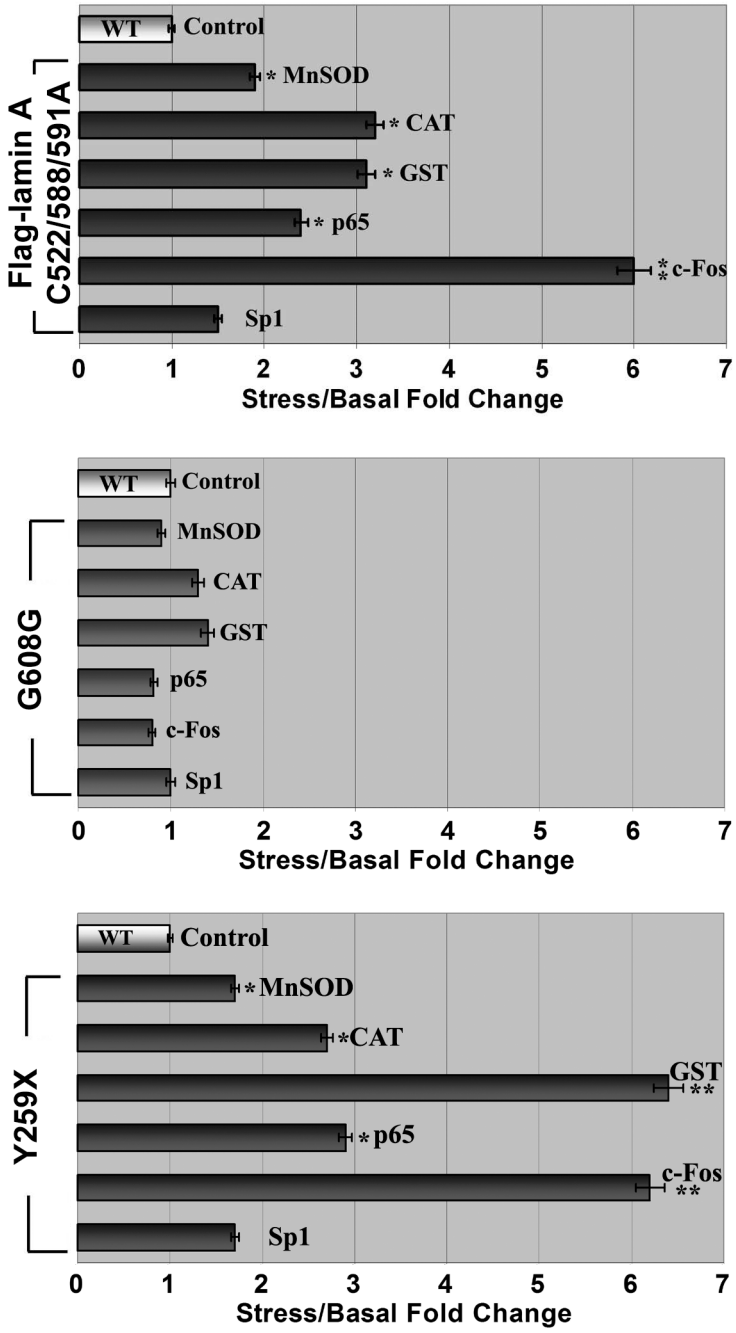

Figure 3.9. C522/588/591A lamin A mutant induces expression of many stress-responsive genes. HDFs expressing Flag-wt lamin A and Flag-C522/588/591A lamin A as well as patient HDFs expressing progerin or that are null for lamin A/C (Y259X) were cultured in the presence (stress) or absence (basal) of 150 μM H2O2 . Total RNA was isolated and cDNA samples subjected to real-time qPCR using primers specific for detoxification enzymes (MnSOD and

CAT), glutathione enzyme (GST) and transcription factors NF-κB (p65), AP-1 (c-Fos) and Sp1. PCR reactions for each sample were performed in triplicates in two independent experiments. Values for each sample were normalised to β-actin. Data were presented as fold change of the ratio between stress-induced and basal levels of gene expression relative to HDFs expressing Flag-wt lamin A, which is set at 1. (Figure kindly provided by Dr Ewa Markiewicz, University of Durham)

3.8 Discussion

3.8.1 The oxidation status of lamin A cysteine residues influences cellular redox homeostasis and the onset of cellular senescence

In this chapter, I propose a novel function for lamin A in the maintenance of cellular redox homeostasis. Lamin A is a target of irreversible oxidative modifications on cysteine residues during cellular aging, which is associated with decreased redox-dependent disulfide bond formation and alterations in nuclear morphology. Furthermore, I have also shown that in response to mild oxidative stress, HDFs require the presence of functional lamin A to correctly activate an adaptive stress response that is characterized by temporary growth arrest and lamin A disulfide bond formation. In order to investigate the role of conserved cysteine residues on lamin A function, I utilised various cysteine-to-alanine lamin A mutants including C522A, which has limited ability to form intra-disulfides, and C522/588/591A, which is unable to form both intra- and inter-disulfide bonds. Expression of Flag-C522/588/591A lamin A in HDFs leads to nuclear disorganisation and high levels of cellular ROS, resulting in ROS-induced DNA damage and the onset of stress induced premature senescence. The increased ROS levels in HDFs expressing Flag-C522/588/591A lamin A appear to result from greatly impaired ROS homeostasis since growth under standard oxygen tension appears to result in high ROS levels. Whether this is a direct consequence of mutating three cysteine residues or a dominant negative effect of impairing lamin filament assembly will need future clarification based on *in vitro* structural studies of lamin filament assembly. Interestingly, other disease-causing *LMNA* mutations that disrupt nuclear morphology such as those causing HGPS (G608G) and AD-EDMD (R453W) also lead to increased cellular ROS levels, but in contrast to Flag-C522/588/591A lamin A, these mutations do not sensitize HDFs to additional low levels of ROS stimulation. Importantly, mutating the common cysteine residue in the Ig fold domain of the lamin A/C tail (C522A) has no affect on ROS stimulation, nuclear morphology or adaptive responses to mild oxidative stress. Lowering of ROS levels in HDFs expressing Flag-cys by either

exogenous treatments with ROS scavengers or growth under low oxygen tension are both able to significantly rescue dysmorphic nuclear morphology, DNA damage and the entry into senescence. Taken together, these findings strongly suggest that lamin A is an essential component of an adaptive cellular response to mild oxidative stress. Furthermore, these findings suggest an essential component of the adaptive response is the ability to form inter-disulfide bonds via the lamin A tail domain.

Protein oxidative damage is known to result in either a loss-of-function or a toxic gain-of-function (Linke and Jakob 2003). The data presented here implies that oxidative damage during cellular aging to cysteine residues in the lamin A tail lead to a loss-of-function, because the phenotype and cellular responses of HDFs expressing Flag-C522/588/591A lamin A are identical to those of HDFs that are functionally null for lamin A (Y259X). In either case, the dominant phenotype is elevated basal levels of ROS (when cells are grown under high oxygen tension) and hyper-sensitivity to mild oxidative stress. Therefore, I propose that lamin A mediates the transient cell cycle arrest that typifies an adaptive response to mild oxidative stress. Moreover, this adaptive response is intimately connected to disulfide bond formation in the lamin A tail.

Disulfide bond formation has been proposed to serve a protective function (Linke and Jakob, 2003) and therefore the simplest explanation for the elevated ROS phenotype observed in HDFs expressing Flag-C522/588/591A lamin A is that it leads to the formation of unstable lamin A dimers. However, this seems unlikely since the mutant is stably expressed in HDFs and is dominant over its endogenous wild type counterpart. The dominant effect of Flag-C522/588/591A lamin A is presumably because lamin A is an obligate homo-dimer (Stuurman et al., 1998), and therefore the Flag-C522/588/591A lamin A would become paired with the endogenous wild type lamin A, which would prevent formation of inter-disulfide bonds in response to oxidative stress. Therefore, an alternative hypothesis is that inter-disulfide bond formation gives rise to conformational changes in the lamin A tail that may modify its binding to cell cycle response

proteins and this is what mediates the adaptive ROS response. If this hypothesis is correct then inter-molecular disulfide bond formation most likely involves sequestration of cell cycle response proteins to the nuclear lamina since HDFs expressing Flag-C522/588/591A lamin A have an equivalent phenotype to HDFs null for lamin A (Y259X).

3.8.2 Lamin A as a mediator of an adaptive response to oxidative stress

Previous studies have shown that oxidative stress leads to cysteine oxidation of many proteins including lamins A/C (Eaton et al., 2003). Whilst cellular senescence has been associated with widespread ROS-related damage that is not targeted to specific proteins, proteins that are highly abundant and contain reactive thiols are the most strongly favoured ROS targets. Such abundant thiol proteins act as redox regulators in cells and only when their thiols become fully oxidized, so do other less abundant thiol proteins become susceptible to ROS (Winterbourn and Hampton 2008). A-type lamins are expressed in all mesenchymal tissues and are highly abundant nuclear proteins, interfacing chromatin and both the nuclear interior and periphery (Hutchison and Worman 2004). Moreover, A-type lamins bind to and regulate a number of proteins that are pivotal to the processes of cell proliferation and cellular senescence (Dechat et al., 2010). Firstly, lamin A has been implicated in p53-dependent DNA damage response pathway (Liu et al., 2005; Varela et al., 2005). This is important because ROS-mediated DNA damage has been implicated in both cellular senescence and organismal aging (Campisi and D'Adda di Fagagna, 2007; Sahin and DePinho, 2010). Furthermore, ROS may also cause telomere damage, which may induce cellular senescence independently of telomere length (Passos et al., 2007). As lamin A is involved in the maintenance of telomeres (Gonzalez-Suarez et al., 2009), this provides another link between lamin A and its role in cellular senescence and also as part of an adaptive response to oxidative stress. Additionally, lamin A also regulates cellular proliferation via the pRb-E2F pathway (Markiewicz et al., 2002, Johnson et al., 2004, van Berlo et al., 2005). More recently, lamin A has also been implicated in regulating proliferation via the AP1

pathway (Ivorra et al., 2006; Gonzalez et al., 2008). Previous studies from our laboratory, as well as data presented in Chapter 4, have shown that depletion of lamin A in HDFs by RNAi leads to impaired cell cycle progression and premature cell cycle arrest (Pekovic et al., 2007). Thus, I propose that lamin A mediates an adaptive response to oxidative stress because it is a highly abundant protein that is ideally positioned both within the nuclear periphery and interior to enable it to regulate various proliferative and senescent pathways, which ultimately make it a target for age-related oxidative damage.

It remains to be determined whether lamin A-interacting proteins are also oxidatively modified during cellular aging. Of note, multiple sequence alignments of the lamin A nucleoplasmic binding partner, LAP2α, revealed that it contains nine unique cysteine residues in its C-terminal region and shares only one cysteine residues with two other LAP2 family members, LAP2β and LAP2γ (Supplementary Figure 6). Future work should therefore seek to determine the role of LAP2α cysteine residues in cellular aging and the implication this has for nucleoplasmic lamin A functions in senescence pathways.

Interestingly, in parallel to these findings, a recent study has implicated B-type lamins in the cellular response to oxidative stress (Malhas et al., 2009). It was previously shown that B-type lamins sequester the transcription factor Oct-1 at the nuclear envelope (Imai et al., 1997). Furthermore, Oct-1 has been shown to regulate genes involved in the oxidative stress response (Tantin et al., 2009). Based on these findings, Malhas et al. showed that *Lmnb1*$^{-/-}$ MEFs exhibited elevated ROS levels and were more susceptible to oxidative stress, with free Oct-1 occupying gene promoters of genes involved in the oxidative stress response, causing their deregulation (Malhas et al., 2009). It therefore seems likely that both A- and B-type lamins contribute to the cellular response to oxidative stress, but via distinct mechanisms. Future work will determine if the known transcription factors that are sequestered at the nuclear envelope in an A-type lamin dependent manner may influence the response to oxidative stress analogously to the lamin B1-Oct-1 relationship.

3.8.3 Possible synergy between oxidative thiol damage to lamin A and the accumulation of prelamin A and progerin during normal aging

Cellular aging of HDFs is associated with loss of nucleoplasmic A-type lamins and the appearance of lamin A disease-linked variants such as progerin and prelamin A (Scafidi and Misteli 2006, Ukekawa et al., 2007). Interestingly, activation of the same cryptic splice site found in HGPS patients (harbouring a G608G mutation, which produces the mutant protein termed progerin) has been detected at low levels in human skin cells and tissues from both young and old individuals (Scaffidi and Misteli 2006). Furthermore, progerin has been detected in a subset of dermal fibroblasts and terminally differentiated keratinocytes in skin biopsies from old individuals (McClintock et al., 2007). Thus, it is has been suggested that the presence of low levels of progerin, in concert with other age-dependent mechanisms, may be required for the observed adverse effects on nuclear morphology and cellular proliferation in aged cells (Kudlow et al., 2007). In this context, the current findings suggest that, in addition to progerin and prelamin A representing important determinants of age-related changes in cells, oxidative damage to lamin A thiols may also have an important influence on cellular aging. Oxidative damage to lamin A thiols may act synergistically with relatively low levels of progerin that could amplify its dominant-negative effects, and in combination, contribute towards a state of cellular senescence. Therefore, in sum, these findings support the concept that lamin A is an important determinant of normal aging.

CHAPTER 4:
LAP2α-LAMIN A/C COMPLEXES GOVERN CELL CYCLE PROGRESSION IN HUMAN DERMAL FIBROBLASTS

4.1 Introduction

4.1.1 Overview

The eukaryotic cell cycle is elegantly controlled by highly evolved mechanisms that co-operate to ensure the accurate transmission of DNA from mother cell to daughter cells. Exquisite regulation of the cell cycle is essential for organismal development and, subsequently, organismal longevity. Importantly, the cell cycle machinery is a prime target for mutations that contribute to many cancers, which may lead to chronic proliferation of cells, a fundamental trait of all cancers (Hanahan and Weinberg, 2011). Therefore, understanding the fundamental processes that operate to control normal cellular proliferation is of basic, as well as clinical, scientific interest.

4.1.2 The role of LAP2α-lamin A/C complexes in G_1/S-phase transition

There is evidence to suggest that nucleoplasmic LAP2α-lamin A/C complexes regulate the G_1/S-phase transition via interaction with pRb (Markiewicz et al., 2002). Previous studies showed that the active hypophosphorylated pRb is tightly bound to the nuclear matrix during G_1 and resists extraction with DNase (Mittnacht and Weinberg, 1991). Hyperphosphorylated pRb bound weakly to the nuclear matrix, suggesting that phosphorylation of pRb disrupts the interaction with the nuclear matrix as cells traverse the G_1/S-phase transition (Mittnacht and Weinberg, 1991). Further work demonstrated that this inactive form of pRb bound to lamin A via the pocket C domain of pRb and was only bound in G_1-phase, when pRb is active in its hypophosphorylated state (Mancini et al., 1994). Importantly, using cells which contained a mutated *RB* gene, pRb was readily solubilised in G_1-phase cells, suggesting that tethering to the nuclear matrix was important for

the tumour suppressor functions of pRb (Mancini et al., 1994). More recent work has dissected these pRb-lamin A/C complexes (Dechat et al., 2000; Markiewicz et al., 2002; Dorner et al., 2006). The lamin A/C-interacting partner LAP2α is found within the nucleoplasm and interacts with lamin A/C (amino acids 319-572) via its C-terminal domain (amino acids 615-693) (Dechat et al., 2000). LAP2α is also able to interact with the pocket C domain of pRb via its own C-terminal region (amino acids 415-615) (Markiewicz et al., 2002; Dorner et al., 2006). This region is downstream of the lamin A/C-interacting domain, thus enabling a trimeric pRb-LAP2α-lamin A/C complex to form (Markiewicz et al., 2002; Dorner et al., 2006). Lamin A/C also interacts with the pocket C domain of pRb via residues 247-355 in the α-helical rod domain (Ozaki et al., 1994). Overexpression of a domain negative lamin B1 mutant sequesters endogenous lamin A/C, LAP2α and pRb into nucleoplasmic aggregates, underlining the interactions between these three proteins (Markiewicz et al., 2002). Importantly, this suggests that LAP2α-lamin A/C complexes may govern the G_1/S-phase transition by promoting pRb nuclear anchorage (Markiewicz et al., 2002). Moreover, LAP2α resides at E2F-dependent promoters, suggesting that the pRb-LAP2α-lamin A/C complex may interact at promoters to inhibit E2F-dependent transcription of S-phase genes (Dorner et al., 2006). Indeed, whilst overexpression of LAP2α in both Hela and mouse 3T3 cells inhibited G_1/S-phase progression, RNAi of endogenous LAP2α in Hela cells enhanced proliferation and also inhibited the ability to exit the cell cycle in response to low serum conditions (Dorner et al., 2006). Furthermore, over-expression of LAP2α inhibited E2F transcriptional activity in mouse 3T3 cells, underlining its negative effect on cell cycle progression (Dorner et al., 2006). However, loss of LAP2α, and indeed lamin A/C, in normal human fibroblasts (HDFs) by RNAi elicits a different cellular response than mouse and transformed human cells (Pekovic et al., 2007). HDFs depleted of either LAP2α or lamin A/C lead to cell cycle arrest by 72 hours post-transfection, as assessed by Ki67 staining (Pekovic et al., 2007). The differences between the two studies probably reflect fundamental differences in the cell types used (Dorner et al., 2006; Pekovic et al., 2007).

4.1.3 Current aims

Previous studies have implicated LAP2α-lamin A/C complexes in the regulation of cell cycle progression with HDFs depleted of either protein undergoing cell cycle arrest. However, the underlying causes of this have yet to be established. In this chapter, I explore in more detail the cell cycle alterations associated with loss of either LAP2α or lamin A/C in HDFs.

4.2 Depletion of LAP2α or lamin A/C causes altered cell cycle progression in HDFs

The nuclear lamins have been implicated in cell cycle progression by a number of studies (Dechat et al., 2010). Both A- and B-type lamins have been suggested to have roles in S-phase progression, however, seemingly contradictory data has underpinned the necessity for a more thorough exploration of A-type lamins in DNA replication (Kennedy et al., 2000; Izumi et al., 2000). Previous work from our laboratory has shown that depleting LAP2α or lamin A/C by RNAi leads to an initial accumulation of G_2/M-phase cells after 48 hours, before entering a G_1-phase arrest after 72 hours, as analysed by single parameter FACS (Pekovic et al., 2007). It was therefore hypothesized that the accumulation of cells transiently in G_2/M-phase after 48 hours may be due to accelerated passage through S-phase, as has been shown previously for *Lap2α*$^{-/-}$ MEFs (Dorner et al., 2006). Experimentally, to circumvent differences in cell cycle phase upon RNAi, HDFs were serum-starved for 5-7 days. HDFs were then stimulated with 10% DMEM to allow re-entry into the cell cycle and transfected with siRNA (Figure 4.1a) (Kill et al., 1991). Depletion of LAP2α or lamin A/C in HDFs by RNAi is first detectable at the protein level by 48 hours and is most prominent by 72 hours with ~ 70% knockdown of LAP2α or lamin A/C protein levels compared to control cells (Figure 4.1d-f). Note that LAP2α protein levels are initially at 0% as LAP2α protein levels are down-regulated in quiescent cells and are then up-regulated in response to mitogenic stimuli (Supplementary Figure 7) (Markiewicz et al., 2002; Pekovic et al., 2007). In order to estimate S-phase fraction, HDFs were labelled after 42 hours post-transfection with EdU (an analogue of BrdU) for 1 hour. Fixed cells were then processed and analysed by FACS using a dual parameter EdU/DNA analysis to obtain the percentage of cells in each phase of the cell cycle. Bivariate histograms were produced from at least three different samples to calculate the mean percentage of cells in each phase of the cell cycle (Figure 4.1b,c).

HDFs transfected with non-targeting control siRNA were predominantly in G_1-phase (~68%) after 43 hours, with ~18% of cells in G_2/M-phase and a minority of cells in S-phase (~13%) (Figure 4.1b,c). In contrast, HDFs depleted of LAP2α or lamin A/C showed a statistically significantly reduced percentage of cells in G_1-phase, ~33% for LAP2α and ~27% for lamin A/C (Figure 4.1b,c). The percentage of cells in S-phase in LAP2α or lamin A/C depleted HDFs was also dramatically increased compared to control cultures, with ~29% for LAP2α and ~25% for lamin A/C. Lastly, analysis of the cytograms revealed a significantly increased percentage of cells in G_2/M-phase for both LAP2α and lamin A/C depleted HDFs, with ~30% for LAP2α and ~38% for lamin A/C compared to control HDFs (~18%) (Figure 4.1b,c). Together, this data suggests that loss of LAP2α and lamin A/C causes altered cell cycle progression as cells passage from quiescence back into the cell cycle.

Figure 4.1. Loss of LAP2α or lamin A/C leads to delayed cell cycle progression. (**a**) Schematic diagram showing the experimental methodology. (**b**) HDFs were transfected with control, LAP2α or lamin A/C siRNA and then labelled with EdU (10μM for 1h) 42h post-transfection before subsequent fixation and analysis by flow cytometry. Representative cytograms are shown. (**c**) Data from cytograms was analysed using FlowJo software and the mean percentage values (*n* = 3-5) + S.D. for each cell cycle phase were calculated. * $p<0.05$ relative to G_1-, S-, or G_2-phase for siCon. (**d**) HDFs transfected with siRNA were harvested after 24, 48 or 72h and protein extracts were subjected to reducing SDS-PAGE and then immunoblotted with anti-lamin A/C, LAP2α or β-actin antibodies. (**e-f**) The level of LAP2α or lamin A/C protein remaining in protein extracts as a function of time (siCon vs. si*LAP2α* and siCon vs. si*LMNA*) was assessed using optical densitometry and expressed as a percentage of the control siRNA, which was set a value of 100%.

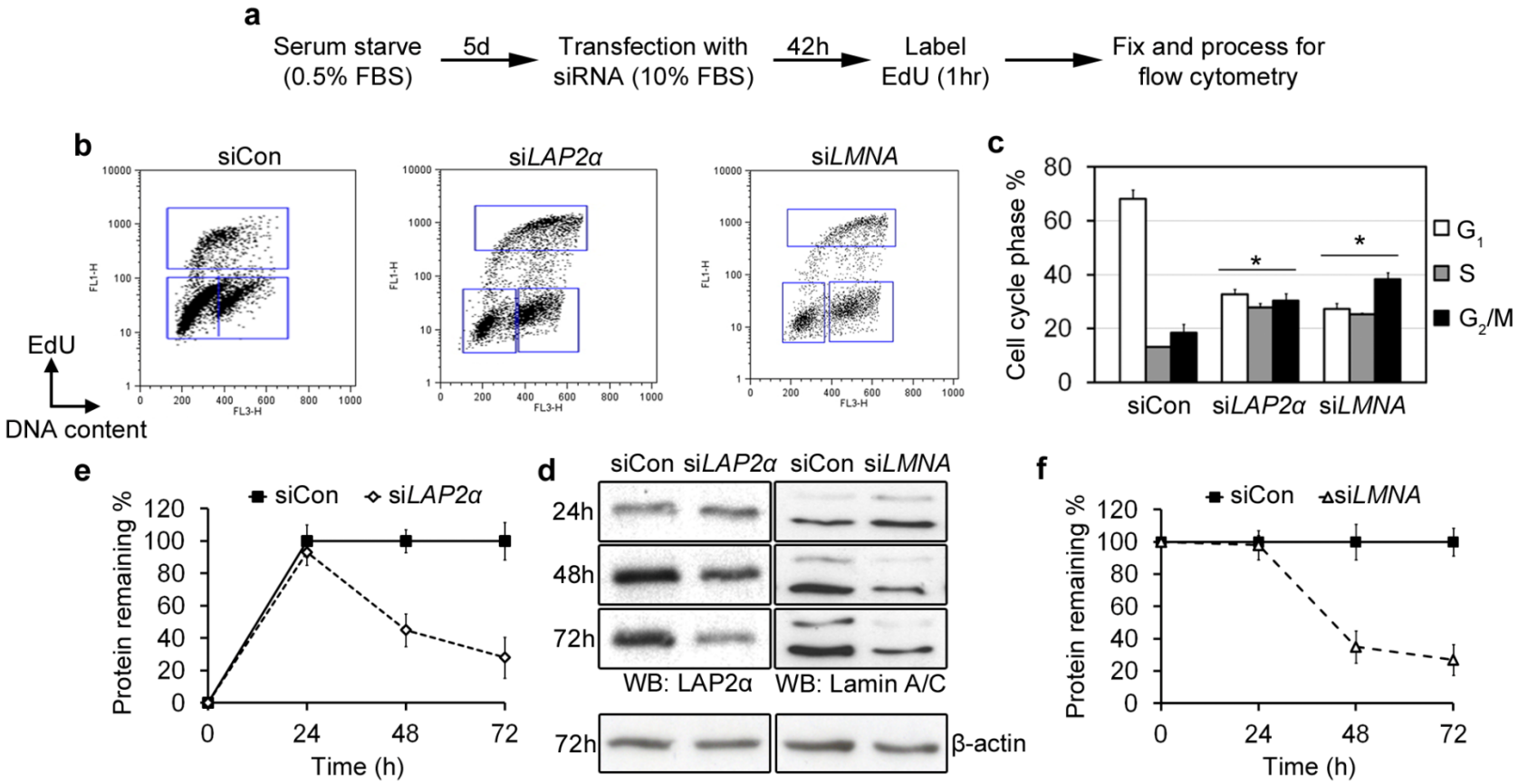
a
Serum starve (0.5% FBS)
5d
Transfection with siRNA (10% FBS)
42h
Label EdU (1hr)
Fix and process for flow cytometry
b
siCon
siLAP2α
siLMNA
EdU
DNA content
c
Cell cycle phase %
G1
S
G2/M
siCon
siLAP2α
siLMNA
d
siCon siLAP2α siCon siLMNA
24h
48h
72h
WB: LAP2α
WB: Lamin A/C
72h
β-actin
e
siCon
siLAP2α
Protein remaining %
Time (h)
f
siCon
siLMNA
Protein remaining %
Time (h)

4.3 Depletion of LAP2α or lamin A/C delays G_1/S-phase progression in HDFs

Based on the findings that loss of either LAP2α or lamin A/C caused altered cell cycle progression, it was unclear how loss of LAP2α or lamin A/C leads to an increased percentage of cells in both S and G_2/M-phases. I therefore sought to investigate whether loss of LAP2α or lamin A/C causes alterations in either G_1/S-phase progression, S-phase duration, or both. Studies in *Lap2α*$^{-/-}$ and *Lmna*$^{-/-}$ MEFs hinted that loss of either protein may lead to either accelerated entry into S-phase or accelerated passage through S-phase, although these two are not mutually exclusive (Johnson et al., 2004; Dorner et al., 2006). To assess these hypotheses directly, it was necessary to estimate the S-phase fraction in LAP2α or lamin A/C depleted HDFs both before and after the 42 hours timepoint previously used for bivariate FACS analysis. To this end, HDFs depleted of LAP2α or lamin A/C were labelled with EdU (for 1 hour) every 3 hours ranging from 23 to 65 hours post-transfection before fixation and processing (Figure 4.2a). The HDFs used in this study exhibit four types of replication patterns when stained with an anti-PCNA antibody (Kill et al., 1991) or, as in this study, labelled with EdU and then detected using an Alexa Fluor 488-conjugated azide that reacts with a side-chain of EdU (Diermeier-Daucher et al., 2009). At the initiation of S-phase, a small number of dim foci are evident and are termed Type I foci. The Type II pattern is granular in appearance and is observed uniformly across the nucleus. Type III nuclei exhibit a punctate pattern with the perinuclear region enriched. The Type IV pattern displayed fewer bright foci and is the last pattern observed (Figure 4.2b).

Initially, the mean percentage of EdU+ cells, i.e. those in S-phase, was analysed over a timecourse from non-targeting control, LAP2α or lamin A/C depleted HDFs. Control HDFs progressed from G_0 (0 hours) through G_1-phase and had entered S-phase by 24 hours, as indicated by the Edu+ cells (Figure 4.2 ‘siCon’). Control HDFs then showed a decrease in EdU+ cells after 27 hours, suggesting

procession through to G_2/M-phase (Figure 4.2c 'siCon'). After ~ 51 hours post-transfection, control HDFs showed an increase in EdU+ cells, indicating that a second round of replication was initiated (Figure 4.2c 'siCon'). The peak of the second round of replication did not reach the levels of the first round of replication, suggesting that the culture had lost synchrony. In contrast to control HDFs, LAP2α or lamin A/C depleted HDFs exhibited a significantly altered EdU+ and hence S-phase distribution over the time-course investigated (Figure 4.2c,d 'si*LAP2α*' and 'si*LMNA*'). Importantly, the progression into S-phase was delayed for LAP2α or lamin A/C depleted HDFs compared to control HDFs, with the EdU+ cells peaking around 39-42 hours (Figure 4.2c,d 'si*LAP2α*' and 'si*LMNA*'). The percentage of cells in S-phase in LAP2α or lamin A/C depleted HDFs then declined to ~15-20% and showed no distinct increase at later time points, indicating that the second round of DNA replication was inhibited or delayed beyond the extent of the times investigated (Figure 4.2c,d). Together, these findings suggest that loss of either LAP2α or lamin A/C in HDFs delays the first G_1/S-phase progression after cell cycle re-entry from G_0.

To explore these findings in more detail, HDFs were then assessed for the S-phase type after 42 hours, as this timepoint was used for flow cytometry analysis previously. Based on the flow cytometry data, I predicted that EdU+ cells in HDFs depleted of either LAP2α or lamin A/C would be in mid-to-late S-phase, whereas control HDFs would show increased early S-phase cells. Indeed, control HDFs typically displayed the Type I (~15%) and II (~64%) patterns, with a minority exhibiting Type III (~12%) and Type IV (~9%) patterns, indicating that the EdU+ cells were mainly in early-mid S-phase (Figure 4.2e). In contrast, LAP2α or lamin A/C depleted HDFs showed an over-representation of Type III and IV S-phase patterns (*p*-values for pattern types observed in si*LAP2α* or si*LMNA* vs. siCon is shown in Figure 4.2e). LAP2α depleted HDFs displayed ~7% Type I, ~48% Type II, 29% Type III and ~16% Type IV patterns (Figure 4.2e). Similarly, lamin A/C depleted HDFs exhibited 10% Type I, 53% Type II, 22% Type III and 15% Type IV patterns (Figure 4.2e). The increased percentage of LAP2α or lamin A/C depleted HDFs showing Type III and IV S-phase patterns indicates that these cells are in

mid to late S-phase by 42 hours. Therefore, in combination with the prior flow cytometry data, this data suggests that, upon re-stimulation from quiescence (G_0), control HDFs proceed through the first S-phase by 24 hours, progress into G2/M and then G1-phase before initiating another round of DNA replication by ~ 51 hours. In contrast, HDFs depleted of LAP2α or lamin A/C progress through the first G_1/S-phase more slowly than control HDFs. Together, these findings suggest that LAP2α and lamin A/C are required for efficient G_1/S-phase progression.

Analysis of the EdU+ data suggested that S-phase duration was unchanged between control HDFs and LAP2α or lamin A/C depleted HDFs, i.e. the rate of decline from the maximum to the minimum percentage of EdU+ cells was similar in these cultures (Figure 4.2c,d). To underline this, I investigated PCNA, an adaptor protein that acts to dramatically enhance the processivity of DNA polymerase δ during chain elongation in DNA synthesis by acting as a loading clamp and encircling DNA (Bowman et al., 2004). Immunoblotting of protein extracts from LAP2α or lamin A/C depleted HDFs revealed that total PCNA levels were unchanged after 48 and 72 hours post-transfection (Figure 4.2f). This suggests that loss of LAP2α or lamin A/C does not affect total PCNA protein levels. In sum, this data suggests that depletion of LAP2α or lamin A/C leads to delayed G_1/S-phase progression in HDFs.

Figure 4.2. Loss of LAP2α or lamin A/C causes delayed G_1/S-phase progression. (**a**) Schematic diagram showing the experimental methodology. (**b**) HDFs grown in culture exhibit four distinct patterns of S-phase staining (I-IV). These patterns can be visualised by labelling HDFs with EdU (10 M) for 1 hour. EdU was detected using an Alexa Fluor 488-conjugated azide that reacts with a side-chain of EdU. (**c,d**) HDFs were transfected with control, LAP2α or lamin A/C siRNA and then labelled with EdU (10μM for 1h) at various times post-transfection before subsequent fixation and analysis by microscopy. The mean percentage of EdU+ cells was calculated from at least 300 cells and the experiment was repeated twice. Error bars represent ± S.D. (**e**) S-phase patterns were analysed 42h post-transfection according to (b). At least 500 EdU positive cells were scored and the experiment was repeated twice. *p*-values are relative to siCon patterns. (**f**) HDFs transfected with siRNA were harvested after 48 or 72h and protein extracts were subjected to reducing SDS-PAGE and then immunoblotted with anti-PCNA or β-actin antibodies.

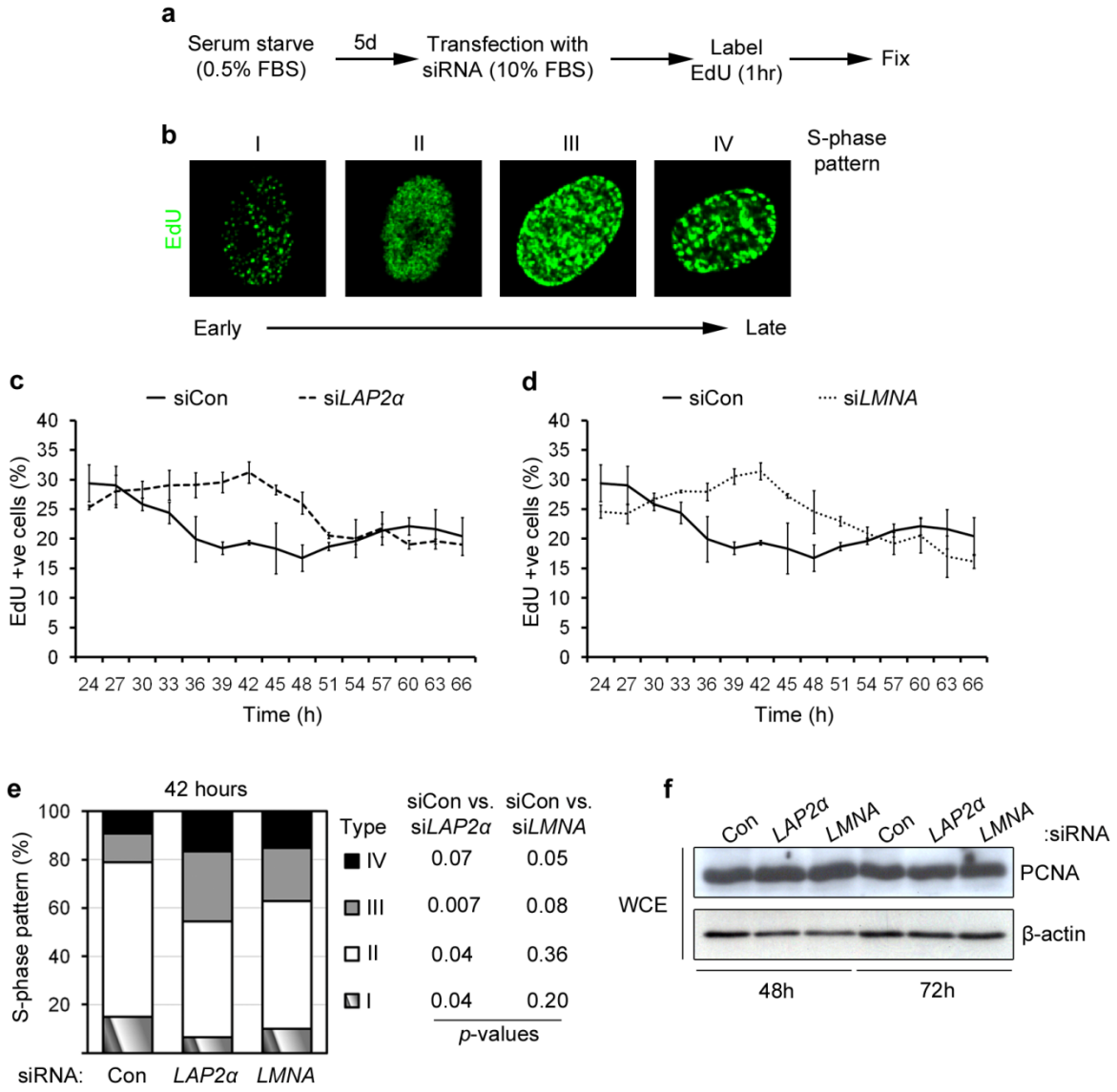
a
Serum starve (0.5% FBS)
5d
Transfection with siRNA (10% FBS)
Label EdU (1hr)
Fix
b
I
II
III
IV
S-phase pattern
EdU
Early
Late
c
siCon
siLAP2α
EdU +ve cells (%)
Time (h)
d
siCon
siLMNA
EdU +ve cells (%)
Time (h)
e
42 hours
S-phase pattern (%)
siRNA: Con LAP2α LMNA
Type
siCon vs. siLAP2α
siCon vs. siLMNA
IV 0.07 0.05
III 0.007 0.08
II 0.04 0.36
I 0.04 0.20
p-values
f
Con LAP2α LMNA Con LAP2α LMNA :siRNA
WCE
PCNA
β-actin
48h
72h

4.4 Depletion of LAP2α or lamin A/C causes transient cell cycle arrest in HDFs

Previous work within our laboratory has shown that HDFs undergo cell cycle arrest in response to either LAP2α or lamin A/C knockdown by RNAi (Pekovic et al., 2007). To re-affirm this, HDFs were synchronised by serum-starvation, transfected with siRNA and then processed for indirect immunofluorescence after 72 hours. Cells were stained the with prototypic cell cycle related nuclear protein Ki67, which is expressed in proliferating cells in all phases of the active cell cycle (G_1, S, G_2, M phases) but is absent when cells enter into a quiescent or senescent state (G_0 phase) (Scholzen and Gerdes, 2000). Control HDFs typically showed between 3 and 10 prominent foci of positive Ki67 staining, whilst HDFs depleted of LAP2α or lamin A/C showed very weak staining or the complete absence of any Ki67 staining, indicating exit from the cell cycle (Figure 4.3a). The number of Ki67+ cells were quantified and results revealed that HDFs transfected with LAP2α or lamin A/C siRNA (~40%) had a significantly lower Ki67+ index than control HDFs (~75%) (Figure 4.3b). The similar cellular phenotype exhibited by depleting HDFs of either LAP2α or lamin A/C may arise because the two proteins exist in a complex within the nucleoplasm (Markiewicz et al., 2002). Indeed, *Lap2alpha*$^{-/-}$ MEFs display a loss of nucleoplasmic lamin A/C, suggesting that it is involved in targeting lamin A/C within the nucleoplasm (Naetar et al., 2008). Therefore, to investigate this in HDFs, co-staining of HDFs depleted of LAP2α with anti-LAP2α and lamin A/C antibodies showed a distinct loss of nucleoplasmic lamin A/C but not nuclear envelope lamin A/C in LAP2α-depleted HDFs (Figure 4.3c). This further corroborates the finding that LAP2α may target a pool of lamin A/C to the nucleoplasm and may explain why depletion of either protein gives rise to similar phenotypes, as shown here (Figure 4.3c).

As I have shown previously, HDFs depleted of LAP2α or lamin A/C show delayed progression through G_1/S-phase before eventual cell cycle exit by 72 hours. To confirm these findings, cellular proliferation curves revealed that whilst control HDFs divided regularly (every ~24 hours by day 4 post-transfection), HDFs

depleted of LAP2α or lamin A/C displayed a significantly reduced proliferative rate (Figure 4.3d). Therefore, together, these results suggest that loss of nucleoplasmic LAP2α or lamin A/C leads to reduced Ki67 positive cells, which causes reduced rates of cellular proliferation.

Following depletion of LAP2α or lamin A/C, HDFs arrest in G_1 phase with a 2N content after 72 hours (Pekovic et al., 2007). This finding, together with the data presented thus far, led me to investigate whether loss of LAP2α or lamin A/C caused cellular senescence. Cellular senescence is governed by two major pathways, the p53 and pRb pathways (Campisi, 2005). The pRb pathway is activated by the cell cycle inhibitor $p16^{INK4A}$, which is one of two major splice products from the *CDKN2A* gene, the other being p14ARF (Lowe and Sherr, 2003). As well as targeting CDK4 directly, thereby inhibiting S-phase progression, $p16^{INK4A}$ directly activates pRb and induces repressive irreversible chromatin formation at E2F loci (Campisi, 2005). Therefore, to assess the nature of the cell cycle arrest, protein extracts were prepared from HDFs depleted of LAP2α or lamin A/C after 120 hours post-transfection. Immunoblotting with an anti-$p16^{INK4A}$ antibody showed no differences in $p16^{INK4A}$ levels, suggesting that the pRb-dependent senescence pathway was not activated (Figure 4.3e). To confirm this finding using an independent assay, HDFs depleted of LAP2α or lamin A/C were fixed after 120 hours post-transfection and stained with a senescence-associated β-galactosidase kit, which is a known to be a robust marker of senescent cells (Dimri et al., 1995). Results indicated that depletion of LAP2α or lamin A/C in HDFs did not induce cells to enter senescence (Figure 4.3f). As a positive control, HDFs were treated with H_2O_2 to promote stress-induced premature senescence (SIPS) (Figure 4.3f). Taken together, this data suggests that depletion of LAP2α or lamin A/C in HDFs induces a transient cell cycle arrest rather than a permanent cell cycle arrest and entry into senescence.

Figure 4.3. Loss of nucleoplasmic LAP2α—lamin A/C complexes leads to transient cell cycle arrest in HDFs. (**a**) G_0-synchronised HDFs were transfected with the indicated siRNAs, fixed after 72h and processed for immunofluorescence with anti-Ki67 and LAP2α antibodies. (**b**) The percentage of Ki67 negative cells from (a) were scored after 72h (* p<0.05 si*LAP2α* vs. siCon; + p<0.05 si*LMNA* vs. siCon). Data represents the mean from duplicate coverslips in three independent experiments. (**c**) HDFs transfected with LAP2α siRNA were fixed after 72h and processed for immunofluorescence with anti-LAP2α and lamin A/C antibodies. Knockdown of LAP2α causes a loss of nucleoplasmic lamin A/C in the transfected cell. The graph shows the lamin A/C fluorescence signal across each nucleus as indicated by the white lines and arrows. (**d**) G_0-synchronised HDFs were transfected with the indicated siRNAs and after 24h counted and seeded in triplicate wells. Cells were then counted every 24h for the next 4 days (* p<0.05 si*LAP2α* vs. siCon; + p<0.05 si*LMNA* vs. siCon). (**e**) HDFs transfected with siRNA were harvested after 120h and protein extracts were subjected to reducing SDS-PAGE and then immunoblotted with anti-$p16^{INK4A}$ or anti-β-tubulin antibodies. (**f**) HDFs transfected with the indicated siRNA were fixed and stained for senescence-associated β-galactosidase activity 120h post-transfection. As a positive control, untransfected HDFs were treated twice with 350μM H_2O_2 within a week, a treatment that has previously been shown to cause stress-induced premature senescence (SIPS). Data represents the mean from three independent experiments.

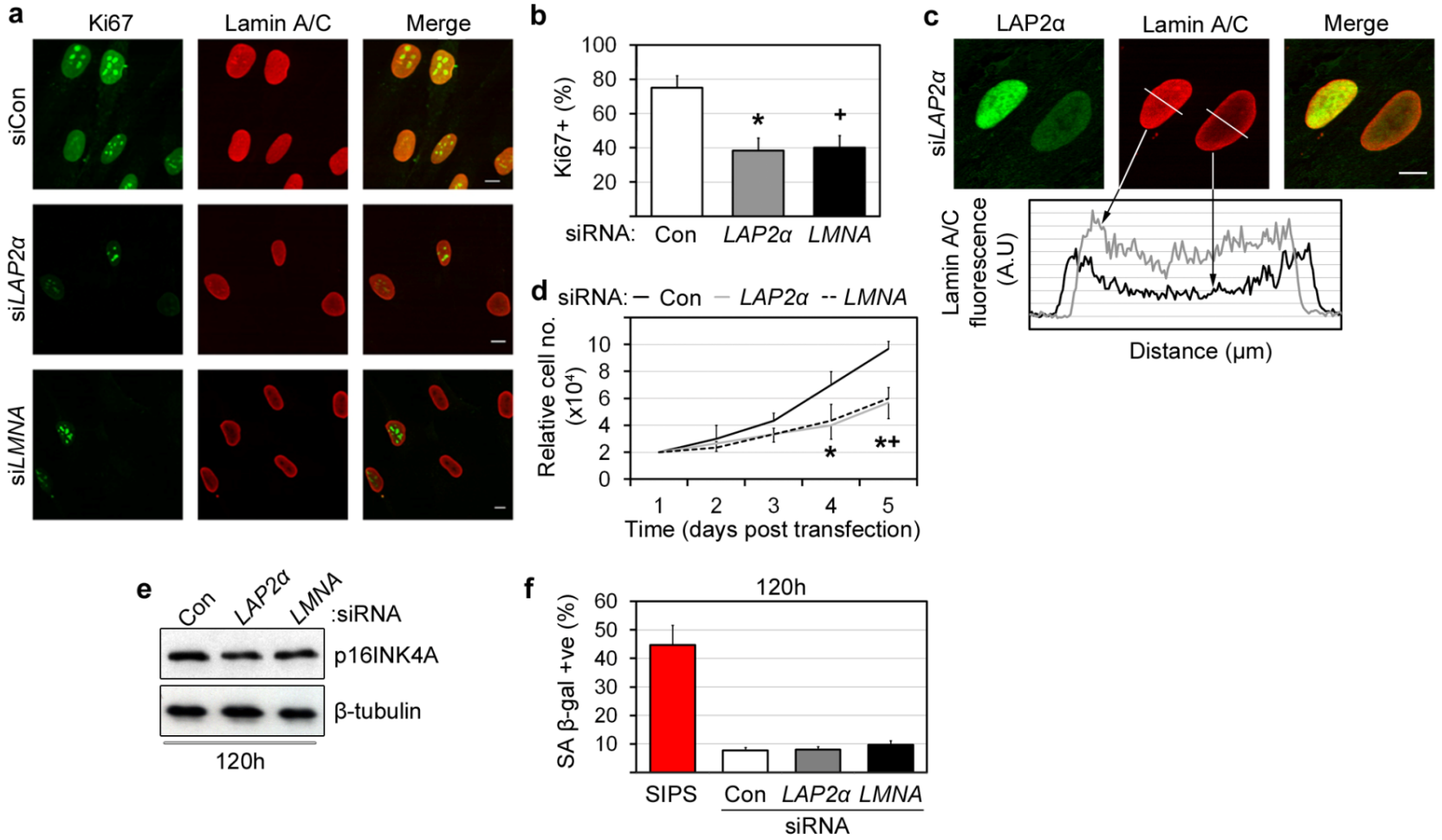
a
Ki67
Lamin A/C
Merge
siCon
siLAP2α
siLMNA
b
Ki67+ (%)
100
80
60
40
20
*
+
siRNA: Con LAP2α LMNA
c
LAP2α
Lamin A/C
Merge
siLAP2α
Lamin A/C fluorescence (A.U)
Distance (μm)
d
siRNA: — Con — LAP2α -- LMNA
Relative cell no. (x10⁴)
10
8
6
4
2
0
1 2 3 4 5
Time (days post transfection)
*
*+
e
Con
LAP2α
LMNA
:siRNA
p16INK4A
β-tubulin
120h
f
120h
SA β-gal +ve (%)
60
50
40
30
20
10
SIPS
Con
LAP2α
LMNA
siRNA

4.5 Cell cycle arrest in LAP2α or lamin A/C depleted HDFs is correlated with high levels of ROS, but not increased double strand breaks

Why should loss of LAP2α or lamin A/C lead to a G_1 arrest by 72 hours? One hypothesis is that loss of nucleoplasmic LAP2α or lamin A/C might cause endogenous DNA damage, therefore activating DNA damage checkpoint pathways that act to arrest cells in order to repair the damage (Jackson and Bartek, 2009). One of the most toxic DNA lesions encountered cells are double strand breaks (DSBs), the presence of which activates DNA damage signalling kinases ATM and ATR leading to the phosphorylation of the tail of the histone variant H2AX adjacent to the site of DNA damage (Ciccia and Elledge, 2010). The generation of γ-H2AX facilitates the focal assembly of DNA repair factors including 53BP1 and MDC1, and also promotes the phosphorylation and activation of Chk1 and Chk2, two protein kinases involved in the DNA damage checkpoint response (Polo and Jackson, 2011). Therefore, to test this hypothesis, HDFs depleted of LAP2α or lamin A/C were fixed after 24, 48 and 72 hours post-transfection and immunostained with an anti-γ-H2AX antibody (Figure 4.4a). Results indicated that depletion of either LAP2α or lamin A/C in HDFs did not induce substantial endogenous DNA damage (Figure 4.4a and data not shown). The radiomimetic chemotherapeutic drug bleomycin is a potent inducer of DSBs and acts as a positive control for the immunostaining. To confirm this, protein extracts were prepared 24, 48 and 72 hours post-transfection and immunoblotting with an anti-γ-H2AX antibody confirmed the absence of endogenous DNA damage in HDFs depleted of LAP2α or lamin A/C (Figure 4.4b). The huge increase in γ-H2AX and the presence of the ubiquitylated species of γ-H2AX in extracts from bleomcyin-treated cells serve as a positive control in the immunoblotting experiments (Huen et al., 2007; Kolas et al., 2007; Mailand et al., 2007).

Another ATM phosphorylation target along with H2AX is the checkpoint protein Chk2 (Chaturvedi et al., 1999; Matsuoka et al., 2000). Chk2 is phosphorylated on seven SQ/TQ motifs, including threonine 68, in response to a variety of DNA damage, some of which are ATM-independent (Matsuoka et al., 2000; Melchionna et al., 2000). Therefore, HDFs depleted of LAP2α or lamin A/C were fixed after 24, 48 and 72 hours post-transfection and immunostained with an anti-phospho-Chk2(Thr68) antibody (Figure 4.4c and data not shown). Results revealed that depletion of either LAP2α or lamin A/C in HDFs did not induce substantial phosphorylation of Chk2 on threonine 68 (Figure 4.4c and data not shown). As a positive control, HDFs were treated with hydroxyurea (HU), which inhibits DNA synthesis by inhibiting ribonucleotide reductase, and leads to Chk2 phosphorylation on threonine 68 (Matsuoka et al., 2000; Platt, 2008). To corroborate the immunostaining data, protein extracts were prepared 24, 48 and 72 hours post-transfection and immunoblotting with an anti-Chk2(Thr68) antibody confirmed the absence of phosphorylated Chk2 on threonine 68 in HDFs depleted of LAP2α or lamin A/C (Figure 4.4d). Together, this data suggests that acute loss of LAP2α or lamin A/C in HDFs does not induce DSBs, and therefore rules out the possibility that DSBs are the underlying cause of the cell cycle arrest observed after 72 hours in HDFs depleted of LAP2α or lamin A/C.

Based on the previous findings that lamin A is involved in the oxidative stress response, I hypothesised that depletion of LAP2α or lamin A/C in HDFs might induce oxidative stress, which may contribute to the cell cycle alterations (Chapter 3). HDFs were synchronised in G_0 by serum-starvation then transfected with siRNA in the presence of 10% serum. After 72 hours cells were then labelled with the fluorescent dye DCF-DA either in the presence or absence of the ROS scavenger N-acetyl cysteine (NAC) and analysed by FACS. Representative cytograms are shown (Figure 4.5a). Basal levels of DCF-DA in HDFs depleted of either LAP2α or lamin A/C were ~ 2-fold higher than in control HDFs, indicating that intracellular ROS levels are elevated in the absence of either LAP2α or lamin A/C (Figure 4.5b). Interestingly, treatment with NAC effectively reduced ROS

levels in HDFs depleted of LAP2α or lamin A/C, although they were still higher than control HDFs, by 76% and 65% respectively (Figure 4.5b). This reduction in ROS levels with NAC treatment was proportionate to the initial ROS levels, as indicated by the similar negative percentage change values from basal to NAC (Figure 4.5c). Together, this data reveals that LAP2α or lamin A/C depletion in HDFs causes increased intracellular ROS levels, which is readily reduced to near control levels with NAC treatment.

To correlate these findings with the observed cellular proliferation defects in HDFs depleted of LAP2α or lamin A/C, I next examined whether long-term anti-oxidant (NAC) treatment of these cells would ameliorate these proliferative defects. HDFs were transfected with control, LAP2α or lamin A/C siRNA and then treated for 1 hour with various concentrations of NAC at 24 hours post-transfection. These treatments were repeated twice more before fixation and immunostaining with anti-Ki67 antibody (Figure 4.6a,b). Quantification of Ki67+ cells revealed that long-term acute NAC treatment caused a dose-dependent inhibition of cellular proliferation in control HDFs, with a significantly reduced percentage of Ki67+ cells after treatment with 10 mM compared to 0.1 mM (Figure 4.6c). As shown previously, LAP2α or lamin A/C depleted cells have a reduced percentage of Ki67+ cells. Treatment of these cells with NAC caused a further smaller reduction (~10% for each) in the percentage Ki67+ cells (Figure 4.6c). This data suggests that the proliferative defects associated with loss of LAP2α or lamin A/C in HDFs cannot be rescued by reducing ROS levels by application of anti-oxidants.

Figure 4.4. Acute loss of nucleoplasmic LAP2α—lamin A/C complexes is not associated with activation of a DNA damage response. (**a**) HDFs transfected with the indicated siRNAs were fixed after 48h and processed for immunofluorescence before staining with anti-γ-H2AX (Ser139) antibody. As a positive control, untransfected HDFs were treated with the bleomycin (20 μg/ml) for 1h. (**b**) HDFs transfected with the indicated siRNA were harvested after 24, 48 or 72h and protein extracts were subjected to reducing SDS-PAGE and then immunoblotted with anti-γ-H2AX (Ser139) antibody. Bleomycin was used as a positive control as in (a) and the presence of the ubiquitylated form of γ-H2AX confirms activation of the DNA damage response in these HDFs (Huen et al., 2007). (**c**) HDFs transfected with the indicated siRNAs were fixed after 48h and processed for immunofluorescence before staining with anti-phospho-Chk2 (Thr68) antibody. As a control, untransfected HDFs were treated with the 20μм hydroxyurea for 16h. (**d**) HDFs transfected with the indicated siRNA were harvested after 24, 48 or 72h and protein extracts were subjected to reducing SDS-PAGE and then immunoblotted with anti-phospho-Chk2 (Thr68) antibody. Hydroxyurea was used as a positive control as in (c).

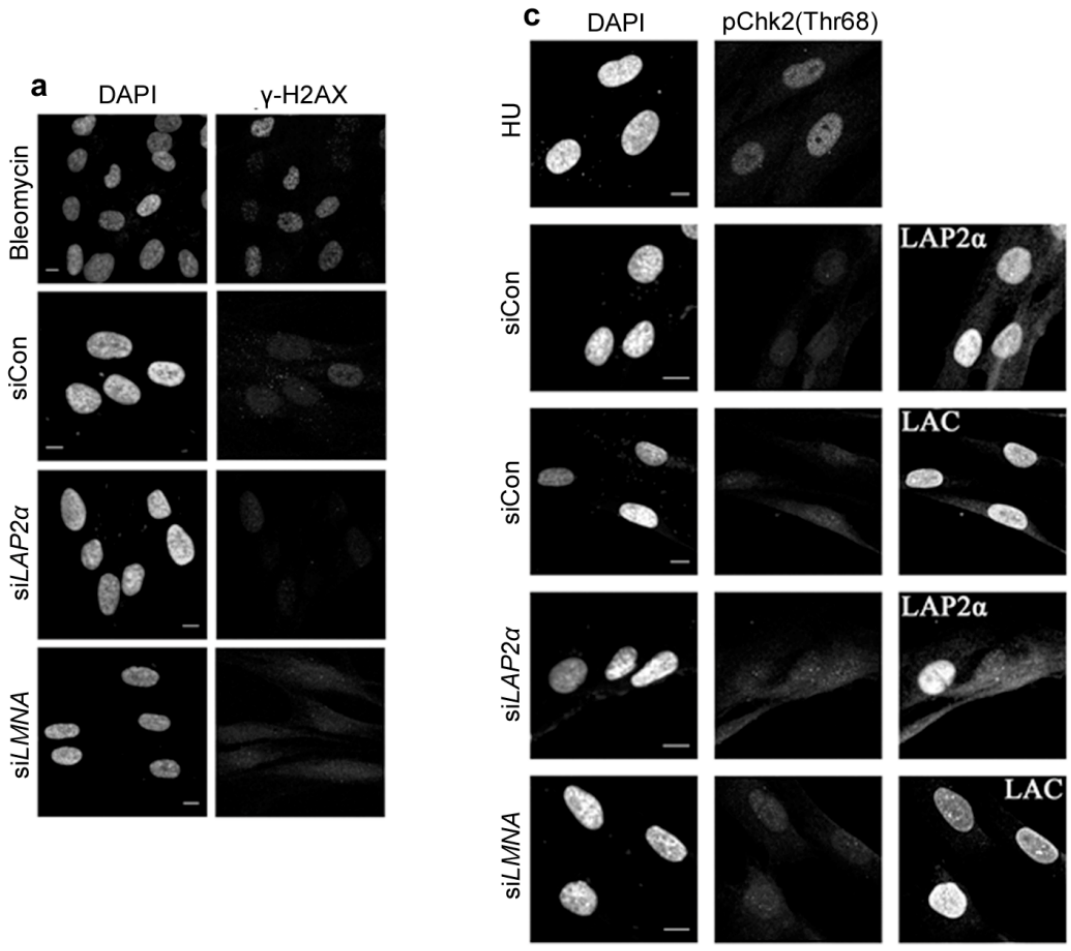
a
DAPI
γ-H2AX
Bleomycin
siCon
siLAP2α
siLMNA
c
DAPI
pChk2(Thr68)
HU
siCon
LAP2α
siCon
LAC
siLAP2α
LAP2α
siLMNA
LAC
b
siRNA:
Bleo
Con
LAP2α
LMNA
Ubi-γ-H2AX
γ-H2AX
24h
48h
72h
Nuclear extract
d
siRNA:
Con
LAP2α
LMNA
HU
phospho-Chk2
(Thr68)
24h
48h
72h

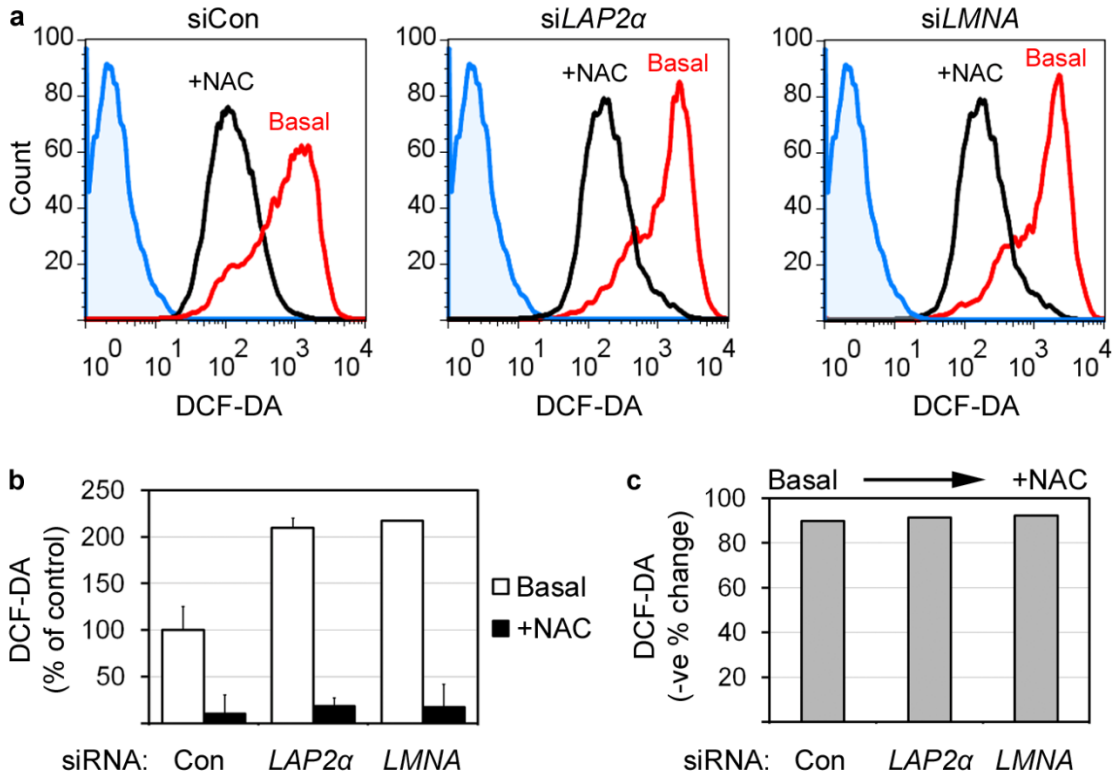

Figure 4.5. HDFs depleted of LAP2α or lamin A/C exhibit high levels of intracellular ROS that can be rescued with NAC treatment. (**a**) HDFs were synchronised in G_0 by serum-starvation before transfection with siRNAs against control, LAP2α or lamin A/C. After 72 hrs cultures were incubated with 5 μM DCF-DA for 1 hr in the presence or absence of the ROS scavenger NAC. HDFs were then analysed by flow cytometry and the resulting histograms of a typical experiment (*n* = 3) are shown. (**b**) Basal levels (±NAC) of intracellular ROS of the above siRNA-transfected HDFs were determined using the FlowJo software and data is expressed as a percentage of control HDFs (-NAC), which are arbitrarily set a value of 100%. (**c**) The negative percentage change of basal ROS levels to +NAC ROS levels was calculated for the siRNA-transfected HDFs.

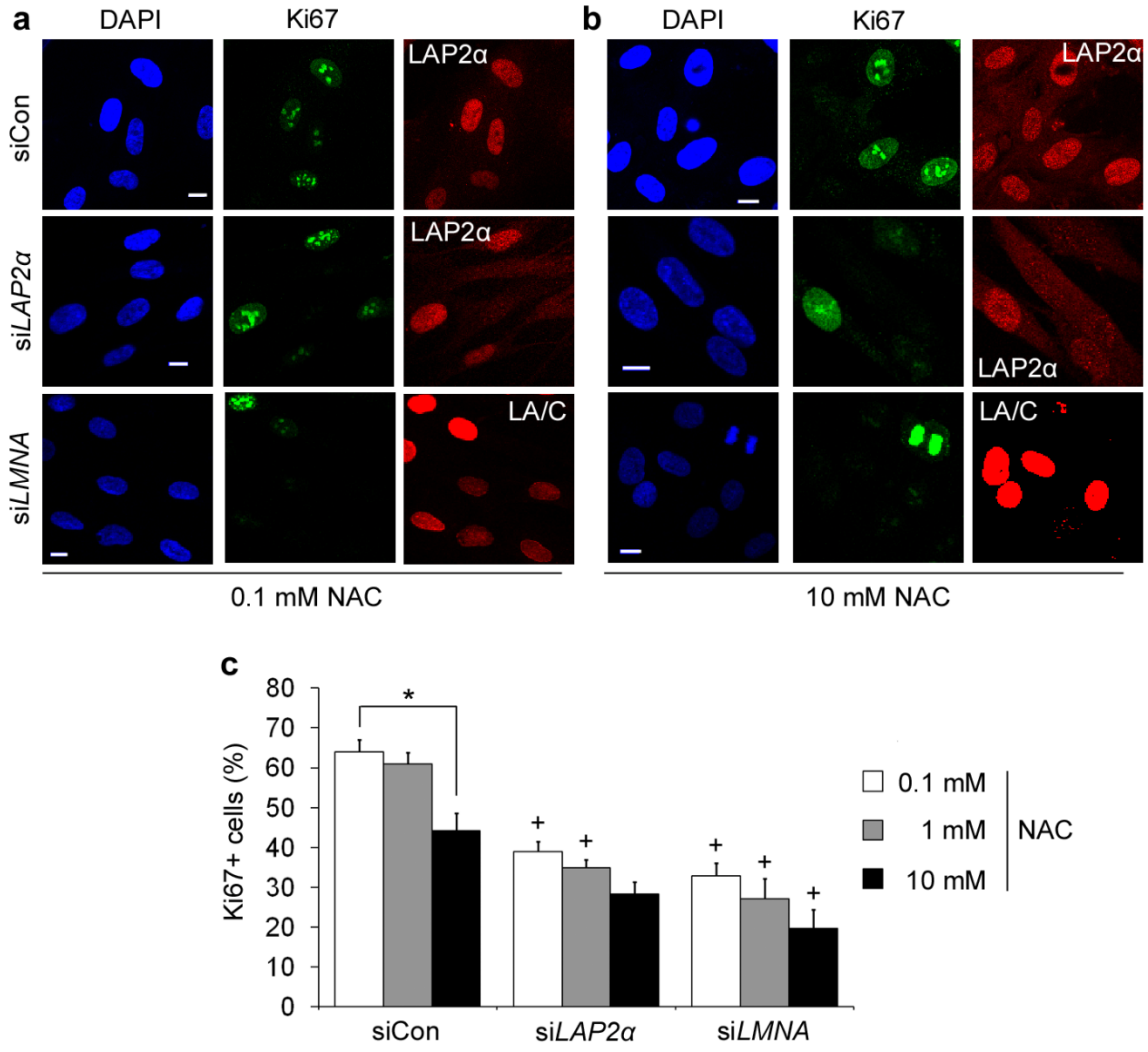

Figure 4.6. Long-term NAC treatment fails to rescue growth defects associated with loss of LAP2α or lamin A/C in HDFs. (**a,b**) HDFs were transfected with siRNAs against control, LAP2α or lamin A/C. After 24 hrs post-transfection, cells were treated with various concentrations of NAC for 1 hour before replacing with fresh medium. This was repeated every 24 hours for a total of 3 treatments. After 96 hours, cells were fixed and processed for immunofluorescence with anti-Ki67, LAP2α or lamin A/C antibodies and counter-stained with DAPI. Untransfected cells provide an internal control. Scale, 10μm. (**c**) Quantification of data obtained from immunofluorescence, *n*= 3, + S.D. * $p<0.05$ siCon (0.1mM NAC) vs. siCon (10mM NAC); + $p<0.05$ siLAP2α or si*LMNA* vs. siCon for corresponding NAC treatment.

4.6 Discussion

4.6.1 LAP2α and lamin A/C are required for normal cell cycle progression in HDFs

LAP2α-lamin A/C complexes have been proposed to govern the G_1/S-phase transition via interaction with pRb (Dorner et al., 2007). Furthermore, A- and B-type lamins have been reported to be involved in S-phase itself, although the exact mechanism remains elusive (Broers et al., 2006). In the present work, I have shown that, in response to re-stimulation from G_0 (or quiescence), HDFs depleted of either LAP2α or lamin A/C undergo delayed G_1/S-phase progression. This was evidenced by bivariate cell cycle analysis, which showed that HDFs depleted of either LAP2α or lamin A/C displayed a greater proportion of cells in S- and G_2/M-phases, with a concomitant decrease in G_1 cells. This suggested that cells were progressing through G_1 to S-phase from quiescence at different rates, either faster or slower, in HDFs depleted of either LAP2α or lamin A/C compared to control HDFs. A time-course assessment of the percentage of cells in S-phase, and which phase of S-phase they were in, revealed that HDFs depleted of either LAP2α or lamin A/C accumulated in S-phase more slowly than control HDFs. This finding does not suggest that S-phase progressed more slowly per se, but rather the entry into S-phase appears delayed. Therefore, at 42 hours, whilst control HDFs have passed through the first S-phase, HDFs depleted of LAP2α or lamin A/C are still in late S-phase as assessed by the replication patterns and flow cytometry. Together, the data suggests that disruption to nucleoplasmic LAP2α or lamin A/C complexes inhibits G_1/S-phase progression upon transition from G_0-G_1-S-phase. This finding is in keeping with previous reports that have utilised HGPS or Y259X HDFs, which both show reduced proliferation rates and reduced phosphorylated pRb levels (Muchir et al., 2003; Goldman et al., 2004; Dechat et al., 2007; Pekovic et al., 2007; Vos et al., 2010). However, these results in human somatic cells are in stark contrast to previous studies using *Lmna*$^{-/-}$ and *Lap2αlpha*$^{-/-}$ MEFs (Johnson et al., 2004; van Berlo et al., 2005; Naetar et al., 2008). These studies have shown that *Lmna*$^{-/-}$ and *Lap2αlpha*$^{-/-}$ MEFs behave in a

similar manner to *Rb*$^{-/-}$ MEFs, which exhibit increased proliferative rates owing to a higher percentage of cells in S-phase (Johnson et al., 2004; van Berlo et al., 2005; Naetar et al., 2008). As LAP2α-lamin A/C complexes interact with active hypophosphorylated pRb, and as pRb levels are lost in *Lmna*$^{-/-}$ MEFs and are deregulated in *Lap2αlpha*$^{-/-}$ MEFs, loss of pRb repressor function in these three genetic backgrounds leads to uncontrolled G_1/S-phase transition due to free E2F, which activates gene transcription necessary for S-phase progression. This simple mechanism may be the dominant pathway in mouse cells but may not be applicable to human cells. It is possible that during the process of transformation these immortalised mouse cell lines have undergone changes that effect the regulation of the cell cycle and its checkpoints. Indeed, in primary *Zmpste24*$^{-/-}$ mouse adult fibroblasts, there is a p53-dependent entry into senescence. Mouse cells are dependent on the p53 pathway for cellular senescence, rather than the pRb pathway, as found in human cells (Campisi, 2005). Therefore, inherent differences between mouse and human cells, as well as embryonic and adult cells, may account for the difference observed here and previously that loss of nucleoplasmic LAP2α-lamin A/C complexes promote G_1/S-phase transition in mouse cells, but inhibits this transition in human cells (Pekovic et al., 2007). This conclusion would suggest that the nucleoplasmic pRb-LAP2α-lamin A/C complex has more precise or previously unrecognised functions than first thought in human somatic cells. In support of this, in human fibroblasts depleted of LAP2α or lamin A/C, total and phosphorylated pRb levels are reduced, but not completely absent, and the localisation of a specific phosphorylated pRb isoform (Ser795) is dramatically altered (Pekovic et al., 2007). In light of these findings and the data presented here, it is possible that LAP2α-lamin A/C complexes provide specificity in nuclear localisation of specific phosphorylated pRb isoforms, which are necessary for optimal G_1/S-phase progression. Therefore, in HDFs depleted of LAP2α or lamin A/C, spatiotemporal regulation of pRb localisation and phosphorylation is deregulated, inhibiting G_1/S-phase progression. Future work should seek to clarify these hypotheses.

The data presented here does not argue for a delay in S-phase duration in response to LAP2α or lamin A/C depletion in HDFs, though it was no tested directly. Conflicting reports have suggested that A-type lamins promote initiation or the elongation phase of DNA synthesis (Broers et al., 2006). No differences were observed in the levels of the elongation factor PCNA in the data presented here, although its activity may be affected by lamin A/C, and possibly LAP2α, loss in HDFs. Future work using aphidicolin to block cells at G_1/S-phase followed by release will allow a more detailed examination of the effect of either LAP2α or lamin A/C loss on the progression through S-phase in HDFs. Further work also needs to clarify the exact role of lamin A/C in DNA replication. Recently, a mammalian *in vitro* DNA replication assay has been developed based on the pEPI-1 plasmid (Rizwani and Chellappan, 2009). Using this system, it will be possible to determine if lamin A/C and mutants found in laminopathy patients affect DNA replication initiation or elongation, if either.

4.6.2 LAP2α and lamin A/C prevent cell cycle arrest in HDFs

Previous work in our laboratory has shown that HDFs depleted of either LAP2α or lamin A/C undergo cell cycle exit after 72 hours post-transfection (Pekovic et al., 2007). Indeed, the present work corroborated this finding. Therefore, to explore the downstream consequences of LAP2α or lamin A/C loss in HDFs I assessed whether these cells might be induced into premature senescence. Prior studies have shown that in the presence of unprocessed prelamin A, in both HGPS and RD, cells undergo premature entry into senescence when grown *in vitro*, therefore providing a link between lamin status and permanent cell cycle exit or senescence (Mounkes et al., 2003; Liu et al., 2006; Hernandez et al., 2010). More importantly, complete loss of A-type lamins in *LMNA*$^{Y259X/Y259X}$ human fibroblasts is associated with premature entry into senescence (Chapter 3; Pekovic et al., 2007). However, in contrast to this, transient knockdown of lamin A/C or its nucleoplasmic binding partner, LAP2α, did not induce cellular senescence in these cells 5 days post-transfection, as assessed by SA β-gal positivity and p16^{INK4A} expression, a known marker of senescent cells (Campisi, 2005). The results in this chapter therefore do

not confirm the hypothesis that loss of LAP2α-lamin A/C complexes induces senescence. How can the apparent discrepancies between these results and the findings using Y259X cells in Chapter 3 be explained? Firstly, as can be seen in Figure 4.1, knockdown of lamin A/C or LAP2α in HDFs is never complete, as has been recognised previously (Pekovic et al., 2007). Moreover, this phenomenon is not specific to the siRNA used as others have reported the inability of HDFs to efficiently respond to RNAi of *LMNA* (Vos et al., 2010). A-type lamins incorporated into the nuclear lamina exhibit a slow turnover rate, as demonstrated by FRAP studies using GFP-tagged lamin A and C (Broers et al., 1999). In contrast, the turnover of nucleoplasmic A-type lamins was much faster. In the present work, depletion of lamin A/C was most evident within the nucleoplasm. This suggests that the altered cell cycle effects demonstrated in this chapter may be due to loss of nucleoplasmic lamin A/C pools, rather than lamin A/C at the nuclear envelope, which were not down-regulated as effectively, probably due to their slow turnover. Importantly, the inability to effectively downregulate lamin A/C completely in HDFs distinguishes the lamin A/C-depleted cells from the Y259X cells, where absolutely no lamin A/C protein is present. The most obvious comparison to make between the two cellular backgrounds (i.e. lamin A/C-depleted HDFs vs. Y259X cells) is nuclear shape. Whilst Y259X exhibit gross changes in nuclear architecture and shape, I could not observe appreciable differences in nuclear shape in lamin A/C-depleted HDFs, most likely due to residual lamin A/C protein (data not shown). Therefore, this may help explain why I could not observe an increase in SA β-gal activity in lamin A/C or LAP2α depleted HDFs, as knockdown was never complete. Secondly, as this assay was carried out on day 5 post-RNAi transfection, future work might examine potential senescent phenotypes using this assay at later timepoints. Indeed, this should be extended to the preparation of protein extracts. Prior studies have shown that $p16^{INK4A}$ expression levels increase notably both *in vitro* and *in vivo* between 1 and 4 weeks in response to UV, oxidative stress, IR and telomere dysfunction (Piepkorn, 2000; Jacobs and De Lange, 2004; Stockl et al., 2006). This delayed induction of $p16^{INK4A}$ is in stark contrast to the rapid induction of $p21^{Cip}$, the transcriptional target of activated p53,

in response to cellular aging *in vitro* (Stein et al., 1999). In this study, induction of $p21^{Cip}$ preceded the induction of $p16^{INK4A}$, with $p21^{Cip}$ expression abruptly downregulated once most cells were positive for SA β-gal activity (Stein et al., 1999). Underlining this, a more recent study has shown that the expression of these two CKIs do not overlap in individual cells (Herbig et al., 2004). Therefore, there are two important avenues to explore in the future to clarify whether depletion of the LAP2α or lamin A/C in HDFs leads to senescence. Firstly, examination of $p16^{INK4A}$ expression levels 5 days post-transfection should be extended beyond this timepoint to between 2-4 weeks post-transfection, with repeated transfections. Secondly, other regulators of the G_1 checkpoint need to be examined, such as $p21^{Cip}$ protein expression, p27 protein levels, cdk2 phosphorylation and Cdc25A protein levels (Bartek and Lukas, 2001). In sum, I suggest that the inability to detect the activation of a senescence programme in HDFs depleted of LAP2α or lamin A/C may be due to a combination of incomplete downregulation of these proteins and the temporal assessment of the entry into senescence.

In light of these suggestions, one potential problem with using later timepoints for both the SA β-gal assay and preparing protein extracts is that the non-transfected cells or cells that have not undergone cell cycle arrest are able to proliferate and become the dominant cell type in the culture. This might be overcome by the production of stable inducible RNAi HDF cell lines. One problem with producing stable inducible knockdown cell lines in HDFs is the finite replicative potential of HDFs, which would age in culture as stable clones were isolated. Therefore this methodology would not represent a good model for studying potential induced senescent pathways or provide a renewable source of cells. Instead, it would be possible to produce stable inducible knockdown HDFs using a human fibroblast cell line that have been immortalised with a retrovirus containing the *hTERT* gene flanked by Cre-recombinase excision sites (Rubio et al., 2002). Importantly, after stable inducible knockdown cells have been created, the *hTERT* gene may be excised by expression of Cre recombinase, therefore rendering the proliferative potential of the fibroblasts as finite, rather than infinite in the presence of hTERT

expression. Once *hTERT* has been excised it would thus be possible to induce stable knockdown of LAP2α or lamins A/C in HDFs and use these cell lines for more in-depth studies of complete loss of either in senescence pathways.

4.6.3 Reducing ROS levels associated with loss of LAP2α or lamin A/C cannot ameliorate proliferative defects

In order to explain the observed cell cycle exit by 72 of either LAP2α or lamin A/C depleted HDFs, I explored the possibility that accumulation of endogenous levels of DNA damage in these cells might lead to G_1 arrest. Notably, I could not detect increases in two ATM targets, γ-H2AX and phospho-Chk2. This was surprising as lamin null HDFs, Y259X cells, display significantly increased levels of endogenous γ-H2AX (Chapter 5). However, based on my previous argument, I would suggest that the incomplete knockdown of either LAP2α or lamin A/C may be one reason why no increase in γ-H2AX and phospho-Chk2 was observed. Alternatively, as the activation of these two targets is in response to double strand breaks (DSBs), other forms of DNA damage may contribute to the G_1 arrest. Alternative DNA damage assays, such as the comet and 8-oxo-dG assays, which detect single strand breaks and oxidative DNA damage, could be used to further interrogate whether these forms of DNA damage contribute to the G_1-arrest in response to loss of lamin A/C or LAP2α. Furthermore, other pathways to explore that are activated in response to DNA damage are the ATR-Chk1 pathway and the p38MAPK-MK2 pathway (Reinhardt and Yaffe, 2009; Ciccia and Elledge, 2010). The ATR-Chk1 pathways is primarily activated in response to single-strand breaks and replication stress, whilst the p38MAPK-MK2 pathways is a general stress pathway that is activated by UV, IR, osmotic stress, heat shock, cytokines and ROS (Reinhardt and Yaffe, 2009).

As A-type lamins are involved in multiple signalling pathways, the observed cell cycle arrest by 72 hours in response to loss of nucleoplasmic LAP2α and lamin A/C appears to be independent of endogenous DNA damage but could be caused by defects in other associated pathways (Pekovic and Hutchison, 2009). Based

on the results presented in Chapter 3, one such pathway I explored was the oxidative stress response. As I found for Y259X cells, HDFs depleted of lamin A/C and its nucleoplasmic binding partner, LAP2α, exhibited ROS levels that were ~ 2-fold higher than control HDFs. Importantly, these levels could be effectively rescued by treatment with the ROS scavenger, NAC. However, long-term acute treatment of LAP2α or lamin A/C depleted HDFs with NAC could not rescue the proliferative defects associated with the down-regulation of either of these proteins. These results suggest that high ROS levels caused by loss of either LAP2α or lamin A/C is not the primary causes of cell cycle arrest. In the context of laminopathies, these results indicate two important conclusions. Firstly, in laminopathies with associated high levels of ROS, patients may be treated with NAC to reduce cellular and systemic ROS levels. For example, it was shown that patient blood samples exhibited high levels of ROS in amyotrophic quadricipital syndrome with cardiac impairment due to mutations in lamin A/C (Charniot et al. 2007). NAC has also been shown to exert protective effects in fibroblasts from patients with Alzheimer's disease, which exhibit high levels of ROS (Moreira et al., 2007). Exploiting NAC to treat laminopathy patients may therefore be a promising avenue to ameliorate some disease phenotypes. Future work should seek to exploit the range of laminopathy mouse models that have been created and empirically determine the effects of anti-oxidants such as NAC on the disease phenotype (Stewart et al., 2007).

CHAPTER 5:
THE ROLE OF A-TYPE LAMINS IN THE DNA DAMAGE RESPONSE

5.1 Introduction

5.1.1 Overview

The genomic integrity of mammalian cells is constantly challenged by endogenous insults of metabolic by-products such as reactive oxygen species (ROS), as well as environmental factors such as chemical agents and ultraviolet (UV) radiation (Ciccia and Elledge, 2010). Limits to the fidelity of DNA metabolism including replication, recombination, and repair also promote genomic instability. Thus, DNA integrity is threatened from multiple sides, with one estimate calculating that each cell may encounter up to 10^5 lesions per cell per day (Hoeijmakers, 2009). To combat this, the DNA damage response (DDR) represents a complex set of spatiotemporal events that are essential for cellular fate in response to genomic insults (Jackson and Bartek, 2009). This vital signal transduction pathway acts as a cellular defence mechanism for the preservation of genomic integrity.

The DNA repair pathway employed by the cell is dictated by the type of genomic insult, which creates different types of DNA damage (Sancar et al., 2004). Damaged DNA is sensed and amplified to expedite a series of sequential events that cooperate to form an integrated network of cellular responses collectively known as the DNA damage response (Figure 5.1). Within the DDR signalling hierarchy, DNA damage sensors transmit the signal to transducers and effectors via mediator proteins. The effector proteins are responsible for impacting on various cellular pathways such as DNA repair, transcriptional response, DNA damage checkpoints and apoptosis, to either repair the DNA or eliminate cells where the damage is beyond repair (Figure 5.1) (Zhou and Elledge, 2000; Jackson and Bartek, 2009). When repair pathways are engaged, it is essential

that these pathways signal to the cell cycle machinery to prevent cell cycle progression in the presence of DNA damage so that the damage is not replicated and inherited by the daughter cell. Thus, failure to cope correctly with DNA damage may cause accumulation of genomic rearrangements that promote tumorigenesis (Bartkova et al., 2006; Di Micco et al., 2006; Halazonetis et al., 2008). Indeed, mutations in genes involved in the DNA damage response often lead to cancer predisposition (e.g. BRCA1 mutations lead to breast and ovarian cancer) and premature aging, therefore highlighting the importance of this signalling pathway as both an anti-oncogenic barrier and essential component of the normal aging process (Halazonetis et al., 2008).

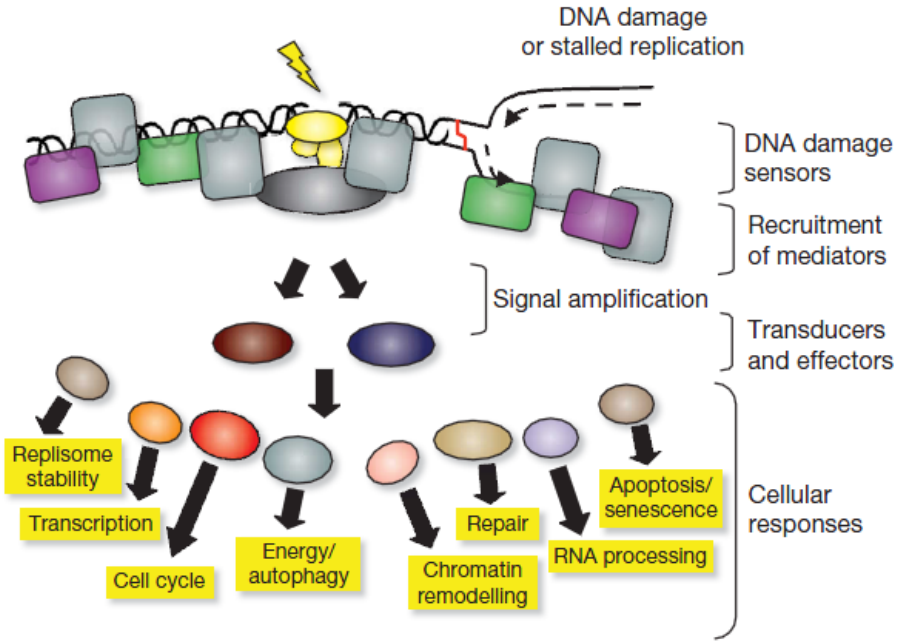

Figure 5.1. The DNA damage response in mammalian cells. The hierarchical nature of the of this signal transduction pathway, via sensors, mediators and then transducers and effectors, is responsible for impacting major biological outputs that together form the DNA damage response. For simplicity, the pathways are shown in a linear manner, however, in reality there is extensive crosstalk between them. DNA damage sensors include the MRN complex, Rad9-Hus1-Rad1 and Rad17. The ATM and ATR kinases, and their downstream targets Chk1 and Chk2, act as transducers and effectors of the DNA damage signal, respectively.

Mediator proteins such as MDC1, 53BP1, BRCA1 and TopBP1 enhance the signal and facilitate an effective DDR and a range of cellular responses (Jackson and Bartek, 2009).

5.1.2 Lamins and the DDR

Defects in prelamin A processing, either in *Zmpste24*$^{-/-}$ MEFs and HGPS cells have been linked to activation of the DDR (Liu et al., 2005; Varela et al., 2005). These cells exhibit increased levels of DNA damage, impaired DNA repair pathways and sensitivity to a range of genotoxic stresses (Liu et al., 2005). One protein important component of the DDR, 53BP1, was shown to exhibit delayed recruitment to sites of DNA damage in HGPS cells, suggesting that the presence of unprocessed prelamin A inhibits the upstream signaling events necessary for the recruitment of 53BP1 (Liu et al., 2005). Further to this, a recent study has shown that *Lmna*$^{-/-}$ MEFs display reduced 53BP1 protein levels (Gonzalez-Suarez et al., 2009). Therefore, as a modulator of 53BP1 levels, A-type lamins have been implicated in the DDR.

5.1.3 Current aims

Previous studies have implicated A-type lamins in the DDR. However, this role has been in the context of unprocessed mutant lamin A. In this chapter, I explore the hypothesis that mature wild type lamin A/C has a role in DNA repair pathways and ultimately genomic maintenance.

5.2 53BP1 co-fractionates with A-type lamins in HDFs

Previous studies have shown that in the presence of unprocessed lamin A, recruitment of 53BP1 to sites of DNA damage is delayed (Liu et al., 2005). Furthermore, a range of GFP-tagged lamin A mutants expressed in HeLa cells have been shown to inhibit 53BP1 foci formation in response to DNA damage (Manju et al., 2006). I therefore postulated that 53BP1 might interact with wild type lamin A/C and if so share some biochemical properties. One characteristic of A-type lamins is their resistance to extraction with detergents and high salts. To investigate if a pool of 53BP1 also co-existed within these A-type lamin fractions, I performed sequential extraction and immunoblotting of proliferating early passage human dermal fibroblasts (HDFs; Ki67 index ~ 70%, data not shown). As expected, lamin A/C and lamin B2 were strongly resistant to all extraction steps; however, 53BP1 existed as three distinct pools. The first pool was readily extracted with Triton X-100 (CSK/T), the second pool was extracted with DNase I and the third was completely resistant to extraction (Figure 5.2a). As a control, blots were probed with anti-histone H2A antibodies. As expected H2A was completely soluble following DNase I treatment (Figure 5.2a, see DNase I S4/P4 lanes). In response to DNA damage, 53BP1 becomes chromatin bound via interaction with methylated lysine 20 of histone H4 (Iwabuchi et al., 2003; Botuyan et al., 2006; Pei et al., 2011). Following treatment of HDFs with 3 Gy ionizing radiation (IR) 53BP1 was completely soluble following DNase I treatment (Figure 5.2b). Furthermore, the level of lamin A/C levels in the S4 fraction also increased, suggesting that a pool, predominantly lamin A, becomes chromatin bound in response to DNA damage (Figure 5.2b). In contrast to this, lamin B1 did not show any differences in extraction properties between untreated and IR (Figure 5.2a,b). To further investigate the status of 53BP1 and A-type lamins in response to DNA damage, HDFs were extracted *in situ* and processed for immunofluorescence (Pekovic et al., 2007). As a positive control, cells were stained with NuMA, a component of the nuclease- and salt-resistant nuclear matrix (Figure 5.2e). Consistent with previous studies, in untreated cells, 53BP1 typically showed a diffuse nucleoplasmic signal with occasional accumulation in 1-5 large foci and an

absence from nucleoli (Figure 5.2c) (Schultz et al., 2000; Lukas et al., 2011). After extraction with nucleases and salt, 53BP1 still existed as a diffuse signal throughout the nucleoplasm (Figure 5.2c). This suggests that, in untreated cells, 53BP1 is largely insoluble in human fibroblasts and is anchored within the nucleus independently of chromatin. Lamins A/C were also resistant to extraction in untreated HDFs, as shown previously (Pekovic et al., 2007). In response to DNA damage, 53BP1 relocalised to ionizing radiation induced foci (IRIF), which were resistant to detergent extraction. However, these foci were fully extracted after treatment with DNase I, reaffirming the finding that in HDFs 53BP1 is chromatin bound after DNA damage (Figure 5.2d). In contrast, lamin A/C did not re-localise to IRIFs 1 hour post-IR and remained largely resistant to all extraction steps (Figure 5.2d). Together, this data suggests that DNA damage causes 53BP1 to relocalise from a nuclear matrix-bound pool to sites of DNA damage in HDFs, whilst lamin A/C localisation and solubility properties remain largely unchanged.

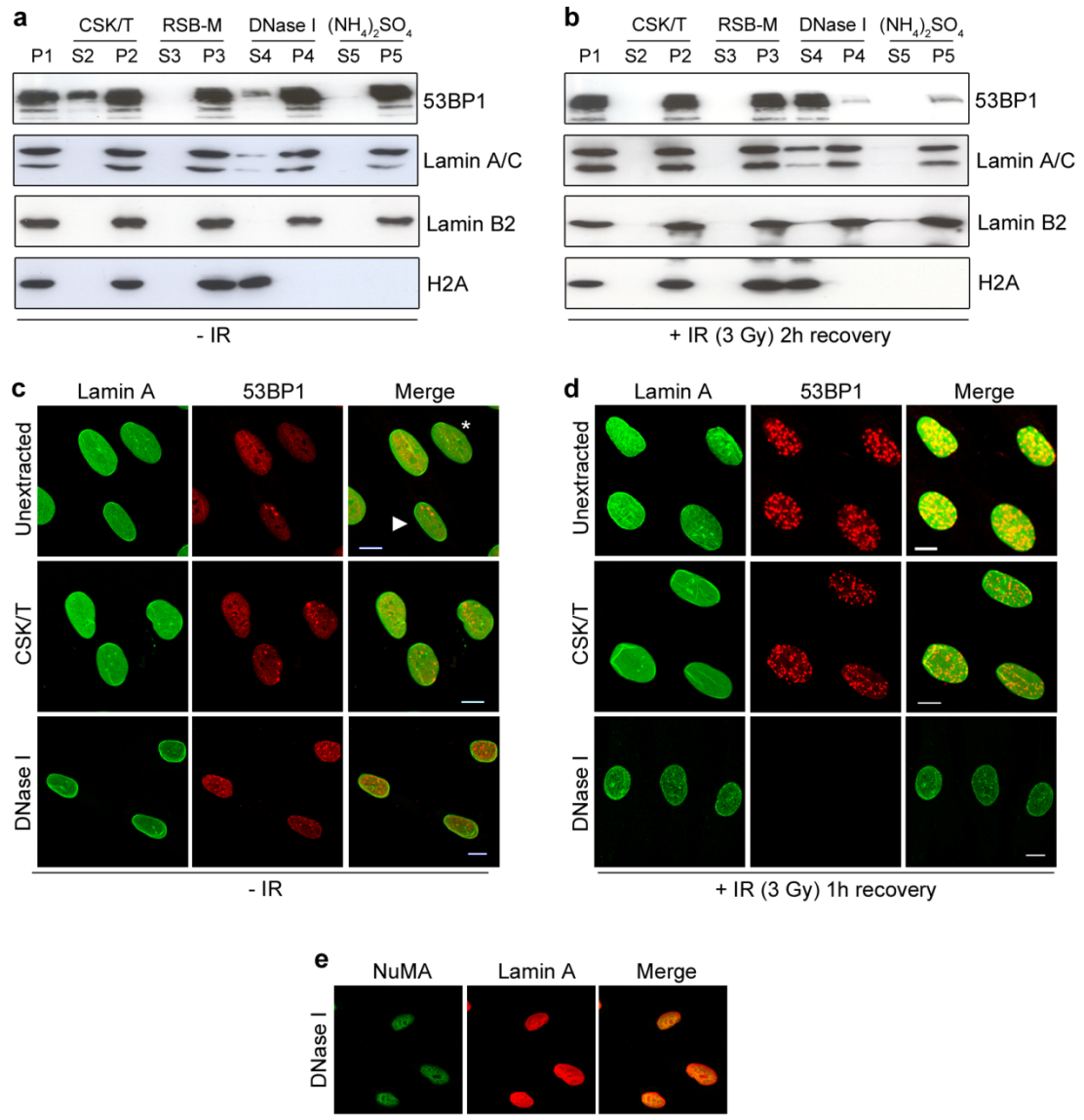

Figure 5.2. 53BP1 cofractionates with lamin A/C in HDFs. (**a-b**) Proliferating HDFs were biochemically fractionated with a sequence of detergent, nuclease and salt extraction, either with (a) or without IR (b). Protein extracts were subjected to reducing SDS-PAGE and immunoblotted with the indicated antibodies. (**c-d**) HDFs were extracted *in situ*, with or without IR treatment, before being processed for immunofluorescence with lamin A and 53BP1 antibodies. (**e**) A positive control for retention of nuclear matrix proteins using anti-NuMA and anti-lamin A antibodies. Scale bars, 10 μm.

5.3 A-type lamins promote genome stability and mediate 53BP1 protein levels

A previous report had shown that immortalised *Lmna*$^{-/-}$ MEFs have reduced 53BP1 protein levels (Gonzalez-Suarez et al., 2009). To corroborate these findings in primary human cells, I performed immunoblotting and immunofluorescence on human fibroblasts harbouring a homozygous Y259X mutation in the *LMNA* gene, which renders these cells lamin A/C-null (Muchir et al., 2003). 53BP1 protein levels were absent from Y259X fibroblasts but readily detectable in normal fibroblasts using both methods (Figure 5.3a). This effect appeared specific to 53BP1 as another DNA damage response protein, Rad51, was expressed at wild type levels (Figure 5.3a). Moreover, the phosphorylated form of H2AX was present at much higher levels in Y259X fibroblasts when compared to controls (Figure 5.3b) and was accumulated in multiple DNA damage foci (Figure 5.3c).

In order to confirm the lamin A/C-dependency of maintaining 53BP1 protein levels, wild type HDFs were depleted of lamin A/C using siRNA. Following siRNA depletion of lamin A/C in HDFs there was a substantial decrease (~75%) in 53BP1 protein levels (Figure 5.3d). This effect was not specific to HDFs as U2OS cells depleted of A-type lamins also showed substantially decreased levels of total 53BP1, with densitometry revealing a decrease of ~65% in 53BP1 protein levels (Figure 5.4a). A previous study showed that loss of pRb protein levels are significantly reduced in *Lmna*$^{-/-}$ MEFs (Johnson et al., 2004). Furthermore, treatment of *Lmna*$^{-/-}$ MEFs with a proteasome inhibitor effectively rescued pRb protein levels, suggesting that the reduced pRb protein levels were due to degradation by the proteasome (Johnson et al.., 2004). Taking inspiration from this, HDFs and Y259X cells were treated with the proteasome inhibitor MG-132. Proteasome inhibition rescued the protein levels of 53BP1 in Y259X HDFs, with densitometry showing a ~3 fold increase in 53BP1 levels in Y259X cells (Figure 5.3e). Furthermore, proteasome inhibition also rescued 53BP1 protein levels in HDFs depleted of lamin A/C by siRNA, with densitometry revealing that the initial

levels were ~50% lower in lamin A/C-depleted HDFs without proteasome inhibition but were similar to control HDFs after proteasome inhibition (Figure 5.4b). However, despite this, when assessed by confocal microscopy, the nuclear localisation of 53BP1 was not restored following proteasome inhibition (Figure 5.3f). Notably, 53BP1 foci were absent in HDFs after proteasome inhibition, which is in keeping with previous reports showing that blocking ubiquitylation events by proteasome inhibition prevents 53BP1 accumulation in foci (Mailand et al., 2007) (Figure 3.5f). Taken together, this data suggests two important findings. Firstly, that lamin A/C is required for the correct localisation of 53BP1 within the nucleus. Secondly, it suggests that cytoplasmic 53BP1 is degraded by the proteasome in the absence of lamin A/C.

Previous data from our laboratory has shown that Y259X HDFs have a low proliferative index and undergo premature senescence (Pekovic et al., 2007). To discount against any cell cycle effects on 53BP1 protein levels, I prepared extracts from proliferating, quiescent and stress-induced prematurely senescent wild type HDFs. Immunoblotting revealed that total lamin A/C and 53BP1 protein levels did not change in these three different proliferative conditions, suggesting that the loss of 53BP1 is not cell cycle specific, but dependent on lamin A/C status (Figure 5.4c). Together, this data suggests that, in the absence of lamin A/C, HDFs exhibit increased genomic instability which is correlated with loss of 53BP1 protein levels, a known mediator of the DDR (Wang et al., 2002).

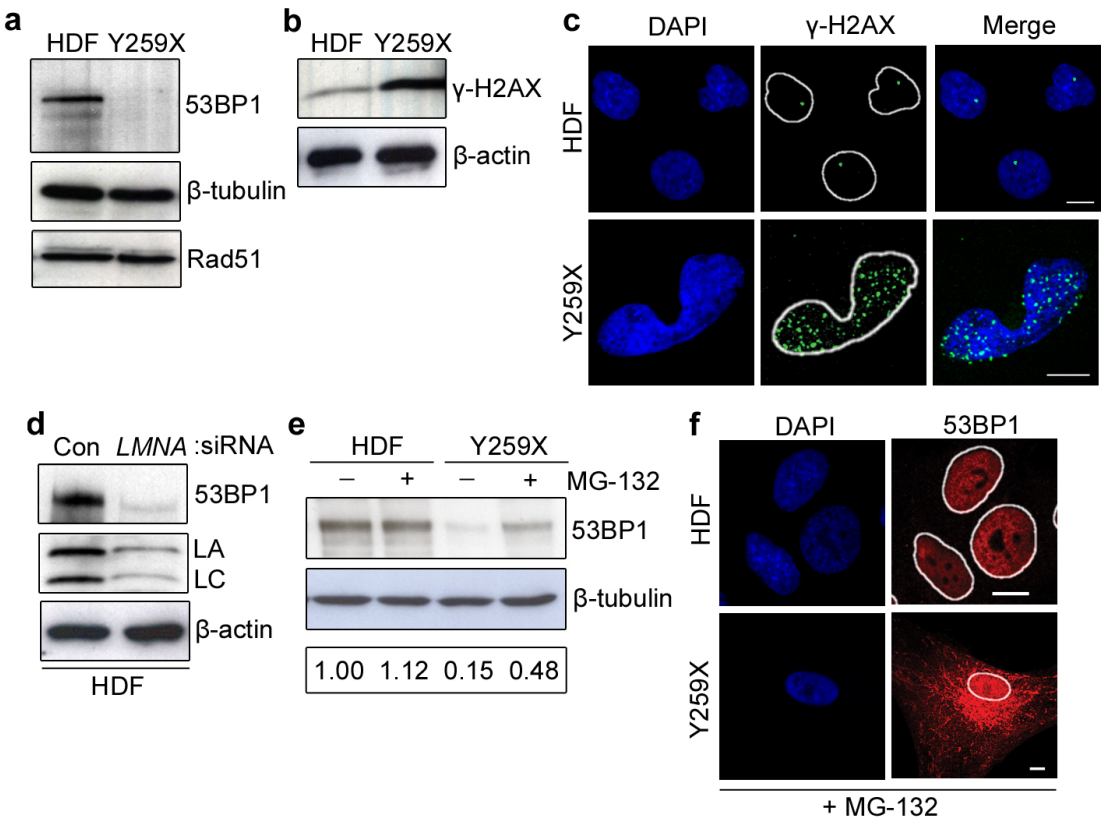

Figure 5.3. A-type lamins promote 53BP1 stability and nuclear localisation. (**a-b**) Whole cell extracts from wild type and Y259X HDFs were analysed by immunoblotting with the indicated antibodies. (**c**) Wild type and Y259X HDFs were fixed, processed for immunofluorescence and co-stained with DAPI and anti-γ-H2AX antibody. (**d**) HDFs were transfected with control (Con) or lamin A/C (*LMNA*) siRNA and whole cell extracts prepared after 72 hours and analysed by immunoblotting with the indicated antibodies. (**e**) Wild type or Y259X HDFs were treated with MG-132 (30 μM) for 6 hours before protein extracts were prepared. Total levels of 53BP1 were assessed by immunoblotting. Boxed values represent 53BP1 protein levels as assessed by densitometry. (**f**) Immunofluorescence analysis of cells from (e) using DAPI and anti-53BP1 antibody. Scale bars, 10 μm.

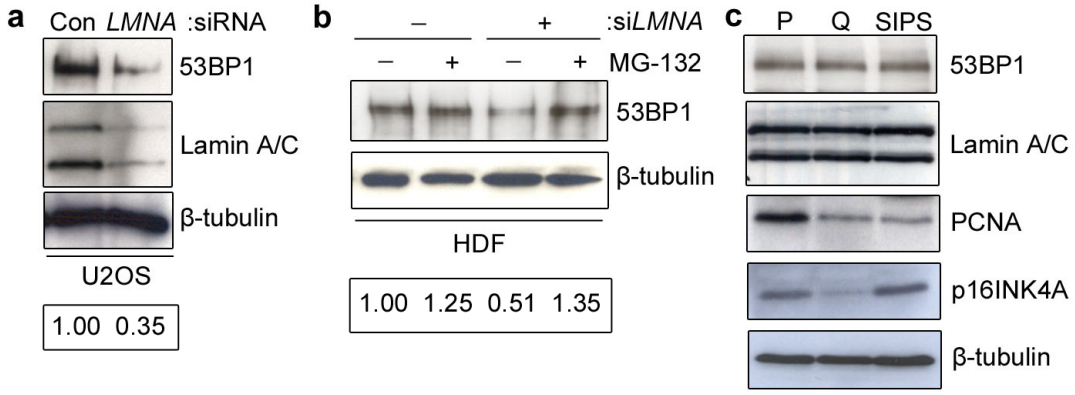

Figure 5.4. Depletion of A-type lamins promotes 53BP1 protein instability. (**a**) U2OS cells were transfected with control (Con) or lamin A/C (*LMNA*) siRNA for 72 hours before whole cell extracts were prepared and 53BP1 levels assessed by immunoblotting. Boxed values represent 53BP1 protein levels as assessed by densitometry. (**b**) HDFs transfected as in (a) were treated with MG-132 (30 μM) for 6 hours before whole cell extracts were assessed by immunoblotting for 53BP1 levels. Boxed values represent 53BP1 protein levels as assessed by densitometry. (**c**) Cell extracts were prepared from proliferating HDFs, quiescent HDFs and HDFs induced to undergo stress-induced premature senescence and protein levels were assessed by immunoblotting with the indicated antibodies.

5.4 53BP1 interacts with A-type lamins via its C-terminal domain, which is lost upon DNA damage

Based on the above findings and previous reports (Gonzalez-Suarez et al., 2009), I sought to determine if the loss of 53BP1 protein levels in the absence of lamin A/C reflected an underlying interaction between lamin A/C and 53BP1. Attempts to immunoprecipitate 53BP1 from endogenous lamin A/C complexes using high salt conditions (500 mM NaCl) were unsuccessful (data not shown). Therefore, I first crosslinked proteins *in vivo* using the reversible protein crosslinker dithiobis (succinimidyl propionate) (DSP), followed by lysis in a low salt buffer (150 mM) and sonication (Fujita et al., 2002; MacKay et al., 2009). Immunoprecipitation of endogenous lamin A/C from HDFs using these conditions showed that 53BP1 was present in lamin A/C immunoprecipitates, but absent from control IgG immunoprecipitates (Figure 5.5a). Importantly, this interaction was clearly decreased following DNA damage. To determine whether 53BP1 preferentially binds lamin A or lamin C, I co-transfected HEK293T cells (which do not express endogenous lamin A/C) with GFP-tagged lamin A or C together with HA-53BP1. Cell extracts were prepared and subjected to immunoprecipitation with GFP-Trap beads. Immunoblotting revealed that HA-53BP1 bound equally to lamin A and C (Figure 5.5b). To confirm these findings, Y259X cells were transfected with GFP-lamin A or GFP-lamin C and the distribution of 53BP1 was investigated by confocal microscopy. Expression of GFP-lamin A and GFP-lamin C both resulted in nuclear localisation of 53BP1, whereas expression of GFP alone did not (Figure 5.6).

To further study the interaction between 53BP1 and lamin A, stable U2OS cell lines expressing GFP or GFP-lamin A were created. As expected, GFP-lamin A localised both at the nuclear envelope and within the nucleoplasm (Figure 5.7a,b). Importantly, endogenous protein levels of 53BP1 were unchanged in U2OS/GFP-lamin A cells. Microscopy revealed that large nucleoplasmic foci of 53BP1 in undamaged cells were largely non-coincident with nucleoplasmic lamin A foci (Figure 5.7c). Lamin A fluorescence signal was typically greater at the nuclear

envelope with a lower fluorescence intensity but uniform distribution within the nucleoplasm, whilst 53BP1 showed a similar uniform distribution in the nucleoplasm with the exception of large foci and absence from nucleoli.

In order to map the lamin A interacting domain of 53BP1, I used a panel of HA-53BP1 constructs and expressed them in U2OS/GFP-lamin A cells. GFP-lamin A complexes were obtained by immunoprecipitation and the bound proteins analysed by immunoblotting. Results revealed that HA-53BP1 constructs containing the Tudor domain interacted strongly with lamin A (represented by + in Figure 5.5d), whilst the HA-53BP1 BRCT domain interacted weakly with lamin A (represented by +/- in Figure 5.5d). Underlining this, densitometry revealed that the HA-53BP1 BRCT signal was only ~20% that of the HA-53BP1 ΔBRCT signal. Therefore, these results strongly suggest that lamin A and C interact with a region surrounding the 53BP1 Tudor domain.

Previous reports have shown that a large number of proteins become phosphorylated upon DNA damage (Matsuoka et al., 2007; Stokes et al., 2007). However, DNA damage-dependent phosphorylation of 53BP1 is independent of its IRIF localisation (Ward et al., 2003). As I have shown that the interaction between lamin A and 53BP1 was decreased by DNA damage, I asked whether phosphorylation events *in toto* were important for this dissociation following DNA damage. I therefore treated U2OS/GFP-lamin A cells with the PIKK-inhibitor, caffeine, for 1 hour prior to IR treatment. Immunoprecipitation of GFP-lamin A complexes showed that endogenous 53BP1 dissociated with GFP-lamin A in response to IR (Figure 5.5e). However, blocking phosphorylation events via caffeine prevented this dissociation following DNA damage, with densitometry revealing that the levels of 53BP1 in caffeine/IR treated GFP-lamin A immunoprecipitates were ~70% of the untreated levels (Figure 5.5e). Together, this data reveals that 53BP1 interacts with A-type lamins via an area surrounding its Tudor domain and this interaction decreases via phosphorylation events in a DNA damage-dependent manner.

Figure 5.5. A-type lamins interact with the 53BP1 C-terminus, which is lost upon DNA damage in a phosphorylation-dependent manner. (**a**) HDFs were crosslinked *in vivo* before cell extracts were prepared and added to antibody-bound Dynabeads. Bound complexes were analysed by immunoblotting with anti-lamin A/C (Jol2) and anti-53BP1 antibodies. (**b**) HEK293T cells were co-transfected with full length HA-53BP1 and either GFP-lamin C or GFP-lamin A and cell extracts were subjected to immunoprecipitation with GFP-Trap beads. Bound complexes were analysed by immunoblotting with anti-HA and anti-GFP antibodies. (**c**) U2OS/GFP-lamin A cells were transfected with HA-53BP1 constructs for 24 hours before extracts were prepared and subjected to immunoprecipitation with GFP-Trap beads. Bound complexes were analysed by immunoblotting with anti-HA and anti-GFP antibodies. (**d**) HA-53BP1 constructs used for interaction studies, fragments that form at IRIFs are indicated (Iwabuchi et al., 2003). (**e**) U2OS/GFP-lamin A cells were pre-treated with caffeine (20 mM) for 1 hour before IR. Extracts were prepared and subjected to immunoprecipitation with GFP-Trap beads followed by immunoblotting. Bound endogenous 53BP1 was assessed using anti-53BP1 antibody.

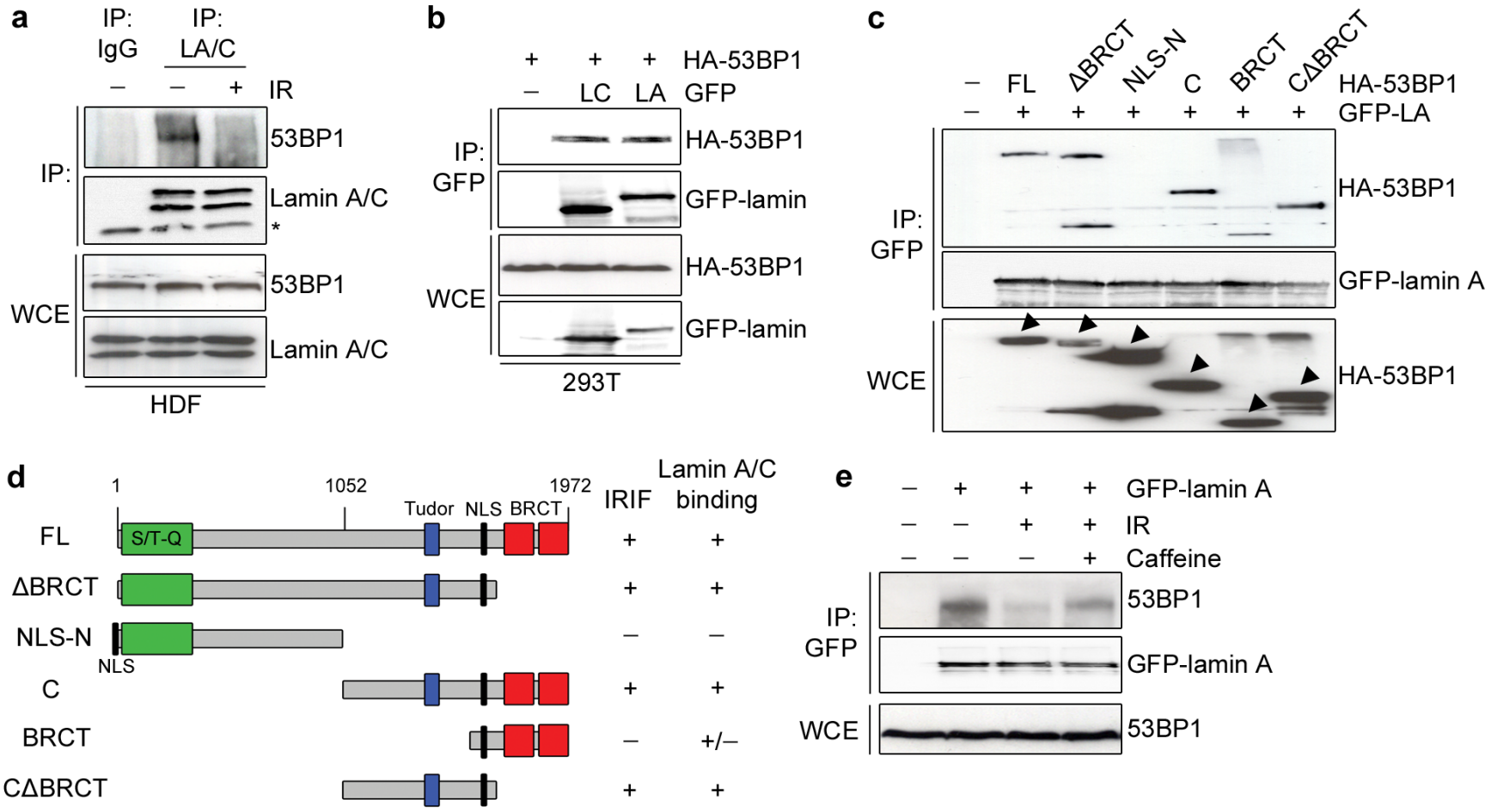
a
IP: IgG
IP: LA/C
– – + IR
IP:
53BP1
Lamin A/C
*
WCE
53BP1
Lamin A/C
HDF
b
+ + + HA-53BP1
– LC LA GFP
IP: GFP
HA-53BP1
GFP-lamin
WCE
HA-53BP1
GFP-lamin
293T
c
– FL ΔBRCT NLS-N C BRCT CΔBRCT HA-53BP1
– + + + + + + GFP-LA
IP: GFP
HA-53BP1
GFP-lamin A
WCE
HA-53BP1
d
1
1052
1972
Tudor NLS BRCT
IRIF
Lamin A/C binding
FL
S/T-Q
+ +
ΔBRCT
+ +
NLS-N
NLS
– –
C
+ +
BRCT
– +/–
CΔBRCT
+ +
e
– + + + GFP-lamin A
– – + + IR
– – – + Caffeine
IP: GFP
53BP1
GFP-lamin A
WCE
53BP1

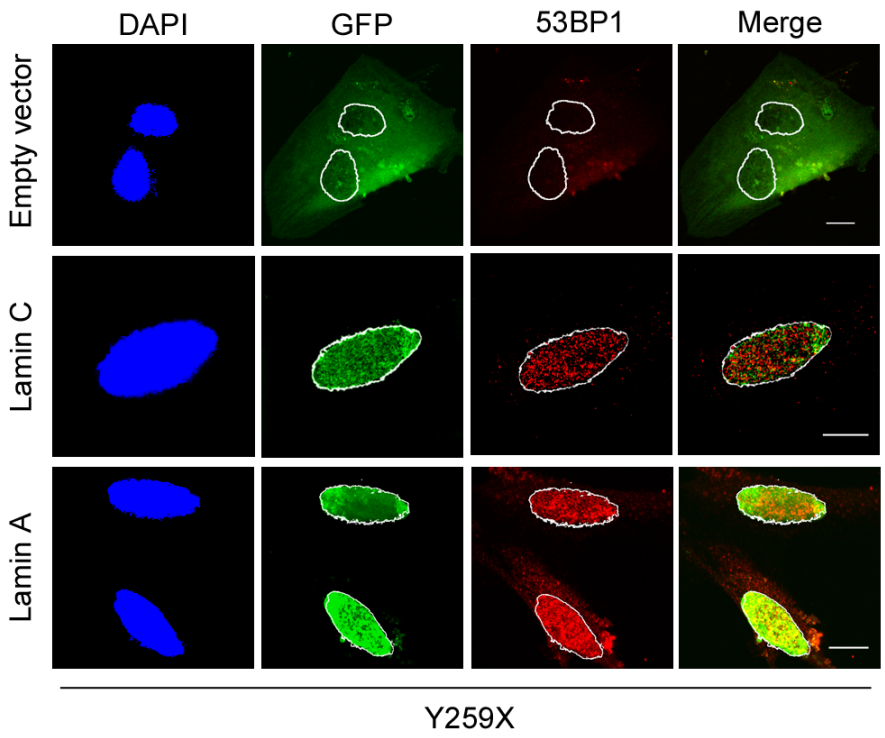

Figure 5.6. Reintroduction of lamin A and C in Y259X cells restores 53BP1 nuclear localization. Y259X cells were transfected with either GFP, GFP-lamin C or GFP-lamin A, fixed after 48 hours and immunostained with anti-53BP1 antibody. Outline indicates area occupied by DAPI signal. Scale bar, 10 μm.

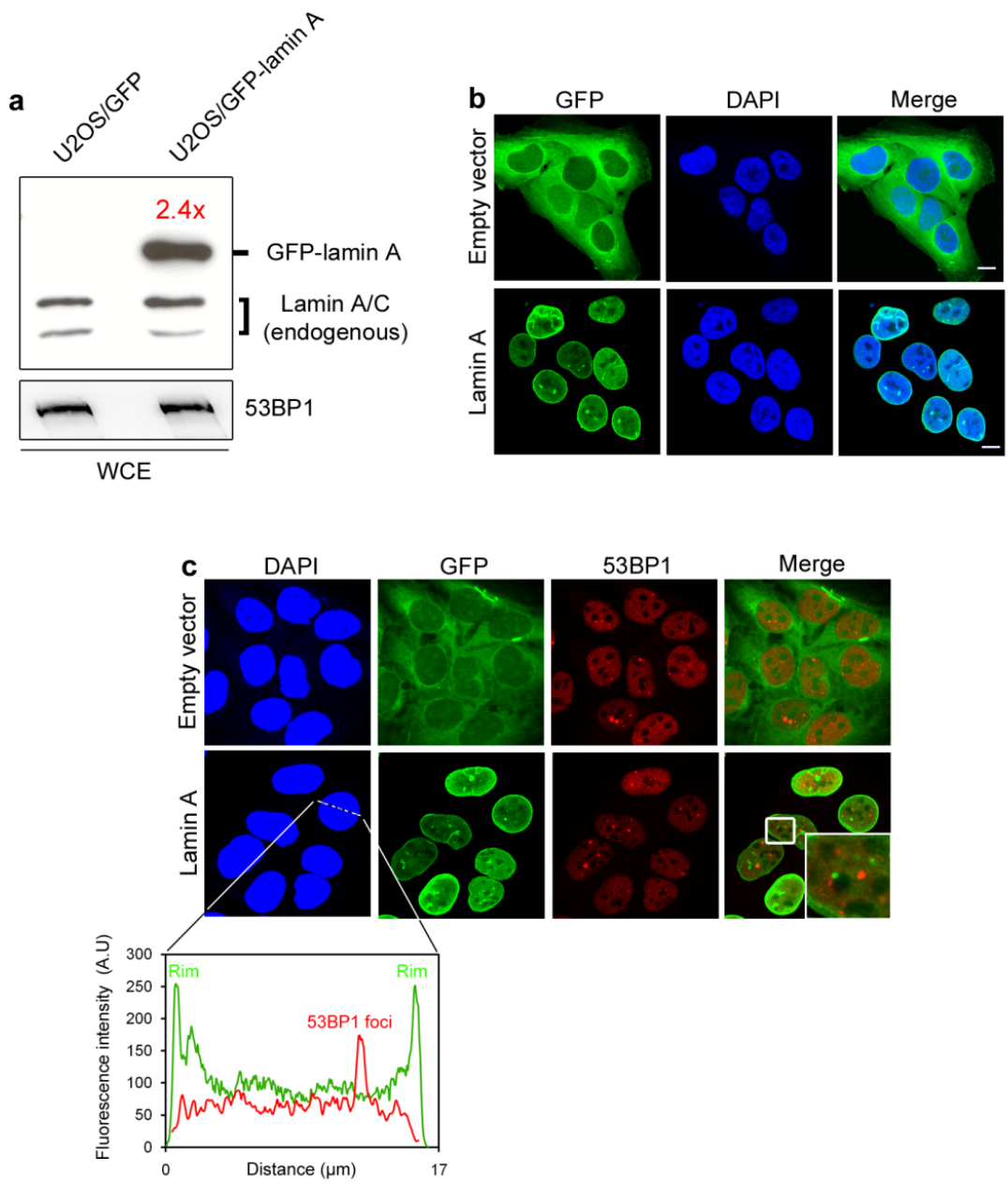

Figure 5.7. Generation of a U2OS/GFP-lamin A stable cell line. (**a**) Whole cell extracts prepared and total levels of lamin A and 53BP1 were assessed by immunoblotting with anti-lamin A/C (Jol2) and 53BP1 antibodies. (**b**) Micrographs of U2OS/GFP and U2OS/GFP-lamin A cells. (**c**) U2OS/GFP and U2OS/GFP-lamin A cells were fixed, processed for immunofluorescence and stained with anti-53BP1 antibody. Graph shows the fluorescence intensity from GFP and 53BP1 signals from the indicated cell. Scale bars, 10 μm.

5.5 Lamin A/C-deficient cells display DNA repair defects and reduced cellular fitness in response to DNA damage

As I have shown that A-type lamins interact with 53BP1, a component of the DNA damage response, I investigated what affect loss of A-type lamins would have on the DNA repair process. I used residual γ-H2AX foci as a readout to assess DNA repair efficiency (Figure 5.8a-d). Cells were treated with a relatively small dose of IR (3 Gy) as it has been shown that cells depleted of 53BP1 display a defective DNA damage response in response to 3 Gy rather than higher doses (10 Gy) (Wang et al., 2002). Even without IR, Y259X cells exhibited increased numbers of γ-H2AX foci compared to wild type HDFs, indicating increased levels of genomic instability even in the absence of genotoxic stress, as noted previously (Figure 5.8e). After IR, which predominantly induces double strand breaks, wild type HDFs were able to effectively repair most DNA damage as γ-H2AX foci numbers over 24 hours. Note that DSB repair was biphasic in nature, with an initial larger fast component, which has been shown to typically represent repair of euchromatin, and a smaller slow component, which represents the repair of heterochromatin (Figure 5.8e) (Goodarzi et al., 2010). In contrast, although Y259X cells were able to induce a similar number of γ-H2AX foci after 0.5 hours compared to wild type HDFs, they exhibited a significant inability to repair late kinetic DSBs (Figure 5.8e). Together, this data suggests that A-type lamins help promote DNA repair in response to genotoxic stress in human fibroblasts.

Double strand breaks generated by IR are scattered randomly throughout the genome. Therefore, to circumvent problems in assaying DNA repair in real time, advances have been made to compartmentalise DSBs using a technique known as laser micro-irradiation (Lukas et al., 2003; 2005). This technique utilises an old finding that incorporation of halogenated thymidine analogs (BrdU, IdU) presensitises DNA to light within the UV-A spectrum, which generates a photochemical reaction to induce DNA damage (Limoli and Ward, 1993). Wild type HDFs and Y259X cells were presensitised by addition of BrdU for 24 hours

before being subject to laser micro-irradiation. Immunostaining revealed reduced γ-H2AX induction in the laser stripes of Y259X cells, with densitometry of the laser stripe revealing that the signal intensity was ~ 50% that of wild type HDFs 0.5 after laser-irradiation (Figure 5.8f). This suggests that phosphorylation of H2AX in these laser stripes is inhibited in the absence of A-type lamins. Notably, this is in direct contrast to the IR data which shows that induction of H2AX phosphorylation is comparable in both Y259X and HDFs (Figure 5.8e,f).

To complement these studies using a different cell line widely used to study the DNA damage response (U2OS cells, derived from an osteosarcoma), I assessed the ability of cells depleted of lamin A/C by RNAi to effectively repair DNA damage. Control or lamin A/C-depleted U2OS ells were treated cells with IR (5 Gy) and whole cell extracts prepared after various time points thereafter. U2OS cells treated with control siRNA exhibited a transient spike in γ-H2AX levels (histone H2A served as a histone loading control), which decreased over time, suggestive of effective DNA repair. In lamin A/C-depleted cells I again observed increased levels of γ-H2AX even in the absence of genotoxic stress (Figure 5.8g). In response to IR, ATM-mediated signalling of γ-H2AX was increased above supra-physiological levels in cells depleted of A-type lamins (Figure 5.8g). Furthermore, lamin A/C-depleted cells still displayed elevated γ-H2AX levels 24 hours post-IR compared to the untreated sample (Figure 5.8g). To assess the long-term effects on cellular fitness in response to DNA damage, colony forming assays revealed that depletion of A-type lamins significantly and reproducibly reduced cellular survival in response to even low doses of IR (Figure 5.8h and Supplementary Figure 8 for knockdown efficiencies). This data strongly suggests that fully processed A-type lamins have a functional role in the DNA repair process and are involved in the maintenance of genomic stability.

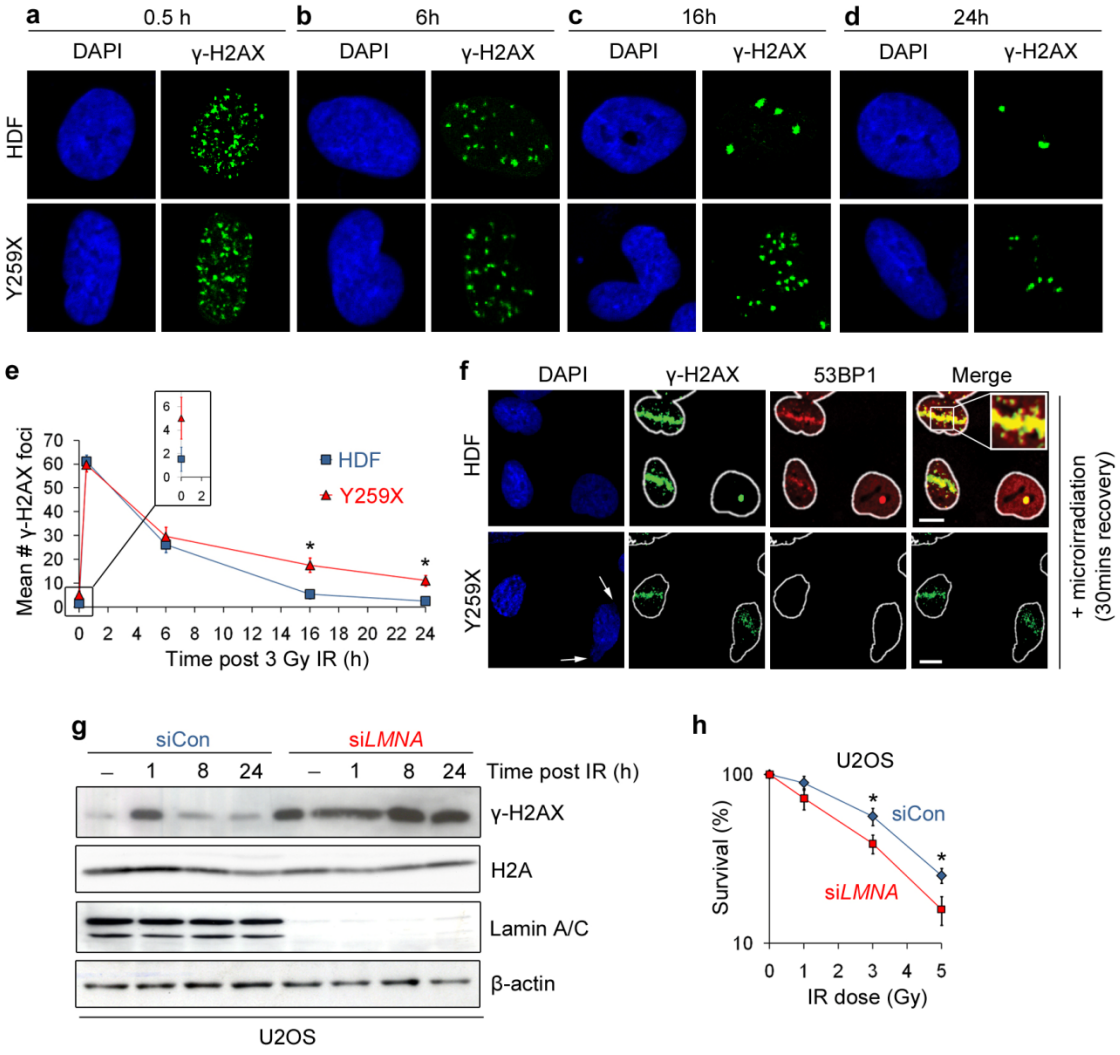

Figure 5.8. A-type lamin depletion inhibits DNA repair and reduces cellular fitness to DNA damage. (**a-d**) HDFs and Y259X cells were treated with IR (3 Gy), fixed at the times indicated and processed for immunofluorescence before staining with anti-γ-H2AX antibody. (**e**) Quantification of data from (a-d). (**f**) HDFs and Y259X were subjected to laser micro-irradiation, fixed after 0.5 h and immunostained with anti-γ-H2AX and 53BP1 antibodies and DAPI. (**g**) U2OS were transfected twice in 24 h with control (siCon) or lamin A/C (si*LMNA*) siRNA and exposed to IR (5 Gy) 72 h later. Whole cell extracts were prepared and assessed by immunoblotting with the indicated antibodies. (**h**) U2OS cells were transfected as in (g) and plated onto 60mm plates 72 h later. The cells were then exposed to varying doses of IR. After 12 days, plates were fixed and stained with

crystal violet and viable colonies counted. Data in (e) and (h) represent the mean ± s.d from three independent experiments. * $p<0.05$ relative to HDFs (e) or siCon (h) at each timepoint. Scale bars, 10 μm.

5.6 Discussion

5.6.1 Lamin A/C as a chromatin binding protein

Previous studies have shown that the production of mutant forms of lamin A, either in RD or HGPS cells, causes increased DNA damage, enhanced downstream signalling events and a failure to repair genotoxic stress-induced DNA damage (Liu et al., 2005; Liu et al., 2006; Liu et al., 2007). A recent study has shown that the DNA damage mediator protein, 53BP1, exhibits reduced protein stability in the absence of A-type lamins using *Lmna*$^{-/-}$ MEFs (Gonzalez-Suarez et al., 2009). Based on this finding, I investigated whether A-type lamins in HDFs might have a similar role and thus implicate A-type lamins in the DDR. Biochemical fractionation results demonstrated that 53BP1 exists in three subpopulations in HDFs: soluble, chromatin-bound and insoluble. The latter pool of 53BP1 co-fractionated with both A- and B-types lamins, both of which are resistant to the fractionation process. In response to DNA damage, biochemical fractionation showed that 53BP1 is almost exclusively chromatin-bound, as described previously for MCF7 cells (Iwabuchi et al., 2003). As the largest pool of 53BP1 in untreated proliferating HDFs was in the insoluble fraction, it seems that this fraction is induced to IRIF upon DNA damage. In contrast, lamin A showed no differential solubility properties in response to DNA damage and although some lamin A was evident in the DNase I digested fraction, this was variable between experiments and thus is likely an artefact. Immunostaining of *in situ* extracted HDFs in response to IR confirmed the loss of 53BP1 in the DNase I digested fraction in response to DNA damage. Again, immunostaining revealed no changes in lamin A/C solubility in response to DNA damage. As lamin A/C has been proposed to be a chromatin scaffold, how might lamin A/C participate in chromatin dynamics during DNA damage? Lamin A forms nucleoplasmic foci in G_1-phase of the cell cycle that colocalises with areas of dense chromatin (Bridger et al., 1993). Furthermore, lamin A/C was shown to be a chromatin-binding protein and the region for this interaction has been mapped to a region after the α-helical coiled-coil domain (Taniura et al., 1995). Interestingly, this region contains a potential

phosphorylation domain with SQ/TQ motifs that are phosphorylated in response to DNA damage (see Chapter 6). The possibility therefore arises that lamin A/C phosphorylation may regulate the ability of the protein to bind chromatin. Future work should seek to clarify the finding that lamin A/C binds core histones, and explore which specific histone lamin A/C interacts with. Recently, a proteomic study of Flag-H2AX-interacting proteins showed a peptide matching lamin A/C was among the proteins identified (Yang et al., 2010). Therefore, whether A-type lamins interact with γ-H2AX at DSBs could be addressed using chromatin immunoprecipitation (ChIP) assays and assessing the presence of lamin A/C in the immunoprecipitates. Mutating residues in the lamin A/C SQ/TQ motif will also provide proof if phosphorylation of lamin A/C regulates chromatin interactions in response to DNA damage. One particular function for any lamin A/C-histone interaction may be to aid chromatin relaxation during DNA damage. Chromatin remodelling and relaxation are essential for the effective recruitment of repair proteins in response to DNA damage (Bao and Shen, 2007; Peng et al., 2009). The role of known chromatin mobility proteins EXPAND1 and KAP1 might also be explored in lamin A/C depleted cells (Ziv et al., 2006; Huen et al., 2010).

5.6.2 A-type lamins do not relocalise to IRIF

One defining characteristic of DDR proteins is their accumulation at IRIF and yet there are a number of other proteins that do not accumulate at IRIF such as p53, Chk1, Chk2, Ku70 and DNA-PK (Bekker-Jensen and Mailand, 2010). These proteins are *bona fide* DDR proteins, and there is evidence to suggest that they only act transiently with areas of DNA damage before embarking on pan-nuclear signaling roles (e.g. for p53, Chk1, and Chk2). In the case of Ku70 and DNA-PK, as only a small number of molecules interact with DNA ends, it is likely that their presence is beyond the limitations of current microscopy techniques (Downs and Jackson, 2004). As a structural component of the nucleus, it is of no surprise that A-type lamins do not relocalise to IRIF. However, based on the observations that proteins such as p53 and Chk1 do not relocalise to IRIF, one mechanism not explored in this study is the potential role that A-type lamins have in various

signaling mechanisms in response to DNA damage (Pekovic and Hutchison, 2009). Lamin A/C-LAP2α complexes tether the tumour suppressor pRb in the nucleoplasm via its C-terminal pocket C region (Markiewicz et al., 2002; Dechat et al., 2004; Dorner et al., 2006). A clear role for lamin A/C-LAP2α complexes in controlling cell cycle progression has therefore been established (Dorner et al., 2006; Pekovic et al., 2007). One avenue of future research should therefore address the role of lamin A/C in controlling cell cycle progression in response to the DNA damage using flow cytometry to determine if loss of A-type lamins has any effects on the G_1-S, intra-S and G_2/M-phase checkpoints.

5.6.3 A-type lamins mediate 53BP1 protein stability

Having determined the biochemical properties of lamin A/C and 53BP1 in HDFs, I then utilised cells harbouring a homozygous Y259X mutation in *LMNA*, rendering these cells null for lamin A/C (Muchir et al., 2003). As has been shown for *Lmna*$^{-/-}$ MEFs, I found barely detectable protein levels of 53BP1, which seemed specific to 53BP1 as analysis of another DDR protein, Rad51, exhibited similar protein levels. In addition, the levels of γ-H2AX were higher in Y259X cells versus wild type HDFs, suggesting increased levels of genomic instability in the absence of A-type lamins. Notably, the effect of A-type loss on 53BP1 was recapitulated by RNAi of lamin A/C in both HDFs and U2OS, suggesting that this phenomenon is not cell-type specific. Moreover, 53BP1 protein levels were unchanged in HDFs in various proliferative states, arguing against cell cycle dependent effects on 53BP1 protein levels. Inhibition of the proteasome rescued protein levels of 53BP1 in both Y259X cells and HDFs depleted of lamin A/C by RNAi. Importantly, even though protein levels were rescued, we did not observe nuclear localisation of 53BP1 in Y259X cells in response to proteasome inhibition, underlining that A-type lamins are important for both the correct nuclear localisation and protein stability of 53BP1. This relationship has striking similarities with the lamin A/C-pRb interaction (Markiewicz et al., 2002; Johnson et al., 2004). It was shown that *Lmna*$^{-/-}$ MEFs exhibit reduced levels of pRb protein levels that are recoverable by

proteasome inhibition, but, as with 53BP1, pRb nuclear localisation was not restored (Johnson et al., 2004).

In order to account for 53BP1 protein loss, I probed whether A-type lamins bound 53BP1. I observed an interaction between 53BP1 in HDFs, which clearly decreased to barely detectable levels 1 hour post-IR. As the antibody used for immunoprecipitation recognised both lamin A and C, I then performed co-immunoprecipitation experiments to determine that 53BP1 was present in both GFP-lamin A and C immunoprecipitates. This is in agreement with previous findings that showed that depleting lamin A/C in wild MEFs followed by restoration of either lamin A or C by over-expressing tagged constructs was sufficient to restore 53BP1 protein levels (Gonzalez-Suarez et al., 2009). Indeed, when I over-expressed GFP-lamin A or C in Y259X cells I observed that 53BP1 protein levels were restored to the nucleus. Together, this data and previous work highlight the importance of both lamin A and C in maintaining 53BP1 protein levels. Furthermore, I would suggest that if the interaction is direct (see below), then the 53BP1 interaction of lamin A and C must be from position 1-572 amino acids, as these are the residues shared by both lamin A and C. Of course, I cannot rule out that the lamin A tail may harbour 53BP1 interacting domains.

To explore the relationship between A-type lamins and 53BP1 in more detail, I generated a stable U2OS/GFP-lamin A cell line. Using these cells, I found that GFP-lamin A was able to efficiently pulldown fragments of HA-53BP1 that contained the Tudor domain. Furthermore, in response to DNA damage the ability of GFP-lamin A to immunoprecipitate endogenous 53BP1 was reduced in U2OS/GFP-lamin A cells, which was reversible by prior treatment with the ATM/ATR inhibitor, caffeine, a known inhibitor of DNA damage phosphorylation events. Future work should seek to confirm whether the relationship between lamin A/C and 53BP1 is direct or mediated by other proteins. This may be addressed by bacterially expressing differentially tagged fragments of lamin A/C and 53BP1 followed by pulldown experiments. Furthermore, to underline the phosphorylation-dependent interaction between lamin A/C and 53BP1 in

response to DNA damage, it will be important to repeat the immunoprecipitation experiments by pre-treating extracts with λ-phosphatase. Despite the need for further studies, these present findings highlight the dynamic phosphorylation-dependent relationship between A-type lamins and 53BP1 in response to DNA damage, and opens the door for a more detailed investigation using the U2OS/GFP-lamin A cells produced here in a proteomic approach to identify proteins that may associate or dissociate with A-type lamins upon DNA damage, and thus might help contribute to effective DNA repair and genomic stability.

5.6.4 A-type lamins promote genomic stability and efficient DNA repair

Previous studies have implicated A-type lamins in preserving genomic integrity (Liu et al., 2005; Gonzalez-Suarez et al., 2009). The presence of a mutant lamin A, progerin or lamin AΔ50, in Hutchinson Gilford Progeria Syndrome (HGPS) cells and the complete absence of A-type lamins in *Lmna*$^{-/-}$ MEFs both lead to increased levels of γ-H2AX, a marker of DNA damage and thus genomic instability (Liu et al., 2005; Gonzalez-Suarez et al., 2009). Similarly, I have shown that Y259X cells have dramatically increased γ-H2AX levels, indicating that loss of A-type lamins in HDFs leads to increased genomic instability. What then is the mechanistic basis for increased genomic instability in cells lacking A-type lamins? The presence of increased γ-H2AX levels in Y259X cells may result from dysfunctional telomeres. It has been observed that HGPS cells have accelerated telomere shortening and progerin-induced DNA damage is correlated with telomeres (Huang et al., 2008; Decker et al., 2009; Benson et al., 2010). Moreover, expression of the catalytic subunit of telomerase, TERT, reduced DNA damage levels and both p53- and pRb-dependent signaling (Benson et al., 2010). Furthermore, *Lmna*$^{-/-}$ MEFs display mislocalised telomeres and accelerated telomeres shortening (Gonzalez-Suarez et al., 2009). Another alternative that I propose is that replication forks may collapse into DSBs in cells lacking A-type lamins. As A-type lamins reportedly bind PCNA and are associated with the initiation of DNA replication, it is possible that, in their absence, spontaneous DSBs may arise from defects in the replication process. Replication fork collapse

in combination with DNA repair defects (see below) may be a plausible suggestion for increased genomic instability in cells lacking A-type lamins. Regardless of the mechanism, it will be important to elucidate whether restoration of 53BP1 in A-type lamin depleted cells may restore genomic stability. These rescue experiments are vital to understanding whether there is more than one mechanism by which A-type lamin loss may affect genomic stability.

Preservation of genomic integrity in somatic cells is vital to cellular function and whilst damage to other macromolecules may be tolerated by renewal, damage to nuclear DNA is irreplaceable. There is therefore a significant evolutionary investment in genomic surveillance and maintenance pathways to faithfully pass on genetic information to daughter cells. Thus, inherent within discussing the genomic instability exhibited in cells lacking A-type lamins should be an exploration of DNA damage repair pathways that may be affected in this genetic background. Based on current understanding of the role of cell cycle position in the choice between NHEJ and HR (i.e. G_1 vs S/G_2) I may now reassess the findings of Liu et al., 2005 (Bartek and Lukas, 2007; Wohlbold and Fisher, 2009). Using *Zmpste24*$^{-/-}$ MEFs, Liu et al. observed a reduced S-phase content and increased G_1-phase content compared to wild type cells (Liu et al., 2005). As HGPS cells undergo premature senescence and have a reduced S-phase index (Goldman et al., 2004), I may conclude generally that unprocessed prelamin A causes proliferative defects that result in both *Zmpste24*$^{-/-}$ MEFs and HGPS cells to have a greater proportion of cells in G_1-phase. As NHEJ is the repair pathway of choice in G_1-phase, we would expect *Zmpste24*$^{-/-}$ MEFs and HGPS to engage this pathway. Indeed, using a fluorescence-based reporter assay, this was found to be the case (Liu et al., 2005). Furthermore, the reduced proportion of S-phase cells more than likely reflects the reduced number of Rad51 foci and impaired engagement of the HR repair pathway (Liu et al., 2005). Thus, as NHEJ is inherently error-prone, I would suggest that the genomic instability in these cells is in part caused by use of this repair pathway rather than the HR repair pathway. Entirely consistent with this is the finding of increased chromosomal aberrations

and in particular more telomere end-fusion products in HGPS cells, reflecting use of the NHEJ pathway (Benson et al., 2010).

In contrast to *Zmpste24*$^{-/-}$ MEFs and HGPS cells, it was reported that *Lmna*$^{-/-}$ MEFs show impaired ability to process dysfunctional telomeres by NHEJ (Gonzalez-Suarez et al., 2009). Flow cytometry analysis in this study could not find any differences in cell cycle phases between immortalised wild type and *Lmna*$^{-/-}$ MEFs, therefore suggesting that it is specifically defects in NHEJ that cause dysfunctional telomere processing, rather due to differences in cell cycle phase (Gonzalez-Suarez et al., 2009). This latter finding is surprising considering a previous report showed a clear increase in the proportion of S-phase cells in *Lmna*$^{-/-}$ MEFs (Johnson et al., 2004). Despite this, the finding that A-type lamins promote 53BP1 stability as demonstrated here and previously, suggests a link between A-type lamins and NHEJ. 53BP1 is involved in the NHEJ pathway by increasing DNA end mobility, either DSBs or telomeres, therefore allowing their effective processing by NHEJ (Dimitrova et al., 2008). A further intriguing link between A-type lamins and NHEJ has come from recent work exploiting unbiased proteomic approaches to identify lamin A binding proteins (Kubben et al., 2010). Among the proteins identified was Ku70, which is part of the Ku70/80 heterodimer complex (Kubben et al., 2010). The Ku70/80 complex is an essential component of the NHEJ pathway and acts as the sensor protein in this pathway, binding to the end of the DSB (Mahaney et al., 2009; Roberts et al., 2010). Ku70/70 also possesses some end processing ability and functions to recruit DNA-dependent protein kinase catalytic subunit (DNA-PKcs) (Roberts et al., 2010). Interestingly, a MudPIT proteomic approach identified DNA-PKcs as a novel progerin-interacting protein in HGPS cells (Liu et al., 2011). Immunoprecipitation experiments confirmed this progerin-interaction was greater than between wild type lamin A and DNA-PKcs. However, analysis of HGPS protein extracts showed decreased levels of DNA-PKcs, suggesting that progerin destabilises DNA-PKcs protein levels (Liu et al., 2011). Furthermore, they also observed decreased levels of the Ku70/80 complex in HGPS. These findings again suggest that presence of mutant lamin A versus absence of A-type lamins has differential outcomes for repair

pathways. However, despite being identified as A-type lamin binding protein, both Ku70 and DNA-PKcs, two of the earliest temporal components of the NHEJ pathway, were found to be unchanged at the protein level in *Lmna*$^{-/-}$ MEFs (Gonzalez-Suarez et al., 2009). Indeed, when I challenged Y259X cells with a low dose of IR they exhibited defects in the repair of DSBs with late kinetics, suggesting that the sensing of DSBs, a role carried out by Ku70/80 and DNA-PKcs, was not impaired in HDFs lacking A-type lamins. Rather than a defect in sensing DSBs, the impaired ability to repair DSBs at late timepoints post-IR in Y259X cells suggests defective repair of heterochromatin regions. Noon et al. showed that loss of 53BP1 conferred a DNA repair cellular phenotype that is epistatic with ATM inhibition, which is characterised by defective repair of heterochromatin regions (Noon et al., 2010). Furthermore, they showed that loss of 53BP1 inhibited the localisation of pKAP-1 at heterochromatin regions of DNA damage (Noon et al., 2010). Future work should thus seek to determine if cells null for lamin A/C exhibit defective repair of heterochromatin in response to DNA damage and the underlying mechanistic basis.

How wild type A-type lamins are involved in the DDR pathways is of great importance as failure of DNA repair mechanisms contribute to cancer progression. In this chapter I have shown that A-type lamins are important for maintaining genomic stability and are involved in effective DNA repair through mechanisms not fully understood. Importantly, it will be of great clinical value to address whether promoter methylation of *LMNA*, and hence its silencing, is associated with an impaired DDR in cancer subtypes.

CHAPTER 6. MODELLING THE LAMIN A/C-53BP1 INTERACTION AND EXPLORATION OF DNA DAMAGE-DEPENDENT A-TYPE LAMIN PHOSPHORYLATION

6.1 Introduction

6.1.1 Lamin networks as indicators of molecular function

The interaction between lamin A/C and various nuclear proteins have implicated A-type lamins in a broad spectrum of cellular processes (see 1.3) (Zastrow et al., 2004; Vlcek and Foisner, 2007). One of these processes, the DNA damage response (DDR), was explored in Chapter 5. To extend these findings, I interrogated the literature and identified proteins implicated in the DNA damage response that interacted either directly with lamin A/C or indirectly via the lamin A/C interacting protein BAF. I found a large set of lamin A/C-interacting proteins, involved in various aspects of the DNA damage response and repair pathways (Figure 6.1). This DNA damage-specific lamin A/C interactome provides a potential mechanistic basis for the DNA repair defects observed in cells lacking lamin A/C, and it is possible that, *a priori*, loss of A-type lamins in cells may affect the functions of these proteins. Despite the obvious need for validation in the context of the DDR, it does suggest that, together with the data in Chapter 5, lamin A/C may actively participate in the DDR. However, how A-type lamins are involved in the DDR remains somewhat elusive.

Of the plethora of post-translational modifications that function within the DDR, one of the earliest and wide-ranging modifications is phosphorylation (Matsuoka et al., 2007; Stokes et al., 2007). Phosphorylation in the DDR activates proteins involved in, but not limited to, DNA repair, cell cycle progression, gene expression, RNA post-transcriptional regulation, nucleic acid metabolism, cell death and cell-cell signaling (Matsuoka et al., 2007). Interestingly, in a proteomic

study identifying proteins phosphorylated in response to UV damage, multiple peptides matching lamin A/C were found (Stokes et al., 2007). However, whether phosphorylation alters lamin A/C function in response to DNA damage remains to be determined.

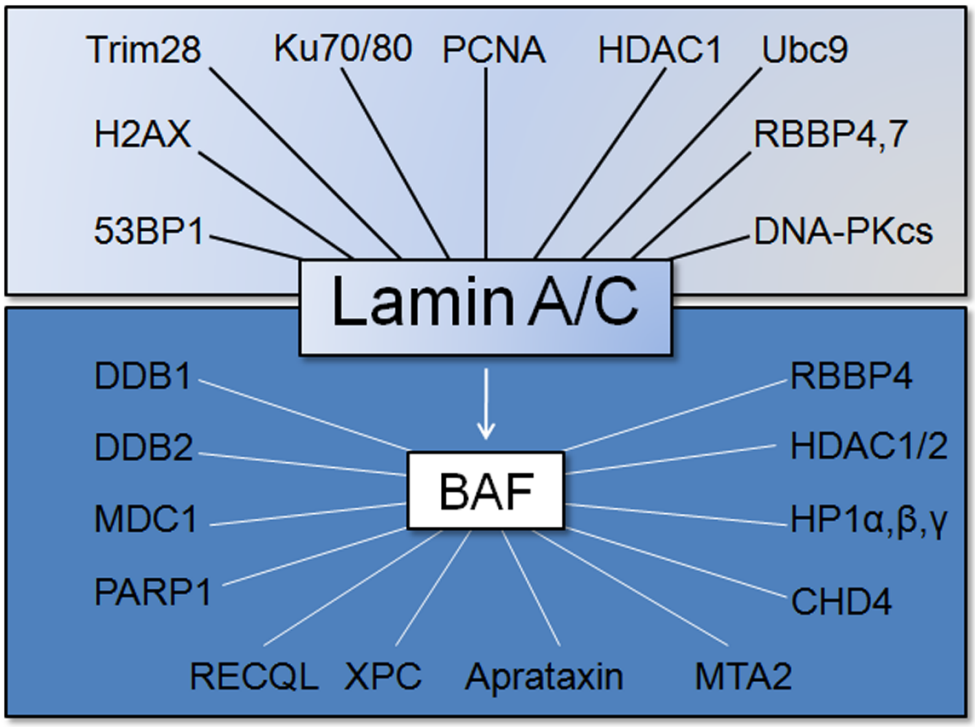

Figure 6.1. DNA damage response proteins that interact either directly or indirectly (via BAF) with lamin A/C.

6.1.2 Current aims

In Chapter 5, I demonstrated that loss of A-type lamins imparts a DNA repair defect on cells, thereby sensitising them to DNA damage. To further explore the role of A-type lamins in the DNA damage response, I assessed whether lamin A/C is phosphorylated in response to DNA damage and modelled the interaction between lamin A/C and 53BP1.

6.2 Modelling the 53BP1-lamin A/C interaction

Based on the data from Chapter 5, in which I showed that lamin A/C interacts with a region surrounding the 53BP1 Tudor domain, I was intrigued by the possible structural relationship between the two. Although I have yet to map the 53BP1-interacting domain of lamin A/C using lamin A or C deletion mutants, I predicted that the Ig-like fold in lamin A/C (Figure 6.2) – a well-known region that binds a variety of other proteins, including PCNA, emerin and LAP2α – might interact with 53BP1 (Zastrow et al., 2004; Shumaker et al., 2008). To assess this potential interaction, I used the protein docking simulation server ClusPro 2.0, which models interactions with four different binding conditions – balanced; electrostatic; hydrophobic; Van der Waals and electrostatic (Kozakov et al., 2010).

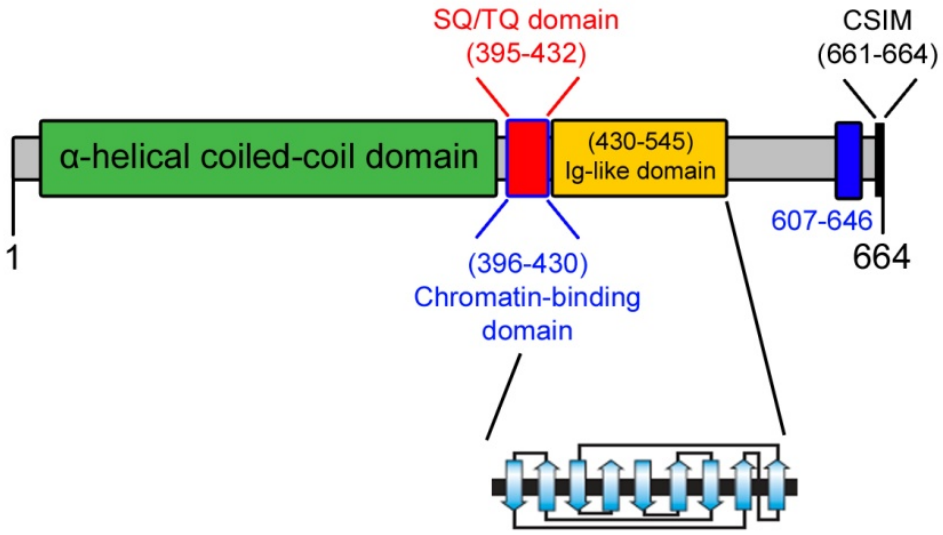

Figure 6.2. The type s Ig-like fold in the lamin A/C C-terminal. (Lower diagram of Ig-like fold taken from Dechat et al., 2010)

The three-dimensional structure of the 53BP1 Tudor domain was previously characterised by X-ray crystallography (Huyen et al., 2004; Botuyan et al., 2006). The Tudor domain consists of two tandem folds with a deep pocket at their interface formed by evolutionarily conserved hydrophobic residues. The presence

of a deep hydrophobic pocket raised the possibility that 53BP1 binds to methylated lysine or arginine residues, because methylated lysine/arginine side chains are long and hydrophobic (Mochan et al., 2004).

Using the lamin A/C Ig-like fold as a receptor (PDB: 1IFR; Dhe-Paganon et al., 2002) and the 53BP1 Tudor domain as a ligand (PDB: 2G3R; Botuyan et al., 2006), I used the protein docking simulation to examine potential interactions between the two. The four top outputs for each modelling condition are shown (Figure 6.3). With the exception of the Van der Waals and electrostatic model which placed the lamin Ig-like fold near to the entrance of the deep pocket of the Tudor domain, the ClusPro simulation results suggest that the lamin Ig-like fold may dock within the deep pocket of the Tudor domain (Figure 6.3).

As previous studies have shown that the deep pocket of the tandem Tudor domain binds methylated lysine/arginine residues, I analysed whether any of the top outputs modelled contained any lysine or arginine residues in the lamin Ig-like fold (Figure 6.4). Using the top prediction from the hydrophobic docking simulation, analysis of the amino acids in closest proximity to the Tudor domain showed a clear absence of any lysine and arginine residues (Figure 6.4). Together with the data from Chapter 5, this modelling data suggests that the lamin A/C Ig-like fold may interact with the 53BP1 Tudor domain, either within the deep pocket or in close proximity to it, which dissociates upon DNA damage, most likely due to the high affinity of the 53BP1 Tudor domain for methylated histone H4, which is increased upon DNA damage (Botuyan et al., 2006; Pei et al., 2011).

To further these findings, I performed a protein docking simulation again using the 53BP1 Tudor domain (PDB; 2G3R), but with a different crystallographic structure of the lamin Ig-like fold (Krimm et al., 2002). The top outputs for each of the four conditions again modelled the lamin Ig-like fold to interact with Tudor domain pocket (Figure 6.5). However, using a different web-based docking simulation, GRAMM-X, the lamin A/C Ig-like fold was predicted to dock to the 53BP1 Tudor domain at a location behind the deep pocket (Figure 6.6). In this scenario, it would

be possible for the 53BP1 Tudor domain to interact with other substrates whilst at the same time interacting with lamin A/C. The predicted docking sites of the ClusPro and GRAMM-X simulations are by no means mutually exclusive, i.e. they may both occur given the correct cellular situation, however, it does underline the need for future experimental data to characterise fully the mode of interaction between lamin A/C and the 53BP1 Tudor domain.

Figure 6.3. The lamin A/C Ig-like fold is predicted to interact with the Tudor domain of 53BP1. Using Cluspro 2.0 protein docking simulation, the lamin A/C Ig-like fold (PDB: 1IFR) and the 53BP1 Tudor domain (PDB: 2G3R) were modelled for potential interactions. The top output in each of the four modelled conditions is shown for (**a**) balanced (**b**) hydrophobic (**c**) electrostatic (**d**) Van der Waals and electrostatic.

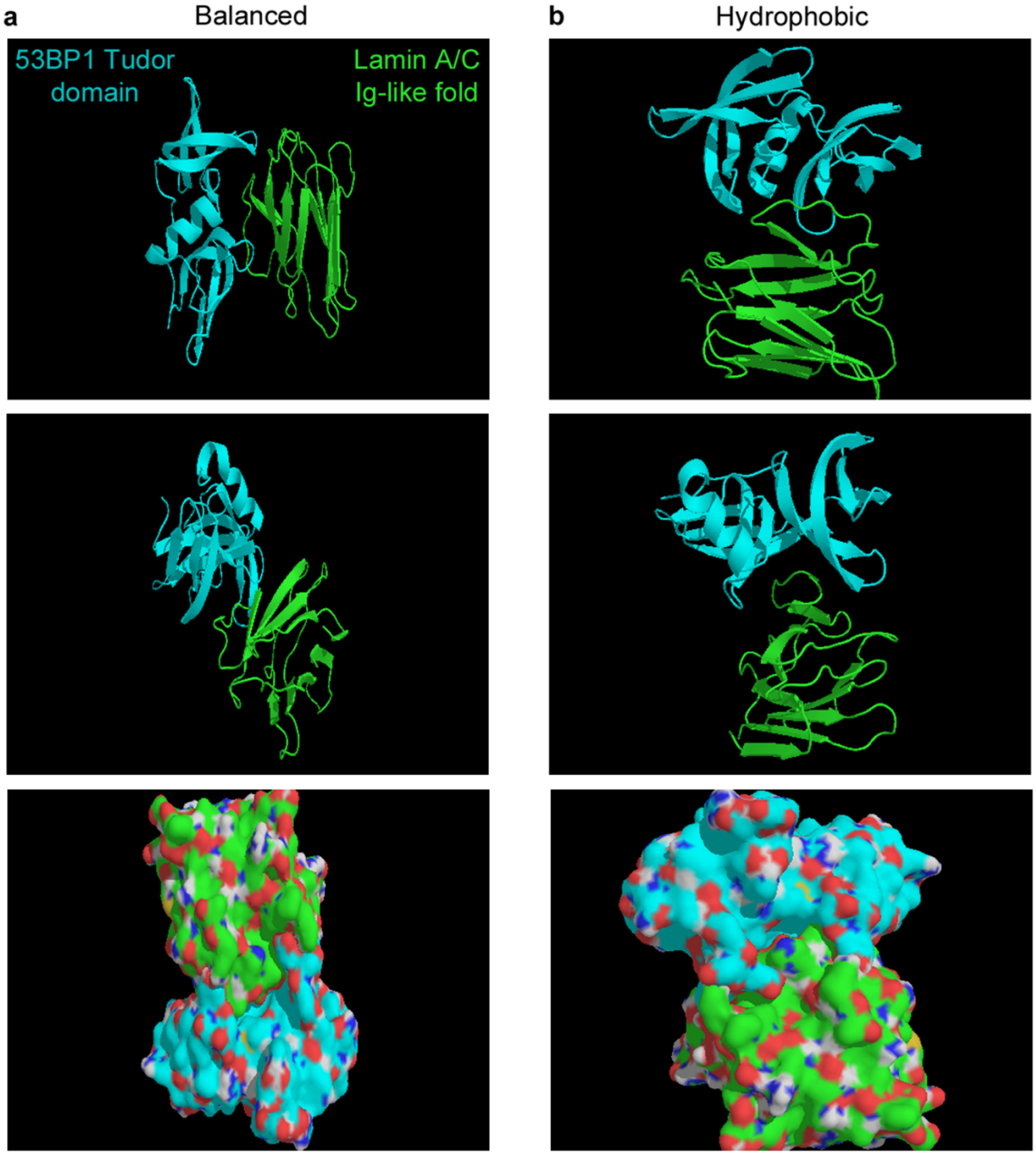
a
Balanced
53BP1 Tudor domain
Lamin A/C Ig-like fold
b
Hydrophobic

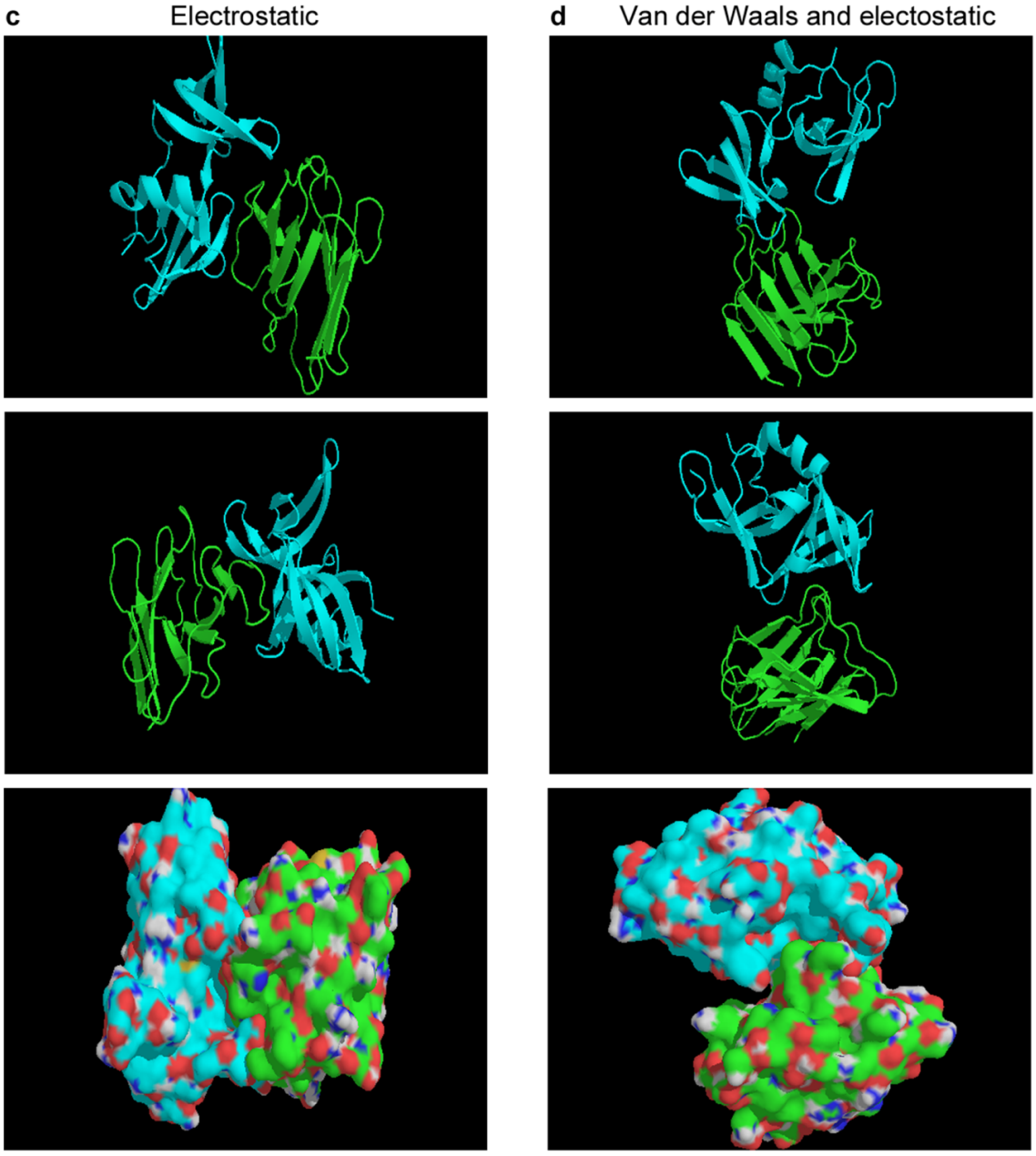
c
Electrostatic
d
Van der Waals and electostatic

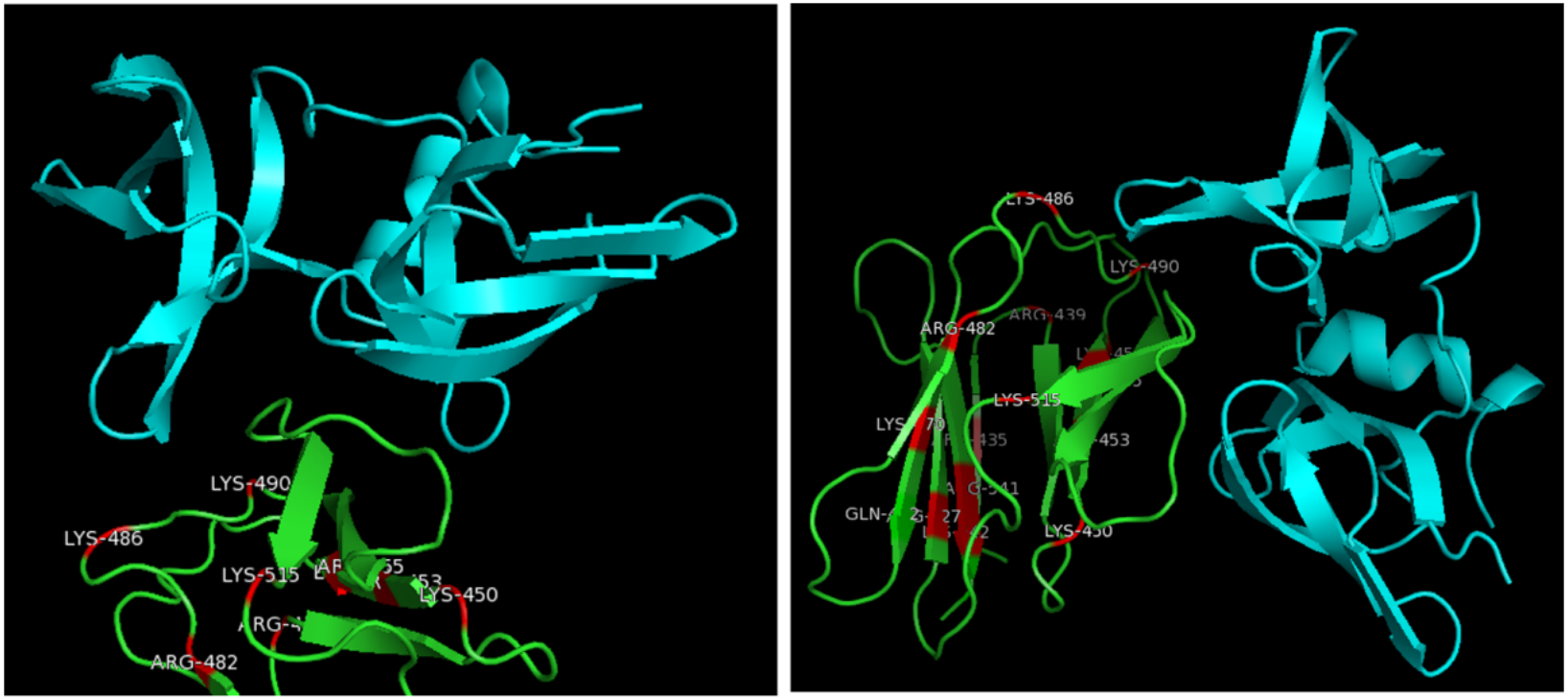

Figure 6.4. Lysine and arginine residues in the lamin A/C Ig-like fold. The lamin Ig-fold is shown in green, the 53BP1 Tudor domain in blue and the lamin A/C Ig-fold lysine and arginine residues are shown in red.

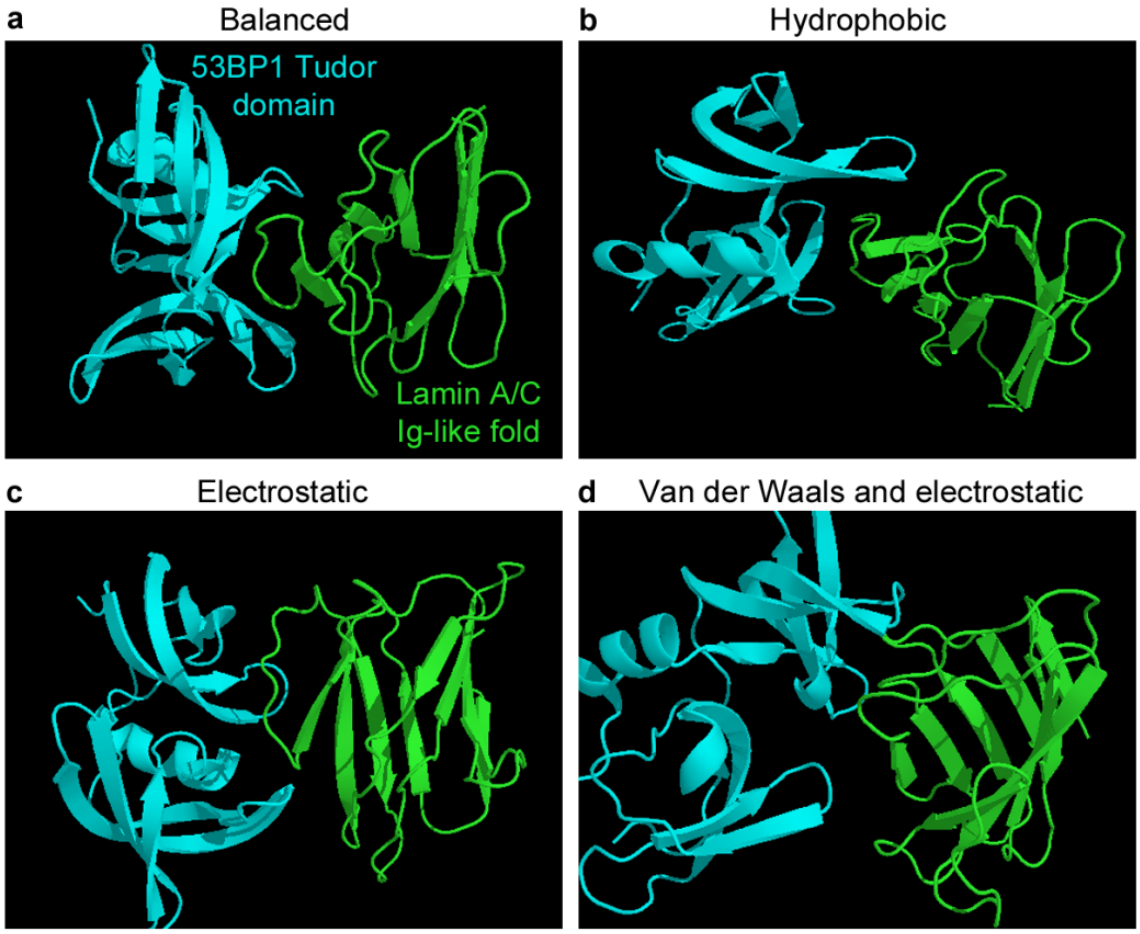

Figure 6.5. The lamin A/C Ig-like fold is predicted to interact with the Tudor domain of 53BP1. Using Cluspro 2.0 protein docking simulation, the lamin A/C Ig-like fold (PDB: 1IVT) and the 53BP1 Tudor domain (PDB: 2G3R) were modelled for potential interactions. The top output in each of the four modelled conditions is shown for (**a**) balanced (**b**) hydrophobic (**c**) electrostatic (**d**) Van der Waals and electrostatic.

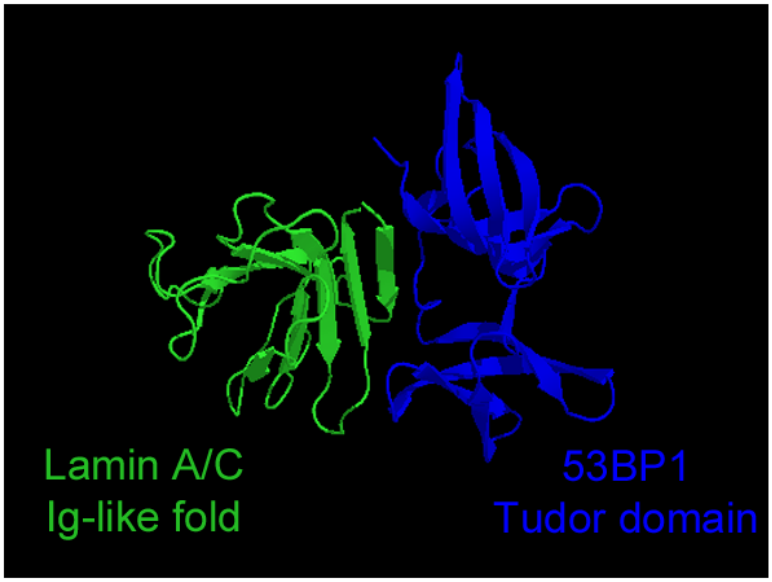

Figure 6.6. Top result using GRAMM-X modeling server. The potential interaction between the lamin A/C Ig-like fold (PDB: 1IFR; Dhe-Paganon et al., 2002) and the 53BP1 Tudor domain (PDB: 2G3R; Botuyan et al., 2006) was modeled using the GRAMM-X server.

6.3 Potential for A-type lamins to be DNA damage-dependent targets of phosphorylation

In response to genotoxic stress, a number of protein kinases are responsible for the phosphorylation of an extensive network of target substrates in a diverse range of cellular processes (Matsuoka et al., 2007; Stokes et al., 2007). Initial protein phosphorylation in the DDR is mainly carried out by the two kinases ATM (ataxia telangiectasia mutated) and ATR (ATM and Rad3-related). Both ATM and ATR prefer phosphorylating serine or theonine residues followed by glutamine (SQ/TQ motifs) (Kim et al., 1999; O'Neil et al., 2000; Zhao et al., 2001). In order to investigate if A-type lamins were phosphorylated in response to DNA damage, I pursued a bioinformatics approach. Using the NetPhos 2.0 server, potential phosphorylation sites were identified, above the threshold, that were distributed throughout the protein. There appeared to be one region after the α-helical rod

domain that showed a large number of potential phosphorylation sites (i.e. above threshold) from position 390-437 (Figure 6.7).

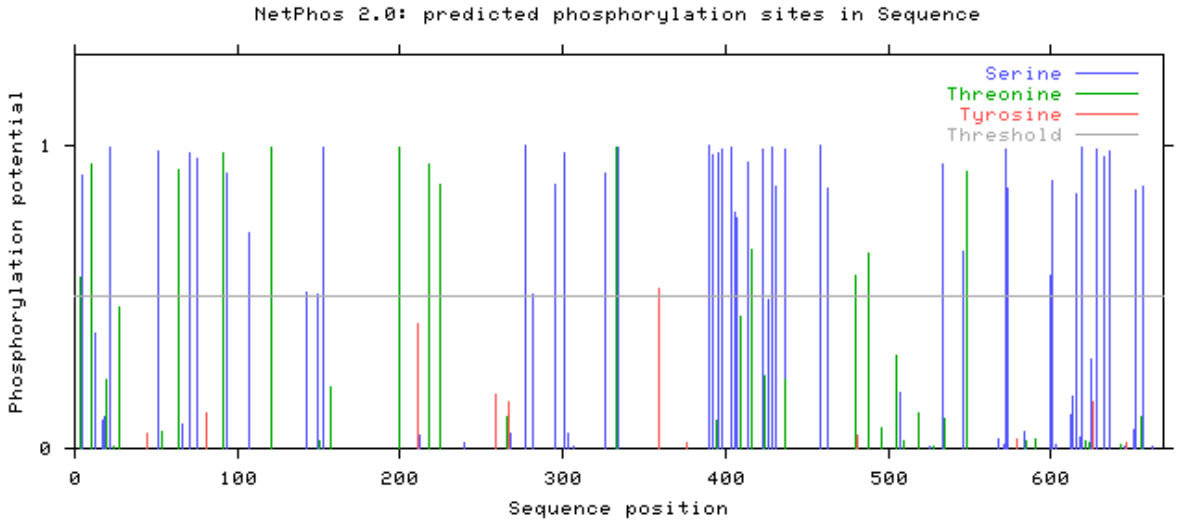

Figure 6.7. Predicted phosphorylation sites in lamin A/C. Potential phosphorylation sites in lamin A and C were generated using the NetPhos 2.0 server (Blom et al., 1999).

Multiple sequence alignments of lamins A, C, B1 and B2 revealed that lamin A/C contains four SQ/TQ motifs after the α-helical rod domain, which is present in both lamin A and C (Figure 6.8a,b). However, none of these SQ/TQ motifs are present in lamins B1 or B2 (Figure 6.8b). Importantly, these four SQ/TQ motifs are conserved throughout the mammalian phylogeny (Figure 6.8c).

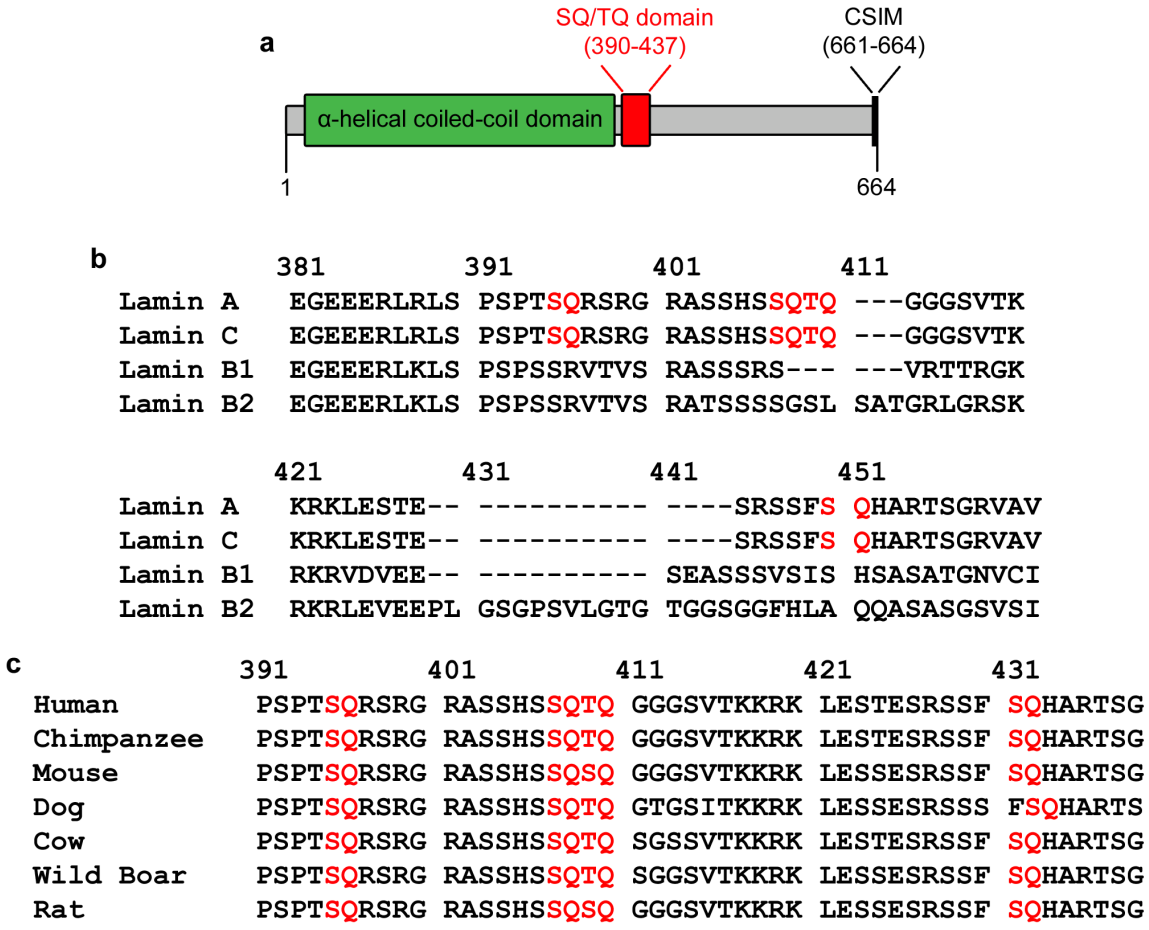

Figure 6.8. SQ/TQ residues are conserved in the mammalian phylogeny. (**a**) Lamin A domain structure. (**b**) Sequence alignment of A-type lamins with lamin B1 and lamin B2. SQ/TQ motifs are shown in red. (**c**) Sequence alignment of lamin A across multiple species.

Using two prediction algorithms to assess potential phosphorylation sites in response to DNA damage (http://elm.eu.org and http://scansite.mit.edu), three amino acids were identified as probable targets that were also found in the 390-437 region: S395, S407, T409 (Figure 6.9a, highlighted red). Further bioinformatic dissection of this region using the Phosphosite protein phosphorylation database revealed that a large number of amino acid residues in this region were phosphorylated in both a DNA damage dependent (Figure 6.9a, in blue) and independent (Figure 6.9a, in pink) manner (www.phosphosite.org). Even though only three sites in this region were predicted to be phosphorylated in response to DNA damage, the database search revealed that up to 10 serine/threonine residues may be phosphorylated *in vivo*, suggesting a degree of promiscuity at the amino acid sequence level for phosphorylation by DNA damage related protein kinases (Supplementary Figure 9).

In order to probe whether A-type lamins were phosphorylated in response to IR *in vivo*, HDFs were treated with IR (10 Gy) before immunoprecipitation of endogenous lamin A/C. Immunoblotting with an anti-phospho-SQ/TQ motif antibody revealed a increase in a band that corresponded to lamin A that was not present in the unspecific IgG (Figure 6.9b). Due to the nature of the antibody, a large unspecific band prevented assessment of lamin C phosphorylation. To further assess lamin A phosphorylation, U2OS/GFP-lamin A cells were treated with IR and extracts subjected to immunoprecipitation with GFP-Trap beads. At the predicted molecular weight there appeared no increase in the level of phosphorylated lamin A (Figure 6.9c). However, the validity of this finding is undermined as there was clearly a band in the control lane prepared from U2OS/GFP cells that the anti-phospho-SQ/TQ antibody recognised. One explanation for this may be that the anti-phospho-SQ/TQ antibody used in this study does not recognise the lamin A/C residues predicted and previously shown to be phosphorylated in response to DNA damage. Further to this, a comparison of the amino acids surrounding the three SQ/TQ residues in lamin A/C with ATM/ATR substrates known to be recognised by the phospho-SQ/TQ antibody shows that the antibody is unlikely to recognise the lamin A/C phospho-SQ/TQ

residues (Figure 6.10a,b). Moreover, a previous sequence analysis of all peptides pulled down by the phospho-SQ/TQ antibody revealed that leucine is the preferred amino acid in the -1 position, which is not present before any of the three potential lamin A/C SQ/TQ phosphorylation sites (Figure 6.10c) (Matsuoka et al., 2007). Therefore, further approaches will be needed in the future to resolve these issues and determine if A-type lamins are phosphorylated *in vivo* and what biological significance, if any, this has for DNA repair, checkpoint control and cell cycle progression.

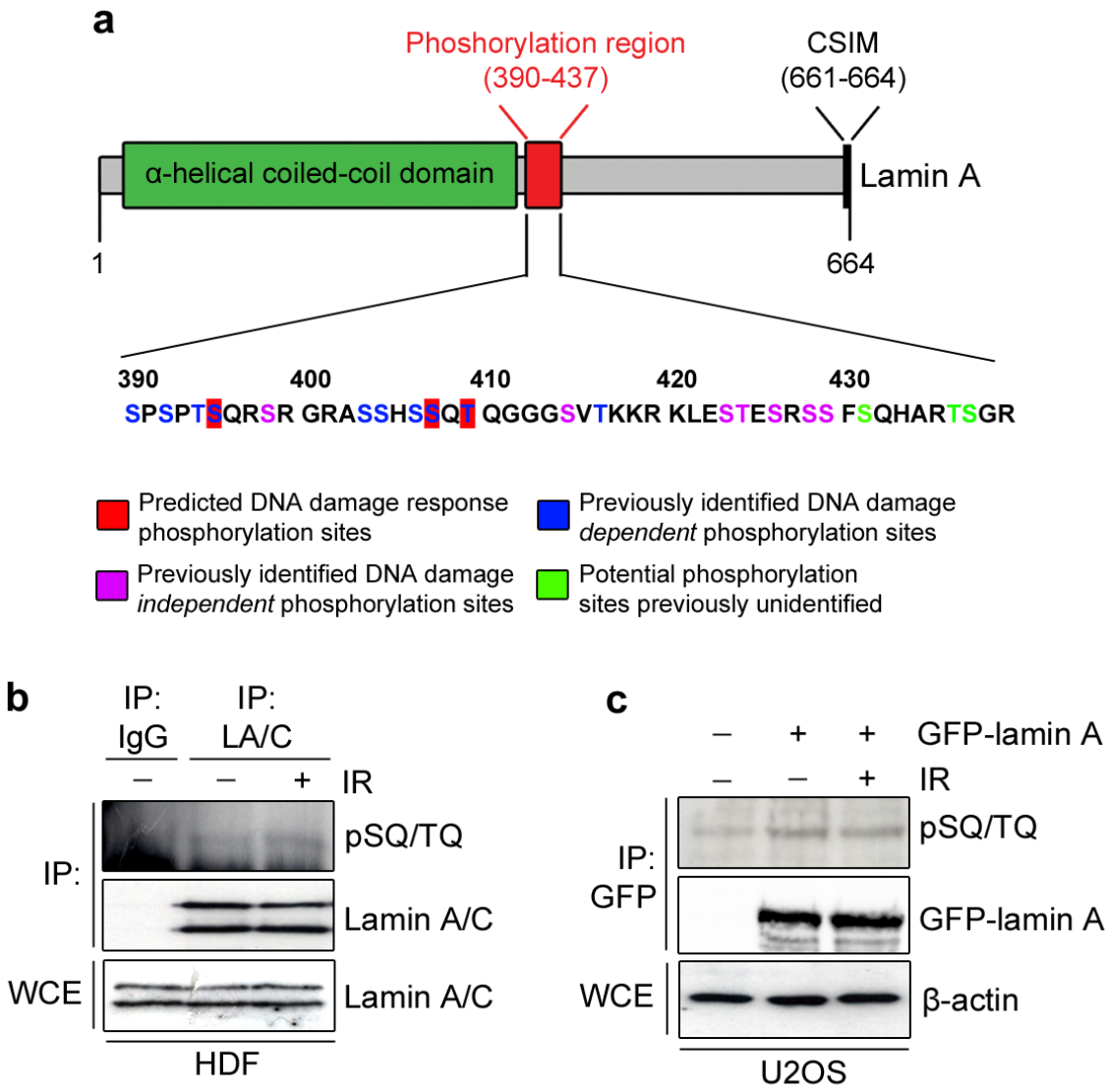

Figure 6.9. Assessing A-type lamin phosphorylation in response to DNA damage. (**a**) Information from www.phosphosite.org was processed and amino acids phosphorylated in a DNA damage-dependent and independent manner are shown in blue and pink, respectively. Potential phospho-SQ/TQ sites and uncharacterised sites are shown in red and green, respectively. (**b**) HDFs were treated with IR (10 Gy) and extracts prepared after 1 hour. After immunoprecipitation, lamin A/C was assessed for phosphorylation by immunoblotting using an anti-phospho-SQ/TQ antibody. (**c**) U2OS/GFP-lamin A were treated with IR (10 Gy) and extracts subjected to immunoprecipitation with

GFP-Trap beads. GFP-lamin A phosphorylation was assessed by immunoblotting using an anti-phospho-SQ/TQ antibody.

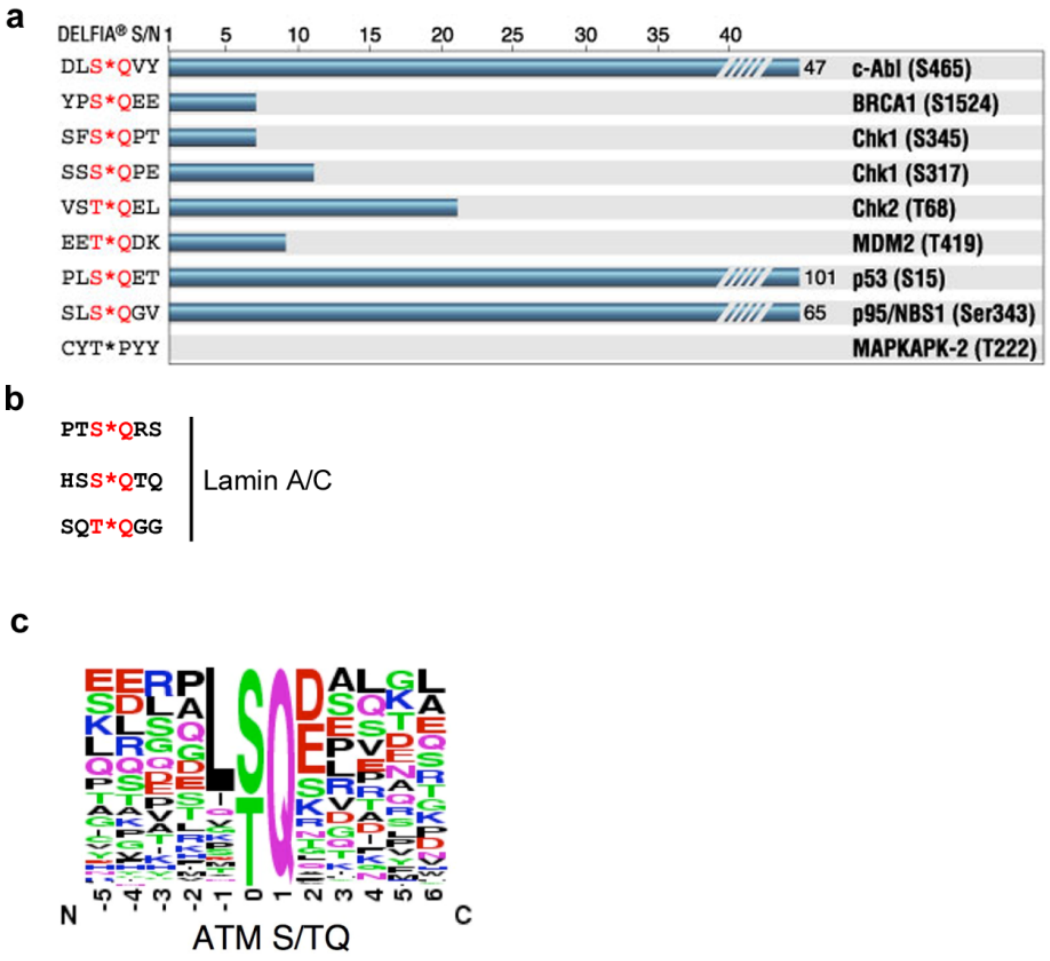

Figure 6.10. Comparison of potential ATM/ATR phosphorylation sites in lamin A/C with other known ATM/ATR targets. (**a**) The phospho-SQ/TQ antibody used in this study from Cell Signalling recognises phosphorylated serine or threonine residues preceded by leucine (L), or similar amino acid, in the -1 position and glutamine (Q) in the +1 position. Corresponding ELISA data (signal:noise ratio) is shown (www.cellsignal.com). (**b**) Three potential phospho-SQ/TQ residues in lamin A/C and neighboring amino acids. (**c**) Distribution of amino acids most commonly found surrounding phospho-SQ/TQ residues (taken from Matsuoka et al., 2007).

6.4 Discussion

6.4.1 Modelling the 53BP1-lamin A/C interaction

As I had determined that both lamin A and C may bind 53BP1, suggesting a binding region common to both, and that C-terminal fragments containing the Tudor domain of 53BP1 were present in GFP-lamin A immunoprecipitates, I postulated whether the Ig-like fold of lamin A/C, which is involved in the interaction with various other proteins, would be able to interact with the Tudor domain of 53BP1. The three-dimensional structures of the lamin A/C Ig-like fold and the Tudor domain of 53BP1 have been characterised by X-ray crystallography (Dhe-Paganon et al., 2002; Krimm et al., 2002; Huyen et al., 2004; Botuyan et al., 2006). Using the ClusPro modelling server, results showed the possibility that the lamin A/C Ig-like fold could interact with the 53BP1 Tudor domain via the hydrophobic pocket of the Tudor domain, a region shown to interact with methylated H4K20. However, using the GRAMM-X server, it showed a contradictory result, underlining the need for direct experimental evidence to probe this hypothesis. Despite this, if the Tudor domain does indeed bind the lamin A/C Ig-like fold then is plausible that, upon DNA damage, methylation of H4K20, which has been shown to increase locally at sites of DSBs, competes for the Tudor domain binding site (Pei et al., 2011). The Tudor domain pocket preferentially binds to arginine and lysine residues (Huyen et al., 2004; Botuyan et al., 2006). However, lamin A/C does not contain any arginine or lysine residues in the vicinity of the proposed interaction based on the protein docking simulation. Therefore, I would suggest that even the lowest of levels of DNA damage would lead to dissociation between the two, allowing 53BP1 to be a sensitive participant of the DDR. A range of Tudor domain mutants that change the surface properties without changing the folding properties do not relocalise to IRIF (Huyen et al., 2004) and whilst these mutants cannot interact with methylated histones, it would be of interest to determine whether they can interact with lamin A/C to help provide evidence for the above DNA damage dependent interaction hypothesis.

The decreased association observed between lamin A/C and 53BP1 in response to DNA damage is not without precedent within the current literature. The mediator protein MDC1 is a 53BP1-associated protein, and this interaction decreases upon DNA damage (Eliezer et al., 2009). Upon DNA damage, it was shown that γ-H2AX competes with the MDC1-interaction site of 53BP1 (Eliezer et al., 2009). As 53BP1 may be recruited by direct γ-H2AX binding and to methylated H4K20 at DSBs, it will be interesting to determine if a γ-H2AX peptide competition assay would disrupt the lamin A/C-53BP1 interaction. Furthermore, it will be of note to ascertain if MDC1 is present in lamin A/C-53BP1 complexes. Both lines of enquiry would help further the understanding of A-type lamins in the DDR and the mechanism by which DNA damage influences the interaction between lamin A/C and 53BP1.

6.4.2 A-type lamins as targets of DNA damage-dependent post-translational modifications

Protein phosphorylation is one of the earliest post-translational modifications that initiates the DDR, primarily through the action of the apical DDR kinases, ATM and ATR (Matsuoka et al., 2007). A database search revealed that A-type lamins may be phosphorylated at multiple residues in response to DNA damage (Supplementary Figure 9). However, there appeared one particular hotspot spanning residues 390-437 that contained 10 DNA damage-dependent phosphorylation residues, 3 of which were SQ/TQ sites. These three SQ/TQ sites were conserved in the mammalian phylogeny. Therefore, to address A-type lamins were phosphorylated *in vivo* in response to DNA damage, endogenous lamin A/C was immunoprecipitated from HDFs and the bound lamin A/C assessed for phosphorylation using an anti-phospho-SQ/TQ motif antibody. A band corresponding to lamin A appeared to show slightly increased reactivity using this antibody in response to DNA damage. However, when I further probed this finding using U2OS/GFP-lamin A cells, there was no difference between untreated and IR-treated GFP-lamin A immunoprecipitates. Furthermore, there was even a signal in the U2OS/GFP control lysates. Analysis of the potential phosphorylation

sites in residues 390-437 revealed that none of the SQ/TQ sites were preceded by a leucine residue, which is present in the antigen used to raise the anti-phospho-SQ/TQ motif antibody. Therefore, whilst proteomic data has identified phosphorylated lamin A/C peptides, it remains to be verified directly. Future proteomic analysis of lamin A/C or GFP-lamin A immunoprecipitates should help uncover whether A-type lamins are indeed phosphorylated in response to DNA damage. I foresee that mutational analysis of serine or threonine residues will prove difficult as so many have been identified as being phosphorylated in response to DNA damage. Therefore, determining the functional significance of A-type lamin phosphorylation will be important. Does it have a signalling role? Does it affect interactions with proteins involved in DNA repair and/or cell cycle progression? Answering such questions should provide a more in-depth understanding of A-type lamin function in the DDR.

Two other post-translational modifications shown to influence the DDR are acetylation and SUMOylation (Polo and Jackson, 2011). Lamin A/C has a consensus SUMOylation site surrounding lysine 201, and is preferentially modified by SUMO-2 conjugates (Zhang and Sarge, 2008). Recent evidence has shown a role for SUMOylation in the regulation of DDR proteins (Galanty et al., 2009; Morris et al., 2009). Ubc9 is the only E2 ligase of the SUMO-conjugation system. It has been shown by yeast two hybrid and subsequent immunoprecipitation experiments that lamin A/C is a Ubc9 binding protein (Zhong et al., 2005). In response to DNA damage Ubc9 forms at sites of double strand breaks and acts in concert with the E3 ligase PIAS4 to SUMOylate 53BP1 and with the E3 ligase PIAS1 to SUMOylate BRCA1. It would therefore be of note to investigate whether lamin A/C is itself SUMOylated in response to DNA damage and whether it has a role in the SUMOylation events of the DDR.

Acetylation of histones and protein in the DDR has been shown to help contribute to effective sensing and repair of DNA damage (Polo and Jackson, 2011). A variety of acetyltransferases and deacetylases are recruited to DNA damage, for example SIRT6 deacetylates CtIP at DNA lesions to promote end resection (Kaidi

et al., 2010). Analysis of the lamin A protein sequence using an acetylation algorithm reveals that lamin A/C has four potential acetylation sites (Supplementary 10) (Basu et al., 2009). Furthermore, one of these sites has been validated, suggesting that acetylation may somehow regulate lamin A/C function (Basu et al., 2009).

In Chapter 5 I provided evidence that A-type lamins are important components of the DDR. In this chapter, I attempted to delineate one mechanism by which A-type lamins may be implicated in the DDR, via phosphorylation, and modelled the 53BP1-lamin A/C interaction as a means to understand their functional inter-relationship. Whilst the latter proved fruitful, it appears that further work and approaches are necessary to understand the post-translational modifications that govern lamin A/C function in response to DNA damage. Thus, it seems that, despite the data presented here and in Chapter 5, our understanding of the role of A-type lamins in the DDR is still in its infancy and future work should seek to build on the insights provided here.

CHAPTER 7. GENERAL DISCUSSION

7.1 A-type lamins and thesis aims

A-type lamins are multifunctional nuclear proteins, involved in a wide range of cellular functions (Andres and Gonzalez, 2009). Mutations in *LMNA* give rise to a broad spectrum of tissue-specific diseases, termed laminopathies. Laminopathies include muscular dystrophy, cardiomyopathy, lipodystrophy, neuropathy and various premature aging syndromes (Broers et al., 2006). Hutchinson-Gilford Progeria Syndrome (HGPS) is one such premature aging syndrome and cells from these patients exhibit a wide range of dysfunctions, including nuclear disorganisation, increased DNA damage, impaired cell cycle progression and premature entry into senescence. Therefore, investigating the roles of lamin A and C in normal cellular processes is vital to understanding the etiology and molecular mechanism of laminopathies. To this end, I interrogated the following hypotheses:

1. Does wild type lamin A/C have a role in normal cellular aging?
2. How do lamin A/C and its nucleoplasmic binding partner LAP2α affect cell cycle progression?
3. What is the role of mature wild type lamin A/C in the DNA damage response?

These three aspects of mature wild type lamin A/C function have not previously been investigated fully. Here, I have provided evidence indicating novel roles for lamin A/C in the normal aging process, as part of an adaptive response to oxidative stress, control of cell cycle progression and the DNA damage response.

7.2 Lamin A function is impaired during normal aging and is a key component of the cellular response to oxidative stress

The increasing life expectancy of individuals in industrialised countries is expected to lead to 1.2 billion people being aged 60 and over by 2025 (Sahin and DePinho, 2010). Providing medical care for this aging population is therefore an important issue for healthcare systems across the world. However, due to the gradual and heterogeneous onset of aging, together with the complex and diverse cellular and tissue phenotypes, research of aging has been difficult. In this light, I sought to understand the role, if any, of wild type mature lamin A/C in the normal aging of human dermal fibroblasts (HDFs). Previous research has indicated that mutations in *LMNA* give rise to premature aging diseases, underlining a possible link between *LMNA* and the normal aging process. To interrogate this hypothesis, in Chapter 3 I have shown that lamin A/C protein levels do not change when HDFs age *in vitro*. Rather, lamin A, but not lamin C, is a target for irreversible oxidative modifications during cellular aging *in vitro*. This oxidation of the cysteine residues in the lamin A C-terminal impairs the ability of lamin A to form intra-molecular and inter-molecular disulfide bonds, resulting in the presence of a monomeric form of lamin A in senescent cells, which is correlated with an increased percentage of dysmorphic nuclei in senescent cells. Furthermore, this impaired disulfide bond formation is correlated with increased endogenous DNA damage, loss of nucleoplasmic lamin A/C, proteolysis of the lamin A C-terminal and loss of nucleoplasmic LAP2α into nuclear aggregates (Pekovic et al., 2007). Moreover, I also observed less lamin A disulfide bond formation in cells from old individuals, which may indicate that impaired lamin A disulfide bond formation may contribute to the aging phenotype *in vivo*. This last observation obviously requires further rigorous examination and mouse models could be generated harbouring various cysteine-to-alanine mutations to test this hypothesis.

That lamin A intra- and inter-disulfide bond formation was readily observed in young cells, but not old cells, suggested that disulfide bond formation may act as a protective mechanism against oxidative stress. In response to low levels of

oxidative stress lamin A undergoes increased disulfide bond formation, which is correlated with a reversible cell cycle arrest. On the other hand, lamin A disulfide bond formation is by-passed at high levels of irreversible oxidative stress. This suggested that lamin A disulfide bond formation is part of a protective response to oxidative stress. Further to this, the expression of a triple lamin A mutant (C522/588/591A) inhibited both intra- and inter-disulfide bond formation in HDFs, which abrogated lamin A function and caused premature entry into senescence. This cellular phenotype was mirrored by loss of *LMNA*, suggesting that the cysteine residues are important for lamin A function in the oxidative stress response and ultimately preventing cellular senescence. Moreover, cells null for *LMNA* (Y259X cells) and cells expressing the C522/588/591A lamin A mutant exhibit high levels of intracellular ROS. HDFs expressing the C522/588/591A lamin A mutant exhibit a range of senescence-associated cellular phenotypes that are reversible by anti-oxidant treatment or growth of cells at low oxygen concentrations. This indicates that ROS are the primary cause of the premature entry into senescence of HDFs expressing the C522/588/591A mutant. How then does this link the role of wild type mature lamin A to the normal aging process? Several lines of evidence have shown that intracellular ROS levels increase with age in a variety of tissues and cellular models (Kregel and Zhang, 2007; Sahin and DePinho, 2010). Increased ROS levels are thought to be due to electrons leaking from the electron transport chain (ETC) in the mitochondria, which can lead to the formation of ROS (Kregel and Zhang, 2007). Oxidative damage to lipids, proteins and DNA all contribute to their age-related functional decline. Based on this, it is plausible to suggest that oxidative damage to wild type mature lamin A in senescent cells is a result of the increased oxidative cellular environment in which they function as cells age *in vitro*. This oxidative damage impairs the ability of the cells to adequately respond to oxidative stress as cells age, as shown here, which ultimately leads to the irreversible withdrawal from the cell cycle, resulting in cellular senescence. This simplistic explanation does not take into account various other mechanisms that contribute to cellular aging such as telomere erosion and DNA damage. Furthermore, it is likely that oxidative

damage to lamin A acts in concert with a broad spectrum of damage to other macromolecules. Therefore, age-related oxidative damage to lamin A may act synergistically with these other mechanisms to contribute to the aging phenotype. Interestingly, cells from normal young and old individuals activate the same cryptic splice site as that used in the premature aging disease Hutchinson-Gilford Progeria Syndrome (HGPS), albeit at much lower levels (Scaffidi and Misteli, 2006). The combination of low levels of progerin and oxidatively damaged lamin A may act together to impair the function of lamin A/C at the nuclear envelope and within the nucleoplasm. Future work should seek to determine whether there is an A-type lamin-dependent decrease in the various signalling pathways controlled by lamin A (e.g. c-Fos), and whether this contributes to the aging phenotype.

7.3 Lamin A/C and LAP2α are important for cell cycle progression

De-regulated and chronic cell cycle progression is a hallmark of most cancers (Hanahan and Weinberg, 2011). During G_1-phase, the decision is made to replicate DNA and complete the cell cycle. LAP2α and lamin A/C have been implicated in the control of the G_1/S-phase transition via interaction with the tumour suppressor, pRb, which is a key factor required for G_1/S-phase transition (Mancini et al., 1994; Mittnacht, 1998; Markiewicz et al., 2002). LAP2α-lamin A/C complexes have been shown to anchor the active hypophosphorylated pRb within G_1-phase cells, which is associated with its tumour suppressor functions (Mancini et al., 1994; Markiewicz et al., 2002). To further explore these findings, in Chapter 4 I have shown that loss of either LAP2α or lamin A/C in HDFs caused delayed G_1/S-phase transition upon G_0-G_1-S-phase progression. This was characterised by altered cell cycle profiles, significantly reduced cellular proliferation rates and a reduced Ki67+ index, a marker of cell cycle arrest. Attempts to delineate the nature of this cell cycle arrest could not find a significant up-regulation of the DDR in response to loss of either LAP2α or lamin A/C in HDFs. However, only markers of double-stranded breaks were used, and future work should address if proteins involved in replication stress are activated in cells depleted of LAP2α or lamin

A/C. In further attempts to understand the nature of the observed cell cycle arrest, I demonstrated that intracellular ROS levels were nearly double in HDFs depleted of LAP2α or lamin A/C, which underlines the role of lamin A in regulating ROS levels, as outlined in Chapter 3. To investigate if increased ROS levels were the causative factor for the cell cycle arrest, cells depleted of LAP2α or lamin A/C were treated with the anti-oxidant NAC for three consecutive days. However, there was no increase in Ki67+ cells, suggesting that cell cycle arrest was independent of ROS levels. Thus, the exact mechanisms underlying the cell cycle arrest remain elusive at this stage. However, investigation of other cell cycle regulators proteins such as p21 and p53 may yield important answers.

7.4 Lamin A/C is a novel regulator of the DNA damage response

DNA damage, either from exogenous or endogenous factors, has been suggested to be a primary driver of aging (Garinis et al., 2008; Hoeijmakers, 2009). Cells have evolved a diverse and complex genomic maintenance system, called the DNA damage response, to sense damage to DNA, trigger signaling cascades and ultimately repair the DNA damage (Jackson and Bartek, 2009). In HGPS, cells exhibit increased endogenous DNA damage and constitutively activated checkpoint signalling, which is correlated with reduced proliferation (Liu et al., 2005; Varela et al., 2005; Liu et al., 2006; Scaffidi and Misteli, 2006). Previous data has also shown that *Lmna*$^{-/-}$ MEFs exhibit decreased protein levels of 53BP1, a mediator protein of the DDR and important component of the NHEJ repair pathway (Gonzalez-Suarez et al., 2009). This implies that wild type lamin A/C may therefore function within the DDR in normal cells. In Chapter 5, I investigated this hypothesis and showed that cells functionally null for *LMNA* (Y259X cells) exhibit increased levels of endogenous DNA damage, suggesting that A-type lamins promote genomic stability. Furthermore, I showed that lamin A/C promotes the nuclear localisation of 53BP1 in undamaged cells and prevents its accumulation in the cytoplasm where it is degraded by the proteasome. Interaction studies revealed that lamin A/C associates with a region surrounding the 53BP1 Tudor domain, a well-known protein-protein interacting module (Fitzgerald et al., 2009).

This interaction decreased in response to DNA damage, in a phosphorylation-dependent manner. Cells depleted of endogenous lamin A/C by siRNA or Y259X cells exhibited a DNA repair defect at late timepoints post-IR, which ultimately led to reduced cellular fitness in response to DNA damage. This last finding is intriguing as loss of 53BP1 in cells confers a DNA repair defect that is epistatic with ATM inhibition in wild type cells (Noon et al., 2010). Moreover, this repair defect in 53BP1 depleted cells is caused by an inability to localise the protein pKAP-1 at sites of DNA damage and heterochromatin is not repaired efficiently (Noon et al., 2010). Based on these findings, it will be of interest to compare Y259X cells, which lack 53BP1, with the cellular phenotype of 53BP1-depleted cells to compare the DNA repair phenotypes. It is possible that the repair defect in Y259X cells actually represents a defect in the repair of heterochromatin. Moreover, it will be important to understand which repair pathways, i.e. homologous recombination (HR) repair or non-homologous end joining (NHEJ) repair, is engaged in cells null for lamin A/C. As NHEJ is associated with the repair of heterochromatin, I would predict that absence of A-type lamins would result in a decrease in NHEJ pathways, although this does not necessarily facilitate a concomitant increase in the HR repair pathway. Future work using widely employed HR and NHEJ fluorescence-based assays in combination with flow cytometry would provide evidence for these predictions.

Based on the finding that A-type lamins are required for genomic stability in normal human fibroblasts, what is the relationship between A-type lamin status and cancer progression? This is not a simple question to answer as various reports have shown that lamin A/C can be down-regulated or up-regulated depending on the cancer subtype. For example, lamin A was shown to be a biomarker of colorectal cancer with patients nearly twice as likely to die if their tumours were lamin A/C positive (Willis et al., 2008). Moreover, lamin A has been identified as a biomarker of prostate cancer (Skvortsov et al., 2011). In contrast, lamin A/C is absent from ovarian cancer cells and tissues, which was correlated with dysmorphic nuclei in these cells (Capo-Chichi et al., 2011). Furthermore, siRNA depletion of lamin A/C in non-cancerous primary ovarian cells promoted

dysmorphic nuclei and aneuploidy, suggesting that loss of A-type lamins is correlated with promotion of ovarian cancer (Capo-Chichi et al., 2011). Therefore, together these contradictory reports suggest that the genetic background of the cancer subtype influences whether lamin A/C status has functional roles in cancer progression. Importantly, lamin A/C positive tumours could be targeted by depleting lamin A/C in combination with radiotherapy, as I have shown in Chapter 5 that cells depleted of lamin A/C exhibit increased sensitivity to DNA damage.

7.5 Linking aging, lamins and the DNA damage response

DNA damage repair pathways are organismal longevity mechanisms that preserve genomic integrity. Failure to repair DNA damage may lead to cell death or cellular senescence, which contributes to tissue and organ decline with age. Alternatively, failure to repair DNA damage can lead to mutations that can drive cancer (Garinis et al., 2008). As organisms age, DNA repair pathways exhibit age-related decline in efficiency, suggesting that DNA damage may be a causative factor of aging (Gorbunova et al., 2007). Indeed, it has been shown that DSBs accumulate with age in mouse tissues (Sedelnikova et al., 2004). In parallel to this, a variety of genetically engineered mouse models with knockouts of genes involved in the DDR give rise to premature aging phenotypes, which suggests that DNA damage is a *bona fide* cause of aging (Garinis et al., 2008). Therefore, linking the findings of Chapter 3, which suggests that lamin A has a role in normal aging process, to the findings in Chapter 5 and 6, it will be interesting to investigate the role of lamin A/C in DNA repair pathways during cellular aging. I would predict that oxidative damage to lamin A would impair its ability to participate in DNA repair in old cells. Does the lamin A/C-53BP1 interaction exhibit age-dependent alterations? Does lamin A form disulfide bonds in response to DNA damage as part of an adaptive protective response, analogous to the oxidative stress response? What levels of DNA damage would lead to disulfide bond formation or by-pass disulfide bond formation? There are thus many questions to answer from the inter-weaving threads from Chapters 3, 5 and 6,

which should provide novel insights into the role of A-type lamins in both the aging process and DNA damage response.

While Chapter 5 focussed on wild type lamin A, I will end by discussing the DDR in the context of mutant lamin A production, which causes the premature aging syndrome HGPS, as this is what stimulated my investigation of the role of wild type A-type lamins in the DDR (Liu et al., 2005). The cascade of signaling events that regulate the recruitment of DDR proteins to DNA lesions has progressed rapidly over the last few years (Bekker-Jensen and Mailand, 2010). Therefore, I may reassess the findings of Liu et al., 2005, in which they showed a distinct delay in the recruitment of 53BP1 in HGPS cells in response to IR. This suggests that the upstream signaling cascade at DSBs in HGPS is impaired somehow. Recently, a study showed that whilst the protein levels of two members of the DNA damage sensing MRN complex, NBS1 and Mre11, were unchanged, their recruitment to sites of IR-induced DNA damage was impaired in a minority of cells (Constantinescu et al., 2010). Is this subtle delay in the recruitment of the MRN complex enough to delay the recruitment of 53BP1 so dramatically in HGPS cells? I would suggest not as only 9% of γ-H2AX foci colocalised with 53BP1 10 minutes after IR (Liu et al., 2005). Therefore, it seems probable that downstream proteins, such as MDC1, RNF8, RNF168 or HERC2 may be destabilised or show reduced activity in the presence of mutant lamin A as these proteins are essential for 53BP1 recruitment (Bekker-Jensen and Mailand, 2010). As well as ubiquitin-adduct formation, the ability to form SUMO-adducts should also be investigated in HGPS to see if they contribute to the delay in 53BP1 recruitment (Galanty et al., 2009; Morris et al., 2009).

Recruitment of 53BP1 to sites of DNA damage appears to be regulated by two independent pathways. One is via the RNF8-RNF168 ubiquitin-dependent signaling axis, even though, paradoxically, 53BP1 has thus far not been shown to bind ubiquitin chains. The other is via the direct methylation of histone H4K20 by MMSET, which in turn is bound directly by the 53BP1 Tudor domain (Botuyan et al., 2006; Pei et al., 2011). This is important because HGPS cells exhibit

epigenetic alterations, including the loss of histone H4K20 methylation (Scaffidi and Misteli, 2006; Shumaker et al., 2006; Gonzalez-Suarez et al., 2009). I would therefore suggest that epigenetic defects in HGPS may also contribute to the delayed recruitment of 53BP1 in these cells.

Together, these defects in DNA damage repair in HGPS cells more than likely contributes to the premature aging phenotype in this disease as a result of tissue wasting and impaired stem cell renewal capabilities (Espada et al., 2008; Scaffidi and Misteli, 2008). Indeed, there is a substantial body of evidence to suggest that defects in DDR genes give rise to an array of premature aging diseases, as mentioned above (Garinis et al., 2008; Jackson and Bartek, 2009; Ciccia and Elledge, 2010). These premature aging diseases suggest that the DDR forms part of normal anti-aging mechanisms. At the cellular level, replicative senescence of cells is caused by telomere erosion which in turn leads to their uncapping and initiates a permanent cell cycle arrest orchestrated by the DDR machinery (D'Adda di Fagana et al., 2003). It has been well documented that HGPS cells undergo premature senescence when grown in culture (Bridger and Kill, 2004). Thus, it seems likely that the progerin-dependent DNA damage seen in HGPS cells contributes to this premature senescence by permanently activating the DDR machinery (Liu et al., 2006). Indeed, transcriptional analyses carried out on tissues from *Zmpste24*-null MEFs showed an up-regulation of classical p53 target genes, which is involved in a pathway that induces cell and tissue senescence and eventually leads to accelerated aging (Campisi, 2005; Varela et al., 2005). That mutations in lamin A give rise to premature aging disorders such as HGPS, which is characterised by increased DNA damage, again suggests that lamin A is a key determinant in aging.

7.6 Conclusion

In this thesis, I have provided evidence to extend previous data implicating A-type lamins in a diverse range of cellular processes. Here, I have underlined a role for lamin A/C and its nucleoplasmic binding partner LAP2α in cell cycle progression. I have provided novel evidence that lamin A is a key determinant in the normal aging process. Furthermore, I have also provided novel evidence to suggest that lamin A/C is required for effective DNA repair and preservation of genomic maintenance. Together, these findings underline the importance of A-type lamins in the maintenance of cellular integrity and ultimately organismal longevity and reflect their fundamental roles as ‘guardians of the soma’.

CHAPTER 8. SUPPLEMENTARY FIGURES

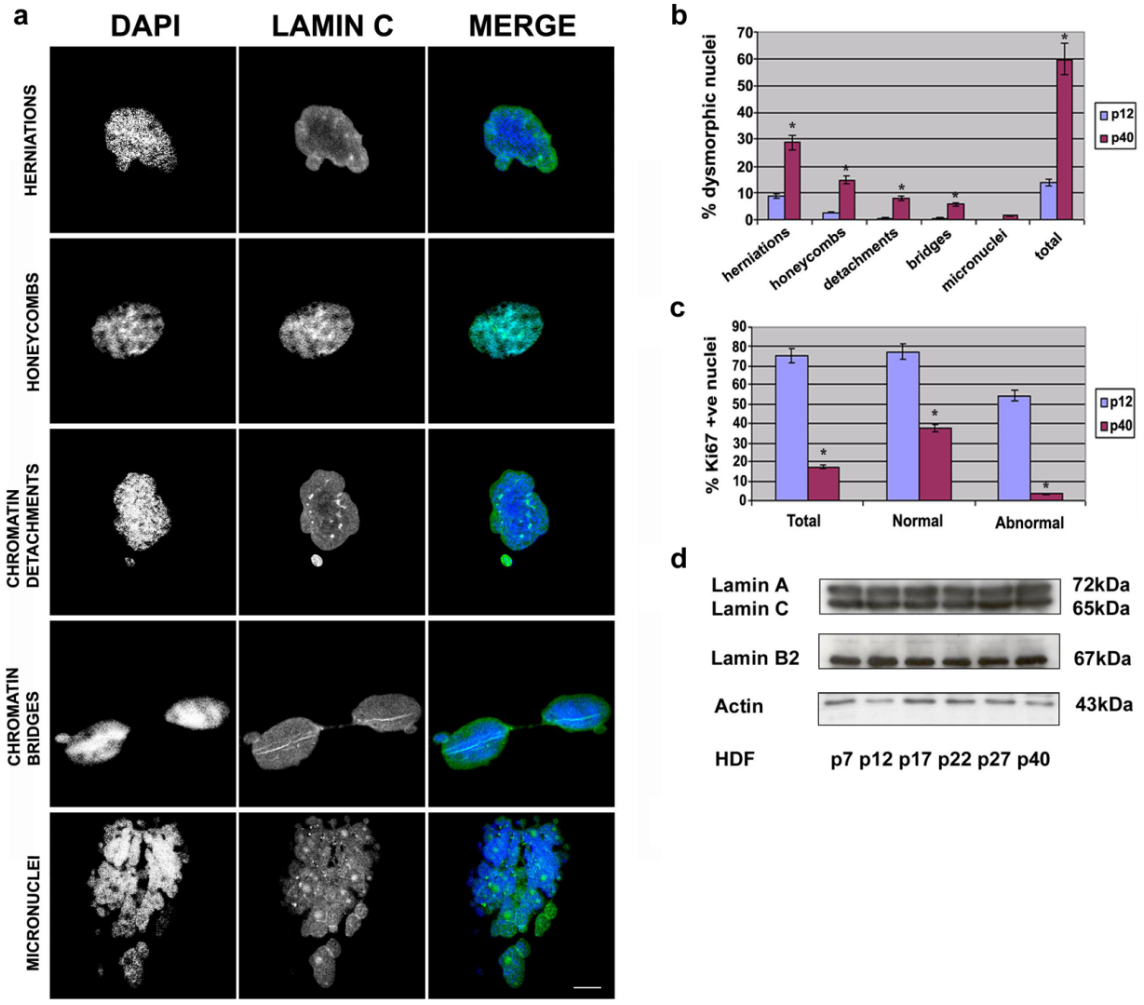

Figure 1. Age-dependent changes in nuclear architecture in HDFs. (**a**) p40 HDFs were immuno-stained with anti-lamin C (RαLC) antibody and DAPI. Micrographs are displayed as black and white or as two-colour merged images (lamin C-green; DAPI-blue). Scale bar 8μm. (**b**) The fractions of total and individual types of dysmorphic nuclei or (**c**) fractions of total Ki67+, normal Ki67+ and dysmorphic Ki67+ nuclei were determined by scoring 300 nuclei on duplicate slides in 4 independent experiments. Means ± S.D. are shown. * $p<0.05$. (**d**) Protein extracts from p7-p44 HDFs were subjected to reducing SDS-PAGE and immunoblotted with anti-lamin A/C (Jol2), anti-lamin B2 (LN43) or anti-β-actin (AC-40) antibodies (Kindly provided by Dr V Pekovic).

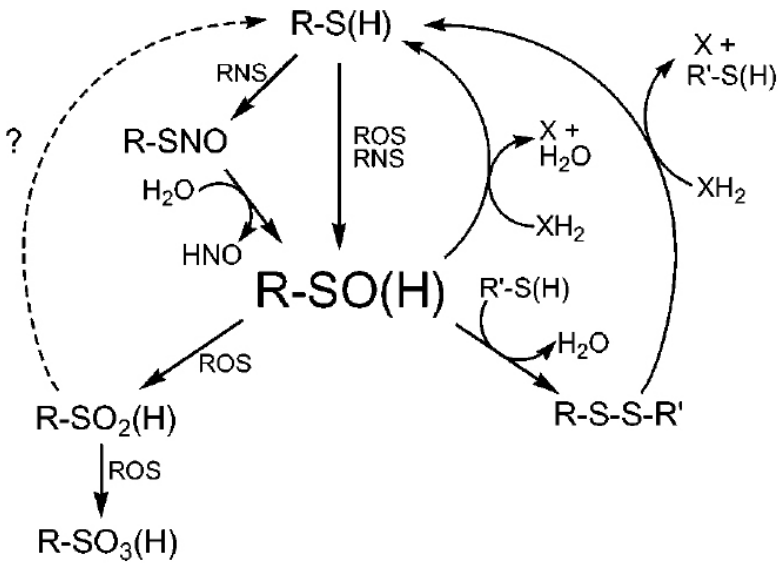

Figure 2. Cysteine sulfenic acid cycles. R-S(H), protein cysteine thiol. R-SO(H), sulfenic acid. R-SO_2(H), sulfinic acid. R-SO_3(H), sulfonic acid. R-S-S-R, protein disulfide. R-SNO, S-nitrosothiols. XH2, reducing agent. (Poole et al., 2004)

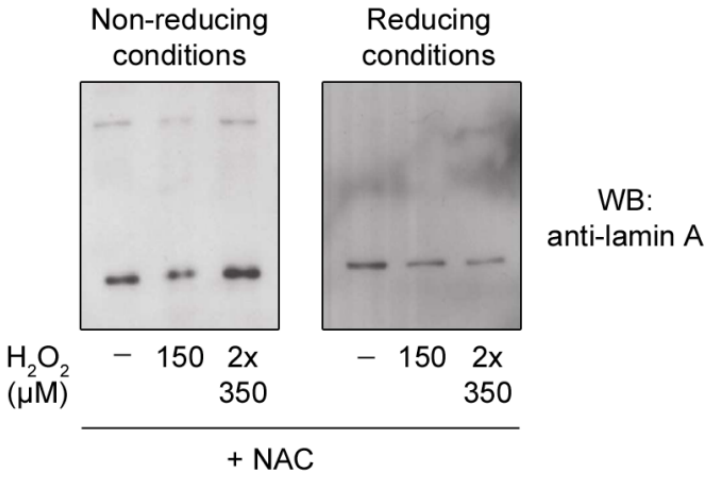

Figure 3. Effect of NAC on lamin A disulfide bond formation. HDFs were pre-treated with 10mM NAC before stimulation with 150 or 2x350μM H_2O_2. Cell extracts were prepared in the presence of NEM, resolved by non-reducing or reducing SDS-PAGE and probed with anti-lamin A (Jol4) antibody.

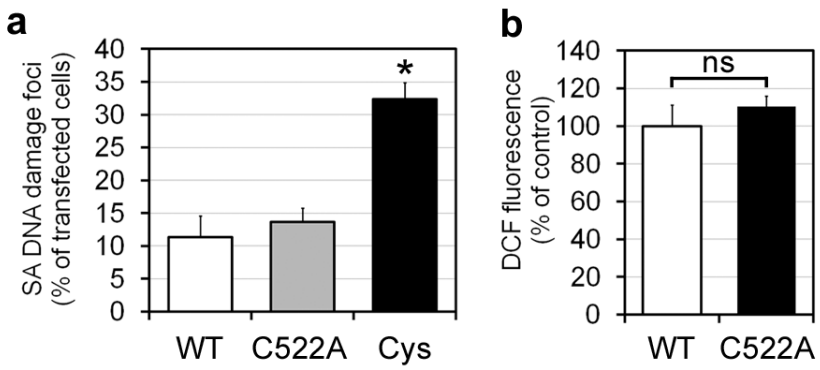

Figure 4. HDFs expressing Flag-C522A lamin A are phenotypically similar to HDFs expressing Flag-wt lamin A. (**a**) Flag-wt, C522A or C552/588/591A (Cys) lamin A were transfected into young (p12) HDFs and immuno-stained with anti-Flag M5 and anti-γ-H2AX antibodies. The fractions of Flag +ve nuclei showing γ-H2AX DNA damage foci were calculated by scoring 300 cells on triplicate coverslips in three independent experiments. (**b**) Transfected Flag-wt and Flag-C522A lamin A HDFs were assessed for basal intracellular ROS levels by measuring DCF fluorescence using flow cytometry. DCF fluorescence is expressed as % relative to Flag-wt HDFs which is set at 100%. Means ± S.D. are shown. *, $p<0.05$ relative to Flag-wt HDFs (a), ns-not significant.

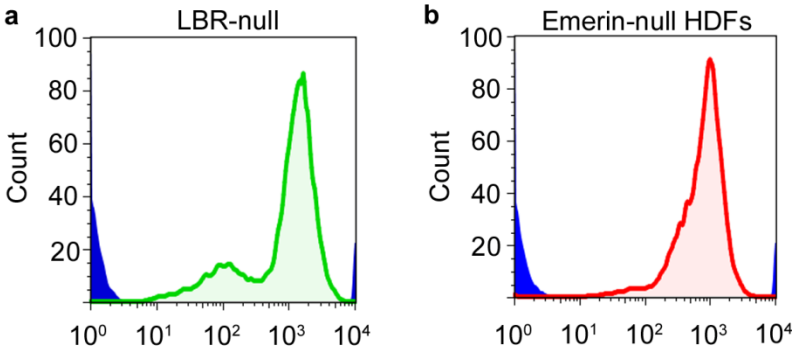

Figure 5. Endogenous ROS levels in LBR and emerin-null HDFs. Basal intracellular ROS levels were determined by measuring relative DCF fluorescence in lamin B receptor (LBR)-null (**a**) and emerin-null (**b**) HDFs. Representative cytograms are shown. Cell control without DCF dye is represented by filled blue peak.

```
     181        191        201        211        221        231
LAP2α DRYSDNEEGK KKEHKKVKST RDIVPFSELG TTPSGGGFFQ GISFPEISTR PPLGSTELQA
LAP2β DRYSDNEEDS KIELKLEK-- ---------- ---------- ---------- ----------
LAP2γ DRYSDNEEDS KIELKLEK-- ---------- ---------- ---------- ----------

     241        251        261        271        281        291
LAP2α AKKVHTSKGD LPREPLVATN LPGRGQLQKL ASERNLFISC KSSHDRCLEK SSSSSSQPEH
LAP2β ---------- --REP----- LKGRAKTPVT LKQR------ RVEHNQSY-- SQAGITETEW
LAP2γ ---------- --REP----- LKGRAKTPVT LKQR------ RVEHNQ---- ----------

     301        311        321        331        341        351
LAP2α SAMLVSTAAS PSLIKETTTG YYKDIVENIC GREKSGIQPL CPERSHISDQ SPLSSKRKAL
LAP2β TSGSSKGGPL QALTRESTRG SRRTPRKRVE TSEHFRIDGP VISESTPIAE TIMASSN---
LAP2γ ---------- ---------- ---------- ---------- ---------- ----------

     361        371        381        391        401        411
LAP2α EESESSQLIS PPLAQAIRDY VNSLLVQGGV GSLPGTSNSM PPLDVENIQK RIDQSKFQET
LAP2β ---------- ---------- -ESLVVNRVT GNFKHASPIL PITEFSDIPR RAPKK-----
LAP2γ ---------- ---------- ---------- ---------- ---------- ----------

     421        431        441        451        461        471
LAP2α EFLSPPRKVP RLSEKSVEER DSGSFVAFQN IPGSELMSSF AKTVVSHSLT TLGLEVAKQS
LAP2β -----PLTRA EVGEKTEERR ---------- ---------- ---------- ----------
LAP2γ ---------- -VGEKTEERR ---------- ---------- ---------- ----------

     481         491        501         511        521         531
LAP2α QHDKIDASEL SFPFHESILK VIEEEWQQVD RQLPSLACKY PVSSREATQI LSVPKVDDEI
LAP2β ---------- ---------- --------VE RDILKEMFPY EAS------- ----------
LAP2γ ---------- ---------- --------VE RDILKEMFPY EAS------- ----------

     541        551        561        571        581        591
LAP2α LGFISEATPL GGIQAASTES CNQQLDLALC RAYEAAASAL QIATHTAFVA KAMQADISQA
LAP2β -------TPT G-----ISAS CRRPIKGAAG RPLELSDFRM EESFSSKYVP KYVPLAD---
LAP2γ -------TPT G-----ISAS CRRPIKGAAG RPLELSDFRM EESFSSKYVP KYVPLAD---

     601        611        621        631        641        651
LAP2α AQILSSDPSR THQALGILSK TYDAASYICE AAFDEVKMAA HTMGNATVGR RYLWLKDCKI
LAP2β ---VKSEKTK KGRSIPVWIK ---ILLFVVV AVFLFLVYQA METNQVNPFS NFLHVDPRKS
LAP2γ ---VKSEKTK KGRSIPVWIK ---ILLFVVV AVFLFLVYQA METNQVNPFS NFLHVDPRKS

     661        671        681        691
LAP2α NLASKNKLAS TPFKGGTLFG GEVCKVIKKR GNKH
LAP2β N--------- ---------- ---------- ----
LAP2γ N--------- ---------- ---------- ----
```

Figure 6. Cysteine residues in the LAP2α-specific C-terminal domain. Multiple sequence alignment of three isoforms of human LAP2: α, β and γ. Cysteine residues are labelled as follows: a single cysteine common to all three LAP2 isoforms (blue), LAP2α specific cysteines (red).

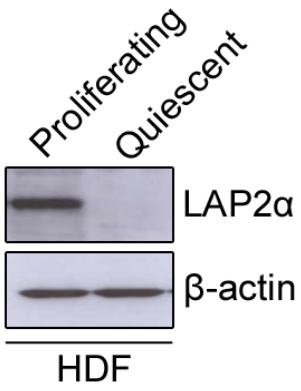

Figure 7. LAP2α protein levels are down-regulated in quiescent HDFs. Protein extracts were prepared from proliferating (P) or quiescent (Q) HDFs and subjected to reducing SDS-PAGE before immunoblotting with anti-LAP2α or β-actin antibodies.

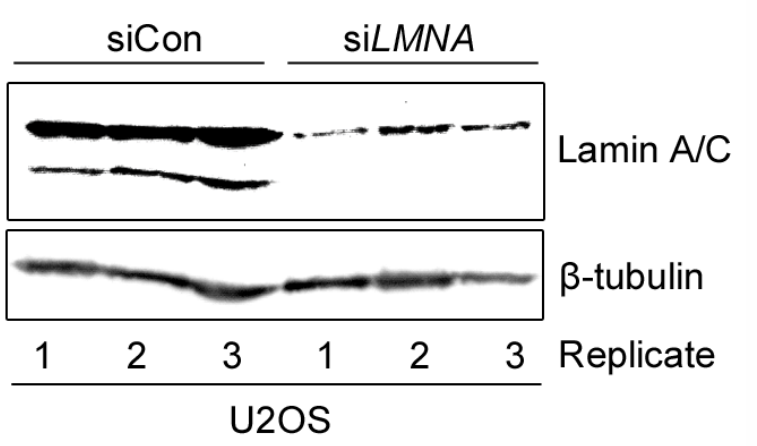

Figure 8. Knockdown efficiencies for clonogenic assay. U2OS cells were transfected with either non-targeting control siRNA or siRNA targeting *LMNA*. After 72 hours, cells were then counted and plated for colony forming assays as shown in Figure 5.8. Remaining cells were pelleted and whole cell extracts were prepared and subjected to reducing SDS-PAGE before immunoblotting with anti-lamin A/C (Jol2) or anti-β-tubulin antibodies to assess knockdown efficiencies.

Amino acid #	Amino acid	Reference(s)
390	**S**	Beausoleil et al., (2006); Trinidad et al., (2006); Dephoure et al., (2008); Wang et al., (2008); Tweedie-Cullen et al., (2009); Bennetzen et al., (2010); Chen et al., (2010); Moritz et al., (2010)
392	**S**	Beausoleil et al., (2006); Wang et al., (2008); Tweedie-Cullen et al., (2009); Bennetzen et al., (2010); Chen et al., (2010); Dephoure et al., (2008); Moritz et al., (2010)
394	**T**	Beausoleil et al., (2006); Tweedie-Cullen et al., (2009)
395	**S**	Beausoleil et al., (2006); Stokes et al., (2007); Dephoure et al., (2008); Bennetzen et al., (2010)
398	**S**	Dephoure et al., (2008); Moritz et al., (2010)
403	**S**	Yang et al., (2006); Tweedie-Cullen et al., (2009); Moritz et al., (2010)
404	**S**	Yang et al., (2006); Tweedie-Cullen et al., (2009); Moritz et al., (2010);
406	**S**	Yang et al., (2006); Wang et al., (2008); Moritz et al., (2010)
407	**S**	Yang et al., (2006); Wang et al., (2008); Tweedie-Cullen et al., (2009); Moritz et al., (2010)
409	**T**	Yang et al., (2006): Moritz et al., (2010)
414	**S**	Moritz et al., (2010)
416	**T**	Yang et al., (2006); Moritz et al., (2010)
423	**S**	Trinidad et al., (2006); Yang et al., (2006)
424	**T**	Trinidad et al., (2006); Yang et al., (2006); Chen et al., (2010)
426	**S**	Trinidad et al., (2006); Chen et al., (2010)
428	**S**	Trinidad et al., (2006)
429	**S**	Trinidad et al., (2006)
431	**S**	(No experimental data)
436	**T**	(No experimental data)
437	**S**	(No experimental data)

Note: not all references have been included. For a more thorough reference list, see www.phosphosite.org

Table 3. Literature based search for A-type lamin phosphorylation sites. Using database searches (www.pubmed.com and www.phosphosite.org) previously identified phosphorylated residues in lamin A/C have been collated with the indicated references.

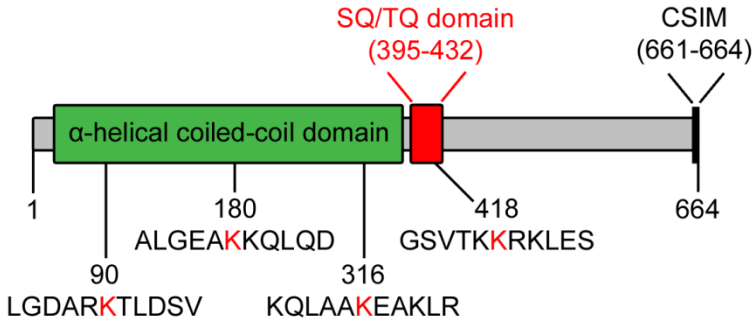

Figure 9. Potential acetylation sites in lamin A/C. Using a prediction algorithm, Basu et al. (2009) identified acetylation sites in lamin A/C, residue 418 was predicted and validated, whilst residues 90, 180 and 316 were only predicted.

REFERENCES

Abraham, R.T. (2001). Cell cycle checkpoint signaling through the ATM and ATR kinases. Genes Dev 15, 2177-2196.

Adams, M.M., and Carpenter, P.B. (2006). Tying the loose ends together in DNA double strand break repair with 53BP1. Cell Div 1, 19.

Agarwal, A.K., and Garg, A. (2006). Genetic disorders of adipose tissue development, differentiation, and death. Annu Rev Genomics Hum Genet 7, 175-199.

Ahel, D., Horejsi, Z., Wiechens, N., Polo, S.E., Garcia-Wilson, E., Ahel, I., Flynn, H., Skehel, M., West, S.C., Jackson, S.P., et al. (2009). Poly(ADP-ribose)-dependent regulation of DNA repair by the chromatin remodeling enzyme ALC1. Science 325, 1240-1243.

Ahel, I., Ahel, D., Matsusaka, T., Clark, A.J., Pines, J., Boulton, S.J., and West, S.C. (2008). Poly(ADP-ribose)-binding zinc finger motifs in DNA repair/checkpoint proteins. Nature 451, 81-85.

Akhtar, A., and Gasser, S.M. (2007). The nuclear envelope and transcriptional control. Nat Rev Genet 8, 507-517.

Al-Hakim, A., Escribano-Diaz, C., Landry, M.C., O'Donnell, L., Panier, S., Szilard, R.K., and Durocher, D. (2010). The ubiquitous role of ubiquitin in the DNA damage response. DNA Repair (Amst) 9, 1229-1240.

Alsheimer, M., and Benavente, R. (1996). Change of karyoskeleton during mammalian spermatogenesis: expression pattern of nuclear lamin C2 and its regulation. Exp Cell Res 228, 181-188.

Alter, B.P., Greene, M.H., Velazquez, I., and Rosenberg, P.S. (2003). Cancer in Fanconi anemia. Blood 101, 2072.

Andreassen, P.R., D'Andrea, A.D., and Taniguchi, T. (2004). ATR couples FANCD2 monoubiquitination to the DNA-damage response. Genes Dev 18, 1958-1963.

Andres, V., and Gonzalez, J.M. (2009). Role of A-type lamins in signaling, transcription, and chromatin organization. The Journal of Cell Biology 187, 945-957.

Arellano, M., and Moreno, S. (1997). Regulation of CDK/cyclin complexes during the cell cycle. Int J Biochem Cell Biol 29, 559-573.

Aressy, B., and Ducommun, B. (2008). Cell cycle control by the CDC25 phosphatases. Anticancer Agents Med Chem 8, 818-824.

Arora, P., Muralikrishna, B., and Parnaik, V.K. (2004). Cell-type-specific interactions at regulatory motifs in the first intron of the lamin A gene. FEBS Lett 568, 122-128.

Artandi, S.E., and DePinho, R.A. (2000). A critical role for telomeres in suppressing and facilitating carcinogenesis. Current Opinion in Genetics & Development 10, 39-46.

Assoian, R.K., and Zhu, X. (1997). Cell anchorage and the cytoskeleton as partners in growth factor dependent cell cycle progression. Curr Opin Cell Biol 9, 93-98.

Attwooll, C., Lazzerini Denchi, E., and Helin, K. (2004). The E2F family: specific functions and overlapping interests. The EMBO Journal 23, 4709-4716.

Atzmon, G., Cho, M., Cawthon, R.M., Budagov, T., Katz, M., Yang, X., Siegel, G., Bergman, A., Huffman, D.M., Schechter, C.B., et al. (2010). Evolution in health and medicine Sackler colloquium: Genetic variation in human telomerase is associated with telomere length in Ashkenazi centenarians. Proceedings of the National Academy of Sciences of the United States of America 107 Suppl 1, 1710-1717.

Bakkenist, C.J., and Kastan, M.B. (2003). DNA damage activates ATM through intermolecular autophosphorylation and dimer dissociation. Nature 421, 499-506.

Bao, Y., and Shen, X. (2007). Chromatin remodeling in DNA double-strand break repair. Current Opinion in Genetics & Development 17, 126-131.

Bardin, A.J., and Amon, A. (2001). Men and sin: what's the difference? Nature Reviews Molecular Cell Biology 2, 815-826.

Barrowman, J., Hamblet, C., George, C.M., and Michaelis, S. (2008). Analysis of prelamin A biogenesis reveals the nucleus to be a CaaX processing compartment. Mol Biol Cell 19, 5398-5408.

Bartek, J., Bartkova, J., and Lukas, J. (1997). The retinoblastoma protein pathway in cell cycle control and cancer. Exp Cell Res 237, 1-6.

Bartek, J., and Lukas, J. (2001). Mammalian G1- and S-phase checkpoints in response to DNA damage. Curr Opin Cell Biol 13, 738-747.

Bartek, J., and Lukas, J. (2007). DNA damage checkpoints: from initiation to recovery or adaptation. Curr Opin Cell Biol 19, 238-245.

Bartek, J., Lukas, J., and Bartkova, J. (2007). DNA damage response as an anti-cancer barrier: damage threshold and the concept of 'conditional haploinsufficiency'. Cell Cycle 6, 2344-2347.

Bartkova, J., Horejsi, Z., Koed, K., Kramer, A., Tort, F., Zieger, K., Guldberg, P., Sehested, M., Nesland, J.M., Lukas, C., et al. (2005). DNA damage response as a candidate anti-cancer barrier in early human tumorigenesis. Nature 434, 864-870.

Bartkova, J., Rezaei, N., Liontos, M., Karakaidos, P., Kletsas, D., Issaeva, N., Vassiliou, L.V., Kolettas, E., Niforou, K., Zoumpourlis, V.C., et al. (2006). Oncogene-induced senescence is part of the tumorigenesis barrier imposed by DNA damage checkpoints. Nature 444, 633-637.

Basu, A., Rose, K.L., Zhang, J., Beavis, R.C., Ueberheide, B., Garcia, B.A., Chait, B., Zhao, Y., Hunt, D.F., Segal, E., et al. (2009). Proteome-wide prediction of acetylation substrates. Proceedings of the National Academy of Sciences of the United States of America 106, 13785-13790.

Batchelor, E., Mock, C.S., Bhan, I., Loewer, A., and Lahav, G. (2008). Recurrent initiation: a mechanism for triggering p53 pulses in response to DNA damage. Mol Cell 30, 277-289.

Beausoleil, S.A., Villen, J., Gerber, S.A., Rush, J., and Gygi, S.P. (2006). A probability-based approach for high-throughput protein phosphorylation analysis and site localization. Nature Biotechnology 24, 1285-1292.

Bekker-Jensen, S., and Mailand, N. (2010). Assembly and function of DNA double-strand break repair foci in mammalian cells. DNA Repair (Amst) 9, 1219-1228.

Bekker-Jensen, S., Rendtlew Danielsen, J., Fugger, K., Gromova, I., Nerstedt, A., Lukas, C., Bartek, J., Lukas, J., and Mailand, N. (2010). HERC2 coordinates ubiquitin-dependent assembly of DNA repair factors on damaged chromosomes. Nature Cell Biology 12, 80-86; sup pp 81-12.

Bengtsson, L., and Wilson, K.L. (2004). Multiple and surprising new functions for emerin, a nuclear membrane protein. Curr Opin Cell Biol 16, 73-79.

Benham, A.M., Cabibbo, A., Fassio, A., Bulleid, N., Sitia, R., and Braakman, I. (2000). The CXXCXXC motif determines the folding, structure and stability of human Ero1-Lalpha. The EMBO Journal 19, 4493-4502.

Bennetzen, M.V., Larsen, D.H., Bunkenborg, J., Bartek, J., Lukas, J., and Andersen, J.S. (2010). Site-specific phosphorylation dynamics of the nuclear proteome during the DNA damage response. Molecular & Cellular Proteomics : MCP 9, 1314-1323.

Benson, E.K., Lee, S.W., and Aaronson, S.A. (2010). Role of progerin-induced telomere dysfunction in HGPS premature cellular senescence. Journal of Cell Science 123, 2605-2612.

Bergo, M.O., Gavino, B., Ross, J., Schmidt, W.K., Hong, C., Kendall, L.V., Mohr, A., Meta, M., Genant, H., Jiang, Y., et al. (2002). Zmpste24 deficiency in mice causes spontaneous bone fractures, muscle weakness, and a prelamin A processing defect. Proceedings of the National Academy of Sciences of the United States of America 99, 13049-13054.

Berkovich, E., Monnat, R.J., Jr., and Kastan, M.B. (2007). Roles of ATM and NBS1 in chromatin structure modulation and DNA double-strand break repair. Nature Cell Biology 9, 683-690.

Besson, A., Dowdy, S.F., and Roberts, J.M. (2008). CDK inhibitors: cell cycle regulators and beyond. Dev Cell 14, 159-169.

Biamonti, G., Giacca, M., Perini, G., Contreas, G., Zentilin, L., Weighardt, F., Guerra, M., Della Valle, G., Saccone, S., Riva, S., et al. (1992). The gene for a novel human lamin maps at a highly transcribed locus of chromosome 19 which replicates at the onset of S-phase. Mol Cell Biol 12, 3499-3506.

Bione, S., Maestrini, E., Rivella, S., Mancini, M., Regis, S., Romeo, G., and Toniolo, D. (1994). Identification of a novel X-linked gene responsible for Emery-Dreifuss muscular dystrophy. Nat Genet 8, 323-327.

Blander, G., de Oliveira, R.M., Conboy, C.M., Haigis, M., and Guarente, L. (2003). Superoxide dismutase 1 knock-down induces senescence in human fibroblasts. The Journal of Biological Chemistry 278, 38966-38969.

Blasco, M.A. (2007). The epigenetic regulation of mammalian telomeres. Nat Rev Genet 8, 299-309.

Blow, J.J., and Dutta, A. (2005). Preventing re-replication of chromosomal DNA. Nature Reviews Molecular Cell Biology 6, 476-486.

Blow, J.J., and Gillespie, P.J. (2008). Replication licensing and cancer--a fatal entanglement? Nat Rev Cancer 8, 799-806.

Blumberg, J. (2004). Use of biomarkers of oxidative stress in research studies. J Nutr 134, 3188S-3189S.

Bodnar, A.G., Ouellette, M., Frolkis, M., Holt, S.E., Chiu, C.P., Morin, G.B., Harley, C.B., Shay, J.W., Lichtsteiner, S., and Wright, W.E. (1998). Extension of life-span by introduction of telomerase into normal human cells. Science 279, 349-352.

Bonne, G., Di Barletta, M.R., Varnous, S., Becane, H.M., Hammouda, E.H., Merlini, L., Muntoni, F., Greenberg, C.R., Gary, F., Urtizberea, J.A., et al. (1999). Mutations in the gene encoding lamin A/C cause autosomal dominant Emery-Dreifuss muscular dystrophy. Nat Genet 21, 285-288.

Bonne, G., Mercuri, E., Muchir, A., Urtizberea, A., Becane, H.M., Recan, D., Merlini, L., Wehnert, M., Boor, R., Reuner, U., et al. (2000). Clinical and molecular genetic spectrum of autosomal dominant Emery-Dreifuss muscular dystrophy due to mutations of the lamin A/C gene. Ann Neurol 48, 170-180.

Botuyan, M.V., Lee, J., Ward, I.M., Kim, J.E., Thompson, J.R., Chen, J., and Mer, G. (2006). Structural basis for the methylation state-specific recognition of histone H4-K20 by 53BP1 and Crb2 in DNA repair. Cell 127, 1361-1373.

Boulton, S.J. (2010). DNA repair: Decision at the break point. Nature 465, 301-302.

Bouwman, P., Aly, A., Escandell, J.M., Pieterse, M., Bartkova, J., van der Gulden, H., Hiddingh, S., Thanasoula, M., Kulkarni, A., Yang, Q., et al. (2010). 53BP1 loss rescues BRCA1 deficiency and is associated with triple-negative and BRCA-mutated breast cancers. Nat Struct Mol Biol 17, 688-695.

Bowman, G.D., O'Donnell, M., and Kuriyan, J. (2004). Structural analysis of a eukaryotic sliding DNA clamp-clamp loader complex. Nature 429, 724-730.

Braig, M., Lee, S., Loddenkemper, C., Rudolph, C., Peters, A.H., Schlegelberger, B., Stein, H., Dorken, B., Jenuwein, T., and Schmitt, C.A. (2005). Oncogene-induced senescence as an initial barrier in lymphoma development. Nature 436, 660-665.

Brehm, A., Miska, E.A., McCance, D.J., Reid, J.L., Bannister, A.J., and Kouzarides, T. (1998). Retinoblastoma protein recruits histone deacetylase to repress transcription. Nature 391, 597-601.

Bridger, J.M., Foeger, N., Kill, I.R., and Herrmann, H. (2007). The nuclear lamina. Both a structural framework and a platform for genome organization. FEBS J 274, 1354-1361.

Bridger, J.M., and Kill, I.R. (2004). Aging of Hutchinson-Gilford progeria syndrome fibroblasts is characterised by hyperproliferation and increased apoptosis. Exp Gerontol 39, 717-724.

Bridger, J.M., Kill, I.R., O'Farrell, M., and Hutchison, C.J. (1993). Internal lamin structures within G1 nuclei of human dermal fibroblasts. Journal of Cell Science 104 (Pt 2), 297-306.

Broers, J.L., Machiels, B.M., van Eys, G.J., Kuijpers, H.J., Manders, E.M., van Driel, R., and Ramaekers, F.C. (1999). Dynamics of the nuclear lamina as monitored by GFP-tagged A-type lamins. Journal of Cell Science 112 (Pt 20), 3463-3475.

Broers, J.L., and Ramaekers, F.C. (2004). Dynamics of nuclear lamina assembly and disassembly. Symp Soc Exp Biol, 177-192.

Broers, J.L., Ramaekers, F.C., Bonne, G., Yaou, R.B., and Hutchison, C.J. (2006). Nuclear lamins: laminopathies and their role in premature ageing. Physiol Rev 86, 967-1008.

Brotherton, D.H., Dhanaraj, V., Wick, S., Brizuela, L., Domaille, P.J., Volyanik, E., Xu, X., Parisini, E., Smith, B.O., Archer, S.J., et al. (1998). Crystal structure of the complex of the cyclin D-dependent kinase Cdk6 bound to the cell-cycle inhibitor p19INK4d. Nature 395, 244-250.

Brown, E.J., and Baltimore, D. (2000). ATR disruption leads to chromosomal fragmentation and early embryonic lethality. Genes Dev 14, 397-402.

Bunting, S.F., Callen, E., Wong, N., Chen, H.T., Polato, F., Gunn, A., Bothmer, A., Feldhahn, N., Fernandez-Capetillo, O., Cao, L., et al. (2010). 53BP1 inhibits homologous recombination in Brca1-deficient cells by blocking resection of DNA breaks. Cell 141, 243-254.

Burke, B., and Roux, K.J. (2009). Nuclei take a position: managing nuclear location. Dev Cell 17, 587-597.

Burke, B., and Stewart, C.L. (2002). Life at the edge: the nuclear envelope and human disease. Nat Rev Mol Cell Biol 3, 575-585.

Burke, B., and Stewart, C.L. (2006). The laminopathies: the functional architecture of the nucleus and its contribution to disease. Annu Rev Genomics Hum Genet 7, 369-405.

Burkhart, D.L., and Sage, J. (2008). Cellular mechanisms of tumour suppression by the retinoblastoma gene. Nat Rev Cancer 8, 671-682.

Burma, S., Chen, B.P., Murphy, M., Kurimasa, A., and Chen, D.J. (2001). ATM phosphorylates histone H2AX in response to DNA double-strand breaks. The Journal of Biological Chemistry 276, 42462-42467.

Caldecott, K.W. (2008). Single-strand break repair and genetic disease. Nat Rev Genet 9, 619-631.

Campisi, J. (1998). The role of cellular senescence in skin aging. J Investig Dermatol Symp Proc 3, 1-5.

Campisi, J. (2003). Cancer and ageing: rival demons? Nat Rev Cancer 3, 339-349.

Campisi, J. (2005). Suppressing cancer: the importance of being senescent. Science 309, 886-887.

Campisi, J., and d'Adda di Fagagna, F. (2007). Cellular senescence: when bad things happen to good cells. Nature Reviews Molecular Cell Biology 8, 729-740.

Cao, H., and Hegele, R.A. (2003). LMNA is mutated in Hutchinson-Gilford progeria (MIM 176670) but not in Wiedemann-Rautenstrauch progeroid syndrome (MIM 264090). J Hum Genet 48, 271-274.

Cao, K., Capell, B.C., Erdos, M.R., Djabali, K., and Collins, F.S. (2007). A lamin A protein isoform overexpressed in Hutchinson-Gilford progeria syndrome interferes with mitosis in progeria and normal cells. Proceedings of the National Academy of Sciences of the United States of America 104, 4949-4954.

Cao, L., Xu, X., Bunting, S.F., Liu, J., Wang, R.H., Cao, L.L., Wu, J.J., Peng, T.N., Chen, J., Nussenzweig, A., et al. (2009). A selective requirement for 53BP1 in the biological response to genomic instability induced by Brca1 deficiency. Mol Cell 35, 534-541.

Capo-Chichi, C.D., Cai, K.Q., Simpkins, F., Ganjei-Azar, P., Godwin, A.K., and Xu, X.X. (2011). Nuclear envelope structural defects cause chromosomal numerical instability and aneuploidy in ovarian cancer. BMC Med 9, 28.

Cardozo, T., and Pagano, M. (2007). Wrenches in the works: drug discovery targeting the SCF ubiquitin ligase and APC/C complexes. BMC Biochem 8 Suppl 1, S9.

Carney, J.P., Maser, R.S., Olivares, H., Davis, E.M., Le Beau, M., Yates, J.R., 3rd, Hays, L., Morgan, W.F., and Petrini, J.H. (1998). The hMre11/hRad50 protein complex and Nijmegen breakage syndrome: linkage of double-strand break repair to the cellular DNA damage response. Cell 93, 477-486.

Cavenee, W.K., Dryja, T.P., Phillips, R.A., Benedict, W.F., Godbout, R., Gallie, B.L., Murphree, A.L., Strong, L.C., and White, R.L. (1983). Expression of recessive alleles by chromosomal mechanisms in retinoblastoma. Nature 305, 779-784.

Celeste, A., Fernandez-Capetillo, O., Kruhlak, M.J., Pilch, D.R., Staudt, D.W., Lee, A., Bonner, R.F., Bonner, W.M., and Nussenzweig, A. (2003). Histone H2AX phosphorylation is dispensable for the initial recognition of DNA breaks. Nature cell biology 5, 675-679.

Chaouch, M., Allal, Y., De Sandre-Giovannoli, A., Vallat, J.M., Amer-el-Khedoud, A., Kassouri, N., Chaouch, A., Sindou, P., Hammadouche, T., Tazir, M., et al. (2003). The phenotypic manifestations of autosomal recessive axonal Charcot-Marie-Tooth due to a mutation in Lamin A/C gene. Neuromuscul Disord 13, 60-67.

Chapman, J.R., and Jackson, S.P. (2008). Phospho-dependent interactions between NBS1 and MDC1 mediate chromatin retention of the MRN complex at sites of DNA damage. EMBO Rep 9, 795-801.

Charniot, J.C., Bonnefont-Rousselot, D., Marchand, C., Zerhouni, K., Vignat, N., Peynet, J., Plotkine, M., Legrand, A., and Artigou, J.Y. (2007). Oxidative stress implication in a new phenotype of amyotrophic quadricipital syndrome with cardiac involvement due to lamin A/C mutation. Free Radic Res 41, 424-431.

Chaturvedi, P., Eng, W.K., Zhu, Y., Mattern, M.R., Mishra, R., Hurle, M.R., Zhang, X., Annan, R.S., Lu, Q., Faucette, L.F., et al. (1999). Mammalian Chk2 is a downstream effector of the ATM-dependent DNA damage checkpoint pathway. Oncogene 18, 4047-4054.

Chaum, E., Yin, J., Yang, H., Thomas, F., and Lang, J.C. (2009). Quantitative AP-1 gene regulation by oxidative stress in the human retinal pigment epithelium. J Cell Biochem 108, 1280-1291.

Chen, H.Z., Tsai, S.Y., and Leone, G. (2009). Emerging roles of E2Fs in cancer: an exit from cell cycle control. Nat Rev Cancer 9, 785-797.

Chen, J.H., Ozanne, S.E., and Hales, C.N. (2005). Heterogeneity in premature senescence by oxidative stress correlates with differential DNA damage during the cell cycle. DNA Repair (Amst) 4, 1140-1148.

Chen, J.H., Stoeber, K., Kingsbury, S., Ozanne, S.E., Williams, G.H., and Hales, C.N. (2004). Loss of proliferative capacity and induction of senescence in oxidatively stressed human fibroblasts. The Journal of Biological Chemistry 279, 49439-49446.

Chen, L., Giorgianni, F., and Beranova-Giorgianni, S. (2010). Characterization of the phosphoproteome in LNCaP prostate cancer cells by in-gel isoelectric focusing and tandem mass spectrometry. J Proteome Res 9, 174-178.

Chen, L., Lee, L., Kudlow, B.A., Dos Santos, H.G., Sletvold, O., Shafeghati, Y., Botha, E.G., Garg, A., Hanson, N.B., Martin, G.M., et al. (2003). LMNA mutations in atypical Werner's syndrome. Lancet 362, 440-445.

Chen, Y., Yang, Y., van Overbeek, M., Donigian, J.R., Baciu, P., de Lange, T., and Lei, M. (2008). A shared docking motif in TRF1 and TRF2 used for differential recruitment of telomeric proteins. Science 319, 1092-1096.

Chou, D.M., Adamson, B., Dephoure, N.E., Tan, X., Nottke, A.C., Hurov, K.E., Gygi, S.P., Colaiacovo, M.P., and Elledge, S.J. (2010). A chromatin localization screen reveals poly (ADP ribose)-regulated recruitment of the repressive polycomb and NuRD complexes to sites of DNA damage. Proceedings of the National Academy of Sciences of the United States of America 107, 18475-18480.

Chung, H.Y., Sung, B., Jung, K.J., Zou, Y., and Yu, B.P. (2006). The molecular inflammatory process in aging. Antioxid Redox Signal 8, 572-581.

Ciccia, A., and Elledge, S.J. (2010). The DNA damage response: making it safe to play with knives. Mol Cell 40, 179-204.

Ciccia, A., Ling, C., Coulthard, R., Yan, Z., Xue, Y., Meetei, A.R., Laghmani el, H., Joenje, H., McDonald, N., de Winter, J.P., et al. (2007). Identification of FAAP24, a Fanconi anemia core complex protein that interacts with FANCM. Mol Cell 25, 331-343.

Cimprich, K.A., and Cortez, D. (2008). ATR: an essential regulator of genome integrity. Nature Reviews Molecular Cell Biology 9, 616-627.

Clevers, H. (2006). Wnt/beta-catenin signaling in development and disease. Cell 127, 469-480.

Cobrinik, D. (2005). Pocket proteins and cell cycle control. Oncogene 24, 2796-2809.

Coffinier, C., Jung, H.J., Li, Z., Nobumori, C., Yun, U.J., Farber, E.A., Davies, B.S., Weinstein, M.M., Yang, S.H., Lammerding, J., et al. (2010). Direct synthesis of lamin A, bypassing prelamin a processing, causes misshapen nuclei in fibroblasts but no detectable pathology in mice. The Journal of Biological Chemistry 285, 20818-20826.

Cohen, M., Lee, K.K., Wilson, K.L., and Gruenbaum, Y. (2001). Transcriptional repression, apoptosis, human disease and the functional evolution of the nuclear lamina. Trends Biochem Sci 26, 41-47.

Coin, F., Oksenych, V., Mocquet, V., Groh, S., Blattner, C., and Egly, J.M. (2008). Nucleotide excision repair driven by the dissociation of CAK from TFIIH. Mol Cell 31, 9-20.

Collis, S.J., Ciccia, A., Deans, A.J., Horejsi, Z., Martin, J.S., Maslen, S.L., Skehel, J.M., Elledge, S.J., West, S.C., and Boulton, S.J. (2008). FANCM and FAAP24 function in ATR-mediated checkpoint signaling independently of the Fanconi anemia core complex. Mol Cell 32, 313-324.

Constantinescu, D., Csoka, A.B., Navara, C.S., and Schatten, G.P. (2010). Defective DSB repair correlates with abnormal nuclear morphology and is improved with FTI treatment in Hutchinson-Gilford progeria syndrome fibroblasts. Exp Cell Res 316, 2747-2759.

Constantinescu, D., Gray, H.L., Sammak, P.J., Schatten, G.P., and Csoka, A.B. (2006). Lamin A/C expression is a marker of mouse and human embryonic stem cell differentiation. Stem Cells 24, 177-185.

Cook, P.J., Ju, B.G., Telese, F., Wang, X., Glass, C.K., and Rosenfeld, M.G. (2009). Tyrosine dephosphorylation of H2AX modulates apoptosis and survival decisions. Nature 458, 591-596.

Coppe, J.P., Kauser, K., Campisi, J., and Beausejour, C.M. (2006). Secretion of vascular endothelial growth factor by primary human fibroblasts at senescence. The Journal of Biological Chemistry 281, 29568-29574.

Coppe, J.P., Patil, C.K., Rodier, F., Krtolica, A., Beausejour, C.M., Parrinello, S., Hodgson, J.G., Chin, K., Desprez, P.Y., and Campisi, J. (2010). A human-like senescence-associated secretory phenotype is conserved in mouse cells dependent on physiological oxygen. PLoS One 5, e9188.

Coppe, J.P., Patil, C.K., Rodier, F., Sun, Y., Munoz, D.P., Goldstein, J., Nelson, P.S., Desprez, P.Y., and Campisi, J. (2008). Senescence-associated secretory phenotypes reveal cell-nonautonomous functions of oncogenic RAS and the p53 tumor suppressor. PLoS Biol 6, 2853-2868.

Corrigan, D.P., Kuszczak, D., Rusinol, A.E., Thewke, D.P., Hrycyna, C.A., Michaelis, S., and Sinensky, M.S. (2005). Prelamin A endoproteolytic processing in vitro by recombinant Zmpste24. Biochem J 387, 129-138.

Cortez, D., Guntuku, S., Qin, J., and Elledge, S.J. (2001). ATR and ATRIP: partners in checkpoint signaling. Science 294, 1713-1716.

Cotterman, R., Jin, V.X., Krig, S.R., Lemen, J.M., Wey, A., Farnham, P.J., and Knoepfler, P.S. (2008). N-Myc regulates a widespread euchromatic program in the human genome partially independent of its role as a classical transcription factor. Cancer Res 68, 9654-9662.

Crisp, M., Liu, Q., Roux, K., Rattner, J.B., Shanahan, C., Burke, B., Stahl, P.D., and Hodzic, D. (2006). Coupling of the nucleus and cytoplasm: role of the LINC complex. Journal of Cell Biology 172, 41-53.

d'Adda di Fagagna, F., Reaper, P.M., Clay-Farrace, L., Fiegler, H., Carr, P., Von Zglinicki, T., Saretzki, G., Carter, N.P., and Jackson, S.P. (2003). A DNA damage checkpoint response in telomere-initiated senescence. Nature 426, 194-198.

Dahl, K.N., Scaffidi, P., Islam, M.F., Yodh, A.G., Wilson, K.L., and Misteli, T. (2006). Distinct structural and mechanical properties of the nuclear lamina in Hutchinson-Gilford progeria syndrome. Proceedings of the National Academy of Sciences of the United States of America 103, 10271-10276.

Davies, B.S., Barnes, R.H., 2nd, Tu, Y., Ren, S., Andres, D.A., Spielmann, H.P., Lammerding, J., Wang, Y., Young, S.G., and Fong, L.G. (2010). An accumulation of non-farnesylated prelamin A causes cardiomyopathy but not progeria. Human Molecular Genetics 19, 2682-2694.

Davies, B.S., Fong, L.G., Yang, S.H., Coffinier, C., and Young, S.G. (2009). The posttranslational processing of prelamin A and disease. Annual Review of Genomics and Human Genetics 10, 153-174.

Davies, K.J. (1999). The broad spectrum of responses to oxidants in proliferating cells: a new paradigm for oxidative stress. IUBMB Life 48, 41-47.

de Klein, A., Muijtjens, M., van Os, R., Verhoeven, Y., Smit, B., Carr, A.M., Lehmann, A.R., and Hoeijmakers, J.H. (2000). Targeted disruption of the cell-cycle checkpoint gene ATR leads to early embryonic lethality in mice. Curr Biol 10, 479-482.

de Lange, T. (2005). Shelterin: the protein complex that shapes and safeguards human telomeres. Genes Dev 19, 2100-2110.

De Sandre-Giovannoli, A., Bernard, R., Cau, P., Navarro, C., Amiel, J., Boccaccio, I., Lyonnet, S., Stewart, C.L., Munnich, A., Le Merrer, M., et al. (2003). Lamin a truncation in Hutchinson-Gilford progeria. Science 300, 2055.

De Sandre-Giovannoli, A., Chaouch, M., Kozlov, S., Vallat, J.M., Tazir, M., Kassouri, N., Szepetowski, P., Hammadouche, T., Vandenberghe, A., Stewart, C.L., et al. (2002). Homozygous defects in LMNA, encoding lamin A/C nuclear-envelope proteins, cause autosomal recessive axonal neuropathy in human (Charcot-Marie-Tooth disorder type 2) and mouse. Am J Hum Genet 70, 726-736.

De Vos, W.H., Houben, F., Hoebe, R.A., Hennekam, R., van Engelen, B., Manders, E.M., Ramaekers, F.C., Broers, J.L., and Van Oostveldt, P. (2010). Increased plasticity of the nuclear envelope and hypermobility of telomeres due to the loss of A-type lamins. Biochim Biophys Acta 1800, 448-458.

Dechat, T., Adam, S.A., Taimen, P., Shimi, T., and Goldman, R.D. (2010). Nuclear lamins. Cold Spring Harb Perspect Biol 2, a000547.

Dechat, T., Gajewski, A., Korbei, B., Gerlich, D., Daigle, N., Haraguchi, T., Furukawa, K., Ellenberg, J., and Foisner, R. (2004). LAP2alpha and BAF transiently localize to telomeres and specific regions on chromatin during nuclear assembly. Journal of Cell Science 117, 6117-6128.

Dechat, T., Gotzmann, J., Stockinger, A., Harris, C.A., Talle, M.A., Siekierka, J.J., and Foisner, R. (1998). Detergent-salt resistance of LAP2alpha in interphase nuclei and phosphorylation-dependent association with chromosomes early in nuclear assembly implies functions in nuclear structure dynamics. The EMBO Journal 17, 4887-4902.

Dechat, T., Korbei, B., Vaughan, O.A., Vlcek, S., Hutchison, C.J., and Foisner, R. (2000). Lamina-associated polypeptide 2alpha binds intranuclear A-type lamins. Journal of Cell Science 113 Pt 19, 3473-3484.

Dechat, T., Shimi, T., Adam, S.A., Rusinol, A.E., Andres, D.A., Spielmann, H.P., Sinensky, M.S., and Goldman, R.D. (2007). Alterations in mitosis and cell cycle progression caused by a mutant lamin A known to accelerate human aging. Proceedings of the National Academy of Sciences of the United States of America 104, 4955-4960.

Dechat, T., Vlcek, S., and Foisner, R. (2000). Review: lamina-associated polypeptide 2 isoforms and related proteins in cell cycle-dependent nuclear structure dynamics. J Struct Biol 129, 335-345.

Decker, M.L., Chavez, E., Vulto, I., and Lansdorp, P.M. (2009). Telomere length in Hutchinson-Gilford progeria syndrome. Mech Ageing Dev 130, 377-383.

Dehay, C., and Kennedy, H. (2007). Cell-cycle control and cortical development. Nat Rev Neurosci 8, 438-450.

Delbarre, E., Tramier, M., Coppey-Moisan, M., Gaillard, C., Courvalin, J.C., and Buendia, B. (2006). The truncated prelamin A in Hutchinson-Gilford progeria syndrome alters segregation of A-type and B-type lamin homopolymers. Hum Mol Genet 15, 1113-1122.

Deng, C., Zhang, P., Harper, J.W., Elledge, S.J., and Leder, P. (1995). Mice lacking p21CIP1/WAF1 undergo normal development, but are defective in G1 checkpoint control. Cell 82, 675-684.

Dephoure, N., Zhou, C., Villen, J., Beausoleil, S.A., Bakalarski, C.E., Elledge, S.J., and Gygi, S.P. (2008). A quantitative atlas of mitotic phosphorylation. Proceedings of the National Academy of Sciences of the United States of America 105, 10762-10767.

Derheimer, F.A., and Kastan, M.B. (2010). Multiple roles of ATM in monitoring and maintaining DNA integrity. FEBS Lett 584, 3675-3681.

Dhe-Paganon, S., Werner, E.D., Chi, Y.I., and Shoelson, S.E. (2002). Structure of the globular tail of nuclear lamin. Journal of Biological Chemistry 277, 17381-17384.

Di Micco, R., Fumagalli, M., Cicalese, A., Piccinin, S., Gasparini, P., Luise, C., Schurra, C., Garre, M., Nuciforo, P.G., Bensimon, A., et al. (2006). Oncogene-induced senescence is a DNA damage response triggered by DNA hyper-replication. Nature 444, 638-642.

Di Micco, R., Fumagalli, M., and d'Adda di Fagagna, F. (2007). Breaking news: high-speed race ends in arrest--how oncogenes induce senescence. Trends Cell Biol 17, 529-536.

Di Micco, R., Sulli, G., Dobreva, M., Liontos, M., Botrugno, O.A., Gargiulo, G., dal Zuffo, R., Matti, V., d'Ario, G., Montani, E., et al. (2011). Interplay between oncogene-induced DNA damage response and heterochromatin in senescence and cancer. Nature Cell Biology 13, 292-302.

Diehl, J.A., Cheng, M., Roussel, M.F., and Sherr, C.J. (1998). Glycogen synthase kinase-3beta regulates cyclin D1 proteolysis and subcellular localization. Genes Dev 12, 3499-3511.

Diermeier-Daucher, S., Clarke, S.T., Hill, D., Vollmann-Zwerenz, A., Bradford, J.A., and Brockhoff, G. (2009). Cell type specific applicability of 5-ethynyl-2'-deoxyuridine (EdU) for dynamic proliferation assessment in flow cytometry. Cytometry A 75, 535-546.

Diffley, J.F., and Labib, K. (2002). The chromosome replication cycle. Journal of Cell Science 115, 869-872.

Difilippantonio, S., Gapud, E., Wong, N., Huang, C.Y., Mahowald, G., Chen, H.T., Kruhlak, M.J., Callen, E., Livak, F., Nussenzweig, M.C., et al. (2008). 53BP1 facilitates long-range DNA end-joining during V(D)J recombination. Nature 456, 529-533.

Difilippantonio, S., and Nussenzweig, A. (2007). The NBS1-ATM connection revisited. Cell Cycle 6, 2366-2370.

Dimitrova, N., Chen, Y.C., Spector, D.L., and de Lange, T. (2008). 53BP1 promotes non-homologous end joining of telomeres by increasing chromatin mobility. Nature 456, 524-528.

Dimri, G.P., Lee, X., Basile, G., Acosta, M., Scott, G., Roskelley, C., Medrano, E.E., Linskens, M., Rubelj, I., Pereira-Smith, O., et al. (1995). A biomarker that identifies senescent human cells in culture and in aging skin in vivo. Proceedings of the National Academy of Sciences of the United States of America 92, 9363-9367.

Ding, L., Getz, G., Wheeler, D.A., Mardis, E.R., McLellan, M.D., Cibulskis, K., Sougnez, C., Greulich, H., Muzny, D.M., Morgan, M.B., et al. (2008). Somatic mutations affect key pathways in lung adenocarcinoma. Nature 455, 1069-1075.

DiTullio, R.A., Jr., Mochan, T.A., Venere, M., Bartkova, J., Sehested, M., Bartek, J., and Halazonetis, T.D. (2002). 53BP1 functions in an ATM-dependent checkpoint pathway that is constitutively activated in human cancer. Nature Cell Biology 4, 998-1002.

Dominguez-Sola, D., Ying, C.Y., Grandori, C., Ruggiero, L., Chen, B., Li, M., Galloway, D.A., Gu, W., Gautier, J., and Dalla-Favera, R. (2007). Non-transcriptional control of DNA replication by c-Myc. Nature 448, 445-451.

Dorner, D., Gotzmann, J., and Foisner, R. (2007). Nucleoplasmic lamins and their interaction partners, LAP2alpha, Rb, and BAF, in transcriptional regulation. FEBS J 274, 1362-1373.

Dorner, D., Vlcek, S., Foeger, N., Gajewski, A., Makolm, C., Gotzmann, J., Hutchison, C.J., and Foisner, R. (2006). Lamina-associated polypeptide 2alpha regulates cell cycle progression and differentiation via the retinoblastoma-E2F pathway. Journal of Cell Biology 173, 83-93.

Downs, J.A., and Jackson, S.P. (2004). A means to a DNA end: the many roles of Ku. Nature Reviews Molecular Cell Biology 5, 367-378.

Draetta, G., and Beach, D. (1988). Activation of cdc2 protein kinase during mitosis in human cells: cell cycle-dependent phosphorylation and subunit rearrangement. Cell 54, 17-26.

Dreuillet, C., Harper, M., Tillit, J., Kress, M., and Ernoult-Lange, M. (2008). Mislocalization of human transcription factor MOK2 in the presence of pathogenic mutations of lamin A/C. Biol Cell 100, 51-61.

Dreuillet, C., Tillit, J., Kress, M., and Ernoult-Lange, M. (2002). In vivo and in vitro interaction between human transcription factor MOK2 and nuclear lamin A/C. Nucleic Acids Res 30, 4634-4642.

Dunn, J.M., Phillips, R.A., Becker, A.J., and Gallie, B.L. (1988). Identification of germline and somatic mutations affecting the retinoblastoma gene. Science 241, 1797-1800.

Duque, G., and Rivas, D. (2006). Age-related changes in lamin A/C expression in the osteoarticular system: laminopathies as a potential new aging mechanism. Mech Ageing Dev 127, 378-383.

Duursma, A.M., and Agami, R. (2005). CDK-dependent stabilization of Cdc6: linking growth and stress signals to activation of DNA replication. Cell Cycle 4, 1725-1728.

Dyer, J.A., Kill, I.R., Pugh, G., Quinlan, R.A., Lane, E.B., and Hutchison, C.J. (1997). Cell cycle changes in A-type lamin associations detected in human dermal fibroblasts using monoclonal antibodies. Chromosome Res 5, 383-394.

Dyer, J.A., Lane, B.E., and Hutchison, C.J. (1999). Investigations of the pathway of incorporation and function of lamin A in the nuclear lamina. Microsc Res Tech 45, 1-12.

Dyson, N. (1998). The regulation of E2F by pRB-family proteins. Genes Dev 12, 2245-2262.

Eaton, P. (2006). Protein thiol oxidation in health and disease: techniques for measuring disulfides and related modifications in complex protein mixtures. Free Radic Biol Med 40, 1889-1899.

Eaton, P., Jones, M.E., McGregor, E., Dunn, M.J., Leeds, N., Byers, H.L., Leung, K.Y., Ward, M.A., Pratt, J.R., and Shattock, M.J. (2003). Reversible cysteine-targeted oxidation of proteins during renal oxidative stress. J Am Soc Nephrol 14, S290-296.

Eferl, R., and Wagner, E.F. (2003). AP-1: a double-edged sword in tumorigenesis. Nat Rev Cancer 3, 859-868.

Elbashir, S.M., Harborth, J., Lendeckel, W., Yalcin, A., Weber, K., and Tuschl, T. (2001). Duplexes of 21-nucleotide RNAs mediate RNA interference in cultured mammalian cells. Nature 411, 494-498.

Eliezer, Y., Argaman, L., Rhie, A., Doherty, A.J., and Goldberg, M. (2009). The direct interaction between 53BP1 and MDC1 is required for the recruitment of 53BP1 to sites of damage. The Journal of Biological Chemistry 284, 426-435.

Elledge, S.J. (1996). Cell cycle checkpoints: preventing an identity crisis. Science 274, 1664-1672.

Ellis, D.J., Jenkins, H., Whitfield, W.G., and Hutchison, C.J. (1997). GST-lamin fusion proteins act as dominant negative mutants in Xenopus egg extract and reveal the function of the lamina in DNA replication. Journal of Cell Science 110 (Pt 20), 2507-2518.

Epstein, J., Williams, J.R., and Little, J.B. (1973). Deficient DNA repair in human progeroid cells. Proceedings of the National Academy of Sciences of the United States of America 70, 977-981.

Eriksson, M., Brown, W.T., Gordon, L.B., Glynn, M.W., Singer, J., Scott, L., Erdos, M.R., Robbins, C.M., Moses, T.Y., Berglund, P., et al. (2003). Recurrent de novo point mutations in lamin A cause Hutchinson-Gilford progeria syndrome. Nature 423, 293-298.

Espada, J., Varela, I., Flores, I., Ugalde, A.P., Cadinanos, J., Pendas, A.M., Stewart, C.L., Tryggvason, K., Blasco, M.A., Freije, J.M., et al. (2008). Nuclear envelope defects cause stem cell dysfunction in premature-aging mice. The Journal of Cell Biology 181, 27-35.

Falck, J., Coates, J., and Jackson, S.P. (2005). Conserved modes of recruitment of ATM, ATR and DNA-PKcs to sites of DNA damage. Nature 434, 605-611.

Falck, J., Mailand, N., Syljuasen, R.G., Bartek, J., and Lukas, J. (2001). The ATM-Chk2-Cdc25A checkpoint pathway guards against radioresistant DNA synthesis. Nature 410, 842-847.

Fatkin, D., MacRae, C., Sasaki, T., Wolff, M.R., Porcu, M., Frenneaux, M., Atherton, J., Vidaillet, H.J., Jr., Spudich, S., De Girolami, U., et al. (1999). Missense mutations in the rod domain of the lamin A/C gene as causes of dilated cardiomyopathy and conduction-system disease. N Engl J Med 341, 1715-1724.

Favale, N.O., Sterin Speziale, N.B., and Fernandez Tome, M.C. (2007). Hypertonic-induced lamin A/C synthesis and distribution to nucleoplasmic speckles is mediated by TonEBP/NFAT5 transcriptional activator. Biochemical and biophysical research communications 364, 443-449.

Fawcett, D.W. (1966). On the occurrence of a fibrous lamina on the inner aspect of the nuclear envelope in certain cells of vertebrates. Am J Anat 119, 129-145.

Fernandez-Capetillo, O., Chen, H.T., Celeste, A., Ward, I., Romanienko, P.J., Morales, J.C., Naka, K., Xia, Z., Camerini-Otero, R.D., Motoyama, N., et al. (2002). DNA damage-induced G2-M checkpoint activation by histone H2AX and 53BP1. Nature Cell Biology 4, 993-997.

Fero, M.L., Rivkin, M., Tasch, M., Porter, P., Carow, C.E., Firpo, E., Polyak, K., Tsai, L.H., Broudy, V., Perlmutter, R.M., et al. (1996). A syndrome of multiorgan hyperplasia with features of gigantism, tumorigenesis, and female sterility in p27(Kip1)-deficient mice. Cell 85, 733-744.

Filesi, I., Gullotta, F., Lattanzi, G., D'Apice, M.R., Capanni, C., Nardone, A.M., Columbaro, M., Scarano, G., Mattioli, E., Sabatelli, P., et al. (2005). Alterations of nuclear envelope and chromatin organization in mandibuloacral dysplasia, a rare form of laminopathy. Physiol Genomics 23, 150-158.

Finlan, L.E., Sproul, D., Thomson, I., Boyle, S., Kerr, E., Perry, P., Ylstra, B., Chubb, J.R., and Bickmore, W.A. (2008). Recruitment to the nuclear periphery can alter expression of genes in human cells. PLoS Genet 4, e1000039.

Fiserova, J., and Goldberg, M.W. (2010). Nucleocytoplasmic transport in yeast: a few roles for many actors. Biochem Soc Trans 38, 273-277.

Fiserova, J., Kiseleva, E., and Goldberg, M.W. (2009). Nuclear envelope and nuclear pore complex structure and organization in tobacco BY-2 cells. Plant J 59, 243-255.

FitzGerald, J.E., Grenon, M., and Lowndes, N.F. (2009). 53BP1: function and mechanisms of focal recruitment. Biochem Soc Trans 37, 897-904.

Foisner, R., and Gerace, L. (1993). Integral membrane proteins of the nuclear envelope interact with lamins and chromosomes, and binding is modulated by mitotic phosphorylation. Cell 73, 1267-1279.

Fong, L.G., Ng, J.K., Lammerding, J., Vickers, T.A., Meta, M., Cote, N., Gavino, B., Qiao, X., Chang, S.Y., Young, S.R., et al. (2006). Prelamin A and lamin A appear to be dispensable in the nuclear lamina. J Clin Invest 116, 743-752.

Fortini, P., and Dogliotti, E. (2007). Base damage and single-strand break repair: mechanisms and functional significance of short- and long-patch repair subpathways. DNA Repair (Amst) 6, 398-409.

Franken, N.A., Rodermond, H.M., Stap, J., Haveman, J., and van Bree, C. (2006). Clonogenic assay of cells in vitro. Nat Protoc 1, 2315-2319.

Frescas, D., and Pagano, M. (2008). Deregulated proteolysis by the F-box proteins SKP2 and beta-TrCP: tipping the scales of cancer. Nat Rev Cancer 8, 438-449.

Freund, A., Orjalo, A.V., Desprez, P.Y., and Campisi, J. (2010). Inflammatory networks during cellular senescence: causes and consequences. Trends Mol Med 16, 238-246.

Friedberg EC. (2001) How nucleotide excision repair protects against cancer. Nat Rev Cancer 1, 22-33.

Friguet, B. (2006). Oxidized protein degradation and repair in ageing and oxidative stress. FEBS Lett 580, 2910-2916.

Frock, R.L., Kudlow, B.A., Evans, A.M., Jameson, S.A., Hauschka, S.D., and Kennedy, B.K. (2006). Lamin A/C and emerin are critical for skeletal muscle satellite cell differentiation. Genes Dev 20, 486-500.

Frolov, M.V., and Dyson, N.J. (2004). Molecular mechanisms of E2F-dependent activation and pRB-mediated repression. Journal of Cell Science 117, 2173-2181.

Fromme, J.C., and Verdine, G.L. (2004). Base excision repair. Adv Protein Chem 69, 1-41.

Fujita, M., Ishimi, Y., Nakamura, H., Kiyono, T., and Tsurumi, T. (2002). Nuclear organization of DNA replication initiation proteins in mammalian cells. The Journal of Biological Chemistry 277, 10354-10361.

Furukawa, K., and Hotta, Y. (1993). cDNA cloning of a germ cell specific lamin B3 from mouse spermatocytes and analysis of its function by ectopic expression in somatic cells. EMBO J 12, 97-106.

Furukawa, K., Inagaki, H., and Hotta, Y. (1994). Identification and cloning of an mRNA coding for a germ cell-specific A-type lamin in mice. Exp Cell Res 212, 426-430.

Furukawa, K., and Kondo, T. (1998). Identification of the lamina-associated-polypeptide-2-binding domain of B-type lamin. Eur J Biochem 251, 729-733.

Furukawa, K., Pante, N., Aebi, U., and Gerace, L. (1995). Cloning of a cDNA for lamina-associated polypeptide 2 (LAP2) and identification of regions that specify targeting to the nuclear envelope. EMBO J 14, 1626-1636.

Gajewski, A., Csaszar, E., and Foisner, R. (2004). A phosphorylation cluster in the chromatin-binding region regulates chromosome association of LAP2alpha. Journal of Biological Chemistry 279, 35813-35821.

Galanty, Y., Belotserkovskaya, R., Coates, J., Polo, S., Miller, K.M., and Jackson, S.P. (2009). Mammalian SUMO E3-ligases PIAS1 and PIAS4 promote responses to DNA double-strand breaks. Nature 462, 935-939.

Galderisi, U., Cipollaro, M., and Giordano, A. (2006). The retinoblastoma gene is involved in multiple aspects of stem cell biology. Oncogene 25, 5250-5256.

Garcia-Higuera, I., Taniguchi, T., Ganesan, S., Meyn, M.S., Timmers, C., Hejna, J., Grompe, M., and D'Andrea, A.D. (2001). Interaction of the Fanconi anemia proteins and BRCA1 in a common pathway. Mol Cell 7, 249-262.

Garg, A., Peshock, R.M., and Fleckenstein, J.L. (1999). Adipose tissue distribution pattern in patients with familial partial lipodystrophy (Dunnigan variety). J Clin Endocrinol Metab 84, 170-174.

Garinis, G.A., van der Horst, G.T., Vijg, J., and Hoeijmakers, J.H. (2008). DNA damage and ageing: new-age ideas for an age-old problem. Nature Cell Biology 10, 1241-1247.

Gartel, A.L., and Tyner, A.L. (1999). Transcriptional regulation of the p21((WAF1/CIP1)) gene. Exp Cell Res 246, 280-289.

Gerace, L., and Foisner, R. (1994). Integral membrane proteins and dynamic organization of the nuclear envelope. Trends Cell Biol 4, 127-131.

Giacinti, C., and Giordano, A. (2006). RB and cell cycle progression. Oncogene 25, 5220-5227.

Gil, J., and Peters, G. (2006). Regulation of the INK4b-ARF-INK4a tumour suppressor locus: all for one or one for all. Nature Reviews Molecular Cell Biology 7, 667-677.

Gilbert, D.M. (2004). In search of the holy replicator. Nature Reviews Molecular Cell Biology 5, 848-855.

Glass, C.A., Glass, J.R., Taniura, H., Hasel, K.W., Blevitt, J.M., and Gerace, L. (1993). The alpha-helical rod domain of human lamins A and C contains a chromatin binding site. EMBO J 12, 4413-4424.

Goldberg, M., Stucki, M., Falck, J., D'Amours, D., Rahman, D., Pappin, D., Bartek, J., and Jackson, S.P. (2003). MDC1 is required for the intra-S-phase DNA damage checkpoint. Nature 421, 952-956.

Goldberg, M.W., Huttenlauch, I., Hutchison, C.J., and Stick, R. (2008). Filaments made from A- and B-type lamins differ in structure and organization. Journal of Cell Science 121, 215-225.

Goldman, R.D., Gruenbaum, Y., Moir, R.D., Shumaker, D.K., and Spann, T.P. (2002). Nuclear lamins: building blocks of nuclear architecture. Genes Dev 16, 533-547.

Goldman, R.D., Shumaker, D.K., Erdos, M.R., Eriksson, M., Goldman, A.E., Gordon, L.B., Gruenbaum, Y., Khuon, S., Mendez, M., Varga, R., et al. (2004). Accumulation of mutant lamin A causes progressive changes in nuclear architecture in Hutchinson-Gilford progeria syndrome. Proc Natl Acad Sci U S A 101, 8963-8968.

Gonzalez, J.M., Navarro-Puche, A., Casar, B., Crespo, P., and Andres, V. (2008). Fast regulation of AP-1 activity through interaction of lamin A/C, ERK1/2, and c-Fos at the nuclear envelope. The Journal of Cell Biology 183, 653-666.

Gonzalez-Suarez, I., Redwood, A.B., Perkins, S.M., Vermolen, B., Lichtensztejin, D., Grotsky, D.A., Morgado-Palacin, L., Gapud, E.J., Sleckman, B.P., Sullivan, T., et al. (2009). Novel roles for A-type lamins in telomere biology and the DNA damage response pathway. The EMBO Journal 28, 2414-2427.

Goodarzi, A.A., Jeggo, P., and Lobrich, M. (2010). The influence of heterochromatin on DNA double strand break repair: Getting the strong, silent type to relax. DNA Repair (Amst) 9, 1273-1282.

Gorbunova, V., Seluanov, A., Mao, Z., and Hine, C. (2007). Changes in DNA repair during aging. Nucleic Acids Research 35, 7466-7474.

Gorbunova, V., Seluanov, A., and Pereira-Smith, O.M. (2002). Expression of human telomerase (hTERT) does not prevent stress-induced senescence in normal human fibroblasts but protects the cells from stress-induced apoptosis and necrosis. Journal of Biological Chemistry 277, 38540-38549.

Gorgoulis, V.G., and Halazonetis, T.D. (2010). Oncogene-induced senescence: the bright and dark side of the response. Curr Opin Cell Biol 22, 816-827.

Gorlich, D., and Kutay, U. (1999). Transport between the cell nucleus and the cytoplasm. Annu Rev Cell Dev Biol 15, 607-660.

Graumann, K., and Evans, D.E. (2011). Nuclear envelope dynamics during plant cell division suggest common mechanisms between kingdoms. Biochem J 435, 661-667.

Green, C.M., Erdjument-Bromage, H., Tempst, P., and Lowndes, N.F. (2000). A novel Rad24 checkpoint protein complex closely related to replication factor C. Curr Biol 10, 39-42.

Gruenbaum, Y., Margalit, A., Goldman, R.D., Shumaker, D.K., and Wilson, K.L. (2005). The nuclear lamina comes of age. Nat Rev Mol Cell Biol 6, 21-31.

Guardavaccaro, D., and Pagano, M. (2006). Stabilizers and destabilizers controlling cell cycle oscillators. Mol Cell 22, 1-4.

Guelen, L., Pagie, L., Brasset, E., Meuleman, W., Faza, M.B., Talhout, W., Eussen, B.H., de Klein, A., Wessels, L., de Laat, W., et al. (2008). Domain organization of human chromosomes revealed by mapping of nuclear lamina interactions. Nature 453, 948-951.

Haddad, J.J. (2002). Antioxidant and prooxidant mechanisms in the regulation of redox(y)-sensitive transcription factors. Cell Signal 14, 879-897.

Haddad, J.J. (2004). Oxygen sensing and oxidant/redox-related pathways. Biochemical and Biophysical Research Communications 316, 969-977.

Hagen, J.L., Krause, D.J., Baker, D.J., Fu, M.H., Tarnopolsky, M.A., and Hepple, R.T. (2004). Skeletal muscle aging in F344BN F1-hybrid rats: I. Mitochondrial dysfunction contributes to the age-associated reduction in VO2max. J Gerontol A Biol Sci Med Sci 59, 1099-1110.

Haithcock, E., Dayani, Y., Neufeld, E., Zahand, A.J., Feinstein, N., Mattout, A., Gruenbaum, Y., and Liu, J. (2005). Age-related changes of nuclear architecture in Caenorhabditis elegans. Proceedings of the National Academy of Sciences of the United States of America 102, 16690-16695.

Halazonetis, T.D., Gorgoulis, V.G., and Bartek, J. (2008). An oncogene-induced DNA damage model for cancer development. Science 319, 1352-1355.

Hall, M., and Peters, G. (1996). Genetic alterations of cyclins, cyclin-dependent kinases, and Cdk inhibitors in human cancer. Adv Cancer Res 68, 67-108.

Hamilton, M.L., Van Remmen, H., Drake, J.A., Yang, H., Guo, Z.M., Kewitt, K., Walter, C.A., and Richardson, A. (2001). Does oxidative damage to DNA increase with age? Proceedings of the National Academy of Sciences of the United States of America 98, 10469-10474.

Han, X., Feng, X., Rattner, J.B., Smith, H., Bose, P., Suzuki, K., Soliman, M.A., Scott, M.S., Burke, B.E., and Riabowol, K. (2008). Tethering by lamin A stabilizes and targets the ING1 tumour suppressor. Nature Cell Biology 10, 1333-1340.

Hanahan, D., and Weinberg, R.A. (2000). The hallmarks of cancer. Cell 100, 57-70.

Hanahan, D., and Weinberg, R.A. (2011). Hallmarks of cancer: the next generation. Cell 144, 646-674.

Hanawalt, P.C. (2007). Paradigms for the three rs: DNA replication, recombination, and repair. Mol Cell 28, 702-707.

Hanawalt, P.C., and Spivak, G. (2008). Transcription-coupled DNA repair: two decades of progress and surprises. Nature Reviews Molecular Cell Biology 9, 958-970.

Hansen, D.V., Loktev, A.V., Ban, K.H., and Jackson, P.K. (2004). Plk1 regulates activation of the anaphase promoting complex by phosphorylating and triggering SCFbetaTrCP-dependent destruction of the APC Inhibitor Emi1. Mol Biol Cell 15, 5623-5634.

Harborth, J., Elbashir, S.M., Bechert, K., Tuschl, T., and Weber, K. (2001). Identification of essential genes in cultured mammalian cells using small interfering RNAs. J Cell Sci 114, 4557-4565.

Harman, D. (1956). Aging: a theory based on free radical and radiation chemistry. J Gerontol 11, 298-300.

Harper, M., Tillit, J., Kress, M., and Ernoult-Lange, M. (2009). Phosphorylation-dependent binding of human transcription factor MOK2 to lamin A/C. FEBS J 276, 3137-3147.

Hartlerode, A.J., and Scully, R. (2009). Mechanisms of double-strand break repair in somatic mammalian cells. Biochem J 423, 157-168.

Hasty, P., Campisi, J., Hoeijmakers, J., van Steeg, H., and Vijg, J. (2003). Aging and genome maintenance: lessons from the mouse? Science 299, 1355-1359.

Hayflick, L., and Moorhead, P.S. (1961). The serial cultivation of human diploid cell strains. Exp Cell Res 25, 585-621.

Heald, R., McLoughlin, M., and McKeon, F. (1993). Human wee1 maintains mitotic timing by protecting the nucleus from cytoplasmically activated Cdc2 kinase. Cell 74, 463-474.

Heessen, S., and Fornerod, M. (2007). The inner nuclear envelope as a transcription factor resting place. EMBO Rep 8, 914-919.

Hegele, R.A. (2003). Lamin mutations come of age. Nat Med 9, 644-645.

Hegele, R.A., Cao, H., Anderson, C.M., and Hramiak, I.M. (2000). Heterogeneity of nuclear lamin A mutations in Dunnigan-type familial partial lipodystrophy. J Clin Endocrinol Metab 85, 3431-3435.

Hegele, R.A., Cao, H., Liu, D.M., Costain, G.A., Charlton-Menys, V., Rodger, N.W., and Durrington, P.N. (2006). Sequencing of the reannotated LMNB2 gene reveals novel mutations in patients with acquired partial lipodystrophy. Am J Hum Genet 79, 383-389.

Hemann, M.T., Hackett, J., A, I.J., and Greider, C.W. (2000). Telomere length, telomere-binding proteins, and DNA damage signaling. Cold Spring Harb Symp Quant Biol 65, 275-279.

Hengst, L., and Reed, S.I. (1998). Inhibitors of the Cip/Kip family. Curr Top Microbiol Immunol 227, 25-41.

Hennekam, R.C. (2006). Hutchinson-Gilford progeria syndrome: review of the phenotype. Am J Med Genet A 140, 2603-2624.

Hennekes, H., and Nigg, E.A. (1994). The role of isoprenylation in membrane attachment of nuclear lamins. A single point mutation prevents proteolytic cleavage of the lamin A precursor and confers membrane binding properties. Journal of Cell Science 107 (Pt 4), 1019-1029.

Herbig, U., Jobling, W.A., Chen, B.P., Chen, D.J., and Sedivy, J.M. (2004). Telomere shortening triggers senescence of human cells through a pathway involving ATM, p53, and p21(CIP1), but not p16(INK4a). Mol Cell 14, 501-513.

Hernandez, L., Roux, K.J., Wong, E.S., Mounkes, L.C., Mutalif, R., Navasankari, R., Rai, B., Cool, S., Jeong, J.W., Wang, H., et al. (2010). Functional coupling between the extracellular matrix and nuclear lamina by Wnt signaling in progeria. Dev Cell 19, 413-425.

Herrmann, H., and Aebi, U. (2004). Intermediate filaments: molecular structure, assembly mechanism, and integration into functionally distinct intracellular Scaffolds. Annu Rev Biochem 73, 749-789.

Heyer, W.D., Ehmsen, K.T., and Liu, J. (2010). Regulation of homologous recombination in eukaryotes. Annu Rev Genet 44, 113-139.

Hiom, K. (2010). Coping with DNA double strand breaks. DNA Repair (Amst) 9, 1256-1263.

Hiratani, I., Takebayashi, S., Lu, J., and Gilbert, D.M. (2009). Replication timing and transcriptional control: beyond cause and effect--part II. Current Opinion in Genetics & Development 19, 142-149.

Ho, G.P., Margossian, S., Taniguchi, T., and D'Andrea, A.D. (2006). Phosphorylation of FANCD2 on two novel sites is required for mitomycin C resistance. Molecular and Cellular Biology 26, 7005-7015.

Hodzic, D.M., Yeater, D.B., Bengtsson, L., Otto, H., and Stahl, P.D. (2004). Sun2 is a novel mammalian inner nuclear membrane protein. The Journal of Biological Chemistry 279, 25805-25812.

Hoeijmakers, J.H. (2001). DNA repair mechanisms. Maturitas 38, 17-22; discussion 22-13.

Hoeijmakers, J.H. (2009). DNA damage, aging, and cancer. The New England Journal of Medicine 361, 1475-1485.

Hoger, T.H., Zatloukal, K., Waizenegger, I., and Krohne, G. (1990). Characterization of a second highly conserved B-type lamin present in cells previously thought to contain only a single B-type lamin. Chromosoma 100, 67-69.

Holtz, D., Tanaka, R.A., Hartwig, J., and McKeon, F. (1989). The CaaX motif of lamin A functions in conjunction with the nuclear localization signal to target assembly to the nuclear envelope. Cell 59, 969-977.

Hopfner, K.P., Craig, L., Moncalian, G., Zinkel, R.A., Usui, T., Owen, B.A., Karcher, A., Henderson, B., Bodmer, J.L., McMurray, C.T., et al. (2002). The Rad50 zinc-hook is a structure joining Mre11 complexes in DNA recombination and repair. Nature 418, 562-566.

Hopfner, K.P., Karcher, A., Craig, L., Woo, T.T., Carney, J.P., and Tainer, J.A. (2001). Structural biochemistry and interaction architecture of the DNA double-strand break repair Mre11 nuclease and Rad50-ATPase. Cell 105, 473-485.

Houben, F., Ramaekers, F.C., Snoeckx, L.H., and Broers, J.L. (2007). Role of nuclear lamina-cytoskeleton interactions in the maintenance of cellular strength. Biochim Biophys Acta 1773, 675-686.

Houben, F., Willems, C.H., Declercq, I.L., Hochstenbach, K., Kamps, M.A., Snoeckx, L.H., Ramaekers, F.C., and Broers, J.L. (2009). Disturbed nuclear orientation and cellular migration in A-type lamin deficient cells. Biochim Biophys Acta 1793, 312-324.

Houliston, E., Guilly, M.N., Courvalin, J.C., and Maro, B. (1988). Expression of nuclear lamins during mouse preimplantation development. Development 102, 271-278.

Hsieh, P., and Yamane, K. (2008). DNA mismatch repair: molecular mechanism, cancer, and ageing. Mech Ageing Dev 129, 391-407.

Huang, S., Risques, R.A., Martin, G.M., Rabinovitch, P.S., and Oshima, J. (2008). Accelerated telomere shortening and replicative senescence in human fibroblasts overexpressing mutant and wild-type lamin A. Exp Cell Res 314, 82-91.

Hubner, M.R., and Spector, D.L. (2010). Chromatin dynamics. Annu Rev Biophys 39, 471-489.

Huen, M.S., and Chen, J. (2010). Assembly of checkpoint and repair machineries at DNA damage sites. Trends in Biochemical Sciences 35, 101-108.

Huen, M.S., Grant, R., Manke, I., Minn, K., Yu, X., Yaffe, M.B., and Chen, J. (2007). RNF8 transduces the DNA-damage signal via histone ubiquitylation and checkpoint protein assembly. Cell 131, 901-914.

Huen, M.S., Huang, J., Leung, J.W., Sy, S.M., Leung, K.M., Ching, Y.P., Tsao, S.W., and Chen, J. (2010). Regulation of chromatin architecture by the PWWP domain-containing DNA damage-responsive factor EXPAND1/MUM1. Mol Cell 37, 854-864.

Huertas, P. (2010). DNA resection in eukaryotes: deciding how to fix the break. Nat Struct Mol Biol 17, 11-16.

Hutchison, C.J. (2002). Lamins: building blocks or regulators of gene expression? Nat Rev Mol Cell Biol 3, 848-858.

Hutchison, C.J., Alvarez-Reyes, M., and Vaughan, O.A. (2001). Lamins in disease: why do ubiquitously expressed nuclear envelope proteins give rise to tissue-specific disease phenotypes? J Cell Sci 114, 9-19.

Hutchison, C.J., and Worman, H.J. (2004). A-type lamins: guardians of the soma? Nat Cell Biol 6, 1062-1067.

Huyen, Y., Zgheib, O., Ditullio, R.A., Jr., Gorgoulis, V.G., Zacharatos, P., Petty, T.J., Sheston, E.A., Mellert, H.S., Stavridi, E.S., and Halazonetis, T.D. (2004). Methylated lysine 79 of histone H3 targets 53BP1 to DNA double-strand breaks. Nature 432, 406-411.

Iacovoni, J.S., Caron, P., Lassadi, I., Nicolas, E., Massip, L., Trouche, D., and Legube, G. (2010). High-resolution profiling of gammaH2AX around DNA double strand breaks in the mammalian genome. The EMBO Journal 29, 1446-1457.

Imai, S., Nishibayashi, S., Takao, K., Tomifuji, M., Fujino, T., Hasegawa, M., and Takano, T. (1997). Dissociation of Oct-1 from the nuclear peripheral structure induces the cellular aging-associated collagenase gene expression. Mol Biol Cell 8, 2407-2419.

Ishiai, M., Kitao, H., Smogorzewska, A., Tomida, J., Kinomura, A., Uchida, E., Saberi, A., Kinoshita, E., Kinoshita-Kikuta, E., Koike, T., et al. (2008). FANCI phosphorylation functions as a molecular switch to turn on the Fanconi anemia pathway. Nat Struct Mol Biol 15, 1138-1146.

Ivorra, C., Kubicek, M., Gonzalez, J.M., Sanz-Gonzalez, S.M., Alvarez-Barrientos, A., O'Connor, J.E., Burke, B., and Andres, V. (2006). A mechanism of AP-1 suppression through interaction of c-Fos with lamin A/C. Genes Dev 20, 307-320.

Iwabuchi, K., Bartel, P.L., Li, B., Marraccino, R., and Fields, S. (1994). Two cellular proteins that bind to wild-type but not mutant p53. Proceedings of the National Academy of Sciences of the United States of America 91, 6098-6102.

Iwabuchi, K., Basu, B.P., Kysela, B., Kurihara, T., Shibata, M., Guan, D., Cao, Y., Hamada, T., Imamura, K., Jeggo, P.A., et al. (2003). Potential role for 53BP1 in DNA end-joining repair through direct interaction with DNA. The Journal of Biological Chemistry 278, 36487-36495.

Iwabuchi, K., Hashimoto, M., Matsui, T., Kurihara, T., Shimizu, H., Adachi, N., Ishiai, M., Yamamoto, K., Tauchi, H., Takata, M., et al. (2006). 53BP1 contributes to survival of cells irradiated with X-ray during G1 without Ku70 or Artemis. Genes Cells 11, 935-948.

Izumi, M., Vaughan, O.A., Hutchison, C.J., and Gilbert, D.M. (2000). Head and/or CaaX domain deletions of lamin proteins disrupt preformed lamin A and C but not lamin B structure in mammalian cells. Mol Biol Cell 11, 4323-4337.

Jackson, S.P., and Bartek, J. (2009). The DNA-damage response in human biology and disease. Nature 461, 1071-1078.

Jacobs, J.J., and de Lange, T. (2004). Significant role for p16INK4a in p53-independent telomere-directed senescence. Curr Biol 14, 2302-2308.

Janaki Ramaiah, M., and Parnaik, V.K. (2006). An essential GT motif in the lamin A promoter mediates activation by CREB-binding protein. Biochemical and biophysical research communications 348, 1132-1137.

Janzen, V., Forkert, R., Fleming, H.E., Saito, Y., Waring, M.T., Dombkowski, D.M., Cheng, T., DePinho, R.A., Sharpless, N.E., and Scadden, D.T. (2006). Stem-cell ageing modified by the cyclin-dependent kinase inhibitor p16INK4a. Nature 443, 421-426.

Jascur, T., and Boland, C.R. (2006). Structure and function of the components of the human DNA mismatch repair system. Int J Cancer 119, 2030-2035.

Jaskelioff, M., Muller, F.L., Paik, J.H., Thomas, E., Jiang, S., Adams, A.C., Sahin, E., Kost-Alimova, M., Protopopov, A., Cadinanos, J., et al. (2011). Telomerase reactivation reverses tissue degeneration in aged telomerase-deficient mice. Nature 469, 102-106.

Jeffrey, P.D., Russo, A.A., Polyak, K., Gibbs, E., Hurwitz, J., Massague, J., and Pavletich, N.P. (1995). Mechanism of CDK activation revealed by the structure of a cyclinA-CDK2 complex. Nature 376, 313-320.

Jeyapalan, J.C., Ferreira, M., Sedivy, J.M., and Herbig, U. (2007). Accumulation of senescent cells in mitotic tissue of aging primates. Mech Ageing Dev 128, 36-44.

Ji, J.Y., Lee, R.T., Vergnes, L., Fong, L.G., Stewart, C.L., Reue, K., Young, S.G., Zhang, Q., Shanahan, C.M., and Lammerding, J. (2007). Cell nuclei spin in the absence of lamin b1. The Journal of Biological Chemistry 282, 20015-20026.

Ji, P., Jiang, H., Rekhtman, K., Bloom, J., Ichetovkin, M., Pagano, M., and Zhu, L. (2004). An Rb-Skp2-p27 pathway mediates acute cell cycle inhibition by Rb and is retained in a partial-penetrance Rb mutant. Mol Cell 16, 47-58.

Jin, J., Cardozo, T., Lovering, R.C., Elledge, S.J., Pagano, M., and Harper, J.W. (2004). Systematic analysis and nomenclature of mammalian F-box proteins. Genes Dev 18, 2573-2580.

Johnson, B.R., Nitta, R.T., Frock, R.L., Mounkes, L., Barbie, D.A., Stewart, C.L., Harlow, E., and Kennedy, B.K. (2004). A-type lamins regulate retinoblastoma protein function by promoting subnuclear localization and preventing proteasomal degradation. Proc Natl Acad Sci U S A 101, 9677-9682.

Johnson, D.G., and Walker, C.L. (1999). Cyclins and cell cycle checkpoints. Annu Rev Pharmacol Toxicol 39, 295-312.

Jones, S., Zhang, X., Parsons, D.W., Lin, J.C., Leary, R.J., Angenendt, P., Mankoo, P., Carter, H., Kamiyama, H., Jimeno, A., et al. (2008). Core signaling pathways in human pancreatic cancers revealed by global genomic analyses. Science 321, 1801-1806.

Jowsey, P., Morrice, N.A., Hastie, C.J., McLauchlan, H., Toth, R., and Rouse, J. (2007). Characterisation of the sites of DNA damage-induced 53BP1 phosphorylation catalysed by ATM and ATR. DNA Repair (Amst) 6, 1536-1544.

Jun, S.H., Kim, T.G., and Ban, C. (2006). DNA mismatch repair system. Classical and fresh roles. FEBS J 273, 1609-1619.

Kadyrov, F.A., Genschel, J., Fang, Y., Penland, E., Edelmann, W., and Modrich, P. (2009). A possible mechanism for exonuclease 1-independent eukaryotic mismatch repair. Proceedings of the National Academy of Sciences of the United States of America 106, 8495-8500.

Kaidi, A., Weinert, B.T., Choudhary, C., and Jackson, S.P. (2010). Human SIRT6 promotes DNA end resection through CtIP deacetylation. Science 329, 1348-1353.

Kamb, A. (1998). Cyclin-dependent kinase inhibitors and human cancer. Curr Top Microbiol Immunol 227, 139-148.

Kasashima, K., Nakamura, Y., and Kozu, T. (2004). Altered expression profiles of microRNAs during TPA-induced differentiation of HL-60 cells. Biochemical and Biophysical Research Communications 322, 403-410.

Kass, E.M., and Jasin, M. (2010). Collaboration and competition between DNA double-strand break repair pathways. FEBS Lett 584, 3703-3708.

Kee, Y., and D'Andrea, A.D. (2010). Expanded roles of the Fanconi anemia pathway in preserving genomic stability. Genes Dev 24, 1680-1694.

Kelly, T.J., and Brown, G.W. (2000). Regulation of chromosome replication. Annual Review of Biochemistry 69, 829-880.

Kennedy, B.K., Barbie, D.A., Classon, M., Dyson, N., and Harlow, E. (2000). Nuclear organization of DNA replication in primary mammalian cells. Genes Dev 14, 2855-2868.

Kenyon, C. (2005). The plasticity of aging: insights from long-lived mutants. Cell 120, 449-460.

Kerzendorfer, C., and O'Driscoll, M. (2009). Human DNA damage response and repair deficiency syndromes: linking genomic instability and cell cycle checkpoint proficiency. DNA Repair (Amst) 8, 1139-1152.

Kill, I.R., Bridger, J.M., Campbell, K.H., Maldonado-Codina, G., and Hutchison, C.J. (1991). The timing of the formation and usage of replicase clusters in S-phase nuclei of human diploid fibroblasts. Journal of Cell Science 100 (Pt 4), 869-876.

Kim, S.T., Lim, D.S., Canman, C.E., and Kastan, M.B. (1999). Substrate specificities and identification of putative substrates of ATM kinase family members. The Journal of Biological Chemistry 274, 37538-37543.

Kim, W.Y., and Sharpless, N.E. (2006). The regulation of INK4/ARF in cancer and aging. Cell 127, 265-275.

Kind, J., and van Steensel, B. (2010). Genome-nuclear lamina interactions and gene regulation. Curr Opin Cell Biol 22, 320-325.

Kinzler, K.W., and Vogelstein, B. (1997). Cancer-susceptibility genes. Gatekeepers and caretakers. Nature 386, 761, 763.

Kirkwood, T. (2006). Ageing: too fast by mistake. Nature 444, 1015-1017.

Kirkwood, T.B. (2002). Evolution of ageing. Mech Ageing Dev 123, 737-745.

Kirkwood, T.B. (2005). Understanding the odd science of aging. Cell 120, 437-447.

Kitten, G.T., and Nigg, E.A. (1991). The CaaX motif is required for isoprenylation, carboxyl methylation, and nuclear membrane association of lamin B2. J Cell Biol 113, 13-23.

Knipscheer, P., Raschle, M., Smogorzewska, A., Enoiu, M., Ho, T.V., Scharer, O.D., Elledge, S.J., and Walter, J.C. (2009). The Fanconi anemia pathway promotes replication-dependent DNA interstrand cross-link repair. Science 326, 1698-1701.

Knudsen, E.S., and Knudsen, K.E. (2008). Tailoring to RB: tumour suppressor status and therapeutic response. Nat Rev Cancer 8, 714-724.

Knudson, A.G., Jr. (1971). Mutation and cancer: statistical study of retinoblastoma. Proceedings of the National Academy of Sciences of the United States of America 68, 820-823.

Kobberling, J., and Dunnigan, M.G. (1986). Familial partial lipodystrophy: two types of an X linked dominant syndrome, lethal in the hemizygous state. J Med Genet 23, 120-127.

Koch, C.A., Agyei, R., Galicia, S., Metalnikov, P., O'Donnell, P., Starostine, A., Weinfeld, M., and Durocher, D. (2004). Xrcc4 physically links DNA end processing by polynucleotide kinase to DNA ligation by DNA ligase IV. The EMBO Journal 23, 3874-3885.

Kolas, N.K., Chapman, J.R., Nakada, S., Ylanko, J., Chahwan, R., Sweeney, F.D., Panier, S., Mendez, M., Wildenhain, J., Thomson, T.M., et al. (2007). Orchestration of the DNA-damage response by the RNF8 ubiquitin ligase. Science 318, 1637-1640.

Korenjak, M., and Brehm, A. (2005). E2F-Rb complexes regulating transcription of genes important for differentiation and development. Curr Opin Genet Dev 15, 520-527.

Kozakov, D., Hall, D.R., Beglov, D., Brenke, R., Comeau, S.R., Shen, Y., Li, K., Zheng, J., Vakili, P., Paschalidis, I., et al. (2010). Achieving reliability and high accuracy in automated protein docking: ClusPro, PIPER, SDU, and stability analysis in CAPRI rounds 13-19. Proteins 78, 3124-3130.

Kozlov, S.V., Graham, M.E., Peng, C., Chen, P., Robinson, P.J., and Lavin, M.F. (2006). Involvement of novel autophosphorylation sites in ATM activation. The EMBO Journal 25, 3504-3514.

Kregel, K.C., and Zhang, H.J. (2007). An integrated view of oxidative stress in aging: basic mechanisms, functional effects, and pathological considerations. Am J Physiol Regul Integr Comp Physiol 292, R18-36.

Krimm, I., Ostlund, C., Gilquin, B., Couprie, J., Hossenlopp, P., Mornon, J.P., Bonne, G., Courvalin, J.C., Worman, H.J., and Zinn-Justin, S. (2002). The Ig-like structure of the C-terminal domain of lamin A/C, mutated in muscular dystrophies, cardiomyopathy, and partial lipodystrophy. Structure 10, 811-823.

Krishnamurthy, J., Ramsey, M.R., Ligon, K.L., Torrice, C., Koh, A., Bonner-Weir, S., and Sharpless, N.E. (2006). p16INK4a induces an age-dependent decline in islet regenerative potential. Nature 443, 453-457.

Krizhanovsky, V., Xue, W., Zender, L., Yon, M., Hernando, E., and Lowe, S.W. (2008). Implications of cellular senescence in tissue damage response, tumor suppression, and stem cell biology. Cold Spring Harb Symp Quant Biol 73, 513-522.

Krtolica, A., Parrinello, S., Lockett, S., Desprez, P.Y., and Campisi, J. (2001). Senescent fibroblasts promote epithelial cell growth and tumorigenesis: a link between cancer and aging. Proceedings of the National Academy of Sciences of the United States of America 98, 12072-12077.

Kubben, N., Voncken, J.W., Demmers, J., Calis, C., van Almen, G., Pinto, Y., and Misteli, T. (2010). Identification of differential protein interactors of lamin A and progerin. Nucleus 1, 513-525.

Kudlow, B.A., Kennedy, B.K., and Monnat, R.J., Jr. (2007). Werner and Hutchinson-Gilford progeria syndromes: mechanistic basis of human progeroid diseases. Nature Reviews Molecular Cell Biology 8, 394-404.

Kumaran, R.I., and Spector, D.L. (2008). A genetic locus targeted to the nuclear periphery in living cells maintains its transcriptional competence. The Journal of Cell Biology 180, 51-65.

Kunkel, T.A., and Erie, D.A. (2005). DNA mismatch repair. Annual Review of Biochemistry 74, 681-710.

Lamarche, B.J., Orazio, N.I., and Weitzman, M.D. (2010). The MRN complex in double-strand break repair and telomere maintenance. FEBS Lett 584, 3682-3695.

Lammerding, J., Schulze, P.C., Takahashi, T., Kozlov, S., Sullivan, T., Kamm, R.D., Stewart, C.L., and Lee, R.T. (2004). Lamin A/C deficiency causes defective nuclear mechanics and mechanotransduction. J Clin Invest 113, 370-378.

Lamond, A.I., and Earnshaw, W.C. (1998). Structure and function in the nucleus. Science 280, 547-553.

Lang, C., and Krohne, G. (2003). Lamina-associated polypeptide 2beta (LAP2beta) is contained in a protein complex together with A- and B-type lamins. European Journal of Cell Biology 82, 143-153.

Lang, C., Paulin-Levasseur, M., Gajewski, A., Alsheimer, M., Benavente, R., and Krohne, G. (1999). Molecular characterization and developmentally regulated expression of Xenopus lamina-associated polypeptide 2 (XLAP2). J Cell Sci 112 (Pt 5), 749-759.

Lanoix, J., Skup, D., Collard, J.F., and Raymond, Y. (1992). Regulation of the expression of lamins A and C is post-transcriptional in P19 embryonal carcinoma cells. Biochem Biophys Res Commun 189, 1639-1644.

Larrea, A.A., Lujan, S.A., and Kunkel, T.A. (2010). SnapShot: DNA mismatch repair. Cell 141, 730 e731.

Larsen, D.H., Poinsignon, C., Gudjonsson, T., Dinant, C., Payne, M.R., Hari, F.J., Danielsen, J.M., Menard, P., Sand, J.C., Stucki, M., et al. (2010). The chromatin-remodeling factor CHD4 coordinates signaling and repair after DNA damage. The Journal of Cell Biology 190, 731-740.

Lavin, M.F. (2008). Ataxia-telangiectasia: from a rare disorder to a paradigm for cell signalling and cancer. Nature Reviews Molecular Cell Biology 9, 759-769.

Lebel, S., Lampron, C., Royal, A., and Raymond, Y. (1987). Lamins A and C appear during retinoic acid-induced differentiation of mouse embryonal carcinoma cells. J Cell Biol 105, 1099-1104.

Lee, D.C., Welton, K.L., Smith, E.D., and Kennedy, B.K. (2009). A-type nuclear lamins act as transcriptional repressors when targeted to promoters. Exp Cell Res 315, 996-1007.

Lee, J.H., Cheong, H.M., Kang, M.Y., Kim, S.Y., and Kang, Y. (2009). Ser1778 of 53BP1 Plays a Role in DNA Double-strand Break Repairs. Korean J Physiol Pharmacol 13, 343-348.

Lee, J.H., Goodarzi, A.A., Jeggo, P.A., and Paull, T.T. (2010). 53BP1 promotes ATM activity through direct interactions with the MRN complex. The EMBO Journal 29, 574-585.

Lee, J.H., and Paull, T.T. (2004). Direct activation of the ATM protein kinase by the Mre11/Rad50/Nbs1 complex. Science 304, 93-96.

Lee, J.H., and Paull, T.T. (2005). ATM activation by DNA double-strand breaks through the Mre11-Rad50-Nbs1 complex. Science 308, 551-554.

Lee, J.S., Hale, C.M., Panorchan, P., Khatau, S.B., George, J.P., Tseng, Y., Stewart, C.L., Hodzic, D., and Wirtz, D. (2007). Nuclear lamin A/C deficiency induces defects in cell mechanics, polarization, and migration. Biophys J 93, 2542-2552.

Lehner, C.F., Furstenberger, G., Eppenberger, H.M., and Nigg, E.A. (1986). Biogenesis of the nuclear lamina: in vivo synthesis and processing of nuclear protein precursors. Proc Natl Acad Sci U S A 83, 2096-2099.

Lelliott, C.J., Logie, L., Sewter, C.P., Berger, D., Jani, P., Blows, F., O'Rahilly, S., and Vidal-Puig, A. (2002). Lamin expression in human adipose cells in relation to anatomical site and differentiation state. J Clin Endocrinol Metab 87, 728-734.

Levy, N., Lopez-Otin, C., and Hennekam, R.C. (2005). Defective prelamin A processing resulting from LMNA or ZMPSTE24 mutations as the cause of restrictive dermopathy. Arch Dermatol 141, 1473-1474.

Lew, D.J., and Kornbluth, S. (1996). Regulatory roles of cyclin dependent kinase phosphorylation in cell cycle control. Curr Opin Cell Biol 8, 795-804.

Li, J., Meyer, A.N., and Donoghue, D.J. (1997). Nuclear localization of cyclin B1 mediates its biological activity and is regulated by phosphorylation. Proceedings of the National Academy of Sciences of the United States of America 94, 502-507.

Li, L., and Zou, L. (2005). Sensing, signaling, and responding to DNA damage: organization of the checkpoint pathways in mammalian cells. J Cell Biochem 94, 298-306.

Lim, R.Y., and Fahrenkrog, B. (2006). The nuclear pore complex up close. Curr Opin Cell Biol 18, 342-347.

Limoli, C.L., and Ward, J.F. (1993). A new method for introducing double-strand breaks into cellular DNA. Radiat Res 134, 160-169.

Lin, F., and Worman, H.J. (1993). Structural organization of the human gene encoding nuclear lamin A and nuclear lamin C. J Biol Chem 268, 16321-16326.

Lin, S.T., and Fu, Y.H. (2009). miR-23 regulation of lamin B1 is crucial for oligodendrocyte development and myelination. Dis Model Mech 2, 178-188.

Linke, K., and Jakob, U. (2003). Not every disulfide lasts forever: disulfide bond formation as a redox switch. Antioxid Redox Signal 5, 425-434.

Liu, B., Wang, J., Chan, K.M., Tjia, W.M., Deng, W., Guan, X., Huang, J.D., Li, K.M., Chau, P.Y., Chen, D.J., et al. (2005). Genomic instability in laminopathy-based premature aging. Nat Med 11, 780-785.

Liu, G.H., Barkho, B.Z., Ruiz, S., Diep, D., Qu, J., Yang, S.L., Panopoulos, A.D., Suzuki, K., Kurian, L., Walsh, C., et al. (2011). Recapitulation of premature ageing with iPSCs from Hutchinson-Gilford progeria syndrome. Nature 472, 221-225.

Liu, T., Ghosal, G., Yuan, J., Chen, J., and Huang, J. (2010). FAN1 acts with FANCI-FANCD2 to promote DNA interstrand cross-link repair. Science 329, 693-696.

Liu, Y., Rusinol, A., Sinensky, M., Wang, Y., and Zou, Y. (2006). DNA damage responses in progeroid syndromes arise from defective maturation of prelamin A. Journal of Cell Science 119, 4644-4649.

Liu, Y., Wang, Y., Rusinol, A.E., Sinensky, M.S., Liu, J., Shell, S.M., and Zou, Y. (2008). Involvement of xeroderma pigmentosum group A (XPA) in progeria arising from defective maturation of prelamin A. FASEB J 22, 603-611.

Lloyd, D.J., Trembath, R.C., and Shackleton, S. (2002). A novel interaction between lamin A and SREBP1: implications for partial lipodystrophy and other laminopathies. Hum Mol Genet 11, 769-777.

Loeb, L.A. (1991). Mutator phenotype may be required for multistage carcinogenesis. Cancer Res 51, 3075-3079.

Loewer, A., Batchelor, E., Gaglia, G., and Lahav, G. (2010). Basal dynamics of p53 reveal transcriptionally attenuated pulses in cycling cells. Cell 142, 89-100.

Lombard, D.B., Chua, K.F., Mostoslavsky, R., Franco, S., Gostissa, M., and Alt, F.W. (2005). DNA repair, genome stability, and aging. Cell 120, 497-512.

Lopez-Garcia, P., and Moreira, D. (2006). Selective forces for the origin of the eukaryotic nucleus. Bioessays 28, 525-533.

Lopez-Soler, R.I., Moir, R.D., Spann, T.P., Stick, R., and Goldman, R.D. (2001). A role for nuclear lamins in nuclear envelope assembly. The Journal of Cell Biology 154, 61-70.

Lou, Z., Minter-Dykhouse, K., Franco, S., Gostissa, M., Rivera, M.A., Celeste, A., Manis, J.P., van Deursen, J., Nussenzweig, A., Paull, T.T., et al. (2006). MDC1 maintains genomic stability by participating in the amplification of ATM-dependent DNA damage signals. Mol Cell 21, 187-200.

Luderus, M.E., den Blaauwen, J.L., de Smit, O.J., Compton, D.A., and van Driel, R. (1994). Binding of matrix attachment regions to lamin polymers involves single-stranded regions and the minor groove. Molecular and Cellular Biology 14, 6297-6305.

Lukas, C., Bartek, J., and Lukas, J. (2005). Imaging of protein movement induced by chromosomal breakage: tiny 'local' lesions pose great 'global' challenges. Chromosoma 114, 146-154.

Lukas, C., Falck, J., Bartkova, J., Bartek, J., and Lukas, J. (2003). Distinct spatiotemporal dynamics of mammalian checkpoint regulators induced by DNA damage. Nature Cell Biology 5, 255-260.

Lukas, C., Savic, V., Bekker-Jensen, S., Doil, C., Neumann, B., Pedersen, R.S., Grofte, M., Chan, K.L., Hickson, I.D., Bartek, J., et al. (2011). 53BP1 nuclear bodies form around DNA lesions generated by mitotic transmission of chromosomes under replication stress. Nature Cell Biology 13, 243-253.

Lukas, J., Lukas, C., and Bartek, J. (2004). Mammalian cell cycle checkpoints: signalling pathways and their organization in space and time. DNA Repair (Amst) 3, 997-1007.

Lukas, J., Sorensen, C.S., Lukas, C., Santoni-Rugiu, E., and Bartek, J. (1999). p16INK4a, but not constitutively active pRb, can impose a sustained G1 arrest: molecular mechanisms and implications for oncogenesis. Oncogene 18, 3930-3935.

Lundberg, A.S., and Weinberg, R.A. (1999). Control of the cell cycle and apoptosis. Eur J Cancer 35, 531-539.

Lutz, R.J., Trujillo, M.A., Denham, K.S., Wenger, L., and Sinensky, M. (1992). Nucleoplasmic localization of prelamin A: implications for prenylation-dependent lamin A assembly into the nuclear lamina. Proc Natl Acad Sci U S A 89, 3000-3004.

Machiels, B.M., Zorenc, A.H., Endert, J.M., Kuijpers, H.J., van Eys, G.J., Ramaekers, F.C., and Broers, J.L. (1996). An alternative splicing product of the lamin A/C gene lacks exon 10. J Biol Chem 271, 9249-9253.

MacKay, C., Declais, A.C., Lundin, C., Agostinho, A., Deans, A.J., MacArtney, T.J., Hofmann, K., Gartner, A., West, S.C., Helleday, T., et al. (2010). Identification of KIAA1018/FAN1, a DNA repair nuclease recruited to DNA damage by monoubiquitinated FANCD2. Cell 142, 65-76.

Mahaney, B.L., Meek, K., and Lees-Miller, S.P. (2009). Repair of ionizing radiation-induced DNA double-strand breaks by non-homologous end-joining. Biochem J 417, 639-650.

Maidment, S.L., and Ellis, J.A. (2002). Muscular dystrophies, dilated cardiomyopathy, lipodystrophy and neuropathy: the nuclear connection. Expert Rev Mol Med 4, 1-21.

Mailand, N., Bekker-Jensen, S., Faustrup, H., Melander, F., Bartek, J., Lukas, C., and Lukas, J. (2007). RNF8 ubiquitylates histones at DNA double-strand breaks and promotes assembly of repair proteins. Cell 131, 887-900.

Mailand, N., and Diffley, J.F. (2005). CDKs promote DNA replication origin licensing in human cells by protecting Cdc6 from APC/C-dependent proteolysis. Cell 122, 915-926.

Mailand, N., Falck, J., Lukas, C., Syljuasen, R.G., Welcker, M., Bartek, J., and Lukas, J. (2000). Rapid destruction of human Cdc25A in response to DNA damage. Science 288, 1425-1429.

Maison, C., Pyrpasopoulou, A., Theodoropoulos, P.A., and Georgatos, S.D. (1997). The inner nuclear membrane protein LAP1 forms a native complex with B-type lamins and partitions with spindle-associated mitotic vesicles. EMBO J 16, 4839-4850.

Malhas, A., Lee, C.F., Sanders, R., Saunders, N.J., and Vaux, D.J. (2007). Defects in lamin B1 expression or processing affect interphase chromosome position and gene expression. The Journal of Cell Biology 176, 593-603.

Malhas, A.N., Lee, C.F., and Vaux, D.J. (2009). Lamin B1 controls oxidative stress responses via Oct-1. The Journal of Cell Biology 184, 45-55.

Mancini, M.A., Shan, B., Nickerson, J.A., Penman, S., and Lee, W.H. (1994). The retinoblastoma gene product is a cell cycle-dependent, nuclear matrix-associated

protein. Proceedings of the National Academy of Sciences of the United States of America 91, 418-422.

Manis, J.P., Morales, J.C., Xia, Z., Kutok, J.L., Alt, F.W., and Carpenter, P.B. (2004). 53BP1 links DNA damage-response pathways to immunoglobulin heavy chain class-switch recombination. Nat Immunol 5, 481-487.

Manju, K., Muralikrishna, B., and Parnaik, V.K. (2006). Expression of disease-causing lamin A mutants impairs the formation of DNA repair foci. Journal of Cell Science 119, 2704-2714.

Mansharamani, M., and Wilson, K.L. (2005). Direct binding of nuclear membrane protein MAN1 to emerin in vitro and two modes of binding to barrier-to-autointegration factor. The Journal of Biological Chemistry 280, 13863-13870.

Margalit, A., Brachner, A., Gotzmann, J., Foisner, R., and Gruenbaum, Y. (2007). Barrier-to-autointegration factor--a BAFfling little protein. Trends Cell Biol 17, 202-208.

Markiewicz, E., Dechat, T., Foisner, R., Quinlan, R.A., and Hutchison, C.J. (2002). Lamin A/C binding protein LAP2alpha is required for nuclear anchorage of retinoblastoma protein. Mol Biol Cell 13, 4401-4413.

Markiewicz, E., Tilgner, K., Barker, N., van de Wetering, M., Clevers, H., Dorobek, M., Hausmanowa-Petrusewicz, I., Ramaekers, F.C., Broers, J.L., Blankesteijn, W.M., et al. (2006). The inner nuclear membrane protein emerin regulates beta-catenin activity by restricting its accumulation in the nucleus. EMBO J 25, 3275-3285.

Martens, U.M., Chavez, E.A., Poon, S.S., Schmoor, C., and Lansdorp, P.M. (2000). Accumulation of short telomeres in human fibroblasts prior to replicative senescence. Exp Cell Res 256, 291-299.

Martin, G.M. (2005). Genetic modulation of senescent phenotypes in Homo sapiens. Cell 120, 523-532.

Martin, L., Crimaudo, C., and Gerace, L. (1995). cDNA cloning and characterization of lamina-associated polypeptide 1C (LAP1C), an integral protein of the inner nuclear membrane. J Biol Chem 270, 8822-8828.

Martins, S., Eikvar, S., Furukawa, K., and Collas, P. (2003). HA95 and LAP2 beta mediate a novel chromatin-nuclear envelope interaction implicated in initiation of DNA replication. J Cell Biol 160, 177-188.

Masai, H., Matsumoto, S., You, Z., Yoshizawa-Sugata, N., and Oda, M. (2010). Eukaryotic chromosome DNA replication: where, when, and how? Annual Review of Biochemistry 79, 89-130.

Masny, P.S., Bengtsson, U., Chung, S.A., Martin, J.H., van Engelen, B., van der Maarel, S.M., and Winokur, S.T. (2004). Localization of 4q35.2 to the nuclear periphery: is FSHD a nuclear envelope disease? Human Molecular Genetics 13, 1857-1871.

Matsuoka, S., Ballif, B.A., Smogorzewska, A., McDonald, E.R., 3rd, Hurov, K.E., Luo, J., Bakalarski, C.E., Zhao, Z., Solimini, N., Lerenthal, Y., et al. (2007). ATM and ATR substrate analysis reveals extensive protein networks responsive to DNA damage. Science 316, 1160-1166.

Matsuoka, S., Rotman, G., Ogawa, A., Shiloh, Y., Tamai, K., and Elledge, S.J. (2000). Ataxia telangiectasia-mutated phosphorylates Chk2 in vivo and in vitro. Proceedings of the National Academy of Sciences of the United States of America 97, 10389-10394.

Matsuura, S., Tauchi, H., Nakamura, A., Kondo, N., Sakamoto, S., Endo, S., Smeets, D., Solder, B., Belohradsky, B.H., Der Kaloustian, V.M., et al. (1998). Positional cloning of the gene for Nijmegen breakage syndrome. Nat Genet 19, 179-181.

Mattout, A., Dechat, T., Adam, S.A., Goldman, R.D., and Gruenbaum, Y. (2006). Nuclear lamins, diseases and aging. Curr Opin Cell Biol 18, 335-341.

McClintock, D., Ratner, D., Lokuge, M., Owens, D.M., Gordon, L.B., Collins, F.S., and Djabali, K. (2007). The mutant form of lamin A that causes Hutchinson-Gilford progeria is a biomarker of cellular aging in human skin. PLoS One 2, e1269.

McKinnon, P.J., and Caldecott, K.W. (2007). DNA strand break repair and human genetic disease. Annual Review of Genomics and Human Genetics 8, 37-55.

McVey, M., and Lee, S.E. (2008). MMEJ repair of double-strand breaks (director's cut): deleted sequences and alternative endings. Trends Genet 24, 529-538.

Meaburn, K.J., Cabuy, E., Bonne, G., Levy, N., Morris, G.E., Novelli, G., Kill, I.R., and Bridger, J.M. (2007). Primary laminopathy fibroblasts display altered genome organization and apoptosis. Aging Cell 6, 139-153.

Meier, A., Fiegler, H., Munoz, P., Ellis, P., Rigler, D., Langford, C., Blasco, M.A., Carter, N., and Jackson, S.P. (2007). Spreading of mammalian DNA-damage response factors studied by ChIP-chip at damaged telomeres. The EMBO journal 26, 2707-2718.

Melander, F., Bekker-Jensen, S., Falck, J., Bartek, J., Mailand, N., and Lukas, J. (2008). Phosphorylation of SDT repeats in the MDC1 N terminus triggers retention of NBS1 at the DNA damage-modified chromatin. The Journal of Cell Biology 181, 213-226.

Melcer, S., Gruenbaum, Y., and Krohne, G. (2007). Invertebrate lamins. Exp Cell Res 313, 2157-2166.

Melchionna, R., Chen, X.B., Blasina, A., and McGowan, C.H. (2000). Threonine 68 is required for radiation-induced phosphorylation and activation of Cds1. Nature Cell Biology 2, 762-765.

Mendez, J., Zou-Yang, X.H., Kim, S.Y., Hidaka, M., Tansey, W.P., and Stillman, B. (2002). Human origin recognition complex large subunit is degraded by ubiquitin-mediated proteolysis after initiation of DNA replication. Mol Cell 9, 481-491.

Mewborn, S.K., Puckelwartz, M.J., Abuisneineh, F., Fahrenbach, J.P., Zhang, Y., MacLeod, H., Dellefave, L., Pytel, P., Selig, S., Labno, C.M., et al. (2010). Altered chromosomal positioning, compaction, and gene expression with a lamin A/C gene mutation. PLoS One 5, e14342.

Milczarek, G.J., Martinez, J., and Bowden, G.T. (1997). p53 Phosphorylation: biochemical and functional consequences. Life Sci 60, 1-11.

Mimitou, E.P., and Symington, L.S. (2008). Sae2, Exo1 and Sgs1 collaborate in DNA double-strand break processing. Nature 455, 770-774.

Minamino, T., and Komuro, I. (2008). Vascular aging: insights from studies on cellular senescence, stem cell aging, and progeroid syndromes. Nat Clin Pract Cardiovasc Med 5, 637-648.

Mittnacht, S. (1998). Control of pRB phosphorylation. Current Opinion in Genetics & Development 8, 21-27.

Mittnacht, S., and Weinberg, R.A. (1991). G1/S phosphorylation of the retinoblastoma protein is associated with an altered affinity for the nuclear compartment. Cell 65, 381-393.

Modrich, P. (2006). Mechanisms in eukaryotic mismatch repair. The Journal of Biological Chemistry 281, 30305-30309.

Moir, R.D., Montag-Lowy, M., and Goldman, R.D. (1994). Dynamic properties of nuclear lamins: lamin B is associated with sites of DNA replication. The Journal of Cell Biology 125, 1201-1212.

Moir, R.D., Spann, T.P., Lopez-Soler, R.I., Yoon, M., Goldman, A.E., Khuon, S., and Goldman, R.D. (2000). Review: the dynamics of the nuclear lamins during the cell cycle-- relationship between structure and function. J Struct Biol 129, 324-334.

Moldovan, G.L., and D'Andrea, A.D. (2009). How the fanconi anemia pathway guards the genome. Annu Rev Genet 43, 223-249.

Molofsky, A.V., Slutsky, S.G., Joseph, N.M., He, S., Pardal, R., Krishnamurthy, J., Sharpless, N.E., and Morrison, S.J. (2006). Increasing p16INK4a expression decreases forebrain progenitors and neurogenesis during ageing. Nature 443, 448-452.

Monnat, R.J., Jr. (2007). From broken to old: DNA damage, IGF1 endocrine suppression and aging. DNA Repair (Amst) 6, 1386-1390.

Moore, J.D., Yang, J., Truant, R., and Kornbluth, S. (1999). Nuclear import of Cdk/cyclin complexes: identification of distinct mechanisms for import of Cdk2/cyclin E and Cdc2/cyclin B1. The Journal of Cell Biology 144, 213-224.

Moreira, P.I., Harris, P.L., Zhu, X., Santos, M.S., Oliveira, C.R., Smith, M.A., and Perry, G. (2007). Lipoic acid and N-acetyl cysteine decrease mitochondrial-related oxidative stress in Alzheimer disease patient fibroblasts. J Alzheimers Dis 12, 195-206.

Morgan, D.O. (1995). Principles of CDK regulation. Nature 374, 131-134.

Morris, J.R., Boutell, C., Keppler, M., Densham, R., Weekes, D., Alamshah, A., Butler, L., Galanty, Y., Pangon, L., Kiuchi, T., et al. (2009). The SUMO modification pathway is involved in the BRCA1 response to genotoxic stress. Nature 462, 886-890.

Moritz, A., Li, Y., Guo, A., Villen, J., Wang, Y., MacNeill, J., Kornhauser, J., Sprott, K., Zhou, J., Possemato, A., et al. (2010). Akt-RSK-S6 kinase signaling networks activated by oncogenic receptor tyrosine kinases. Science signaling 3, ra64.

Mounkes, L.C., Kozlov, S., Hernandez, L., Sullivan, T., and Stewart, C.L. (2003). A progeroid syndrome in mice is caused by defects in A-type lamins. Nature 423, 298-301.

Mounkes, L.C., and Stewart, C.L. (2004). Aging and nuclear organization: lamins and progeria. Curr Opin Cell Biol 16, 322-327.

Muchir, A., Bonne, G., van der Kooi, A.J., van Meegen, M., Baas, F., Bolhuis, P.A., de Visser, M., and Schwartz, K. (2000). Identification of mutations in the gene encoding lamins A/C in autosomal dominant limb girdle muscular dystrophy with atrioventricular conduction disturbances (LGMD1B). Hum Mol Genet 9, 1453-1459.

Muchir, A., van Engelen, B.G., Lammens, M., Mislow, J.M., McNally, E., Schwartz, K., and Bonne, G. (2003). Nuclear envelope alterations in fibroblasts from LGMD1B patients carrying nonsense Y259X heterozygous or homozygous mutation in lamin A/C gene. Exp Cell Res 291, 352-362.

Munger, K. (2003). Clefts, grooves, and (small) pockets: the structure of the retinoblastoma tumor suppressor in complex with its cellular target E2F unveiled. Proceedings of the National Academy of Sciences of the United States of America 100, 2165-2167.

Muralikrishna, B., and Parnaik, V.K. (2001). SP3 and AP-1 mediate transcriptional activation of the lamin A proximal promoter. Eur J Biochem 268, 3736-3743.

Murray, A.W. (2004). Recycling the cell cycle: cyclins revisited. Cell 116, 221-234.

Musacchio, A., and Hardwick, K.G. (2002). The spindle checkpoint: structural insights into dynamic signalling. Nature Reviews Molecular Cell Biology 3, 731-741.

Naetar, N., and Foisner, R. (2009). Lamin complexes in the nuclear interior control progenitor cell proliferation and tissue homeostasis. Cell Cycle 8, 1488-1493.

Naetar, N., Hutter, S., Dorner, D., Dechat, T., Korbei, B., Gotzmann, J., Beug, H., and Foisner, R. (2007). LAP2alpha-binding protein LINT-25 is a novel chromatin-associated protein involved in cell cycle exit. J Cell Sci 120, 737-747.

Naetar, N., Korbei, B., Kozlov, S., Kerenyi, M.A., Dorner, D., Kral, R., Gotic, I., Fuchs, P., Cohen, T.V., Bittner, R., et al. (2008). Loss of nucleoplasmic LAP2alpha-lamin A complexes causes erythroid and epidermal progenitor hyperproliferation. Nature Cell Biology 10, 1341-1348.

Nakada, S., Tai, I., Panier, S., Al-Hakim, A., Iemura, S., Juang, Y.C., O'Donnell, L., Kumakubo, A., Munro, M., Sicheri, F., et al. (2010). Non-canonical inhibition of DNA damage-dependent ubiquitination by OTUB1. Nature 466, 941-946.

Nakajima, N., and Abe, K. (1995). Genomic structure of the mouse A-type lamin gene locus encoding somatic and germ cell-specific lamins. FEBS Lett 365, 108-114.

Nakamura, K., Sakai, W., Kawamoto, T., Bree, R.T., Lowndes, N.F., Takeda, S., and Taniguchi, Y. (2006). Genetic dissection of vertebrate 53BP1: a major role in non-homologous end joining of DNA double strand breaks. DNA Repair (Amst) 5, 741-749.

Nakayama, K., Nagahama, H., Minamishima, Y.A., Miyake, S., Ishida, N., Hatakeyama, S., Kitagawa, M., Iemura, S., Natsume, T., and Nakayama, K.I. (2004). Skp2-mediated degradation of p27 regulates progression into mitosis. Dev Cell 6, 661-672.

Narita, M., Nunez, S., Heard, E., Lin, A.W., Hearn, S.A., Spector, D.L., Hannon, G.J., and Lowe, S.W. (2003). Rb-mediated heterochromatin formation and silencing of E2F target genes during cellular senescence. Cell 113, 703-716.

Nasmyth, K. (2005). How do so few control so many? Cell 120, 739-746.

Navarro, C.L., De Sandre-Giovannoli, A., Bernard, R., Boccaccio, I., Boyer, A., Genevieve, D., Hadj-Rabia, S., Gaudy-Marqueste, C., Smitt, H.S., Vabres, P., et al. (2004). Lamin A and ZMPSTE24 (FACE-1) defects cause nuclear disorganization and identify restrictive dermopathy as a lethal neonatal laminopathy. Hum Mol Genet 13, 2493-2503.

Negrini, S., Gorgoulis, V.G., and Halazonetis, T.D. (2010). Genomic instability--an evolving hallmark of cancer. Nature Reviews Molecular Cell Biology 11, 220-228.

Nguyen, V.Q., Co, C., and Li, J.J. (2001). Cyclin-dependent kinases prevent DNA re-replication through multiple mechanisms. Nature 411, 1068-1073.

Nicolette, M.L., Lee, K., Guo, Z., Rani, M., Chow, J.M., Lee, S.E., and Paull, T.T. (2010). Mre11-Rad50-Xrs2 and Sae2 promote 5' strand resection of DNA double-strand breaks. Nat Struct Mol Biol 17, 1478-1485.

Niedernhofer, L.J., Lalai, A.S., and Hoeijmakers, J.H. (2005). Fanconi anemia (cross)linked to DNA repair. Cell 123, 1191-1198.

Nigg, E.A. (2001). Mitotic kinases as regulators of cell division and its checkpoints. Nature Reviews Molecular Cell Biology 2, 21-32.

Nikolova, V., Leimena, C., McMahon, A.C., Tan, J.C., Chandar, S., Jogia, D., Kesteven, S.H., Michalicek, J., Otway, R., Verheyen, F., et al. (2004). Defects in nuclear structure and function promote dilated cardiomyopathy in lamin A/C-deficient mice. J Clin Invest 113, 357-369.

Nili, E., Cojocaru, G.S., Kalma, Y., Ginsberg, D., Copeland, N.G., Gilbert, D.J., Jenkins, N.A., Berger, R., Shaklai, S., Amariglio, N., et al. (2001). Nuclear membrane protein LAP2beta mediates transcriptional repression alone and together with its binding partner GCL (germ-cell-less). J Cell Sci 114, 3297-3307.

Nilsson, I., and Hoffmann, I. (2000). Cell cycle regulation by the Cdc25 phosphatase family. Prog Cell Cycle Res 4, 107-114.

Noon, A.T., Shibata, A., Rief, N., Lobrich, M., Stewart, G.S., Jeggo, P.A., and Goodarzi, A.A. (2010). 53BP1-dependent robust localized KAP-1 phosphorylation is essential for heterochromatic DNA double-strand break repair. Nature Cell Biology 12, 177-184.

Nouspikel, T. (2009). DNA repair in mammalian cells : Nucleotide excision repair: variations on versatility. Cellular and molecular life sciences : CMLS 66, 994-1009.

Novelli, G., and D'Apice, M.R. (2003). The strange case of the "lumper" lamin A/C gene and human premature ageing. Trends Mol Med 9, 370-375.

Novelli, G., Muchir, A., Sangiuolo, F., Helbling-Leclerc, A., D'Apice, M.R., Massart, C., Capon, F., Sbraccia, P., Federici, M., Lauro, R., et al. (2002). Mandibuloacral dysplasia is caused by a mutation in LMNA-encoding lamin A/C. Am J Hum Genet 71, 426-431.

Nurse, P. (2000). A long twentieth century of the cell cycle and beyond. Cell 100, 71-78.

Nurse, P. (2004). Wee beasties. Nature 432, 557.

O'Driscoll, M., Ruiz-Perez, V.L., Woods, C.G., Jeggo, P.A., and Goodship, J.A. (2003). A splicing mutation affecting expression of ataxia-telangiectasia and Rad3-related protein (ATR) results in Seckel syndrome. Nat Genet 33, 497-501.

Okumura, K., Hosoe, Y., and Nakajima, N. (2004). c-Jun and Sp1 family are critical for retinoic acid induction of the lamin A/C retinoic acid-responsive element. Biochemical and Biophysical Research Communications 320, 487-492.

Okumura, K., Nakamachi, K., Hosoe, Y., and Nakajima, N. (2000). Identification of a novel retinoic acid-responsive element within the lamin A/C promoter. Biochemical and Biophysical Research Communications 269, 197-202.

O'Neill, T., Dwyer, A.J., Ziv, Y., Chan, D.W., Lees-Miller, S.P., Abraham, R.H., Lai, J.H., Hill, D., Shiloh, Y., Cantley, L.C., et al. (2000). Utilization of oriented peptide libraries to identify substrate motifs selected by ATM. The Journal of Biological Chemistry 275, 22719-22727.

Osorio, F.G., Varela, I., Lara, E., Puente, X.S., Espada, J., Santoro, R., Freije, J.M., Fraga, M.F., and Lopez-Otin, C. (2010). Nuclear envelope alterations generate an aging-like epigenetic pattern in mice deficient in Zmpste24 metalloprotease. Aging Cell 9, 947-957.

Ostlund, C., Bonne, G., Schwartz, K., and Worman, H.J. (2001). Properties of lamin A mutants found in Emery-Dreifuss muscular dystrophy, cardiomyopathy and Dunnigan-type partial lipodystrophy. J Cell Sci 114, 4435-4445.

O'Sullivan, R.J., and Karlseder, J. (2010). Telomeres: protecting chromosomes against genome instability. Nature Reviews Molecular Cell Biology 11, 171-181.

Ozaki, T., Saijo, M., Murakami, K., Enomoto, H., Taya, Y., and Sakiyama, S. (1994). Complex formation between lamin A and the retinoblastoma gene product: identification of the domain on lamin A required for its interaction. Oncogene 9, 2649-2653.

Padiath, Q.S., Saigoh, K., Schiffmann, R., Asahara, H., Yamada, T., Koeppen, A., Hogan, K., Ptacek, L.J., and Fu, Y.H. (2006). Lamin B1 duplications cause autosomal dominant leukodystrophy. Nat Genet 38, 1114-1123.

Pajerowski, J.D., Dahl, K.N., Zhong, F.L., Sammak, P.J., and Discher, D.E. (2007). Physical plasticity of the nucleus in stem cell differentiation. Proceedings of the National Academy of Sciences of the United States of America 104, 15619-15624.

Park, C.J., and Choi, B.S. (2006). The protein shuffle. Sequential interactions among components of the human nucleotide excision repair pathway. FEBS J 273, 1600-1608.

Parrinello, S., Samper, E., Krtolica, A., Goldstein, J., Melov, S., and Campisi, J. (2003). Oxygen sensitivity severely limits the replicative lifespan of murine fibroblasts. Nature Cell Biology 5, 741-747.

Parsons, D.W., Jones, S., Zhang, X., Lin, J.C., Leary, R.J., Angenendt, P., Mankoo, P., Carter, H., Siu, I.M., Gallia, G.L., et al. (2008). An integrated genomic analysis of human glioblastoma multiforme. Science 321, 1807-1812.

Parsons, D.W., Li, M., Zhang, X., Jones, S., Leary, R.J., Lin, J.C., Boca, S.M., Carter, H., Samayoa, J., Bettegowda, C., et al. (2011). The genetic landscape of the childhood cancer medulloblastoma. Science 331, 435-439.

Passos, J.F., Saretzki, G., and von Zglinicki, T. (2007). DNA damage in telomeres and mitochondria during cellular senescence: is there a connection? Nucleic Acids Res 35, 7505-7513.

Paulin-Levasseur, M., Scherbarth, A., Traub, U., and Traub, P. (1988). Lack of lamins A and C in mammalian hemopoietic cell lines devoid of intermediate filament proteins. Eur J Cell Biol 47, 121-131.

Peeper, D.S., Upton, T.M., Ladha, M.H., Neuman, E., Zalvide, J., Bernards, R., DeCaprio, J.A., and Ewen, M.E. (1997). Ras signalling linked to the cell-cycle machinery by the retinoblastoma protein. Nature 386, 177-181.

Pegoraro, G., Kubben, N., Wickert, U., Gohler, H., Hoffmann, K., and Misteli, T. (2009). Ageing-related chromatin defects through loss of the NURD complex. Nature Cell Biology 11, 1261-1267.

Pei, H., Zhang, L., Luo, K., Qin, Y., Chesi, M., Fei, F., Bergsagel, P.L., Wang, L., You, Z., and Lou, Z. (2011). MMSET regulates histone H4K20 methylation and 53BP1 accumulation at DNA damage sites. Nature 470, 124-128.

Pekovic, V., Harborth, J., Broers, J.L., Ramaekers, F.C., van Engelen, B., Lammens, M., von Zglinicki, T., Foisner, R., Hutchison, C., and Markiewicz, E. (2007). Nucleoplasmic LAP2alpha-lamin A complexes are required to maintain a proliferative state in human fibroblasts. J Cell Biol 176, 163-172.

Pekovic, V., and Hutchison, C.J. (2009). A-type lamins, disease and ageing: a stress-induced relationship? SEB Exp Biol Ser 62, 139-170.

Peng, G., Yim, E.K., Dai, H., Jackson, A.P., Burgt, I., Pan, M.R., Hu, R., Li, K., and Lin, S.Y. (2009). BRIT1/MCPH1 links chromatin remodelling to DNA damage response. Nature Cell Biology 11, 865-872.

Pennisi, E. (2004). Evolutionary biology. The birth of the nucleus. Science 305, 766-768.

Peters, J.M. (2006). The anaphase promoting complex/cyclosome: a machine designed to destroy. Nature Reviews Molecular Cell Biology 7, 644-656.

Pickersgill, H., Kalverda, B., de Wit, E., Talhout, W., Fornerod, M., and van Steensel, B. (2006). Characterization of the Drosophila melanogaster genome at the nuclear lamina. Nat Genet 38, 1005-1014.

Piepkorn, M. (2000). The expression of p16(INK4a), the product of a tumor suppressor gene for melanoma, is upregulated in human melanocytes by UVB irradiation. J Am Acad Dermatol 42, 741-745.

Platt, O.S. (2008). Hydroxyurea for the treatment of sickle cell anemia. The New England journal of medicine 358, 1362-1369.

Poehlmann, A., and Roessner, A. (2010). Importance of DNA damage checkpoints in the pathogenesis of human cancers. Pathol Res Pract 206, 591-601.

Polager, S., and Ginsberg, D. (2008). E2F - at the crossroads of life and death. Trends Cell Biol 18, 528-535.

Pollex, R.L., and Hegele, R.A. (2004). Hutchinson-Gilford progeria syndrome. Clin Genet 66, 375-381.

Polo, S.E., and Jackson, S.P. (2011). Dynamics of DNA damage response proteins at DNA breaks: a focus on protein modifications. Genes Dev 25, 409-433.

Polo, S.E., Kaidi, A., Baskcomb, L., Galanty, Y., and Jackson, S.P. (2010). Regulation of DNA-damage responses and cell-cycle progression by the chromatin remodelling factor CHD4. The EMBO Journal 29, 3130-3139.

Poole, L.B., Karplus, P.A., and Claiborne, A. (2004). Protein sulfenic acids in redox signaling. Annu Rev Pharmacol Toxicol 44, 325-347.

Pugh, G.E., Coates, P.J., Lane, E.B., Raymond, Y., and Quinlan, R.A. (1997). Distinct nuclear assembly pathways for lamins A and C lead to their increase during quiescence in Swiss 3T3 cells. J Cell Sci 110 (Pt 19), 2483-2493.

Qin, X.Q., Chittenden, T., Livingston, D.M., and Kaelin, W.G., Jr. (1992). Identification of a growth suppression domain within the retinoblastoma gene product. Genes Dev 6, 953-964.

Rahman-Roblick, R., Roblick, U.J., Hellman, U., Conrotto, P., Liu, T., Becker, S., Hirschberg, D., Jornvall, H., Auer, G., and Wiman, K.G. (2007). p53 targets identified by protein expression profiling. Proceedings of the National Academy of Sciences of the United States of America 104, 5401-5406.

Raschle, M., Knipscheer, P., Enoiu, M., Angelov, T., Sun, J., Griffith, J.D., Ellenberger, T.E., Scharer, O.D., and Walter, J.C. (2008). Mechanism of replication-coupled DNA interstrand crosslink repair. Cell 134, 969-980.

Reddel, C.J., and Weiss, A.S. (2004). Lamin A expression levels are unperturbed at the normal and mutant alleles but display partial splice site selection in Hutchinson-Gilford progeria syndrome. Journal of Medical Genetics 41, 715-717.

Reddy, K.L., Zullo, J.M., Bertolino, E., and Singh, H. (2008). Transcriptional repression mediated by repositioning of genes to the nuclear lamina. Nature 452, 243-247.

Reinhardt, H.C., and Yaffe, M.B. (2009). Kinases that control the cell cycle in response to DNA damage: Chk1, Chk2, and MK2. Curr Opin Cell Biol 21, 245-255.

Reitman, M.L., Arioglu, E., Gavrilova, O., and Taylor, S.I. (2000). Lipoatrophy revisited. Trends Endocrinol Metab 11, 410-416.

Rizwani, W., and Chellappan, S.P. (2009). In vitro replication assay with mammalian cell extracts. Methods Mol Biol 523, 203-216.

Rober, R.A., Weber, K., and Osborn, M. (1989). Differential timing of nuclear lamin A/C expression in the various organs of the mouse embryo and the young animal: a developmental study. Development 105, 365-378.

Roberts, S.A., Strande, N., Burkhalter, M.D., Strom, C., Havener, J.M., Hasty, P., and Ramsden, D.A. (2010). Ku is a 5'-dRP/AP lyase that excises nucleotide damage near broken ends. Nature 464, 1214-1217.

Rodriguez, S., Coppede, F., Sagelius, H., and Eriksson, M. (2009). Increased expression of the Hutchinson-Gilford progeria syndrome truncated lamin A transcript during cell aging. Eur J Hum Genet 17, 928-937.

Rogakou, E.P., Boon, C., Redon, C., and Bonner, W.M. (1999). Megabase chromatin domains involved in DNA double-strand breaks in vivo. The Journal of Cell Biology 146, 905-916.

Rubio, M.A., Kim, S.H., and Campisi, J. (2002). Reversible manipulation of telomerase expression and telomere length. Implications for the ionizing radiation response and replicative senescence of human cells. The Journal of Bological Chemistry 277, 28609-28617.

Rusinol, A.E., and Sinensky, M.S. (2006). Farnesylated lamins, progeroid syndromes and farnesyl transferase inhibitors. J Cell Sci 119, 3265-3272.

Russo, A.A., Jeffrey, P.D., Patten, A.K., Massague, J., and Pavletich, N.P. (1996). Crystal structure of the p27Kip1 cyclin-dependent-kinase inhibitor bound to the cyclin A-Cdk2 complex. Nature 382, 325-331.

Russo, A.A., Tong, L., Lee, J.O., Jeffrey, P.D., and Pavletich, N.P. (1998). Structural basis for inhibition of the cyclin-dependent kinase Cdk6 by the tumour suppressor p16INK4a. Nature 395, 237-243.

Sadoni, N., Langer, S., Fauth, C., Bernardi, G., Cremer, T., Turner, B.M., and Zink, D. (1999). Nuclear organization of mammalian genomes. Polar chromosome territories build up functionally distinct higher order compartments. J Cell Biol 146, 1211-1226.

Sahin, E., Colla, S., Liesa, M., Moslehi, J., Muller, F.L., Guo, M., Cooper, M., Kotton, D., Fabian, A.J., Walkey, C., et al. (2011). Telomere dysfunction induces metabolic and mitochondrial compromise. Nature 470, 359-365.

Sahin, E., and Depinho, R.A. (2010). Linking functional decline of telomeres, mitochondria and stem cells during ageing. Nature 464, 520-528.

Sancar, A., Lindsey-Boltz, L.A., Unsal-Kacmaz, K., and Linn, S. (2004). Molecular mechanisms of mammalian DNA repair and the DNA damage checkpoints. Annual Review of Biochemistry 73, 39-85.

Santamaria, D., Barriere, C., Cerqueira, A., Hunt, S., Tardy, C., Newton, K., Caceres, J.F., Dubus, P., Malumbres, M., and Barbacid, M. (2007). Cdk1 is sufficient to drive the mammalian cell cycle. Nature 448, 811-815.

Savic, V., Yin, B., Maas, N.L., Bredemeyer, A.L., Carpenter, A.C., Helmink, B.A., Yang-Iott, K.S., Sleckman, B.P., and Bassing, C.H. (2009). Formation of dynamic gamma-H2AX domains along broken DNA strands is distinctly regulated by ATM and MDC1 and dependent upon H2AX densities in chromatin. Mol Cell 34, 298-310.

Scaffidi, P., and Misteli, T. (2006). Lamin A-dependent nuclear defects in human aging. Science 312, 1059-1063.

Scaffidi, P., and Misteli, T. (2008). Lamin A-dependent misregulation of adult stem cells associated with accelerated ageing. Nature Cell Bology 10, 452-459.

Schafer, K.A. (1998). The cell cycle: a review. Vet Pathol 35, 461-478.

Schape, J., Prausse, S., Radmacher, M., and Stick, R. (2009). Influence of lamin A on the mechanical properties of amphibian oocyte nuclei measured by atomic force microscopy. Biophys J 96, 4319-4325.

Schirmer, E.C., and Gerace, L. (2004). The stability of the nuclear lamina polymer changes with the composition of lamin subtypes according to their individual binding strengths. J Biol Chem 279, 42811-42817.

Scholzen, T., and Gerdes, J. (2000). The Ki-67 protein: from the known and the unknown. J Cell Physiol 182, 311-322.

Schreiber, V., Dantzer, F., Ame, J.C., and de Murcia, G. (2006). Poly(ADP-ribose): novel functions for an old molecule. Nature Reviews Molecular Cell Biology 7, 517-528.

Schultz, L.B., Chehab, N.H., Malikzay, A., and Halazonetis, T.D. (2000). p53 binding protein 1 (53BP1) is an early participant in the cellular response to DNA double-strand breaks. The Journal of Cell Biology 151, 1381-1390.

Schulze, S.R., Curio-Penny, B., Speese, S., Dialynas, G., Cryderman, D.E., McDonough, C.W., Nalbant, D., Petersen, M., Budnik, V., Geyer, P.K., et al. (2009). A comparative study of Drosophila and human A-type lamins. PLoS One 4, e7564.

Schumacher, B., Garinis, G.A., and Hoeijmakers, J.H. (2008). Age to survive: DNA damage and aging. Trends Genet 24, 77-85.

Sclafani, R.A., and Holzen, T.M. (2007). Cell cycle regulation of DNA replication. Annu Rev Genet 41, 237-280.

Sedelnikova, O.A., Horikawa, I., Zimonjic, D.B., Popescu, N.C., Bonner, W.M., and Barrett, J.C. (2004). Senescing human cells and ageing mice accumulate DNA lesions with unrepairable double-strand breaks. Nature Cell Biology 6, 168-170.

Senior, A., and Gerace, L. (1988). Integral membrane proteins specific to the inner nuclear membrane and associated with the nuclear lamina. J Cell Biol 107, 2029-2036.

Serra, V., von Zglinicki, T., Lorenz, M., and Saretzki, G. (2003). Extracellular superoxide dismutase is a major antioxidant in human fibroblasts and slows telomere shortening. The Journal of Biological Chemistry 278, 6824-6830.

Serrano, M., Lin, A.W., McCurrach, M.E., Beach, D., and Lowe, S.W. (1997). Oncogenic ras provokes premature cell senescence associated with accumulation of p53 and p16INK4a. Cell 88, 593-602.

Shaklai, S., Somech, R., Gal-Yam, E.N., Deshet-Unger, N., Moshitch-Moshkovitz, S., Hirschberg, K., Amariglio, N., Simon, A.J., and Rechavi, G. (2008). LAP2zeta binds BAF and suppresses LAP2beta-mediated transcriptional repression. European Journal of Cell Biology 87, 267-278.

Sharpless, N.E. (2005). INK4a/ARF: a multifunctional tumor suppressor locus. Mutat Res 576, 22-38.

Sherr, C.J. (2004). Principles of tumor suppression. Cell 116, 235-246.

Sherr, C.J., and McCormick, F. (2002). The RB and p53 pathways in cancer. Cancer Cell 2, 103-112.

Sherr, C.J., and Roberts, J.M. (1995). Inhibitors of mammalian G1 cyclin-dependent kinases. Genes Dev 9, 1149-1163.

Sherr, C.J., and Roberts, J.M. (1999). CDK inhibitors: positive and negative regulators of G1-phase progression. Genes Dev 13, 1501-1512.

Sherr, C.J., and Roberts, J.M. (2004). Living with or without cyclins and cyclin-dependent kinases. Genes Dev 18, 2699-2711.

Shevelyov, Y.Y., Lavrov, S.A., Mikhaylova, L.M., Nurminsky, I.D., Kulathinal, R.J., Egorova, K.S., Rozovsky, Y.M., and Nurminsky, D.I. (2009). The B-type lamin is required for somatic repression of testis-specific gene clusters. Proceedings of the National Academy of Sciences of the United States of America 106, 3282-3287.

Shiloh, Y. (2003). ATM: ready, set, go. Cell Cycle 2, 116-117.

Shimi, T., Pfleghaar, K., Kojima, S., Pack, C.G., Solovei, I., Goldman, A.E., Adam, S.A., Shumaker, D.K., Kinjo, M., Cremer, T., et al. (2008). The A- and B-type nuclear lamin networks: microdomains involved in chromatin organization and transcription. Genes Dev 22, 3409-3421.

Shumaker, D.K., Dechat, T., Kohlmaier, A., Adam, S.A., Bozovsky, M.R., Erdos, M.R., Eriksson, M., Goldman, A.E., Khuon, S., Collins, F.S., et al. (2006). Mutant nuclear lamin A leads to progressive alterations of epigenetic control in premature aging. Proceedings of the National Academy of Sciences of the United States of America 103, 8703-8708.

Shumaker, D.K., Solimando, L., Sengupta, K., Shimi, T., Adam, S.A., Grunwald, A., Strelkov, S.V., Aebi, U., Cardoso, M.C., and Goldman, R.D. (2008). The highly conserved nuclear lamin Ig-fold binds to PCNA: its role in DNA replication. The Journal of Cell Biology 181, 269-280.

Sibanda, B.L., Chirgadze, D.Y., and Blundell, T.L. (2010). Crystal structure of DNA-PKcs reveals a large open-ring cradle comprised of HEAT repeats. Nature 463, 118-121.

Silvius, J.R., and l'Heureux, F. (1994). Fluorimetric evaluation of the affinities of isoprenylated peptides for lipid bilayers. Biochemistry 33, 3014-3022.

Simsek, D., and Jasin, M. (2010). Alternative end-joining is suppressed by the canonical NHEJ component Xrcc4-ligase IV during chromosomal translocation formation. Nat Struct Mol Biol 17, 410-416.

Sinclair, D.A., and Oberdoerffer, P. (2009). The ageing epigenome: damaged beyond repair? Ageing Res Rev 8, 189-198.

Sjoblom, T., Jones, S., Wood, L.D., Parsons, D.W., Lin, J., Barber, T.D., Mandelker, D., Leary, R.J., Ptak, J., Silliman, N., et al. (2006). The consensus coding sequences of human breast and colorectal cancers. Science 314, 268-274.

Skaar, J.R., and Pagano, M. (2009). Control of cell growth by the SCF and APC/C ubiquitin ligases. Curr Opin Cell Biol 21, 816-824.

Skvortsov, S., Schafer, G., Stasyk, T., Fuchsberger, C., Bonn, G.K., Bartsch, G., Klocker, H., and Huber, L.A. (2011). Proteomics profiling of microdissected low- and high-grade prostate tumors identifies Lamin A as a discriminatory biomarker. J Proteome Res 10, 259-268.

Smeenk, G., Wiegant, W.W., Vrolijk, H., Solari, A.P., Pastink, A., and van Attikum, H. (2010). The NuRD chromatin-remodeling complex regulates signaling and repair of DNA damage. The Journal of Cell Biology 190, 741-749.

Smogorzewska, A., Desetty, R., Saito, T.T., Schlabach, M., Lach, F.P., Sowa, M.E., Clark, A.B., Kunkel, T.A., Harper, J.W., Colaiacovo, M.P., et al. (2010). A genetic screen identifies FAN1, a Fanconi anemia-associated nuclease necessary for DNA interstrand crosslink repair. Mol Cell 39, 36-47.

Smogorzewska, A., Matsuoka, S., Vinciguerra, P., McDonald, E.R., 3rd, Hurov, K.E., Luo, J., Ballif, B.A., Gygi, S.P., Hofmann, K., D'Andrea, A.D., et al. (2007). Identification of the FANCI protein, a monoubiquitinated FANCD2 paralog required for DNA repair. Cell 129, 289-301.

Somech, R., Shaklai, S., Geller, O., Amariglio, N., Simon, A.J., Rechavi, G., and Gal-Yam, E.N. (2005). The nuclear-envelope protein and transcriptional repressor LAP2beta interacts with HDAC3 at the nuclear periphery, and induces histone H4 deacetylation. J Cell Sci 118, 4017-4025.

Spann, T.P., Goldman, A.E., Wang, C., Huang, S., and Goldman, R.D. (2002). Alteration of nuclear lamin organization inhibits RNA polymerase II-dependent transcription. J Cell Biol 156, 603-608.

Spann, T.P., Moir, R.D., Goldman, A.E., Stick, R., and Goldman, R.D. (1997). Disruption of nuclear lamin organization alters the distribution of replication factors and inhibits DNA synthesis. J Cell Biol 136, 1201-1212.

Spycher, C., Miller, E.S., Townsend, K., Pavic, L., Morrice, N.A., Janscak, P., Stewart, G.S., and Stucki, M. (2008). Constitutive phosphorylation of MDC1 physically links the MRE11-RAD50-NBS1 complex to damaged chromatin. The Journal of Cell Biology 181, 227-240.

Starr, D.A., and Han, M. (2003). ANChors away: an actin based mechanism of nuclear positioning. Journal of Cell Science 116, 211-216.

Stein, G.H., Drullinger, L.F., Soulard, A., and Dulic, V. (1999). Differential roles for cyclin-dependent kinase inhibitors p21 and p16 in the mechanisms of senescence and differentiation in human fibroblasts. Molecular and Cellular Biology 19, 2109-2117.

Stevaux, O., and Dyson, N.J. (2002). A revised picture of the E2F transcriptional network and RB function. Curr Opin Cell Biol 14, 684-691.

Stewart, C., and Burke, B. (1987). Teratocarcinoma stem cells and early mouse embryos contain only a single major lamin polypeptide closely resembling lamin B. Cell 51, 383-392.

Stewart, C.L., Kozlov, S., Fong, L.G., and Young, S.G. (2007). Mouse models of the laminopathies. Exp Cell Res 313, 2144-2156.

Stewart, G.S., Maser, R.S., Stankovic, T., Bressan, D.A., Kaplan, M.I., Jaspers, N.G., Raams, A., Byrd, P.J., Petrini, J.H., and Taylor, A.M. (1999). The DNA double-strand break repair gene hMRE11 is mutated in individuals with an ataxia-telangiectasia-like disorder. Cell 99, 577-587.

Stierle, V., Couprie, J., Ostlund, C., Krimm, I., Zinn-Justin, S., Hossenlopp, P., Worman, H.J., Courvalin, J.C., and Duband-Goulet, I. (2003). The carboxyl-terminal region common to lamins A and C contains a DNA binding domain. Biochemistry 42, 4819-4828.

Stiff, T., O'Driscoll, M., Rief, N., Iwabuchi, K., Lobrich, M., and Jeggo, P.A. (2004). ATM and DNA-PK function redundantly to phosphorylate H2AX after exposure to ionizing radiation. Cancer Res 64, 2390-2396.

Stockl, P., Hutter, E., Zwerschke, W., and Jansen-Durr, P. (2006). Sustained inhibition of oxidative phosphorylation impairs cell proliferation and induces premature senescence in human fibroblasts. Experimental gerontology 41, 674-682.

Stokes, M.P., Rush, J., Macneill, J., Ren, J.M., Sprott, K., Nardone, J., Yang, V., Beausoleil, S.A., Gygi, S.P., Livingstone, M., et al. (2007). Profiling of UV-induced ATM/ATR signaling pathways. Proceedings of the National Academy of Sciences of the United States of America 104, 19855-19860.

Stucki, M., and Jackson, S.P. (2004). MDC1/NFBD1: a key regulator of the DNA damage response in higher eukaryotes. DNA Repair (Amst) 3, 953-957.

Stucki, M., and Jackson, S.P. (2006). gammaH2AX and MDC1: anchoring the DNA-damage-response machinery to broken chromosomes. DNA Repair (Amst) 5, 534-543.

Stuurman, N., Heins, S., and Aebi, U. (1998). Nuclear lamins: their structure, assembly, and interactions. J Struct Biol 122, 42-66.

Sullivan, T., Escalante-Alcalde, D., Bhatt, H., Anver, M., Bhat, N., Nagashima, K., Stewart, C.L., and Burke, B. (1999). Loss of A-type lamin expression compromises nuclear envelope integrity leading to muscular dystrophy. J Cell Biol 147, 913-920.

Sun, Y., Jiang, X., Chen, S., Fernandes, N., and Price, B.D. (2005). A role for the Tip60 histone acetyltransferase in the acetylation and activation of ATM. Proceedings of the National Academy of Sciences of the United States of America 102, 13182-13187.

Sun, Y., Jiang, X., Xu, Y., Ayrapetov, M.K., Moreau, L.A., Whetstine, J.R., and Price, B.D. (2009). Histone H3 methylation links DNA damage detection to activation of the tumour suppressor Tip60. Nature Cell Biology 11, 1376-1382.

Sun, Y., Xu, Y., Roy, K., and Price, B.D. (2007). DNA damage-induced acetylation of lysine 3016 of ATM activates ATM kinase activity. Molecular and Cellular Biology 27, 8502-8509.

Susaki, E., and Nakayama, K.I. (2009). Functional similarities and uniqueness of p27 and p57: insight from a knock-in mouse model. Cell Cycle 8, 2497-2501.

Suzuki, K., Mori, I., Nakayama, Y., Miyakoda, M., Kodama, S., and Watanabe, M. (2001). Radiation-induced senescence-like growth arrest requires TP53 function but not telomere shortening. Radiat Res 155, 248-253.

Takai, H., Smogorzewska, A., and de Lange, T. (2003). DNA damage foci at dysfunctional telomeres. Curr Biol 13, 1549-1556.

Takizawa, C.G., and Morgan, D.O. (2000). Control of mitosis by changes in the subcellular location of cyclin-B1-Cdk1 and Cdc25C. Curr Opin Cell Biol 12, 658-665.

Tang, C.W., Maya-Mendoza, A., Martin, C., Zeng, K., Chen, S., Feret, D., Wilson, S.A., and Jackson, D.A. (2008). The integrity of a lamin-B1-dependent nucleoskeleton is a fundamental determinant of RNA synthesis in human cells. Journal of cell science 121, 1014-1024.

Taniguchi, T., Garcia-Higuera, I., Xu, B., Andreassen, P.R., Gregory, R.C., Kim, S.T., Lane, W.S., Kastan, M.B., and D'Andrea, A.D. (2002). Convergence of the fanconi anemia and ataxia telangiectasia signaling pathways. Cell 109, 459-472.

Taniura, H., Glass, C., and Gerace, L. (1995). A chromatin binding site in the tail domain of nuclear lamins that interacts with core histones. J Cell Biol 131, 33-44.

Tantin, D., Schild-Poulter, C., Wang, V., Hache, R.J., and Sharp, P.A. (2005). The octamer binding transcription factor Oct-1 is a stress sensor. Cancer Res 65, 10750-10758.

Tazir, M., Azzedine, H., Assami, S., Sindou, P., Nouioua, S., Zemmouri, R., Hamadouche, T., Chaouch, M., Feingold, J., Vallat, J.M., et al. (2004). Phenotypic variability in autosomal recessive axonal Charcot-Marie-Tooth disease due to the R298C mutation in lamin A/C. Brain 127, 154-163.

Thiery, J.P., Acloque, H., Huang, R.Y., and Nieto, M.A. (2009). Epithelial-mesenchymal transitions in development and disease. Cell 139, 871-890.

Thoma, B.S., and Vasquez, K.M. (2003). Critical DNA damage recognition functions of XPC-hHR23B and XPA-RPA in nucleotide excision repair. Mol Carcinog 38, 1-13.

Thompson, L.J., Bollen, M., and Fields, A.P. (1997). Identification of protein phosphatase 1 as a mitotic lamin phosphatase. The Journal of Biological chemistry 272, 29693-29697.

Tiwari, B., Muralikrishna, B., and Parnaik, V.K. (1998). Functional analysis of the 5' promoter region of the rat lamin A gene. DNA Cell Biol 17, 957-965.

Toth, J.I., Yang, S.H., Qiao, X., Beigneux, A.P., Gelb, M.H., Moulson, C.L., Miner, J.H., Young, S.G., and Fong, L.G. (2005). Blocking protein farnesyltransferase improves nuclear shape in fibroblasts from humans with progeroid syndromes. Proc Natl Acad Sci U S A 102, 12873-12878.

Toussaint, O., Medrano, E.E., and von Zglinicki, T. (2000). Cellular and molecular mechanisms of stress-induced premature senescence (SIPS) of human diploid fibroblasts and melanocytes. Exp Gerontol 35, 927-945.

Trinidad, J.C., Specht, C.G., Thalhammer, A., Schoepfer, R., and Burlingame, A.L. (2006). Comprehensive identification of phosphorylation sites in postsynaptic density preparations. Molecular & cellular proteomics : MCP 5, 914-922.

Trujillo, K.M., Yuan, S.S., Lee, E.Y., and Sung, P. (1998). Nuclease activities in a complex of human recombination and DNA repair factors Rad50, Mre11, and p95. The Journal of Biological Chemistry 273, 21447-21450.

Tweedie-Cullen, R.Y., Reck, J.M., and Mansuy, I.M. (2009). Comprehensive mapping of post-translational modifications on synaptic, nuclear, and histone proteins in the adult mouse brain. J Proteome Res 8, 4966-4982.

Tzur, Y.B., Wilson, K.L., and Gruenbaum, Y. (2006). SUN-domain proteins: 'Velcro' that links the nucleoskeleton to the cytoskeleton. Nature Reviews Molecular Cell Biology 7, 782-788.

Ukekawa, R., Miki, K., Fujii, M., Hirano, H., and Ayusawa, D. (2007). Accumulation of multiple forms of lamin A with down-regulation of FACE-1 suppresses growth in senescent human cells. Genes Cells 12, 397-406.

Ulbert, S., Antonin, W., Platani, M., and Mattaj, I.W. (2006). The inner nuclear membrane protein Lem2 is critical for normal nuclear envelope morphology. FEBS Lett 580, 6435-6441.

Uziel, T., Lerenthal, Y., Moyal, L., Andegeko, Y., Mittelman, L., and Shiloh, Y. (2003). Requirement of the MRN complex for ATM activation by DNA damage. The EMBO Journal 22, 5612-5621.

van Attikum, H., and Gasser, S.M. (2009). Crosstalk between histone modifications during the DNA damage response. Trends Cell Biol 19, 207-217.

Van Berlo, J.H., Voncken, J.W., Kubben, N., Broers, J.L., Duisters, R., van Leeuwen, R.E., Crijns, H.J., Ramaekers, F.C., Hutchison, C.J., and Pinto, Y.M. (2005). A-type lamins are essential for TGF-beta1 induced PP2A to dephosphorylate transcription factors. Hum Mol Genet 14, 2839-2849.

van Engelen, B.G., Muchir, A., Hutchison, C.J., van der Kooi, A.J., Bonne, G., and Lammens, M. (2005). The lethal phenotype of a homozygous nonsense mutation in the lamin A/C gene. Neurology 64, 374-376.

Varela, I., Cadinanos, J., Pendas, A.M., Gutierrez-Fernandez, A., Folgueras, A.R., Sanchez, L.M., Zhou, Z., Rodriguez, F.J., Stewart, C.L., Vega, J.A., et al. (2005). Accelerated ageing in mice deficient in Zmpste24 protease is linked to p53 signalling activation. Nature 437, 564-568.

Varela, I., Tarpey, P., Raine, K., Huang, D., Ong, C.K., Stephens, P., Davies, H., Jones, D., Lin, M.L., Teague, J., et al. (2011). Exome sequencing identifies frequent mutation of the SWI/SNF complex gene PBRM1 in renal carcinoma. Nature 469, 539-542.

Varon, R., Vissinga, C., Platzer, M., Cerosaletti, K.M., Chrzanowska, K.H., Saar, K., Beckmann, G., Seemanova, E., Cooper, P.R., Nowak, N.J., et al. (1998). Nibrin, a novel DNA double-strand break repair protein, is mutated in Nijmegen breakage syndrome. Cell 93, 467-476.

Vasile, E., Tomita, Y., Brown, L.F., Kocher, O., and Dvorak, H.F. (2001). Differential expression of thymosin beta-10 by early passage and senescent vascular endothelium is modulated by VPF/VEGF: evidence for senescent endothelial cells in vivo at sites of atherosclerosis. FASEB J 15, 458-466.

Vaughan, A., Alvarez-Reyes, M., Bridger, J.M., Broers, J.L., Ramaekers, F.C., Wehnert, M., Morris, G.E., Whitfield, W.G.F., and Hutchison, C.J. (2001). Both emerin and lamin C depend on lamin A for localization at the nuclear envelope. Journal of Cell Science 114, 2577-2590.

Vergnes, L., Peterfy, M., Bergo, M.O., Young, S.G., and Reue, K. (2004). Lamin B1 is required for mouse development and nuclear integrity. Proc Natl Acad Sci U S A 101, 10428-10433.

Vermeulen, K., Van Bockstaele, D.R., and Berneman, Z.N. (2003). The cell cycle: a review of regulation, deregulation and therapeutic targets in cancer. Cell Prolif 36, 131-149.

Vijg, J., and Campisi, J. (2008). Puzzles, promises and a cure for ageing. Nature 454, 1065-1071.

Vlcek, S., Dechat, T., and Foisner, R. (2001). Nuclear envelope and nuclear matrix: interactions and dynamics. Cell Mol Life Sci 58, 1758-1765.

Vlcek, S., and Foisner, R. (2007). A-type lamin networks in light of laminopathic diseases. Biochim Biophys Acta 1773, 661-674.

Vlcek, S., Just, H., Dechat, T., and Foisner, R. (1999). Functional diversity of LAP2alpha and LAP2beta in postmitotic chromosome association is caused by an alpha-specific nuclear targeting domain. EMBO J 18, 6370-6384.

Vodermaier, H.C. (2004). APC/C and SCF: controlling each other and the cell cycle. Curr Biol 14, R787-796.

Volkmer, E., and Karnitz, L.M. (1999). Human homologs of Schizosaccharomyces pombe rad1, hus1, and rad9 form a DNA damage-responsive protein complex. The Journal of Biological Chemistry 274, 567-570.

Vousden, K.H., and Prives, C. (2009). Blinded by the Light: The Growing Complexity of p53. Cell 137, 413-431.

Waga, S., Li, R., and Stillman, B. (1997). p53-induced p21 controls DNA replication. Leukemia 11 Suppl 3, 321-323.

Wallace, D.C. (2005). A mitochondrial paradigm of metabolic and degenerative diseases, aging, and cancer: a dawn for evolutionary medicine. Annu Rev Genet 39, 359-407.

Waltes, R., Kalb, R., Gatei, M., Kijas, A.W., Stumm, M., Sobeck, A., Wieland, B., Varon, R., Lerenthal, Y., Lavin, M.F., et al. (2009). Human RAD50 deficiency in a Nijmegen breakage syndrome-like disorder. American journal of human genetics 84, 605-616.

Wang, B., Matsuoka, S., Carpenter, P.B., and Elledge, S.J. (2002). 53BP1, a mediator of the DNA damage checkpoint. Science 298, 1435-1438.

Wang, H., Bauzon, F., Ji, P., Xu, X., Sun, D., Locker, J., Sellers, R.S., Nakayama, K., Nakayama, K.I., Cobrinik, D., et al. (2010). Skp2 is required for survival of aberrantly proliferating Rb1-deficient cells and for tumorigenesis in Rb1+/- mice. Nat Genet 42, 83-88.

Wang, X., Kennedy, R.D., Ray, K., Stuckert, P., Ellenberger, T., and D'Andrea, A.D. (2007). Chk1-mediated phosphorylation of FANCE is required for the Fanconi anemia/BRCA pathway. Molecular and Cellular Biology 27, 3098-3108.

Wang, Z., Gucek, M., and Hart, G.W. (2008). Cross-talk between GlcNAcylation and phosphorylation: site-specific phosphorylation dynamics in response to globally elevated O-GlcNAc. Proc Natl Acad Sci U S A 105, 13793-13798.

Ward, I.M., Minn, K., Jorda, K.G., and Chen, J. (2003). Accumulation of checkpoint protein 53BP1 at DNA breaks involves its binding to phosphorylated histone H2AX. The Journal of Biological Chemistry 278, 19579-19582.

Ward, I.M., Reina-San-Martin, B., Olaru, A., Minn, K., Tamada, K., Lau, J.S., Cascalho, M., Chen, L., Nussenzweig, A., Livak, F., et al. (2004). 53BP1 is required for class switch recombination. The Journal of Cell Biology 165, 459-464.

Wei, S., and Sedivy, J.M. (1999). Expression of catalytically active telomerase does not prevent premature senescence caused by overexpression of oncogenic Ha-Ras in normal human fibroblasts. Cancer Res 59, 1539-1543.

Weiss, R.S., Enoch, T., and Leder, P. (2000). Inactivation of mouse Hus1 results in genomic instability and impaired responses to genotoxic stress. Genes Dev 14, 1886-1898.

Wilhelmsen, K., Ketema, M., Truong, H., and Sonnenberg, A. (2006). KASH-domain proteins in nuclear migration, anchorage and other processes. Journal of Cell Science 119, 5021-5029.

Williams, G.J., Lees-Miller, S.P., and Tainer, J.A. (2010). Mre11-Rad50-Nbs1 conformations and the control of sensing, signaling, and effector responses at DNA double-strand breaks. DNA Repair (Amst) 9, 1299-1306.

Williams, R.S., Dodson, G.E., Limbo, O., Yamada, Y., Williams, J.S., Guenther, G., Classen, S., Glover, J.N., Iwasaki, H., Russell, P., et al. (2009). Nbs1 flexibly tethers Ctp1 and Mre11-Rad50 to coordinate DNA double-strand break processing and repair. Cell 139, 87-99.

Williams, R.S., Williams, J.S., and Tainer, J.A. (2007). Mre11-Rad50-Nbs1 is a keystone complex connecting DNA repair machinery, double-strand break signaling, and the chromatin template. Biochem Cell Biol 85, 509-520.

Willis, N.D., Cox, T.R., Rahman-Casans, S.F., Smits, K., Przyborski, S.A., van den Brandt, P., van Engeland, M., Weijenberg, M., Wilson, R.G., de Bruine, A., et al. (2008). Lamin A/C is a risk biomarker in colorectal cancer. PLoS One 3, e2988.

Wilson, K.A., and Stern, D.F. (2008). NFBD1/MDC1, 53BP1 and BRCA1 have both redundant and unique roles in the ATM pathway. Cell Cycle 7, 3584-3594.

Winterbourn, C.C., and Hampton, M.B. (2008). Thiol chemistry and specificity in redox signaling. Free Radic Biol Med 45, 549-561.

Wohlbold, L., and Fisher, R.P. (2009). Behind the wheel and under the hood: functions of cyclin-dependent kinases in response to DNA damage. DNA Repair (Amst) 8, 1018-1024.

Wood, L.D., Parsons, D.W., Jones, S., Lin, J., Sjoblom, T., Leary, R.J., Shen, D., Boca, S.M., Barber, T., Ptak, J., et al. (2007). The genomic landscapes of human breast and colorectal cancers. Science 318, 1108-1113.

Worman, H.J., and Bonne, G. (2007). "Laminopathies": a wide spectrum of human diseases. Exp Cell Res 313, 2121-2133.

Worman, H.J., and Courvalin, J.C. (2005). Nuclear envelope, nuclear lamina, and inherited disease. Int Rev Cytol 246, 231-279.

Worman, H.J., and Gundersen, G.G. (2006). Here come the SUNs: a nucleocytoskeletal missing link. Trends Cell Biol 16, 67-69.

Wydner, K.L., McNeil, J.A., Lin, F., Worman, H.J., and Lawrence, J.B. (1996). Chromosomal assignment of human nuclear envelope protein genes LMNA, LMNB1, and LBR by fluorescence in situ hybridization. Genomics 32, 474-478.

Xiao, A., Li, H., Shechter, D., Ahn, S.H., Fabrizio, L.A., Erdjument-Bromage, H., Ishibe-Murakami, S., Wang, B., Tempst, P., Hofmann, K., et al. (2009). WSTF regulates the H2A.X DNA damage response via a novel tyrosine kinase activity. Nature 457, 57-62.

Xie, A., Hartlerode, A., Stucki, M., Odate, S., Puget, N., Kwok, A., Nagaraju, G., Yan, C., Alt, F.W., Chen, J., et al. (2007). Distinct roles of chromatin-associated proteins MDC1 and 53BP1 in mammalian double-strand break repair. Mol Cell 28, 1045-1057.

Yamasaki, L., and Pagano, M. (2004). Cell cycle, proteolysis and cancer. Curr Opin Cell Biol 16, 623-628.

Yang, F., Stenoien, D.L., Strittmatter, E.F., Wang, J., Ding, L., Lipton, M.S., Monroe, M.E., Nicora, C.D., Gristenko, M.A., Tang, K., et al. (2006). Phosphoproteome profiling of human skin fibroblast cells in response to low- and high-dose irradiation. J Proteome Res 5, 1252-1260.

Yang, J., Bardes, E.S., Moore, J.D., Brennan, J., Powers, M.A., and Kornbluth, S. (1998). Control of cyclin B1 localization through regulated binding of the nuclear export factor CRM1. Genes Dev 12, 2131-2143.

Yang, J., and Kornbluth, S. (1999). All aboard the cyclin train: subcellular trafficking of cyclins and their CDK partners. Trends Cell Biol 9, 207-210.

Yang, X., Zou, P., Yao, J., Yun, D., Bao, H., Du, R., Long, J., and Chen, X. (2010). Proteomic dissection of cell type-specific H2AX-interacting protein complex associated with hepatocellular carcinoma. J Proteome Res 9, 1402-1415.

You, Z., Chahwan, C., Bailis, J., Hunter, T., and Russell, P. (2005). ATM activation and its recruitment to damaged DNA require binding to the C terminus of Nbs1. Molecular and Cellular Biology 25, 5363-5379.

Yu, H., and Yao, X. (2008). Cyclin B1: conductor of mitotic symphony orchestra. Cell Res 18, 218-220.

Yuan, J., and Chen, J. (2010). MRE11-RAD50-NBS1 complex dictates DNA repair independent of H2AX. The Journal of Biological Chemistry 285, 1097-1104.

Yuan, J., Simos, G., Blobel, G., and Georgatos, S.D. (1991). Binding of lamin A to polynucleosomes. The Journal of Biological Chemistry 266, 9211-9215.

Zastrow, M.S., Vlcek, S., and Wilson, K.L. (2004). Proteins that bind A-type lamins: integrating isolated clues. Journal of Cell Science 117, 979-987.

Zhang, J., Lian, Q., Zhu, G., Zhou, F., Sui, L., Tan, C., Mutalif, R.A., Navasankari, R., Zhang, Y., Tse, H.F., et al. (2011). A human iPSC model of Hutchinson Gilford Progeria reveals vascular smooth muscle and mesenchymal stem cell defects. Cell Stem Cell 8, 31-45.

Zhang, R., Poustovoitov, M.V., Ye, X., Santos, H.A., Chen, W., Daganzo, S.M., Erzberger, J.P., Serebriiskii, I.G., Canutescu, A.A., Dunbrack, R.L., et al. (2005). Formation of MacroH2A-containing senescence-associated heterochromatin foci and senescence driven by ASF1a and HIRA. Dev Cell 8, 19-30.

Zhang, Y.Q., and Sarge, K.D. (2008). Sumoylation regulates lamin A function and is lost in lamin A mutants associated with familial cardiomyopathies. The Journal of Cell Biology 182, 35-39.

Zhao, H., and Piwnica-Worms, H. (2001). ATR-mediated checkpoint pathways regulate phosphorylation and activation of human Chk1. Molecular and Cellular Biology 21, 4129-4139.

Zhong, N., Radu, G., Ju, W., and Brown, W.T. (2005). Novel progerin-interactive partner proteins hnRNP E1, EGF, Mel 18, and UBC9 interact with lamin A/C. Biochemical and Biophysical Research Communications 338, 855-861.

Zhou, B.B., and Elledge, S.J. (2000). The DNA damage response: putting checkpoints in perspective. Nature 408, 433-439.

Zhu, L., Enders, G., Lees, J.A., Beijersbergen, R.L., Bernards, R., and Harlow, E. (1995). The pRB-related protein p107 contains two growth suppression domains: independent interactions with E2F and cyclin/cdk complexes. The EMBO Journal 14, 1904-1913.

Zhu, Z., Chung, W.H., Shim, E.Y., Lee, S.E., and Ira, G. (2008). Sgs1 helicase and two nucleases Dna2 and Exo1 resect DNA double-strand break ends. Cell 134, 981-994.

Zink, D., Amaral, M.D., Englmann, A., Lang, S., Clarke, L.A., Rudolph, C., Alt, F., Luther, K., Braz, C., Sadoni, N., et al. (2004). Transcription-dependent spatial arrangements of CFTR and adjacent genes in human cell nuclei. J Cell Biol 166, 815-825.

Ziv, Y., Bielopolski, D., Galanty, Y., Lukas, C., Taya, Y., Schultz, D.C., Lukas, J., Bekker-Jensen, S., Bartek, J., and Shiloh, Y. (2006). Chromatin relaxation in response to DNA double-strand breaks is modulated by a novel ATM- and KAP-1 dependent pathway. Nature Cell Biology 8, 870-876.

Zou, L., and Elledge, S.J. (2003). Sensing DNA damage through ATRIP recognition of RPA-ssDNA complexes. Science 300, 1542-1548.

Zou, L., and Stillman, B. (1998). Formation of a preinitiation complex by S-phase cyclin CDK-dependent loading of Cdc45p onto chromatin. Science 280, 593-596.